Terranes affinity
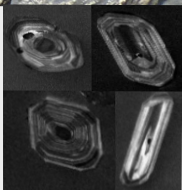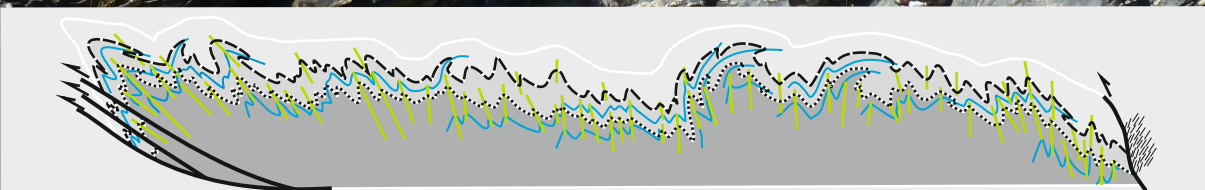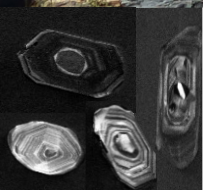# and Variscan transpressional evolution
# of Rheic-related units in SW Iberia

Irene Pérez Cáceres

Departamento de Geodinámica

Universidad de Granada

Terranes affinity
and Variscan transpressional evolution
of Rheic-related units in SW Iberia

Memoria de Tesis Doctoral

presentada por la Licenciada en Geología Irene Pérez Cáceres

para optar al Grado de Doctora por la Universidad de Granada.

Granada, 23 de Febrero de 2017

Fdo. Irene Pérez Cáceres

VºBº del Director

Fdo. David Jesús Martínez Poyatos

El doctorando / The *doctoral candidate* **[Irene Pérez Cáceres]** y los directores de la tesis / and the thesis supervisor/s: **[David J. Martínez Poyatos]**

Garantizamos, al firmar esta tesis doctoral, que el trabajo ha sido realizado por el doctorando bajo la dirección de los directores de la tesis y hasta donde nuestro conocimiento alcanza, en la realización del trabajo, se han respetado los derechos de otros autores a ser citados, cuando se han utilizado sus resultados o publicaciones.

/
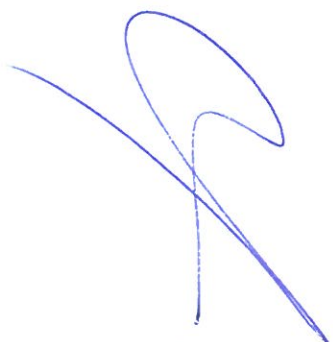
Guarantee, by signing this doctoral thesis, that the work has been done by the doctoral candidate under the direction of the thesis supervisor/s and, as far as our knowledge reaches, in the performance of the work, the rights of other authors to be cited (when their results or publications have been used) have been respected.

Lugar y fecha / Place and date:

Granada, a 23 de Febrero de 2017

Director/es de la Tesis / *Thesis supervisor/s;*   Doctorando / *Doctoral candidate:*

Firma / Signed   Firma / Signed

Foi nesta altura que, em profusão e diversidade internacional, apareceram os geólogos. (…)

agora chegavam em força os sábios da terra e das terras,

os averiguadores de movimentos e acidentes, estratos e blocos erráticos,

de martelinho na mão, batendo em tudo quanto fosse pedra ou pedra parecesse.

JOSÉ SARAMAGO

A jangada de pedra

Index

Agradecimientos

Durante los cuatro años de realización de esta tesis doctoral, han sido muchas las personas que me han ayudado y apoyado, y en este apartado quiero mostrarles mi agradecimiento.

En primer lugar, quiero agradecer a mi director de tesis, David Jesús Martínez Poyatos, por confiar en mí para este proyecto. Siempre estaré agradecida por todo lo que he aprendido bajo su dirección. Además, Antonio Azor Pérez y muy especialmente José Fernando Simancas Cabrera han tenido también una participación muy activa como codirectores (aunque formalmente no aparezcan como tales debido a las restricciones que impone la normativa al respecto), y a los tres quiero agradecerles su dedicación y apoyo continuos. Quiero destacar que para mí, el principal resultado de estos años es el aprendizaje científico, académico y personal, y se lo debo a ellos tres.

Fernando y David disfrutando del paisaje del Pulo do Lobo.

Asimismo, también quiero dar las gracias a otros investigadores de la Universidad de Granada que han enriquecido este estudio. Gracias a Fernando Nieto García que siempre me facilitó el trabajo con la preparación de muestras y análisis de difracción de rayos X, y con quien además aprendí mucho sobre mineralogía y metamorfismo. Agradezco también la ayuda de Aitor Cambeses Torres, cuyas investigaciones previas simplificaron la recopilación de datos en mi tesis. Además, su experiencia en geocronología y geoquímica me ayudaron a resolver problemas en el laboratorio y dudas en la interpretación de los resultados. Gracias a Pilar Navas-Parejo, quien me enseñó a trabajar en el laboratorio y me aconsejó en mis inicios en el análisis de circones e interpretación paleogeográfica. También quiero prestar atención a Antonio Jabaloy Sánchez, quien siempre estuvo dispuesto a ayudarme en todo lo necesario. No puedo olvidar a Isabel Nieto García, Isabel Sánchez

Fuera de Granada quiero agradecer ante todo a toda mi familia (canaria y viguesa) por su constante apoyo e interés, particularmente a mis padres José María y Nieves, y a mi hermano Jose, quienes me aconsejan y me animan incondicionalmente. Si algo cambiaría de estos años, sería haber estado más tiempo con vosotros.

Gracias también a Cris y a Tatiana y a todos mis amigos de Vigo, quienes siguen haciéndome sentir en casa cuando estoy allí. Me siento muy orgullosa de todos los años de nuestra amistad. Agradecer a María y Jaime, mi pareja del norte, nuestros encuentros tan necesarios. A mis compañeras geólogas de carrera Cris, Ana y María, con quienes guardo una gran amistad y siguen animándome. Y a mis amigos de Máster por nuestras quedadas anuales navideñas, en las que seguimos conversando de piedras y en donde tanto sigo aprendiendo.

Gracias a todos por haber contribuido en mi formación como investigadora.

Abstract

The Rheic Ocean closure led to the Variscan collision between Laurussia and Gondwana and concluded with the formation of the Pangea supercontinent in late Paleozoic time. Other minor terranes were also involved in the Variscan Cycle, e.g. Avalonia and Armorica.

This Thesis deals with the Variscan tectonometamorphic evolution of the SW Iberian Variscides, constituted by the southern Central Iberian Zone (CIZ), the Ossa-Morena Zone (OMZ) and the South Portuguese Zone (SPZ). The main focus is put on the OMZ/SPZ boundary, which is interpreted as the Rheic Ocean suture and attests the collision of Avalonia (SPZ) with a north-Gondwanan terrane (OMZ). Three tectonics units have been classically related to the OMZ/SPZ suture: (i) the Beja-Acebuches amphibolites (BAA), a metamafic unit interpreted as a Rheic ophiolite; (ii) the Pulo do Lobo unit, a low-grade metasedimentary unit with minor MORB-like metabasalts, considered as the remnant of a Rheic subduction-related accretionary prism; and (iii) the allochthonous Cubito-Moura unit, which appears emplaced onto the southern OMZ and contains Ordovician? MORB-featured rocks and Devonian? high-pressure metamorphic assemblages.

Concerning the paleogeographic significance of the SPZ, a good number of SHRIMP U/Pb detrital zircon age populations from Devonian-Carboniferous rocks of the northern SPZ have been obtained in order to estimate provenance sources and maximum depositional ages. The results are compatible with an Avalonian affinity of the SPZ, particularly regarding the latest Devonian Horta da Torre formation of the Pulo do Lobo unit. The lower formations of the Pulo do Lobo unit (Pulo do Lobo and Ribeira de Limas formations) and that of the Iberian Pyrite belt (Ronquillo formation) can be considered as equivalent according to their similar inherited zircon content, depositional age, lithology and polyphasic deformation, thus challenging the classical interpretation of the Pulo do Lobo unit as exotic with respect to the SPZ.

New structural and geochronological data have been obtained in order to improve the knowledge of the geometry and timing of the Variscan tectonometamorphic evolution of the OMZ/SPZ suture-related units. The interplay between folding and high- to low-temperature ductile shearing of the BAA has been studied, with particular emphasis on structural mapping, which, in turn, has allowed the recognition of the large-scale Quintos fold. We have also characterized the polyphasic Devonian to Carboniferous deformation of the Pulo do Lobo unit at different scales, from thin-sections to regional kilometric cross-sections. The MORB-like metamafic rocks of the Pulo do Lobo belt have yielded (SHRIMP U/Pb on zircons) Mississipian ages, thus having been reinterpreted (as previously was done for the BAA) as formed during an Early Carboniferous intraorogenic transtensional and magmatic event that obscured the former Rheic suture zone. The collision was resumed after this transtensional stage in an oblique left-lateral scenario that gave way to the majority of structures described in this Thesis.

The very low- to low-grade metamorphic evolution of the Pulo do Lobo unit has been studied by applying three different methodologies. Two metamorphic events have been distinguished based on phyllosilicate growth in relation to the regional foliations: the

Devonian M1 corresponds to the epizone, and the Carbonifeous M2 to the anchizone/epizone boundary. The white-mica *b* parameter and celadonite content indicate low-pressure conditions, which question the interpretation of the Pulo do Lobo belt as an accretionary prism.

Finally, the large-scale kinematics of the Variscan collision between the CIZ/OMZ/SPZ has been quantified by using all the available data (fold, shear zone and fault patterns, tectonic fabrics and finite strain) on suitable transpressional scenarios for each structural domain. The total collisional convergence surpasses 1000 km, most of them corresponding to left-lateral displacement parallel to terrane boundaries. This left-lateral kinematics contrasts with the dextral component that prevailed elsewhere in the Variscan orogen, having been explained in the context of an Avalonian plate promontory (currently represented by the SPZ) that entered the northern Gondwanan or Armorican margin.

Resumen

La colisión Varisca entre Laurusia y Gondwana se produjo debido al cierre del Océano Rheico y concluyó al final del Paleozoico con la formación del supercontinente Pangea. Otros terrenos de menor tamaño también estuvieron involucrados en el ciclo Varisco, e.g. Avalonia y Armórica.

Esta Tesis trata sobre la evolución tectonometamórfica del SO del Macizo Ibérico, que está constituido por el sur de la Zona Centro Ibérica (ZCI), la Zona de Ossa-Morena (ZOM) y la Zona Sudportuguesa (ZSP). El objetivo principal ha sido el estudio del límite ZOM/ZSP, interpretado generalmente como la sutura del Océano Rheico debido a la colisión de Avalonia (ZSP) con el margen norte de Gondwana (ZOM). Tres unidades tectónicas han sido relacionadas con la sutura ZOM/ZSP: (i) las anfibolitas de Beja-Acebuches (ABA), una unidad metamáfica interpretada como la ofiolita del Océano Rheico; (ii) la unidad del Pulo do Lobo, una unidad metasedimentaria de bajo grado, que contiene metabasaltos de afinidad MORB, y que se ha considerado en su conjunto como un prisma de acreción relacionado con la subducción del Océano Rheico; y (iii) la unidad alóctona del Cubito-Moura, que aparece emplazada sobre el sur de la ZOM, y contiene rocas de afinidad MORB Ordovícicas? y rocas metamórficas de alta presión Devónicas?.

Respecto al significado paleogeográfico de la ZSP, se dataron poblaciones de circones detríticos para estimar las fuentes de procedencia y las edades máximas de sedimetación. Los resultados son compatibles con la afinidad avaloniana de la ZSP, particularmente de la formación Horta da Torre del Devónico Superior. Las formaciones inferiores de la unidad Pulo do Lobo (Pulo do Lobo s. str. y Ribeira de Limas) y las equivalentes de la Faja Pirítica (Formación Ronquillo) muestran un contenido similar de circones heredados, lo que unido a su semejanza en edad de sedimentación, litología y deformación polifásica, pone en duda la interpretación clásica de Pulo do Lobo como unidad exótica respecto a la ZSP.

Se han obtenido también nuevos datos estructurales y geocronológicos para mejorar la información sobre la geometría y las edades de la evolución tectonometamórfica de las unidades de sutura en el contacto ZOM/ZSP. Se ha estudiado la relación entre plegamiento y deformación dúctil de las ABA, con particular énfasis en la cartografía estructural, lo cual ha permitido el reconocimiento del pliegue de Quintos. La deformación polifásica devónica y carbonífera de la unidad Pulo do Lobo ha sido caracterizada a diferentes escalas, desde el estudio de lámina delgada, a cortes geológicos de escala regional. La edad de los metabasaltos MORB de la unidad del Pulo do Lobo ha resultado ser Misisipiense, por lo que su origen está relacionado con en el evento magmático y transtensional que ocultó los restos de la sutura Rheica. Después de este evento transtensivo, se retomó la colisión oblicua izquierda que dio lugar a la mayoría de las estructuras que se describen en esta Tesis.

La evolución metamórfica de grado bajo a muy bajo de la unidad del Pulo do Lobo se estudió aplicando tres metodologías diferentes. Se distinguieron dos eventos metamórficos de acuerdo con el crecimiento de filosilicatos: el evento devónico M1 corresponde a la epizona, y el evento carbonífero M2 al límite anquizona/epizona. El parámetro b de la

mica blanca y el contenido en celadonita indican condiciones de baja presión, lo que pone en duda la interpretación de la unidad del Pulo do Lobo como un prisma de acreción.

Finalmente, se ha cuantificado a gran escala la cinemática de la colisión Varisca entre las ZCI/ZOM/ZSP usando todos los datos disponibles (plegamiento, cizallamiento y fracturación, fábricas tectónicas y deformación finita) en ambientes transpresivos para cada dominio estructural. La convergencia colisional total sobrepasa los 1000 km, que en su mayoría corresponden a desplazamientos izquierdos paralelos a los límites entre terrenos. Esta cinemática izquierda contrasta con la componente derecha que domina el Orógeno Varisco, y se justifica como un saliente de Avalonia (actualmente representada por la ZSP) que se introdujo en el margen septentrional de Gondwana o en Armórica.

Chapter I

Introduction

1. Geographic location

The area of study in this Thesis is an E-W elongated band located in the SW part of the Iberian Peninsula (Fig. 1.1a). This area comprises the northern Huelva province and, a small part of the northern Sevilla province in Spain, as well as the central and eastern parts of the Beja district in Portugal (Fig. 1.1b). From a topographic point of view, this region is characterized by a moderate local relief (≈600 m.a.s.l. in the east that progressively descends to ≈200 m.a.s.l. in the west). The landscape is variably eroded and incised by a dense hydrographic network with numerous streams that flow into the Odiel, Tinto, Rivera del Chanza and Guadiana rivers. In Spain, the Sierra de Aracena and Picos de Aroche Natural Park (714 m of maximum altitude) consists in a number of E-W oriented valleys and ridges parallel to the structural grain. In Portugal, the local relief is smaller, with the exception of the sectors incised by the Guadiana river.
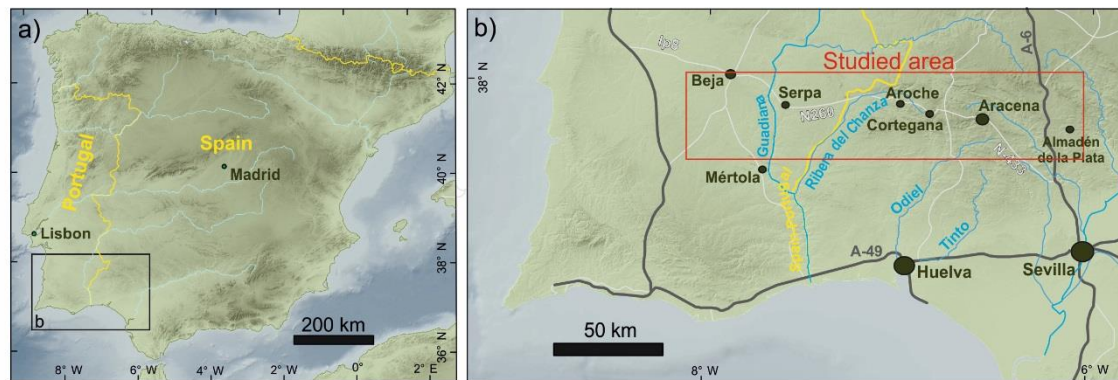
Figure 1.1. a) Geographic location of the SW Iberian Peninsula. b) Geographic map of the SW Iberian Peninsula with location of the studied area. The Spanish/Portuguese border, main towns, roads and rivers are shown.

2. The Iberian Massif in the context of the Variscides

2.1. The Variscan belt

The end of Paleozoic times was a period of collision between two major continents, Laurussia and Gondwana, which gave way to the Variscan/Appalachian orogenic belt (Fig. 1.2a; e.g. Matte, 1986). The Variscides are referred as the part of this belt extending from Morocco to Central Europe through Iberia (Fig. 1.2b). The NW front of the Variscan belt (the Laurussia side) is well defined from England to Germany. By contrast, the SE front of the Variscides (the Gondwanan foreland) is not well defined due to Alpine reworking that difficults paleogeographic and paleotectonic interpretations (Fig. 1.2b).

Regarding the Paleozoic paleogeographical evolution, paleomagnetic and paleontological data basically agree on the existence of three major continental blocks (Laurentia, Baltica and Gondwana, separated by the Iapetus and Tornquist oceans) up to early Ordovician times (Fig. 1.2a). The subsequent fragmentation of northern Gondwana gave way to the formation of Avalonia (and other Gondwana-derived terranes such as Ganderia, Meguma, Carolina, Armorica, and Florida) and the birth of the Rheic Ocean separating Avalonia and

Gondwana. The amalgamation of Avalonia with Baltica closed the Tornquist Ocean at latemost Ordovician times, while the docking with Laurentia closed the Iapetus Ocean at Silurian/Lower Devonian times. Finally, the closure of the Rheic Ocean gave way to the Carboniferous assembly of Laurentia-Baltica-Avalonia with Gondwana, with the formation of the Pangea supercontinent (Fig. 1.2; e.g. Matte, 2001; Nance et al., 2012).

The recognition and correlation of high-pressure metamorphic and ophiolitic belts along the Variscan orogen constitute a key constraint for paleotectonic and paleogeographic reconstructions. These data apparently indicate where subduction events took place and oceanic-like crust existed sometime in the geological past, but the width of the putative oceanic domains is unknown, and the correlation of the disparate high-pressure/ophiolitic belts is controversial. The available paleobiological, paleomagnetic and geological evidence suggests that the Variscan Orogen must include the major suture of the Rheic Ocean, as well as some second-order sutures related to the amalgamation of terranes of arguable significance (e.g. Matte, 1991, 2001; Franke, 2000, 2014).
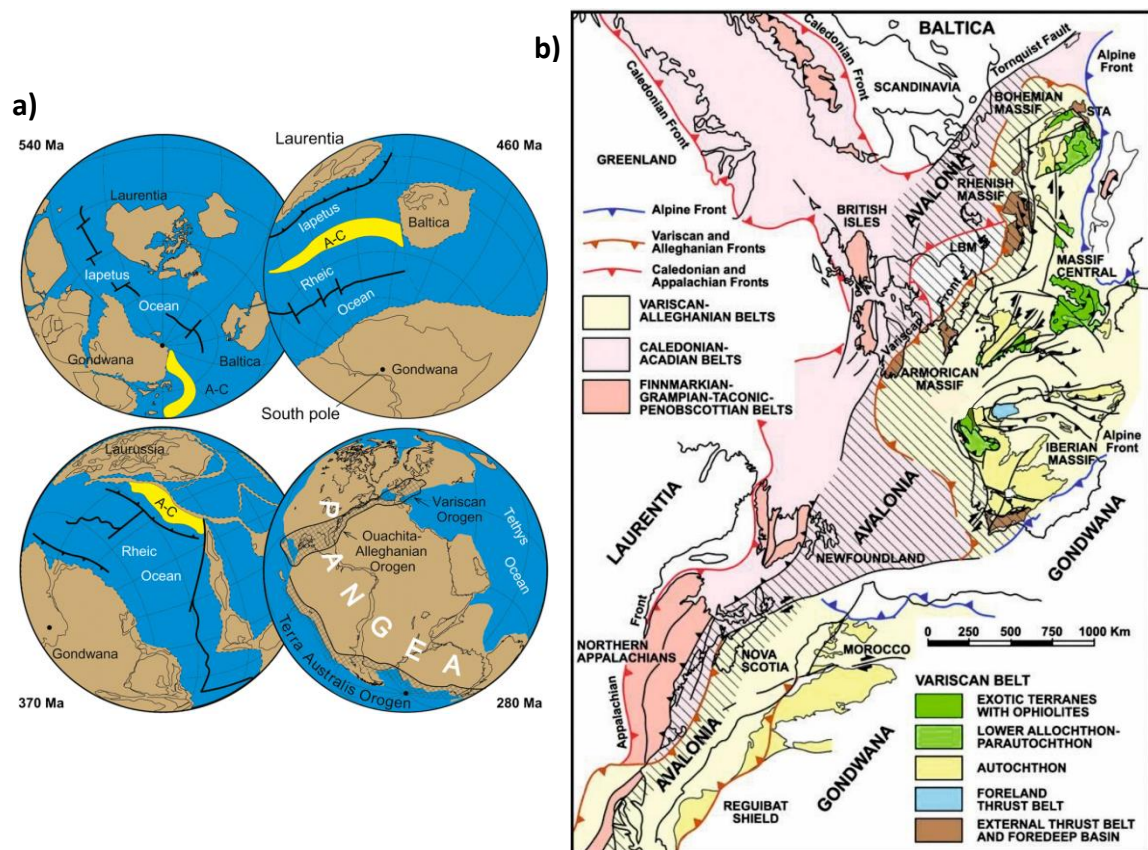
Figure 1.2. a) Accretion of Pangea (280 Ma) after the Paleozoic evolution of Laurentia, Baltica, Gondwana and Avalonia-Carolinia (A-C); modified from Nance et al. (2010). b) Location of Iberia as part of the Paleozoic orogenic belts at the end of the Variscan collision between Laurentia-Baltica, Gondwana and other intervening terranes; modified from Murphy et al. (2016).

The basement of the Variscides contains calc-alkaline magmatic bodies and thick siliciclastic-volcanoclastic greywacke deposits of late Neoproterozoic (Ediacaran) age, which are said to belong to a Cadomian magmatic arc (Murphy et al., 2002).

At late Cambrian-early Ordovician times, the drift of terranes such as Carolinia and Avalonia from the northern border of the Gondwana supercontinent started to form the Rheic Ocean that characterizes the Variscan Cycle (Fig. 1.2a). The arrival of Laurussia to collide with Gondwana added an Avalonian basement to the dominant Cadomian-Gondwanan one of the Variscan orogenic belt.

2.2. The Iberian Massif

In the Iberian Peninsula, the Variscan orogen forms a vast outcrop that has been divided into a number of zones (Fig. 1.3). The currently consensual zoning is made up of the Cantabrian (CZ), Western Asturian-Leonese (WALZ), Central Iberian (CIZ), Galicia Tras-Os-Montes (GTMZ), Ossa-Morena (OMZ) and South Portuguese (SPZ) zones, referred hereafter by their abbreviations. It is commonly interpreted that the CZ faces the Gondwanan foreland, while the SPZ faces the Avalonian (Laurentian) foreland (e.g. Matte, 1991; Quesada, 1991; Ribeiro et al., 1995, 2007; Franke, 2000; Simancas et al., 2005; Murphy et al., 2016).

The CZ-WALZ boundary is an antiform cored by Neoproterozoic rocks (Narcea antiform), which can be considered as the passage from the external (CZ) to the internal zones in this transect of the Iberian Variscides. The structure of the CZ is dominated by east-vergent folds and thrusts. The seismic image under the Narcea antiform shows a lower crustal wedge that evidences an abrupt deepening (i.e. thickening) of the deformation, in contrast to the thin-skinned tectonics that characterizes the CZ (Gutiérrez-Alonso, 1995; Pérez-Estaún et al., 1995).

The WALZ-CIZ boundary has been located along the linear outcrop of the Ollo de Sapo metaigneous unit (orthogneisses, metarhyolites and ignimbrites of Early Ordovician age; Julivert et al., 1974; Montero et al., 2007) (Fig. 1.3), or along the Viveiro fault and its SE passage to the Caurel-Truchas fold (Martínez Catalán, 1985; Martínez Catalán et al., 1992). At first sight, none of the two proposed boundaries seem to be a main tectonic feature, though the CIZ adjacent to this boundary exhibits a contrasting abundance of Carboniferous granitoids, midcrustal Variscan stacking and exhumation of deep metamorphic rocks, i.e. an intense crustal thickening that might be related to intracontinental subduction (Macaya et al., 1991; Barbero and Villaseca, 2000; Simancas et al., 2013).

The GTMZ is made up of parautochtonous sequences and allochthonous complexes thrust onto the CIZ autochthon, the latter representing the section of the Gondwanan margin that escaped to continental subduction during the Variscan Cycle. Three groups of allochthonous units (Upper, Ophiolitic and Basal) and a frontal tectonic mélange appear in the GTMZ. The ophiolitic units as a whole represent an unrooted suture of disputed correlation with either the Rheic Ocean itself or another Variscan ocean (Arenas, 1984; Martínez Catalán et al., 2007; 2009). Below the ophiolitic units, the parautochthonous

sequences (Farias et al., 1987; Ribeiro et al., 1990) comprise latest Ediacaran to latest Cambrian metasediments of northern Gondwana provenance (Díez-Fernández et al., 2010). The parautochthonous sequences underwent HP/LT metamorphism dated at ≈370 Ma (Martínez Catalán et al., 1996; Abati et al., 2010), while the exhumation to intermediate-pressure conditions occurred at ≈350-340 Ma (Rodríguez et al., 2003).
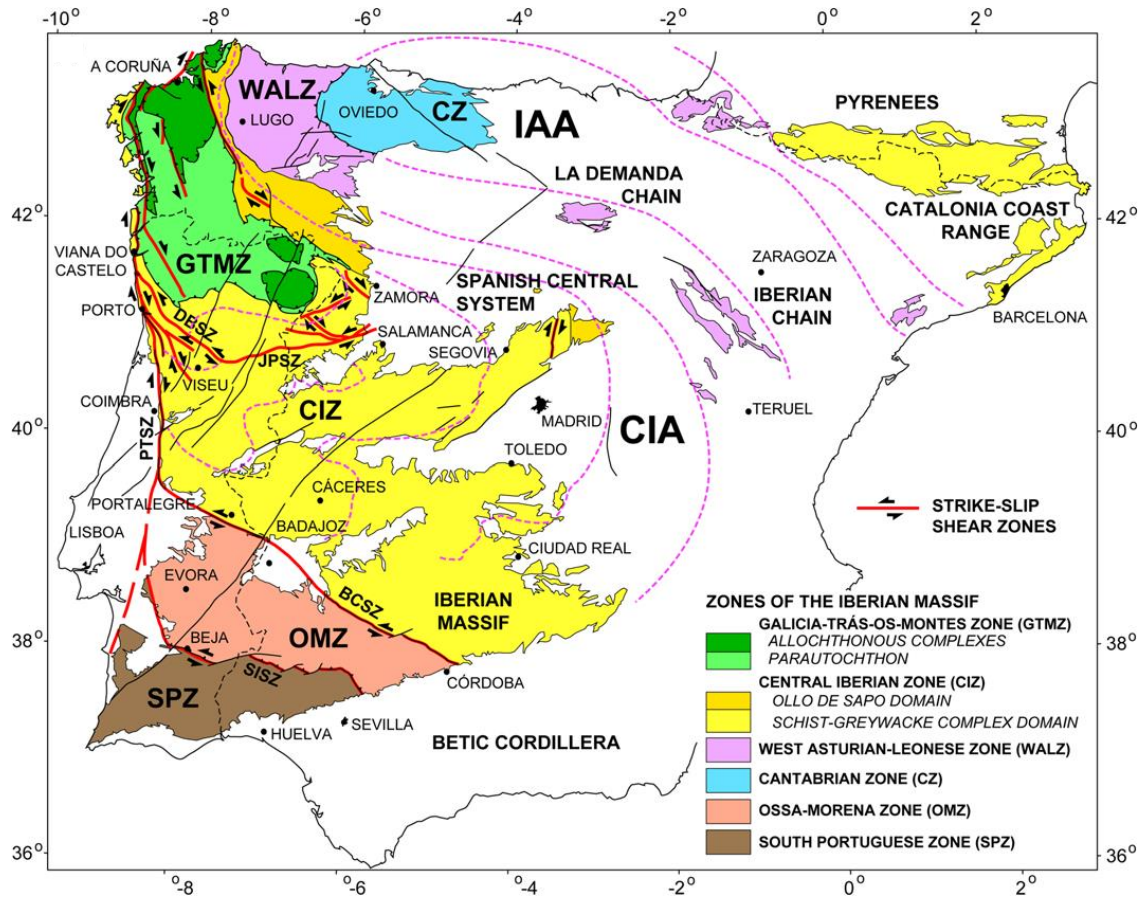
Figure 1.3. Outcrops of the Variscan basement in the Iberian Peninsula (except those of the Betic Cordillera) and subdivision into zones. The Central Iberian (CIA) and Ibero-Armorican (IAA) arcs are outlined. Shear zones: BCSZ, Badajoz-Córdoba; DBSZ, Douro-Beira; JPSZ, Juzbado-Penalva; PTSZ, Porto-Tomar; SISZ, Southern Iberian. Modified from Martínez Catalán et al. (2014).

The two southern zone boundaries of the Iberian Variscides (CIZ/OMZ and OMZ/SPZ) and the unrooted GTMZ may represent orogenic sutures (Fig. 1.3). The CIZ/OMZ boundary is classically located at the main tectonic band represented by the Badajoz-Córdoba Shear Zone (BCSZ; Burg et al., 1981) or Tomar-Badajoz-Córdoba Shear Zone (TBCSZ), also called Central Unit (Azor et al., 1994a). The BCSZ is of conflicting Variscan-only or Cadomian-Variscan significance. Moreover, some authors prefer to locate the CIZ/OMZ boundary north of the BCSZ, just at or near the Pedroches Batholith (Fig. 1.4), because the Ediacaran rocks cropping out north and south of the BCSZ are very similar, while they differ with those north of the Pedroches area (Eguiluz et al., 2000; San José et al., 2004; Martín Parra et al., 2006). The OMZ/SPZ boundary is classically

interpreted as the suture of the Rheic Ocean, though its current appearance is obscured by a protracted collisional evolution.

Following the above brief description of the Variscides and the geological zonation of the Iberian Massif, now the geological evolution of Iberia is introduced from the Ediacaran to the end of the Variscan Cycle. Cadomian calc-alkaline magmatism is well represented in SW Iberia (Sánchez Carretero et al., 1989, 1990; Pin et al., 2002; Bandrés et al., 2004; Simancas et al., 2004; Henriques et al., 2015) and also locally in NW Iberia (Fernández-Suárez et al., 1998). Cadomian deformation/metamorphism is locally observed as a low-grade foliation dated at 560-550 Ma (Blatrix and Burg, 1981; Dallmeyer and Quesada, 1992) in Ediacaran rocks (Serie Negra formation) at the southernmost CIZ; recently, a 540 Ma amphibolite facies metamorphic event has been described close to the CIZ/OMZ boundary (Henriques et al., 2015). To the north, in the inner CIZ, the Cadomian deformation is manifested as an angular unconformity (the so-called intra-Alcudian unconformity; Ortega and González Lodeiro, 1986; Palero, 1993) that has been constrained to develop between 575 and 555 Ma (Talavera et al., 2015). In the Iberian Chain of NE Iberia (Fig. 1.3), a poorly deformed conglomerate of Lower Cambrian age contains pebbles with internal deformation occurred at low-grade conditions (Abalos, 2001). In NW Iberia, large asymmetric folds with axial planar cleavage, truncated by Lower Cambrian conglomerates, have been estimated to develop between 560 and 540 Ma (Díaz García, 2006), in accordance with some $^{40}Ar/^{39}Ar$ age data on single detrital muscovite grains, which were mostly derived from proximal sources and record low-temperature processes (Gutiérrez-Alonso et al., 2005).

The Cambrian starts everywhere in Iberia with transgressive siliciclastic deposits, passing upwards to carbonate or mixed terrigenous/carbonate platform deposits (Liñán et al., 2002). Therefore, a generalized stage of tectonic inactivity seems to have prevailed at early Cambrian times in extended domains of the Variscides. Moreover, according to geochemistry of sediments (Fuenlabrada et al., 2016), Ediacaran greywackes from the CIZ were associated with a mature active margin (volcanic arc), while Cambrian shales fit better with a more stable context in which cratonic sources had a higher contribution; i.e. the regional setting during the Ediacaran/Lower Cambrian transition evolved from an active margin (end of the Cadomian belt) to a more stable context related to the onset of a passive continental margin (inception of the Variscan Cycle).

During Cambrian to Lower Ordovician times, signs of instability started to appear in the form of passage to terrigenous sediments and associated tholeitic-alkaline volcanics that have been interpreted as the beginning of the rifting affecting the northern border of Gondwana (Liñán and Quesada, 1990; Crowley et al., 2000). Subsequently, the Ordovician to Devonian stratigraphy of Iberia indicates a relatively stable passive continental margin that would continue to the north into the Rheic and/or other oceanic realm(s). Then, the Carboniferous period (and also the Devonian and Permian by sectors) constitutes the time-span of the Variscan orogeny.

Synorogenic flysch deposits mark the climax of collisional deformation, which corresponds to Visean-Bashkirian times for the external SPZ and CZ (e.g. Oliveira, 1990; Fernández et al., 2004, respectively). Molassic basins with undeformed basal Autunian sediments mark an

upper boundary for the age of deformation, which is thus found to finish at the end of the Carboniferous (e.g. Arche and López-Gómez, 1996; Sierra and Moreno, 2004; Dinis et al., 2012). However, paleomagnetic evidence suggests that the strong arcuate shape of the northern Iberian Variscides may have developed at latest Carboniferous-earliest Permian times (Weil et al. 2001, 2013; Gutiérrez-Alonso et al., 2004; Pastor-Galán et al., 2015; Fernández-Lozano et al., 2016). Regarding orogenic magmatism, late- to post-collisional granitic magmatism extends from late Carboniferous to earliest Permian times (e.g. Bea, 2004; Gutiérrez-Alonso et al., 2011; Pereira et al., 2015a).

3. Southwest Iberia

This transect of the Variscan belt comprises the southern CIZ, the OMZ and the SPZ (Fig. 1.4). Two outstanding features characterize the Variscan collisional evolution of the SW Iberian Massif: (i) the presence of an intraorogenic early Carboniferous extensional/transtensional stage (e.g. Simancas et al., 2003, 2006; Azor et al., 2008; Pereira et al., 2012) and (ii) the left-lateral component of the collision (e.g. Burg et al., 1981; Crespo-Blanc and Orozco, 1988). A good deal of stratigraphic, tectonometamorphic, geochronological and geochemical data endorse the existence of a Devonian collisional event followed by a Mississippian transtensional one that gave way to widespread flysch basins and (mostly mafic) magmatism in SW Iberia. The left-lateral displacements in SW Iberia contrast with the dextral tectonics recognized in most of the regions of the Variscan/Appalachian Orogen (e.g. Shelley and Bossière, 2000). This particular kinematics has been classically related to the formation and tightening of the Ibero-Armorican Arc (Matte and Ribeiro, 1975; Brun and Burg, 1982) (Fig. 1.3). However, the reassessment of this orocline as an essentially very late Variscan (early Permian) structure (Weil et al., 2000) has questioned this interpretation. An alternative explanation for the left-lateral kinematics in SW Iberia was provided by considering a paleogeographic Avalonian? (Laurentian) promontory, which collided with the northern Gondwana margin during the Variscan orogeny (Simancas et al., 2005).

The evolution of the SW Iberian Massif has been intensely debated regarding the Cadomian or Variscan age of the main deformational and metamorphic events in the southernmost CIZ, the CIZ/OMZ boundary and the inner OMZ. An increasing number of geochronological and structural data favor that both the main structures and the associated metamorphism are Variscan in age (e.g. Azor et al., 1993; Ordóñez-Casado, 1998; Pereira et al., 2010, 2012). On the contrary, the Cadomian orogeny is mainly witnessed by the presence of subduction-related Ediacaran igneous rocks (Sánchez Carretero et al., 1989, 1990; Pin et al., 2002; Bandrés et al., 2004; Simancas et al., 2004; Henriques et al., 2015) or simple late Ediacaran unconformities (e.g. Ortega and González Lodeiro, 1986). A tectonometamorphic Cadomian imprint has only been demonstrated in a few localities of the southernmost CIZ (Blatrix and Burg, 1981; Dallmeyer and Quesada, 1992).

A new discussion regarding the structure of the OMZ comes from a recent proposition that considers it as a Variscan mega-nappe spreading from the Allochthonous Complexes of NW Iberia, also covering the Central Spanish System and most of the southern CIZ

(Díez Fernández and Arenas, 2015 and 2016; Arenas et al., 2016a; Díez Fernández et al., 2016). These authors claim that the same pile of allochthonous units recognized in NW Iberia (e.g. Martínez Catalán et al., 2009; Arenas et al., 2016b) also exists in the OMZ, thus proposing a huge continuous nappe emplaced eastward? at Mississippian time onto the Gondwana margin (Díez Fernández and Arenas, 2016; Díez Fernández et al., 2016). This hypothesis is exclusively based on the correlation of high-pressure metamorphic "belts" and MORB-type metabasites from NW to SW Iberia, which would be part of a single and huge high-pressure and ophiolitic allochthonous complex, i.e. they would attest a single suture, instead of two as considered by other authors (e.g. Matte, 1991; Simancas et al., 2002). This proposal has a number of structural and kinematic inconsistencies that were already stated by Simancas et al. (2016). Moreover, the Mississippian period, as indicated above, is a transtensional stage in the whole SW Iberian Massif with widespread basin formation and magmatism, without evidences of nappe emplacement.
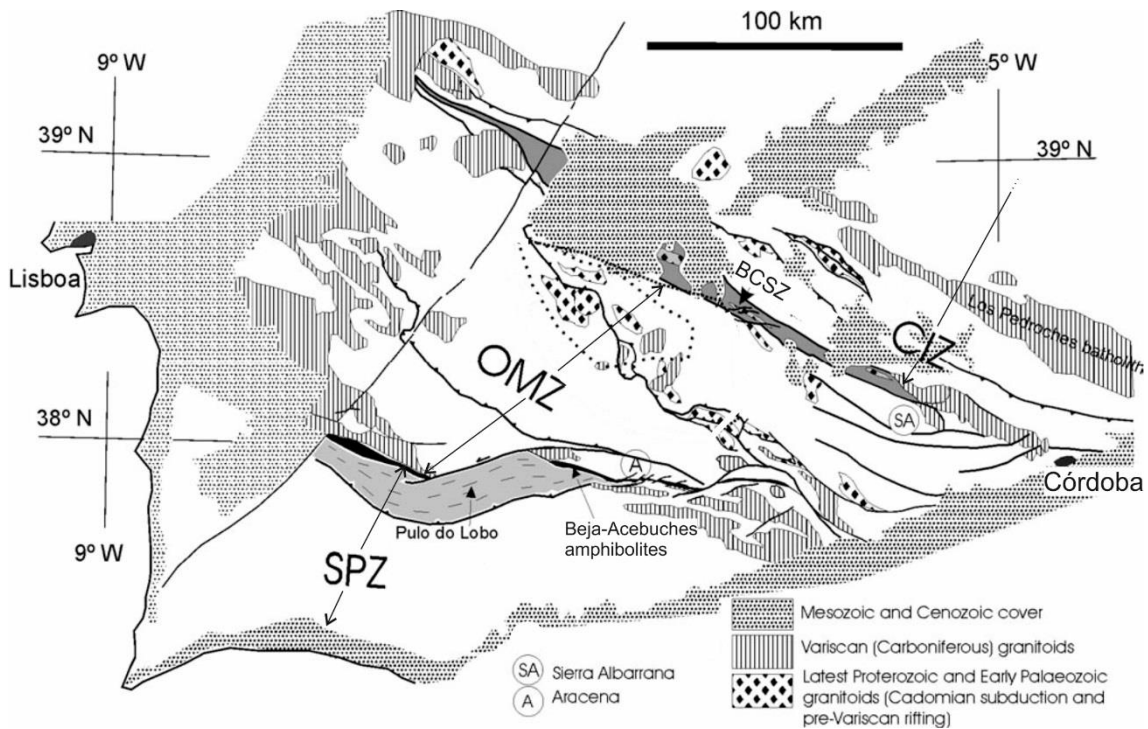
Figure 1.4. Geological sketch of SW Iberian Massif, showing the location of the Central Iberian Zone (CIZ), the Ossa-Morena Zone (OMZ) and the South Portuguese Zone (SPZ), as well as their boundaries (BCSZ: Badajoz-Córdoba Shear Zone; and Beja-Acebuches amphibolites). Modified from Simancas et al. (2004).

3.1. Southern Central Iberian Zone

The southern CIZ is characterized by large outcrops of the pre-Ordovician 'Alcudian' (Schist-Greywacke Complex), unconformably overlaid by an Ordovician-Devonian passive-margin succession (Fig. 1.5a). The intra-Alcudian unconformity separates the Lower Alcudian succession, affected by Cadomian folds without associated foliation and metamorphism, from the Upper Alcudian succession (Ortega and González Lodeiro, 1986; Palero, 1993).

The first Variscan deformation is Late Devonian in age, having only affected the Espiel Thrust Sheet, which is an allochthonous unit located at the southernmost CIZ next to the boundary with the OMZ (Fig. 1.5). Here, the Ediacaran to Lower/Middle Devonian succession was deformed by syn-metamorphic kilometric NE-vergent recumbent folds and related ductile shearing (Azor et al., 1994b; Martínez Poyatos, 1997; Martínez Poyatos et al., 1995a, 1995b and 1998a). The rocks show a penetrative planar-linear fabric parallel to the axial planes of the folds. The stretching lineation is parallel to the fold axes, while asymmetrical structures reveal top-to-the-SE kinematics. The metamorphic conditions range from the chlorite zone in the NW to the sillimanite zone in the SE, with a low- to intermediate-pressure gradient (Martínez Poyatos et al., 2001). These eo-Variscan structures are interpreted as formed during the transpressional CIZ/OMZ collision, being the NE-vergent folds of the southernmost CIZ retro-vergent structures with respect to the coeval SW-vergent folds in the OMZ (e.g., Simancas et al., 2001). The recumbent folds of the CIZ were unconformably covered by lower- to middle Carboniferous sediments as piggy-back basins during the NE-directed thrusting of the Espiel Thrust Sheet (Martínez Poyatos et al., 1998b) onto the Pedroches Basin (see below).

In the southern CIZ, the transtensional scenario that characterized SW Iberia in the early Carboniferous, gave way to subsidence with the accumulation of a thick flysch succession (the Culm-facies Pedroches Basin; Fig. 1.5a; Gabaldón et al., 1985) that widely crops out along a NW-SE trending band located to the north of the CIZ/OMZ boundary. The visible thickness of this basin exceeds 6000 m. Basaltic volcanism accompanied the beginning of the sedimentation mostly in the SW part of the basin, attesting significant lithospheric thinning (Armendáriz et al., 2008). Additional evidence of transtensional crustal thinning is given by the left-lateral to normal, high- to low-temperature, ductile- to brittle shearing recorded at the CIZ/OMZ boundary (Azor et al., 1994b).

Km-scale NW-SE trending upright folds of late Mississippian to Pennsylvanian age dominate the cartographic pattern in the whole southern CIZ (Fig. 1.5). The associated regional metamorphism was of very low- to low-grade, with a low- to intermediate-pressure gradient (López Munguira et al., 1991; Martínez Poyatos et al., 2001).

The late Variscan deformation in the CIZ is characterized by transcurrent ductile-brittle shear zones and low-angle extensional shear zones. In the southern CIZ, two important extensional shear zones have been reported, namely the Toledo (Hernández Enrile, 1991; Barbero, 1995) and the Puente Génave/Castelo de Vide (Martín Parra et al., 2006) shear zones.

The ALCUDIA deep seismic reflection profile (Martínez Poyatos et al., 2012) has improved the knowledge of the crustal structure of the southern CIZ. The Moho discontinuity is subhorizontal and located at 10 s (≈30 km). The reflectivity of the upper crust is not very intense, probably due to the dominant monotonous lithologies (Schist-Greywacke Complex and granite intrusions), though the variably dipping reflectors correlate well with surface geology. By contrast, intense reflectivity in the decoupled middle-lower crust is depicted by numerous high-amplitude and laterally coherent events. This pervasive seismic fabric is subhorizontal in the central part of the section, while it reveals two large-scale contractional structures at both ends of the seismic profile.
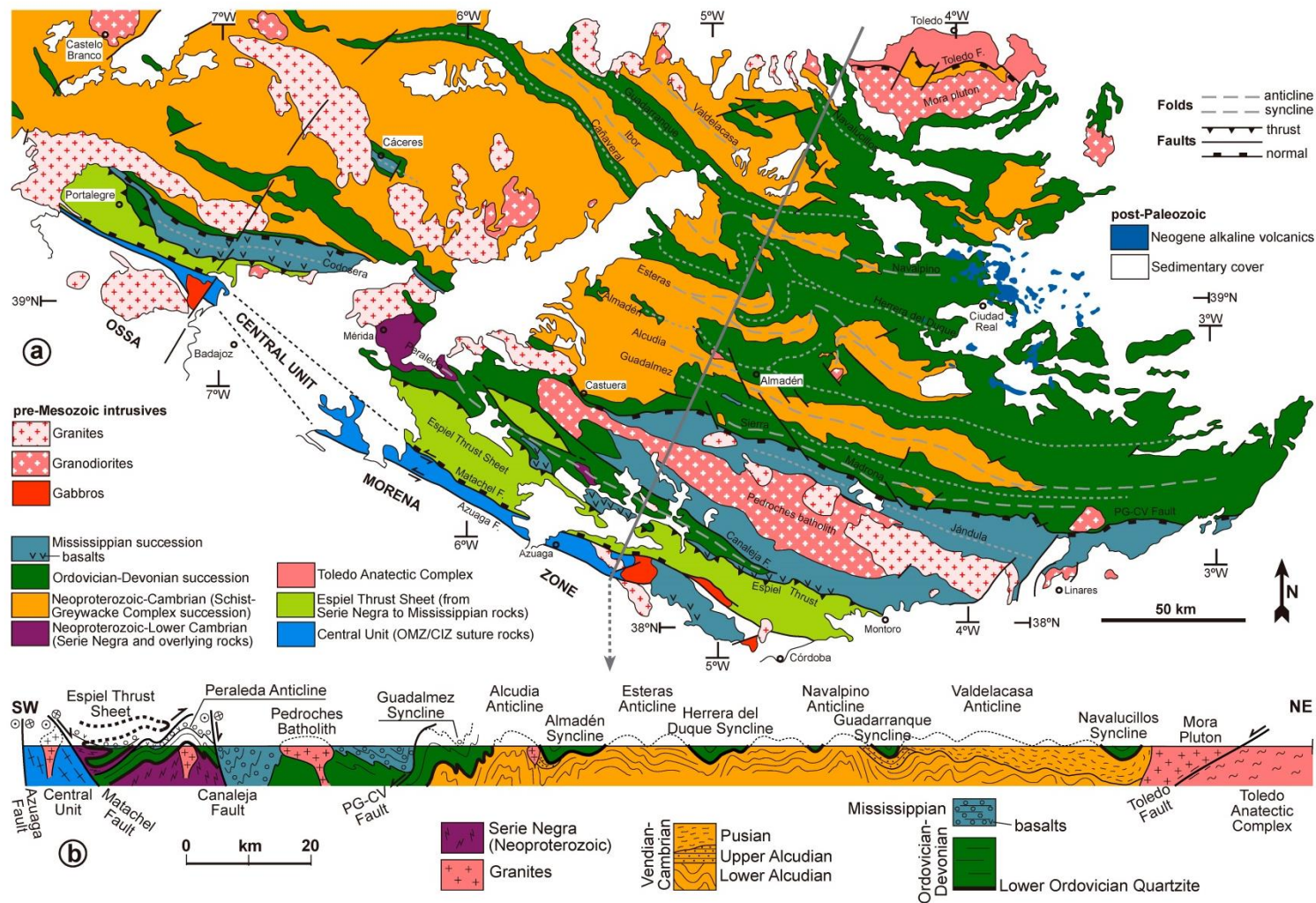
Figure 1.5. a) Geological map of the southern Central Iberian Zone. b) Generalized geological cross-section along the grey line of the map in Fig. 1.5a. Modified from Martínez Poyatos et al. (2012).

3.2. The CIZ/OMZ boundary: The Badajoz-Córdoba Shear Zone

The boundary between the CIZ and the OMZ was first interpreted as a major left-lateral subvertical ductile shear zone, namely the Badajoz-Córdoba Shear Zone (BCSZ; Burg et al., 1981; Matte, 1986), running for 300 km in SW Iberia with a NW-SE orientation (Fig. 1.4). According to some authors, the BCSZ would represent a polyorogenic terrane that underwent a high-pressure, high-temperature late Precambrian (Cadomian) metamorphism, followed by a low-grade Late Paleozoic one (Variscan) (Quesada, 1990; Abalos et al., 1991 and 2002; Eguiluz et al., 2000; Ribeiro et al., 2007). Nevertheless, a good number of geochronological and structural data indicate that the metamorphic evolution of the BCSZ is entirely Variscan in age (e.g. Azor et al., 1993 and 1994a; Ordóñez-Casado, 1998; Pereira et al., 2010 and 2012).

The BCSZ consists in metasediments, orthogneisses and amphibolites organized in a sequence in which the structural top is located to the NE. The geochemical and geochronological data of sheet-shaped strongly deformed bodies of the amphibolites showed the existence of dikes intruded into a continental basement during the late Cadomian orogeny, and tectonic lenses of an Early Paleozoic oceanic-like crust (Ordóñez-Casado, 1998; Gómez-Pugnaire et al., 2003). The structure of the BCSZ as observed in the field basically consists in a NW-SE oriented km-scale cartographic band of strongly sheared rocks, which are affected by minor later folds and cut across by later NW-SE striking brittle faults. Thus, ductile shearing penetrated the whole unit, giving way to an intense mylonitic foliation that strikes on average NW-SE with dominant steep dips to the NE. The stretching lineation is subhorizontal or gently plunging to the NW or to the SE. Shear criteria indicate a left-lateral sense of movement when the foliation is steeply dipping and top-to-the-NW when the foliation dips moderately to the NE. To the NE, the upper BCSZ is cut cut by the Matachel Fault, which dips to the NE and has a normal component, i.e. it downthrows the southernmost CIZ rocks (Fig. 1.5b; Azor et al., 1994a).

The metamorphic evolution of the lower part of the BCSZ is characterized by an initial high-pressure/intermediate-temperature event (Abalos et al., 1991) with peak-pressure conditions of ≈19 kbar and 550 ° C, followed by a high-pressure/high-temperature one with peak temperatures of ≈725° C (López Sánchez-Vizcaíno et al., 2003). The upper part of the BCSZ recorded only intermediate-pressure/intermediate-temperature conditions (the micaschists contain garnet and rare kyanite; Abalos, 1990; Azor, 1994a; Azor et al., 1997) with peak pressures of ≈10 kbar and temperatures of ≈500 ºC. The high-pressure metamorphism recorded in the BCSZ can be related to Variscan underthrusting beneath the southern border of the CIZ in an early compressional stage whose structural record became completely obliterated by the later shearing that penetrates the whole unit. This shearing produced the retrogression of the high-pressure assemblages first to amphibolite and then to greenschist facies assemblages while the rocks were being exhumed to upper crustal levels (Azor et al., 1994a; Simancas et al., 2001).

The available geochronological data on the metamorphic evolution of the BCSZ mostly constrain the temperature peak conditions (≈340 Ma) and the subsequent retrogression to amphibolite (≈335 Ma) and greenschist (≈330 Ma) facies conditions (Blatrix and Burg, 1981; Quesada and Dallmeyer, 1994; Ordóñez-Casado, 1998; Pereira et al., 2010).

The IBERSEIS (Fig. 1.6) and ALCUDIA seismic profiles have imaged a NE-dipping slab down to the middle crust (Simancas et al., 2003; Martínez Poyatos et al., 2012). These geophysical data, together with the available geochemical and geochronological data, suggest the existence of some sort of narrow? oceanic realm between the OMZ and CIZ in Lower Paleozoic times.
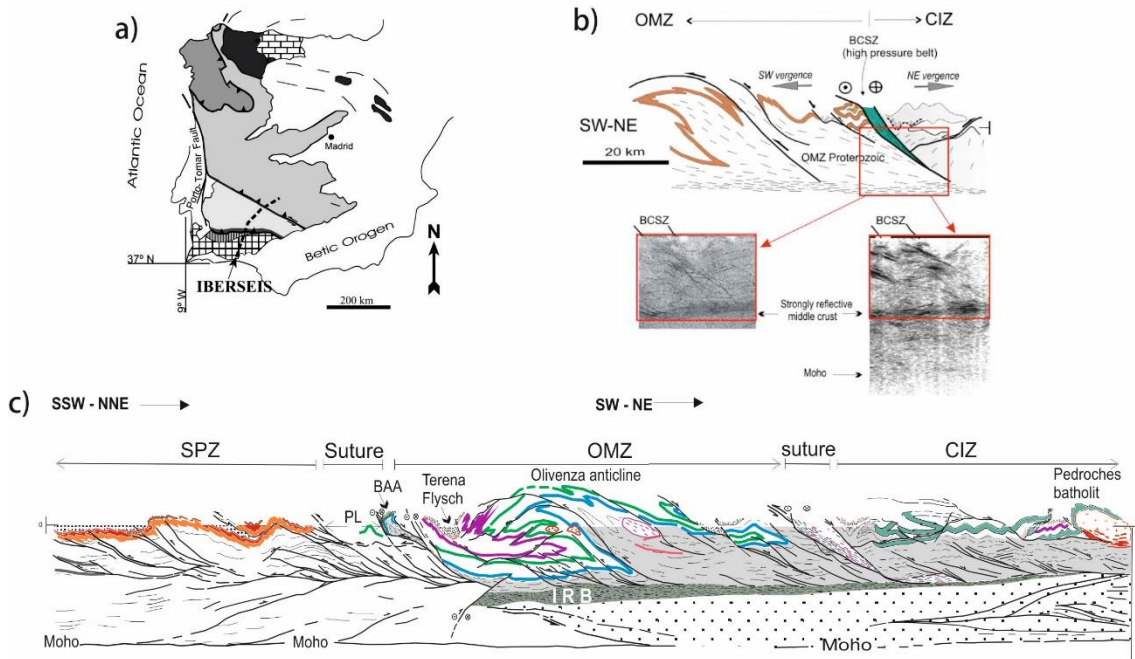
Figure 1.6. a) Location of the IBERSEIS deep reflection seismic profile in the SW Iberian Massif, crosscutting the South Portuguese Zone (SPZ), the Ossa-Morena Zone (OMZ) and the southernmost Central Iberian Zone (CIZ) perpendicularly to the main geological structures. b) Cross-section and seismic windows through the OMZ/CIZ boundary, showing the NE-dipping BCSZ and the opposite structural vergence at both sides. c) Crustal architecture of SW Iberia, according to the interpretation of the IBERSEIS seismic profile. IRB: Iberseis Reflective Body; BAA: Beja-Acebuches Amphibolites; PL: Pulo do Lobo. Modified from Simancas et al., 2003.

3.3. The Ossa-Morena Zone

The OMZ (Fig. 1.7) is distinguished by: (i) its particular Ediacaran and lower Paleozoic sedimentary sequences that are quite distinctive with respect to other Variscan Zones in the Iberian Massif, and (ii) its relative abundance of late Ediacaran and middle Cambrian to Ordovician volcanic and plutonic rocks.

The crustal structure of the OMZ is well constrained from geological mapping and the IBERSEIS seismic surveys (Fig. 1.6c; Simancas et al., 2003, 2006; Palomeras et al., 2009). On a large scale, the OMZ must be viewed as a continental piece deformed in-between two suture contacts, namely the contact with the CIZ and the contact with the SPZ. Subduction at the CIZ/OMZ boundary seems to have accommodated most of the shortening in the OMZ interior, while the OMZ/SPZ boundary would account for the shortening measured in the SPZ.

The OMZ interior can be divided into two domains, namely the Estremoz-Monesterio domain to the north and the Évora-Aracena domain to the south, separated by the Santo Aleixo thrust (Fig. 1.7). Both domains share the NW-SE structural grain, and SW-vergent folds and thrusts (e.g. Vauchez, 1975; Expósito 2000; Simancas et al., 2001; Expósito et al., 2002). However, the rocks of the Estremoz-Monesterio domain exhibit only very low or low-grade Variscan metamorphism, while in the Evora-Aracena domain low-pressure/high-temperature metamorphic rocks crop out in the core of Carboniferous extensional dome-shaped sectors.

The first Variscan structures in the Estremoz-Monesterio domain are recumbent km-scale NW-SE oriented SW-vergent folds, whose axial traces show rather complex map patterns due to the interference with later upright folds. This folding episode probably started in the Lower Devonian according to the age of the older syn-orogenic sediments in the Terena basin (Piçarra, 1998; Pereira et al. 1999; Rocha et al., 2010). Although the time gap between these early syn-orogenic sediments and the underlying deformed rocks is minimal, the existence of an unconformity in-between has been demonstrated through detailed structural mapping (Expósito, 2000; Expósito et al., 2002; Azor et al., 2004).

The recumbent folds are cross-cut by SW-directed thrusts generated as a continuation of the same shortening episode. The most important of these structures is the Olivenza-Monesterio thrust (Fig. 1.7; Eguiluz, 1987; Expósito 2000; Expósito et al., 2002).

The early Carboniferous transtensional intraorogenic episode gave way to low- to high-angle normal faults and several sedimentary basins (Santos de Maimona, Toca da Moura and Cabrela basins (Giese, 1994; Expósito, 2000; Expósito et al., 2002; Simancas et al., 2003; Oliveira et al., 2006).

The Variscan collision was resumed after the transtensional stage, giving way to large-scale, open to tight, NW-SE oriented folds, and high-angle reverse faults (Fig. 1.5c). These folds are generally upright. Finally, strike-slip left-lateral faults developed mostly at both boundaries of the OMZ (Fig. 1.7).

In the southern OMZ, the Évora-Aracena unit crops out as NW-SE elongated structural domes (Evora, Aracena and Lora del Río sectors; Fig. 1.7), being characterized by high-temperature/low-pressure metamorphism that occurred at 345-335 Ma (Bard, 1977; Crespo-Blanc, 1991; Carvalhosa, 1999; Apraiz and Eguiluz, 2002; Díaz-Azpiroz et al., 2004; Pereira et al., 2006 and 2009). Despite the dominant high-grade rocks and the intense deformation, some of the original lithologies are still recognizable and correspond to the classical Ediacaran to Cambrian succession of the OMZ. The dominant structure is a widespread NW-SE oriented moderate to steeply-dipping mylonitic foliation with a gently-plunging stretching lineation, generally coaxial with the later fold axes. Reliable shear criteria have not been described yet due to poor exposure and overprinting by subsequent deformation. However, normal to left-lateral movements seem to dominate, which have been interpreted as compatible with an oblique extensional scenario (Pereira et al., 2009).
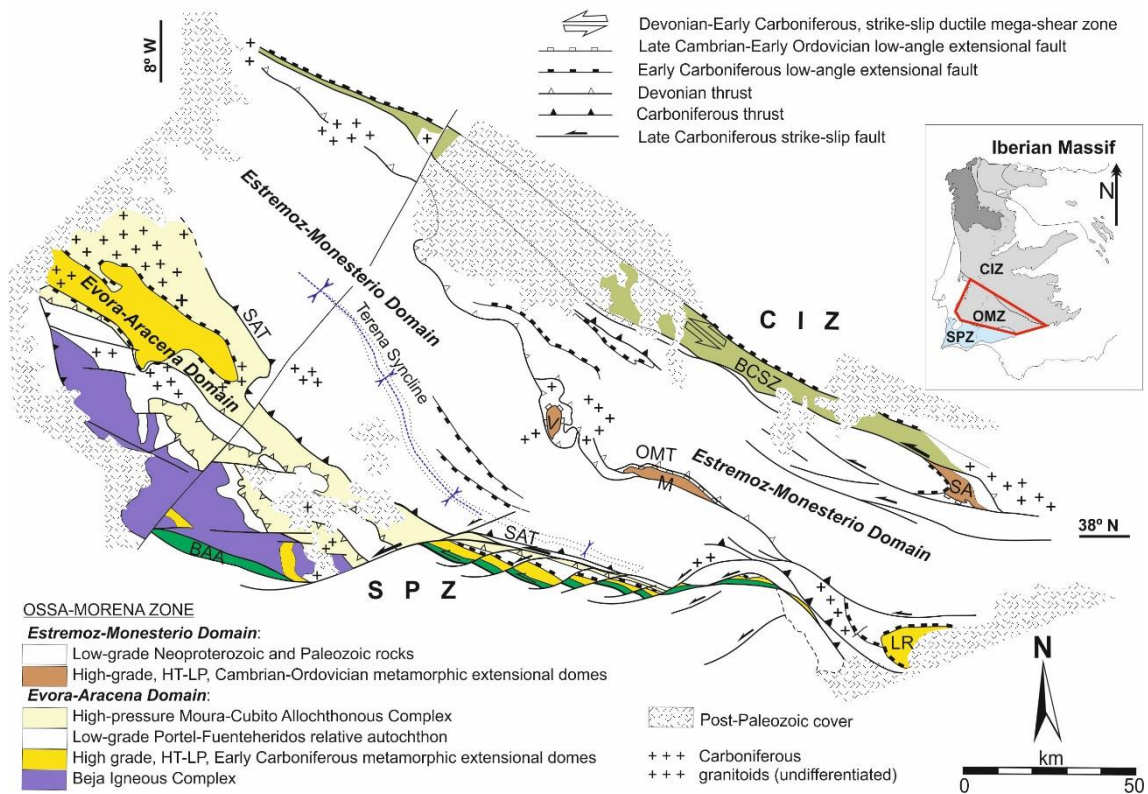
Figure 1.7: Domains of the Ossa-Morena Zone and its main structures. Location of the map is shown in the inset of the Iberian Massif. BAA: Beja-Acebuches Amphibolites; BCSZ: Badajoz-Córdoba Shear Zone; CIZ: Central Iberian Zone; LR: Lora del Río dome; M: Monesterio dome; OMT: Olivenza Montesterio Thrust; OMZ: Ossa-Morena Zone; SA: Sierra Albarrana dome; SAT: Santo Aleixo Thrust; SPZ: South Portuguese Zone; V: Valuengo dome).

An early Carboniferous low-angle normal fault system separates the high-grade/low-pressure Evora-Aracena domes from the overlying low-grade Portel-Fuenteheridos unit (Fig. 1.7), which also features the classical stratigraphy of the OMZ, with the Ediacaran Serie Negra, the latemost Ediacaran Malcocinado formation and the Cambrian succession. The structure of this unit is similar to the one observed in the Estremoz-Monesterio domain, i.e. first generation recumbent folds affected by upright second generation ones. The Portel-Fuenteheridos unit constitutes the para-autochthon of the overlying allochthonous HP Cubito-Moura unit, which, in turn, is related to the OMZ/SPZ suture (see below).

3.4. The South Portuguese Zone

The South Portuguese Zone (SPZ) constitutes the southernmost part of the Iberian Massif, being characterized by its restricted stratigraphic range at surface from the Givetian to the Pennsylvanian (Schermerhorn, 1971; Oliveira, 1990; González et al., 2004; Pereira et al., 2008). The SPZ can be considered as the southern external foreland fold and thrust belt of

the Iberian Variscides but, contrarily to the CZ in north Iberia, it shows a low- to very low-grade slaty cleavage.

The SPZ can be divided into three main belts or units, namely (from north to south) the Pulo do Lobo unit, the Iberian Pyrite unit and the Flysch unit, each one featuring distinctive stratigraphy and deformation (Fig. 1.8). The Pulo do Lobo unit is composed of polydeformed low-grade Middle Devonian to Mississippian metasediments and contains also some MORB-featured greenschists lenses. It has been classically interpreted as the subduction-related accretionary prism formed by the Rheic Ocean closure between the OMZ and the SPZ (e.g. Eden and Andrews, 1990; Braid et al., 2012). Because of that, the Pulo do Lobo belt will be introduced below in section 3.5.3, as part of the OMZ/SPZ boundary. The Iberian Pyrite unit attests the most complete (Givetian to Serpukhovian) and lithologically varied stratigraphy, while the Flysch unit is a thick clastic sequence of Mississippian to Pennsylvanian age.

The older rocks of the SPZ (Givetian-Frasnian metasediments) crop out at the Pulo do Lobo unit (Pulo do Lobo and Ribeira de Limas formations) and at the eastern Iberian Pyrite unit (Fig. 1.8; Ronquillo formation; Simancas, 1983; González et al., 2004) and they show a pre-Carbonifeorus foliation. The classic tectonic context given to the Devonian deformation around the OMZ/SPZ boundary has been a northward directed subduction (SPZ underneath the OMZ; e.g. Silva et al., 1990; Eden, 1991; Braid et al., 2010). However, Azor et al. (2008) and Ponce et al. (2012) have proposed an opposite Devonian subduction polarity.

The Devonian deformation was separated from the Carboniferous one by a transtensional event that is particularly well represented by the Volcanosedimentary Complex with associated giant sulphide deposits, which are interpreted by most authors as the consequence of a pervasive rifting event (e.g. Schermerhorn, 1971; Munhá et al., 1983; Oliveira, 1990; Barrie et al., 2002; Thièblemont et al., 1998; Valenzuela et al., 2011). Moreover, at the eastern SPZ there are remarkable volumes of gabbros, diorites and granitic rocks coeval with the Volcanosedimentary Complex (Fig. 1.8; Simancas, 1983; Barrie et al. 2002; Dunning et al. 2002; de la Rosa and Castro, 2004).

Following the transtensional and magmatic event, the orogenic shortening was resumed originating south-vergent folds and thrusts that typify the deformation of the entire SPZ. As imaged in the IBERSEIS deep seismic reflection profile (Fig. 1.6c; Simancas et al., 2003), the Carboniferous deformation that characterizes the whole SPZ constitutes a south-vergent fold-and-thrust belt detached at a mid-crustal level. Deformation migrated southwards from the northern border of the SPZ to the southernmost SPZ, being heralded by flysch deposits that start in the late Visean at the northern Iberian Pyrite unit and are progressively younger southwards, ending in the Moscovian at the SW corner of the SPZ (Oliveira, 1990). Metamorphism is of low- to very low-grade in the SPZ (Munhá, 1979; Simancas, 1983; Abad et al., 2001, 2004).
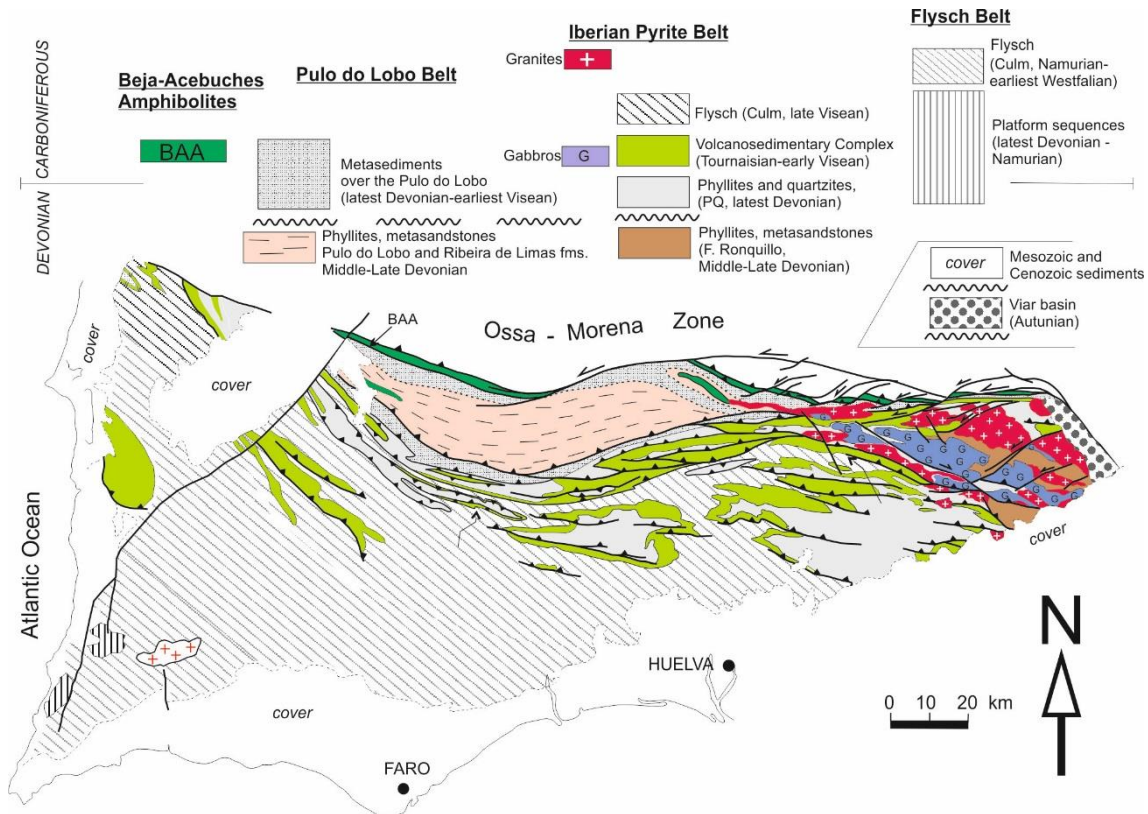
Figure 1.8. Geological map of the South Portuguese Zone with the three units distinguished (Pulo do Lobo, Iberian Pyrite and Flysch). Modified from Simancas, 2004.

A Pennsyvanian brittle strike-slip fault system stands out on the geological map of the OMZ/SPZ boundary, penetrating the easternmost SPZ (Figs. 1.7 and 1.8; Simancas, 1983; Quesada, 1991; Crespo-Blanc, 1992). E-W to NE-SW trending left-lateral faults largely dominate the fault system. The development of this brittle strike-slip shear zone around the OMZ/SPZ boundary might have been coeval with the latest deformation at the southwesternmost SPZ (the Carrapateira thrust; Silva et al., 1990).

3.5. The boundary between the Ossa-Morena and South Portuguese Zones

This boundary has been traditionally interpreted as the main Variscan suture, constituted by the remnant of the closure of the Rheic Ocean and the subsequent collision of the Avalonian border of Laurussia (represented by the SPZ) with the complex border of northern Gondwana (represented by the OMZ) (e.g. Crespo-Blanc and Orozco, 1988; Fonseca and Ribeiro, 1993; Fonseca et al., 1999; Simancas et al., 2003; Aráujo et al., 2005). This interpretation has been sustained by the presence of three units with oceanic and/or high-pressure rocks, namely the allochthonous Cubito-Moura unit (located above the Évora-Aracena Domain in the southwest OMZ), the Beja-Acebuches Amphibolites (BAA) unit (located along the OMZ/SPZ boundary itself), and the Pulo do Lobo unit (located just to the south of the BAA unit, and representing the northernmost unit of the SPZ) (Fig. 1.9). At the OMZ/SPZ boundary a remarkable ductile shear zone (the Southern Iberian

Shear Zone) has been interpreted as related to the emplacement of the BAA ophiolite-like unit (Crespo-Blanc and Orozco, 1988; Quesada et al., 1994; Díaz-Azpiroz and Fernández, 2005). The three mentioned unit are introduced below, keeping in mind that the BAA unit and the Pulo do Lobo units will be described in depth in the following chapters of this Thesis.

3.5.1. The Cubito-Moura unit

The Cubito-Moura unit tectonically overlies the low-grade Portel-Fuenteheridos unit or the HT-LP domes of the Évora-Aracena domain (Figs. 1.7 and 1.9). It is mainly constituted by micaschists, though at some places includes tectonic intercalations of different rock-types, such as MORB-featured metabasites, eclogitic metabasites, marbles, gneisses and black schists. All of these rock types, except the MORB-type metabasites, can be correlated with less deformed and metamorphosed lithologies of the Ediacaran and Early Paleozoic formations of the autochthonous OMZ. Thus, this unit was considered as an allochthonous complex constituted by the scraped off-cover of the OMZ continental margin, with some small fragments of oceanic crust (Fonseca et al., 1999; Araújo et al., 2005; Ribeiro et al., 2010). Regarding the MORB-featured metabasites, the only available protolith age is Ordovician (six zircon grains dated by U/Pb at ≈480 Ma; Pedro et al., 2010), thus being compatible with a Rheic Ocean attribution.

The metamorphic evolution of the Cubito-Moura unit has been established drawing on the eclogite and blueschist facies assemblages preserved in metabasites, as well as from PT calculations performed on the metapelitic assemblages. Thus, the eclogitic assemblages led Fonseca et al. (1999) to propose peak conditions of ≈16 kbar and 650 °C. The blueschist assemblages have yielded conditions of 11-12 kbar and 300-450 °C (Fonseca et al., 1999; Rubio Pascual et al., 2013). In the metapelites, chlorite - white K-mica - quartz ± chloritoid multi-equilibrium calculations yielded peak pressure conditions in the range 9-12 kbar at temperatures of 300-400 °C (Booth Rea et al., 2006; Ponce et al., 2012). All of these data show a high-pressure and intermediate- to low-temperature metamorphic event in the Cubito-Moura unit, which attests an early collisional stage (see below) that has been tentatively attributed to the Late Devonian (371 ± 17 Ma; Moita et al., 2005).

In the Cubito-Moura unit, the first deformational event recognized in metapelites is represented by a fabric characterized by stretching/mineral lineation (L1) and foliation (S1), which would have been formed during the early exhumation of the HP-LT rocks. L1 is well preserved only in early metamorphic quartz veins, while S1 is a relict microstructure in the metapelites (Booth-Rea et al., 2006; Ponce et al., 2012). The restored trend of L1 after unfoldig later folds is ≈N70ºE (Ponce et al., 2012). Quartz microfabric points to top-to-the-east movement, thus attesting an oblique left-lateral collisional scenario in SW Iberia since the very beginning of the Variscan orogeny. A top-to-the-north kinematics has been described in some metabasites of the Cubito-Moura unit (Araújo et al., 2005) and it has been interpreted as representing an Early Carboniferous extensional event (Rosas et al., 2008). A second deformational event produced a very penetrative crenulation cleavage (S2) that transposes the previous S1, without associated stretching or mineral lineation. Mesoscopic folds of this second deformation trend around N135ºE. Later penetrative

deformation gave way to upright folds, sometimes with axial-plane crenulation foliation (S3).
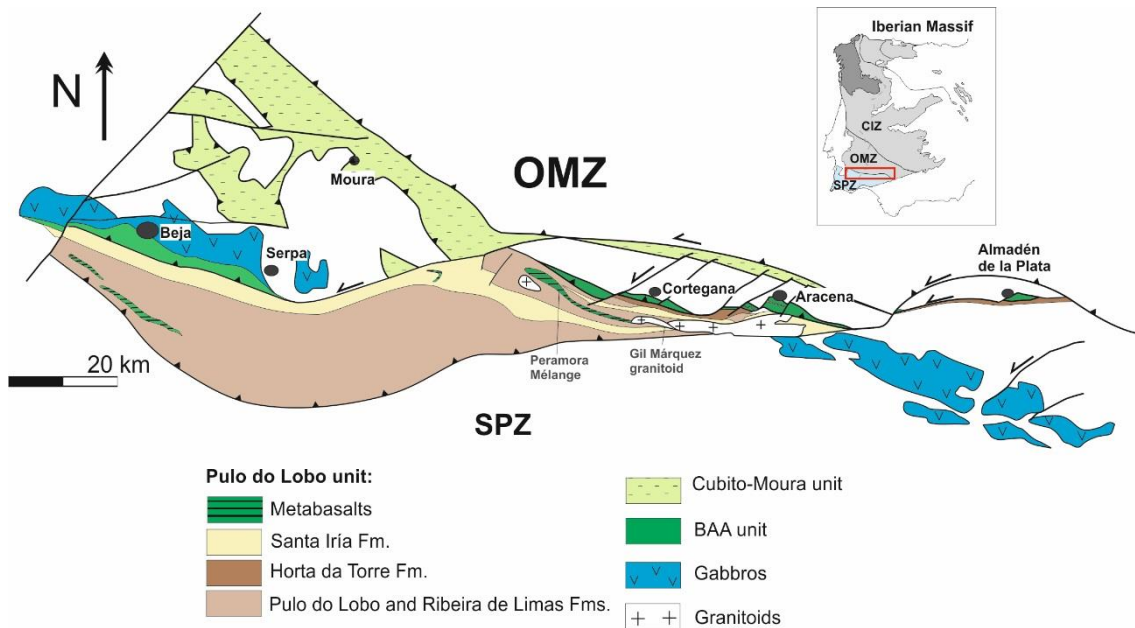
Figure 1.9. Map with the main units related to the boundary between the Ossa-Morena Zone (OMZ) and the South Portuguese Zone (SPZ): Pulo do Lobo, Cubito-Moura and Beja-Acebuches Amphibolites. Location of the map is shown in the inset of the Iberian Massif.

3.5.2. The Beja-Acebuches Amphibolite unit

The BAA unit crops out as a 0.5-3.5 km-wide strip of metamafic rocks (from greenschists to metagabbros, locally ultramafic rocks), continuous along the OMZ/SPZ boundary (Fig. 1.9; Bard, 1977; Fonseca and Ribeiro, 1993; Quesada et al., 1994; Castro et al., 1996). SHRIMP U-Pb zircon ages from MORB-featured rocks of this unit range from 332 to 340 Ma, having been interpreted as corresponding to the crystallization of the mafic protoliths (Azor et al., 2008 and 2009). A first and direct implication of these early Carboniferous ages is that the BAA unit can no longer be viewed as an ophiolite belonging to the Rheic Ocean suture, since this oceanic domain was presumably closed in Devonian times. Accordingly, the preferred interpretation for the BAA unit is that it represents a narrow and very ephemeral realm of oceanic-like crust that opened in early Carboniferous times, after total consumption of the Rheic Ocean. On the contrary, Murphy et al. (2016) have suggested that the Ocean Rheic lithosphere might have survived until Early Carboniferous times in SW Iberia due to the existence of an oceanic re-entrant along the Gondwana margin. It must be stressed however that the presence of collisional structures of Devonian age in the Cubito-Moura unit can be argued to undermine this hypothesis. Furthermore, the palynological content of Upper Devonian and Lower Carboniferous sediments at both sides of the BAA unit is similar (Pereira et al., 2006), thus suggesting that the OMZ and SPZ were already welded in Late Devonian time.

The ages reported for the BAA metamafic protoliths are slightly younger or virtually coincident with other published ages of mafic, intermediate and felsic rocks outcropping close to the OMZ/SPZ boundary and in the interior of the OMZ (e.g. Romeo et al., 2006; Jesus et al., 2007; Ordóñez-Casado et al., 2008; Pin et al., 2008; Gladney et al., 2014; Cambeses, 2015; Pereira et al., 2015b), highlighting the importance of the early Carboniferous magmatic event in SW Iberia.

3.5.3. The Pulo do Lobo unit

The Pulo do Lobo unit is made up of four metasedimentary formations affected by very low- to low-grade metamorphism (Figs. 1.8 and 1.9). The lowermost formation (Pulo do Lobo formation) is constituted by phyllites with abundant quartz veins. Upwards, the Ribeira de Limas Formation is constituted by quartz-sandstone and phyllite alternances. These two lower formations are Givetian-Frasnian in age (Pereira et al., 2008). The Santa Iría formation unconformably overlyies the lower formations, being constituted by slates and greywackes. The Horta da Torre formation is constituted by phyllites alternating with thick quartzite beds, and crops out sandwiched in-between late faults along a narrow band just south of the BAA unit. The Santa Iría and Horta da Torre formations are latest Devonian-early Carboniferous in age (Pereira et al., 2008). Regarding the paleogeographic affinity of the Pulo do Lobo unit, Braid et al. (2012) provided with inherited detrital zircon age populations that led them to propose that it could have been part of Avalonia.

The Pulo do Lobo unit has undergone a complex polyphasic deformation already recognized by previous authors (e.g. Crespo-Blanc, 1991; Silva el al., 1990; Fonseca, 2005). Some descriptions of the Pulo do Lobo macrostructure have considered a simple antiformal structure (Oliveira et al., 1986; Onézime et al., 2002). This unit has also been interpreted as an imbricated tectonic mélange (Eden and Andrews, 1990; Eden, 1991; Onézime et al., 2002, 2003; Braid et al., 2010). Finally, Martínez Poza et al. (2012), based on detailed structural observations, performed two long cross-sections through the Pulo do Lobo unit in the Spanish sector; this work has served as the starting point of the structural study of the Pulo do Lobo in is Thesis.

Imbricated with the Pulo do Lobo rocks, some metric intercalations of N-MORB greenschists have been described cropping out in the core of a late antiform (Los Ciries antiform; Apalategui et al., 1983), namely the Peramora Mélange (Munhá, 1983; Giese and Bühn, 1993; Dahn et al., 2014). Similar mafic rocks have been mapped on other sectors of the Pulo do Lobo unit, as the Alájar Mélange beween Aracena and Cortegana (Eden, 1991; Dahn et al., 2014) and the Trindade metabasalts in the surroundings of Trindade village to the south of Beja (Oliveira and Pereira, 1992). The Peramora and Alájar mélanges contain decimetric- to metric-scale grey quartzite lenses and greenschist phacoids imbricated in a pelitic or greenish matrix (Eden, 1991; Eden and Andrews, 1990). Braid et al. (2011) and Dahn et al. (2014) have reported diverse geochemical and geochronological data of these mélanges. The interpretation usually given to these imbrications is that they belonged to an accretionary prism related to the closure of the Rheic Ocean (e.g. Eden and Andrews, 1990; Braid et al., 2010; Dahn et al., 2014).

4. Aims and structure of thePh. D. Thesis

Detrital zircon content in metasedimentary rocks has become an important tool to decipher paleogeographic/paleotectonic scenarios. In the case of the Caledonian-Variscan-Appalachian terranes, several issues concerning their paleogeographic location are subject to intense research and debate. Thus, a first target of this Thesis has been to obtain a good number of detrital zircon age data in order to reevaluate the paleogeographical attribution of the SPZ (Avalonian affinity) and the Ediacaran to Early Paleozoic paleotectonic evolution of the whole SW Iberian Variscides (chapter 2).

The previous dating of the protoliths of the Beja Acebuches Amphibolites as early Carboniferous (Azor et al., 2008 and 2009), means that the interpretation of the OMZ/SPZ boundary as the Rheic suture needs to be reconsidered. Thus, to better constrain the knowledge of this boundary, the second aim of this Thesis has been the structural analysis of the Beja-Acebuches Amphibolite and the Pulo do Lobo units, as well as the dating of key lithologies, such as the MORB-featured metabasalts imbricated in the Pulo do Lobo unit (chapter 3).

Besides the structural analysis, the knowledge of the very low- to low-grade metamorphism of the Pulo do Lobo unit has been studied with the idea of better characterize its metamorphic evolution, and to check the feasibility of usually accepted interpretations of this unit as a subduction-related accretionary prism (chapter 4).

Finally, the last aim of this Thesis was to integrate the available data on the evolution of SW Iberia in appropriate geometric and kinematic models which lead to estimate the significant left-lateral displacements during the Variscan collision in this region of the Variscides (chapter 5).

Chapter 6 underlines the main conclusions obtained in this Thesis.

Complementary material is included as appendix.

5. Methodologies

In order to achieve the aims of this Thesis referred above, in addition to detailed structural work (field cartography and microstructural analysis), a number of laboratory techniques have been used:

- Massive U/Pb zircon dating of detrital zircons has been performed with the SHRIMP at the Ibersims laboratory (Universidad de Granada).

- U/Pb zircon dating of igneous protoliths was also done with the SHRIMP at the Ibersims laboratory of the Universidad de Granada.

- Geothermobarometry of metapelites has been performed through: (i) X-Ray diffraction on powdered samples, at the Departamento de Mineralogía y Petrología of the Universidad de Granada; (ii) EPMA chemical maps on thin sections of samples, at the Institut des Sciences de la Terre in Grenoble; and (iii) Raman spectrometry on carbonaceous matter on

thin sections of samples, at the Institut de Mineralogie et de Physique des Milieux Condenses in Paris.

References

Abad, I., Mata, M.P., Nieto, F., Velilla, N., 2001. The phyllosilicates in diagenetic-metamorphic rocks of the South Portuguese Zone, southwestern Portugal. The Canadian Mineralogist 39(6), 1571-1589.

Abad, I., Nieto, F., Velilla, N., Simancas, J.F., 2004. La Zona Sudportuguesa. Metamorfismo. In: Vera, J.A. (ed.), Geología de España. SGE-IGME, Madrid, 209-211.

Abalos, B., Gil Ibarguchi, J.I., Eguiluz, L., 1991. Cadomian subduction/collision and Variscan transpression in the Badajoz-Córdoba shear belt, southwest Spain. Tectonophysics 199, 51-72.

Abalos, B., 2001. Nuevos datos microestructurales sobre la existencia de deformaciones precámbricas en la Sierra de la Demanda (Cordillera Ibérica). Geogaceta 30, 3-6.

Abalos, B., Carreras, J., Druguet, E., Escuder Viruete, J., Gómez Pugnaire, M.T., Álvarez, S.L., Quesada, C., Rodríguez Fernández, L.R., Gil Ibarguchi, J.I., 2002. Variscan and Pre-Variscan Tectonics. In: Gibbons, W., Moreno, M.T. (eds.), The Geology of Spain. Geological Society, London, 155-183.

Abati, J., Gerdes, A., Fernández-Suárez, J., Arenas, R., Whitehouse, M.J., Díez Fernández, R., 2010. Magmatism and early-Variscan continental subduction in the northern Gondwana margin recorded in zircons from the basal units of Galicia, NW Spain. Geological Society of America Bulletin 122, (1-2), 219-235. doi: 10.1130/b26572.1.

Apalategui, O., Barranco, E., Contreras, F., Delgado, M., Roldán, F.J., 1983. Hoja 916, Aroche, Mapa Geológico de España a escala 1:50000, Inst. Geológico y Minero de España, Madrid.

Apraiz, A., Eguiluz, L., 2002. Hercynian tectono-thermal evolution associated with crustal extension and exhumation of the Lora del Río metamorphic core complex (Ossa-Morena zone, Iberian Massif, SW Spain). Interational Journal of Earth Sciences 91, 76–92. doi: 10.1007/s005310100206.

Araújo, A., Fonseca, P., Munhá, J., Moita, P., Pedro, J., Ribeiro, A., 2005. The Moura Phyllonitic Complex: An accretionary complex related with obduction in the southern Iberia Variscan suture. Geodinamica Acta 18, 375-388.

Arche, A., López-Gómez, J., 1996. Origin of the Permian-Triassic Iberian Basin, central-eastern Spain. Tectonophysics 266, 443-464.

Arenas, R., 1984. Características y significado del volcanismo ordovícico-silúrico de la serie autóctona envolvente del Macizo de Cabo Ortegal (Galicia, NW España). Revista Materiales Procesos Geológicos 11, 135-144.

Arenas, R., Díez Fernández, R., Rubio Pascual, F.J., Sánchez Martínez, S., Martín Parra, L.M., Matas, J., González del Tánago, J., Jiménez-Díaz, A., Fuenlabrada, J.M., Andonaegui, P., Garcia-Casco, A., 2016a. The Galicia–Ossa-Morena Zone: Proposal for a new zone of the Iberian Massif. Variscan implications. Tectonophysics 681, 135-143. doi: 10.1016/j.tecto.2016.02.030.

Arenas, R., Sánchez Martínez, S., Díez Fernández, R., Gerdes, A., Abati, J., Fernández-Suárez, J., Andonaegui, P., González Cuadra, P, López Carmona, A., Albert, R., Fuenlabrada, J.M., Rubio Pascual, F.J., 2016b. Allochthonous terranes involved in the Variscan suture of NW Iberia: A review of their origin and tectonothermal evolution. Earth-Science Reviews 161, 140-178. doi: 10.1016/j.earscirev.2016.08.010.

Armendáriz, M., López-Guijarro R., Quesada C., Pin C., Bellido, F., 2008. Genesis and evolution of a syn-orogenic basin in transpression: Insights from petrography, geochemistry and Sm–Nd systematics in the Variscan Pedroches basin (Mississippian, SW Iberia). Tectonophysics 461, 395-413.

Azor, A., González Lodeiro, F., Simancas, J.F., 1993. Cadomian subduction/collision and Variscan transpression in the Badajoz-Córdoba Shear Belt, southwest Spain: a discussion on the age of the main tectonometamorphic events. Tectonophysics 217, 343-346.

Azor, A., González Lodeiro, F., Simancas, J.F., 1994a. Tectonic evolution of the boundary between the Central Iberian and Ossa-Morena zones (Variscan belt, southwest Spain). Tectonics 13, 45-61.

Azor, A., González Lodeiro, F., Martínez Poyatos, D., Simancas, J.F., 1994b. Regional significance of kilometric-scale NE-vergent recumbent folds associated with E- to SE-directed shear on the southern border of the Central Iberian Zone (Hornachos-Oliva region, Variscan belt, Iberian Peninsula). Geologische Rundschau 83, 377-387.

Azor, A., Simancas, J.F., Expósito, I., Gonzalez Lodeiro, F., Martínez Poyatos, D., 1997. Deformation of garnets in a low-grade shear zone. Journal of Structural Geology 19, 1137-1148.

Azor, A., Expósito, I., Gonzalez Lodeiro, F., Simancas, J.F., Martínez Poyatos, D., 2004. Zona de Ossa-Morena. Estructura y metamorfismo. In: Vera, J.A. (Ed.), Geología de España, SGE-IGME, Madrid, 173-189.

Azor, A., Rubatto, D., Simancas, J.F., González Lodeiro, F., Martínez Poyatos, D., Martín Parra, L.M., Matas, J., 2008. Rheic Ocean ophiolitic remnants in Southern Iberia questioned by SHRIMP U-Pb zircon ages on the Beja-Acebuches amphibolites. Tectonics, 27, TC5014, doi: 10.1029/2009TC002527.

Azor, A., Rubatto, D., Marchesi, C., Simancas, J.F., González Lodeiro, F., Martínez Poyatos, D., Martín Parra, L.M., Matas, J., 2009. Reply to comment by C. Pin and J. Rodríguez on "Rheic Ocean ophiolitic remnants in southern Iberia questioned by SHRIMP U-Pb zircon ages on the Beja-Acebuches amphibolites". Tectonics 28(5), TC5014. doi: 10.1029/2009TC002527.

Bandrés, A., Eguiluz, L., Pin, C., Paquette, J.L., Ordóñez-Casado, B., Le Fèvre, B., Ortega, L.A., Gil Ibaguchi, J.I., 2004. The northern Ossa-Morena Cadomian batholith (Iberian Massif): magmatic arc origin and early evolution. International Journal of Earth Sciences 93, 860-885.

Barbero, L., 1995. Granulite-facies metamorphism in the Anatectic Complex of Toledo, Spain: late Hercynian tectonic evolution by crustal extension. Journal of the Geological Society 152(2), 365-382.

Barbero, L., Villaseca, C., 2000. Eclogite facies relics in metabasites Sierra de Guadarrama (Spanish Central System): PT estimations and implications for from the the Hercynian evolution. Mineralogical Magazine 64(5), 815-836.

Bard, J.P., 1977. Signification tectonique des métatholeites d'affinité abyssale de la ceinture de basse pression d'Aracena (Huelva, Espagne). Bulletin de la Société géologique de France 19, 385-393.

Barrie, C.T., Amelin, Y., Pascual, E., 2002. U-Pb Geochronology of VMS mineralization in Iberian Pyrite Belt. Mineralium Deposita 37, 684-703.

Bea, F., 2004. La naturaleza del magmatismo de la Zona Centroibérica: consideraciones generales y ensayo de correlación. In: Vera, J.A. (ed.), Geología de España. SGE-IGME, Madrid, 199-201.

Blatrix, P., Burg, J.P., 1981. $^{40}Ar/^{39}Ar$ dates from the Sierra Morena (Southern Spain): Variscan metamorphism and Cadomian orogeny. Neues Jahrbuch für Mineralogie–Monatshefte 10, 470-478.

Booth-Rea, G., Simancas, J.F., Azor, A., Azañón, J.M., Gonzalez Lodeiro, F., Fonseca, P., 2006. HP-LT Variscan metamorphism in the Cubito-Moura schists (Ossa-Morena Zone, southern Iberia). Comptes Rendus Geoscience 338(16), 1260-1267.

Braid, J.A., Murphy J.B., Quesada, C., 2010. Structural analysis of an accretionary prism in a continental collisional setting, the Late Paleozoic Pulo do Lobo Zone, Southern Iberia. Gondwana Research, 17(2-3), 422-439.

Braid, J.A., Murphy, J.B., Quesada, C., Mortensen, J., 2011. Tectonic escape of a crustal fragment during the closure of the Rheic Ocean: U-Pb detrital zircon data from the Late Palaeozoic Pulo do Lobo and South Portuguese zones, southern Iberia. Journal of the Geological Society of London 168, 383-392. doi: 10.1144/0016-76492010-104.

Braid, J.A., Murphy, J.B., Quesada, C., Bickerton, L., Mortensen, J., 2012. Probing the composition of unexposed basement, South Portuguese Zone, southern Iberia: implications for the connections between the Appalachian and Variscan orogens. Canadian Journal of Earth Sciences 49, 591-613. doi: 10.1139/E11-071.

Brun, J.P., Burg, J.P., 1982. Combined thrusting and wrenching in the Ibero-Armorican arc: a corner effect during continental collision. Earth and Planetary Science Letters 61, 319-332.

Burg, J.P., Iglesias, M., Laurent, P., Matte, P., Ribeiro, A., 1981. Variscan intracontinental deformation: The Coimbra-Córdoba Shear zone (SW Iberian Peninsula). Tectonophysics 78, 161-177.

Cambeses, A., 2015. Ossa-Morena Zone Variscan "Calc-Alkaline" hybrid rocks: Interaction of mantle- and crustal-derived magmas as a result of intra-orogenic extension-related intraplating. Ph. D. Tesis, Universidad de Granada, 450 pp.

Carvalhosa, A., 1999. Carta geológica de Portugal: Notícia explicativa da Folha 36-C Arraiolos. Instituto Geológico e Mineiro, Lisboa, Portugal, scale 1:50000.

Castro, A., Fernández, C., De la Rosa, J.D., Moreno Ventas, I., Rogers, G., 1996. Significance of MORB-derived amphibolites from the Aracena metamorphic belt, southwest Spain. Journal of Petrology 37(2), 235-260.

Crespo-Blanc, A., 1991. Evolución geotectónica del contacto entre la zona de Ossa-Morena y la zona Surportuguesa en las sierras de Aracena y Aroche (Macizo Ibérico Meridional): Un contacto mayor en la cadena Hercínica Europea. Ph. D. Thesis, Universidad de Granada, 327 pp.

Crespo-Blanc, A., 1992. Structure and kinematics of a sinistral transpressive suture between the Ossa-Morena and the South Portuguese Zones, South Iberian Massif. Journal of the Geological Society, London, 149, 401-411.

Crespo-Blanc, A., Orozco, M., 1988. The southern Iberian shear zone: a major boundary in the Hercynian folded belt. Tectonophysics 148, 221-227.

Crowley, Q.G., Floyd, P.A., Winchester, J.A., Franke, W., Holland, J.G., 2000. Early Palaeozoic rift-related magmatism in Variscan Europe: fragmentation of the Armorican Terrane Assemblage. Terra Nova 12, 171-180.

Dahn, D.R.L., Braid, J.A., Murphy, J.B., Quesada, C., Dupuis, N., McFarlane, C.R.M., 2014. Geochemistry of the Peramora Melange and Pulo do Lobo schist: geochemical investigation and tectonic interpretation of mafic melange in the Pangean suture zone, Southern Iberia. International Journal of Earth Sciences 103, 1415-1431.

Dallmeyer, R.D., Quesada, C., 1992. Cadomian vs. Variscan evolution of the Ossa-Morena Zone (SW Iberia): field and ^{40}Ar/^{39}Ar mineral age constraints. Tectonophysics 216, 339-364.

De la Rosa, J.D., Castro, A., 2004. Magmatismo de la Zona Sudportuguesa. In: Vera, J.A. (ed.) Geología de España. SGE-IGME, Madrid, 215-222.

Díaz Azpiroz, M., Fernández, C., 2005. Kinematic analysis of the southern Iberian shear zone and tectonic evolution of the Acebuches metabasites (SW Variscan Iberian Massif). Tectonics 24, TC3010. doi: 10.1029/2004TC001682.

Díaz Azpiroz, M., Castro, A., Fernández, C., López, S., Fernández Caliani, J.C., Moreno-Ventas, I., 2004. The contact between the Ossa-Morena and the South Portuguese zones: Characteristics and significance of the Aracena metamorphic belt, in its central sector between Aroche and Aracena (Huelva). Journal of Iberian Geology 30, 23-51.

Díaz García, F., 2006. Geometry and regional significance of Neoproterozoic (Cadomian) structures of the Narcea Antiform, NW Spain. Journal of the Geological Society, London, 163, 499-508.

Díez Fernández, R., Arenas, R., 2015. The Late Devonian Variscan suture of the Iberian Massif: A correlation of high-pressure belts in NW and SW Iberia. Tectonophysics 654, 96-100. doi: 10.1016/j.tecto.2015.05.001.

Díez Fernández, R., Arenas, R., 2016. Reply to Comment on "The Late Devonian Variscan suture of the Iberian Massif: A correlation of high-pressure belts in NW and SW Iberia". Tectonophysics 670, 155-160. doi: 10.1016/j.tecto.2015.11.033.

Díez Fernández, R., Martínez Catalán, J.R., Gerdes, A., Abati, J., Arenas, R., Fernández-Suárez, J., 2010. U-Pb ages of detrital zircons from the Basal allochthonous units of NW Iberia: Provenance and paleoposition on the northern margin of Gondwana during the Neoproterozoic and Paleozoic. Gondwana Research 18, 385-399. doi: 10.1016/j.gr.2009.12.006.

Díez Fernández, R., Arenas, R., Pereira, F.M., Sánchez Martínez, S., Albert, R., Martín Parra, L.M., Rubio Pascual, F.J., Matas, J., 2016. Tectonic evolution of Variscan Iberia: Gondwana-Laurussia collision revisited. Earth Science Reviews 162, 269-292. doi: 10.1016/j.earscirev.2016.08.002.

Dinis, P., Andersen, T., Machado, G., Guimaraes, F., 2012. Detrital zircon U-Pb ages of a late-Variscan Carboniferous succession associated with the Porto-Tomar shear zone (West

Portugal): Provenance implications. Sedimentary Geology 273-274, 19-29. doi: 10.1016/j.sedgeo.2012.06.007.

Dunning, G.R., Díez Montes, A., Matas, J., Martín Parra, L.M., Almarza, J., Donaire M., 2002. Geocronología U/Pb del volcanismo ácido y granitoides de la Faja Pirítica Ibérica (Zona Surportuguesa). Geogaceta 32, 127-130.

Eden, C.P., 1991. Tectonostratigraphic analysis of the northern extent of the oceanic exotic terrane, Northwestern Huelva Province, Spain. Ph. D. Thesis, University of Southhampton, 214 pp.

Eden, C.P., Andrews, J.R., 1990. Middle to Upper Devonian mélanges in SW Spain and their relationship to the Meneage Formation in south Cornwall. Proceedings Ussher Society 7, 217-222.

Eguiluz, L., 1987. Petrogénesis de rocas ígneas y metamórficas en el antiforme de Burguillos Monesterio. Macizo Ibérico. PhD Thesis, University of País Vasco, 456pp.

Eguiluz, L., Gil Ibarguchi, J.I., Ábalos, B., Apraiz, A., 2000. Superposed Hercynian and Cadomian orogenic cycles in the Ossa-Morena zone and related areas of the Iberian Massif. Geological Society of America Bulletin 112, 1398-1413.

Expósito, I., 2000. Evolución estructural de la mitad septentrional de la Zona de Ossa-Morena y su relación con el límite Zona de Ossa Morena/Zona Centroibérica. Ph. D. Thesis, Universidad de Granada, 296 pp.

Expósito, I., Simancas, J.F., González Lodeiro, F., Azor, A., Martínez Poyatos, D., 2002. Estructura de la mitad septentrional de la zona de Ossa-Morena: Deformación en el bloque inferior de un cabalgamiento cortical de evolución compleja. Revista de la Sociedad Geológica de España 15, 3-14.

Farias, P., Gallastegui, G., González Lodeiro, F., Marquínez, J., Martín Parra, L.M., Martínez Catalán, J.R., de Pablo Maciá, J.G., Rodríguez Fernández, L.R., 1987. Aportaciones al conocimiento de la litoestratigrafía y estructura de Galicia Central. Memórias da Faculdade de Ciências da Universidade do Porto 1, 411-431.

Fernández, L.P., Bahamonde, J.R., Barba, P., Colmenero, J.R., Heredia, N., Rodríguez-Fernández, L.R., Salvador, C., Sánchez de Posada, L.C., Villa, E., Merino-Tomé, O., Motis, K., 2004. Zona Cantábrica. Estratigrafía. Secuencia sinorogénica. In: Vera, J.A. (Ed.), Geología de España, SGE-IGME, Madrid, 34-42.

Fernández-Lozano, J., Pastor-Galán, D., Gutiérrez-Alonso, G., Franco, P., 2016. New kinematic constraints on the Cantabrian orocline: A paleomagnetic study from the Peñalba and Truchas synclines, NW Spain. Tectonophysics 681, 195-208. doi: 10.1016/j.tecto.2016.02.019.

Fernández-Suárez, J., Gutiérrez-Alonso, G., Jenner, G.A., Jackson, S.E., 1998. Geochronology and geochemistry of the Pola de Allande granitoids (northern Spain): their bearing on the Cadomian-Avalonian evolution of northwest Iberia. Canadian Journal of Earth Sciences 35,1-15.

Fonseca, P., 2005. O terreno acrecionário do Pulo do Lobo: implicaçoes geodinâmicas da sutura com a Zona de Ossa-Morena (SW da Cadeia Varisca Ibérica). Cadernos do Laboratorio Xeolóxico de Laxe 30, 213-222.

Fonseca, P., Ribeiro, A., 1993. Tectonics of the Beja-Acebuches ophiolite - a major suture in the Iberian Variscan foldbelt. Geologische Rundschau 82, 440-447.

Fonseca, P., Munhá, J., Pedro, J., Rosas, F., Moita, P., Araujo, A., Leal, N., 1999. Variscan ophiolites and high-pressure metamorphism in southern Iberia. Ofioliti, 24, 259-268.

Franke, W., 2000. The mid-European segment of the Variscides: tectonostratigraphic units, terrane boundaries and plate tectonic evolution. Geological Society, London, Special Publications, 179, 35-61.

Franke, W., 2014. Topography of the Variscan orogen in Europe: failed-not collapsed. International Journal of Earth Sciences 103, 1471-1499. doi: 10.1007/s00531-014-1014-9.

Fuenlabrada, J.M., Pieren, A.P., Díez Fernández, R., Sánchez Martínez, S., Arenas, R., 2016. Geochemistry of the Ediacaran-Early Cambrian transition in Central Iberia : Tectonic setting and isotopic sources. Tectonophysics 681, 15-30. doi: 10.1016/j.tecto.2015.11.013.

Gabaldón, V., Garrote, A., Quesada, C., 1985. Geología del Carbonífero Inferior del Norte de la Zona de Ossa-Morena. Introducción a la excursión. Temas Geológico-Mineros, IGME, 101-137.

Giese, U., Bühn, B., 1993. Early Paleozoic rifting and bimodal volcanism in the Ossa-Morena Zone of south-west Spain. Geologische Rundschau 83, 143-160.

Gladney, E.R., Braid J.A., Murphy J.B., Quesada C., McFarlane, C.R.M., 2014. U-Pb geochronology and petrology of the late Paleozoic Gil Marquez pluton: magmatism in the Variscan suture zone, southern Iberia, during continental collision and the amalgamation of Pangea, International Journal of Earth Sciences 103(5), 1433-1451.

Gómez-Pugnaire, M.T., Azor, A., Fernández Soler, J.M., López Sánchez-Vizcaíno, V., 2003. The amphibolites from the Ossa-Morena/Central Iberian Variscan suture (southwestern Iberian Massif): Geochemistry and tectonic interpretation. Lithos, 68(1), 23-42. doi: 10.1016/S0024-4937(03)00018-5.

González, F., Moreno, C., López, M.J., Dino, R., Antonioli, L., 2004. Palinoestratigrafía del Grupo Pizarroso-cuarcítico del sector más oriental de la Faja Pirítica Ibérica, SO de España. Revista Española de Micropaleontología 36, 279-304.

Gutiérrez-Alonso, G., 1995. Structure of the Internal-External Transition Zone in the northern Iberian Massif: implications for the interpretation of deep crustal seismic profiles. Revista de la Sociedad Geológica de España 8, 322-330.

Gutiérrez-Alonso, G., Fernández-Suárez, J., Weil, A.B., 2004. Orocline triggered lithospheric delamination. Geological Society of America, Special Paper 383, 121-130.

Gutiérrez-Alonso, G., Fernández-Suárez, J., Collins, A.S., Abad, I., Nieto, F., 2005. Amazon and Mesoproterozoic basement in the core of the Ibero-Armorican Arc: [40]Ar/[39]Ar detrital mica ages complement the zircon's tale. Geology 33, 637-640. doi: 10.1130/G21485.1.

Gutiérrez-Alonso, G., Fernández-Suárez, J., Jeffries, T.E., Johnston, S.T., Pastor-Galán, D., Murphy, B.J., Franco, M.P., Gonzalo, J.C., 2011. Diachronous post-orogenic magmatism within a developing orocline in Iberia, European Variscides. Tectonics 30, TC5008. doi: 10.1029/2010TC002845.

Henriques, S.B.A., Neiva, A.M.R., Ribeiro, M.L., Dunning, G.R., Tagcmanová, L., 2015. Evolution of a Neoproterozoic suture in the Iberian Massif, Central Portugal: New U-Pb ages of igneous and metamorphic events at the contact between the Ossa Morena Zone and Central Iberian Zone. Lithos 220-223, 43-59. doi: 10.1016/j.lithos.2015.02.001.

Hernández Enrile, J.L., 1991. Extensional tectonics of the Toledo ductile-brittle shear zone, central Iberian Massif. Tectonophysics 191, 311-324.

Jesus, A.P., Munhá, J., Mateus, A., Tassinari, C., Nutman, A.P., 2007. The Beja Layered Gabbroic Sequence (Ossa-Morena Zone, Southern Portugal): geochronology and geodynamic implications. Geodinamica Acta 20, 139-157. doi: 10.3166/ga.20.139-157.

Julivert, M., Fontboté, J.M., Ribeiro, A., Nabais-Conde, L.E., 1974. Mapa Tectónico de la Península Ibérica y Baleares escala 1:1.000.000. Inst. Geológico y Minero de España, Madrid, Memoria explicativa, 113.

Liñán, E., Quesada. C., 1990. Ossa-Morena Zone. Stratigraphy. Rift Phase (Cambrian). In: Dallmeyer, R.D., Martínez García, E. (eds.), Pre-Mesozoic Geology of Iberia. Springer Verlag, Berlin, 259-266.

Liñán, E., Gozalo, R., Palacios, T., Gámez Vintaned, J.A., Ugidos, J.M., Mayoral, E., 2002. Cambrian. In: Gibbons, W., Moreno, M.T. (eds.), The Geology of Spain. Geological Society, London, 17-29.

López Munguira, A., Nieto, F., Pardo, E.S., Velilla, N., 1991. The composition of phyllosilicates in Precambrian, low-grademetamorphic, clastic rocks from the Southern Hesperian Massif (Spain) used as an indicator to metamorphic conditions. Precambrian Research 53(3-4), 267-279.

López Sánchez-Vizcaíno, V., Gómez Pugnaire, M.T., Azor, A., Fernández Soler, J.M., 2003. Phase diagram sections applied to amphibolites: a case study from the Ossa-Morena/Central Iberian Variscan suture (Southwestern Iberian Massif). Lithos 68, 1-21.

Macaya, J., González Lodeiro, F., Martínez Catalán, J.R., Alvarez, F., 1991. Continuous deformation, ductile thrusting and backfolding of cover and basement in the Sierra de Guadarrama, Hercynian orogen of central Spain. Tectonophysics 191(3), 291-309. doi: 10.1016/0040-1951(91)90063-X.

Martín Parra, L.M., González Lodeiro, F., Martínez Poyatos, D., Matas, J., 2006. The Puente Génave-Castelo de Vide shear zone (southern Central Iberian Zone, Iberian Massif): geometry, kinematics and regional implications. Bulletin de la Société Géologique de France 177(4), 191-202. doi: 10.2113/gssgfbull.177.4.191.

Martínez Catalán, J.R., 1985. Estratigrafía y estructura del Domo de Lugo:(Sector Oeste de la Zona Asturoccidental-leonesa). Corpus Geol. Gallaeacie (2º Serie), 2, 1-291.

Martínez Catalán, J.R., Rodríguez, M.H., Alonso, P.V., Pérez-Estaún, A., González Lodeiro, F., 1992. Lower Paleozoic extensional tectonics in the limit between the West Asturian-Leonese and Central Iberian Zones of the Variscan fold-belt in NW Spain. Geologische Rundschau 81(2), 545-560.

Martínez Catalán, J.R., Arenas, R., Díaz García, F., Rubio Pascual, F.J., Abati, J., Marquínez, J., 1996. Variscan exhumation of a subducted Paleozoic continental margin: The basal units of the Ordenes Complex, Galicia, NW Spain. Tectonics 15, 106-121.

Martínez Catalán, J.R., Arenas, R., Díaz García, F., González Cuadra, P., Gómez Barreiro, J., Abati, J., Castiñeiras, P., Fernández-Suárez, J., Sánchez Martínez, S., Andonaegui, P., González Clavijo, E., Díez Montes, A., Rubio Pascual, F., Valle Aguado, B., 2007. Space and time in the tectonic evolution of the northwestern Iberian Massif: Implications for the Variscan belt. In: Hatcher Jr., R.D., Carlson, M.P., McBride, J.H., Martínez Catalán, J.R., (eds.), 4-D Framework of Continental Crust. Geological Society of America, Boulder, 403-423.

Martínez Catalán, J.R., Arenas, R., Abati, J., Sánchez Martínez, S., Díaz García, F., Fernández-Suárez, J., González Cuadra, P., Castiñeiras, P., Gómez Barreiro, J., Díez Montes, A., González Clavijo, E., Rubio Pascual, F.J., Andonaegui, P., Jeffries, T.E., Alcock, J.E., Díez Fernández, R., López Carmona, A., 2009. A rootless suture and the loss of the roots of a mountain chain: The Variscan belt of NW Iberia. Comptes Rendus Geoscience 341, 114-126. doi: 10.1016/j.crte.2008.11.004.

Martínez Catalán, J.R., Rubio Pascual, F.J., Díez Montes, A., Díez Fernández, R., Gómez Barreiro, J., Dias Da Silva, Í., González Clavijo, E., Ayarza, P., Alcock, J.E., 2014. The late Variscan HT/LP metamorphic event in NW and Central Iberia: relationships to crustal thickening, extension, orocline development and crustal evolution. Geological Society, London, Special Publications 405(1), 225-247.

Martínez Poyatos, D., 1997. Estructura del borde meridional de la Zona Centroibérica y su relación con el contacto entre las Zonas Centroibérica y de Ossa-Morena. Ph. D. Thesis, Universidad de Granada, 295 pp.

Martínez Poyatos, D., Azor, A., González Lodeiro, F., Simancas, J.F., 1995a. Timing of the Variscan structures on both sides of the Ossa Morena/Central Iberian contact (south-west Iberian Massif). Comptes Rendus de l'Académie des Sciences de Paris 321(II), 609-615.

Martínez Poyatos, D., Simancas, J.F., Azor, A., González Lodeiro, F., 1995b. La estructura del borde meridional de la Zona Centroibérica en sector suroriental de la provincia de Badajoz. Revista de la Sociedad Geológica de España 8, 41-50.

Martínez Poyatos, D., Simancas, J.F., Azor, A., González Lodeiro, F., 1998a. La estructura del borde meridional de la Zona Centroibérica (Macizo Ibérico) en el norte de la provincia de Córdoba. Revista de la Sociedad Geológica de España 11, 87-94.

Martínez Poyatos, D., Simancas, J.F., Azor, A., González Lodeiro, F., 1998b. Evolution of a Carboniferous piggyback basin in the southern Central Iberian Zone (Variscan Belt, SE Spain). Bulletin de la Société Géologique de France 169, 573-578.

Martínez Poyatos, D., Nieto, F., Azor, A., Simancas, J.F., 2001. Relationships between very low-grade metamorphism and tectonic deformation: Examples from the southern Central Iberian Zone (Iberian Massif, Variscan Belt). Journal of the Geological Society 158, 953-968. doi: 10.1144/0016-764900-206.

Martínez Poyatos, D., Carbonell, R., Palomeras, I., Simancas, J.F., Ayarza, P., Martí, D., Azor, A., Jabaloy, A., González Cuadra, P., Tejero, R., Martín Parra, L.M., Matas, J., González Lodeiro, F., Pérez-Estaún, A., García Lobón, J.L., Mansilla, L., 2012. Imaging the crustal structure of the Central Iberian Zone (Variscan Belt): The ALCUDIA deep seismic reflection transect. Tectonics 31, TC3017. doi: 10.1029/2011TC002995.

Martínez Poza, A.I., Martínez Poyatos D.J., Simancas J.F., Azor, A., 2012. La estructura varisca de la Unidad del Pulo do Lobo (SO del Macizo Ibérico) en las transversales de Aroche y Rosal de la Frontera (Huelva). Geogaceta 52, 21-24.

Matte, P., 1986. Tectonics and plate tectonics model for the Variscan belt of Europe. Tectonophysics 126, 329-374.

Matte, P., 1991. Accretionary history and crustal evolution of the Variscan Belt in western Europe. Tectonophysics 196, 309-339.

Matte, P., 2001. The Variscan collage and orogeny (480-290 Ma) and the tectonic definition of the Armorica microplate: A review. Terra Nova 13, 122-128.

Matte, P., Ribeiro, A., 1975. Forme et orientation de la virgation hercynienne de Galice. Relations avec le plissement et hypothèses sur la genèse de l'arc Ibero-Armoricaine. Comptes Rendus Seances Académie Sciences Paris, 280D, 2825-2828.

Moita, P., Munhá, J., Fonseca, P., Pedro, J., Araújo, A., Tassinari, C., Palacios, T., 2005. Phase equilibria and geochronology of Ossa-Morena eclogites. Actas do XIV Semana de Gequímica / VIII Congresso de geoquímica dos Países de Língua Portuguesa, 2, 471-474.

Montero, P., Bea, F., González-Lodeiro, F., Talavera, C., Whitehouse, M.J., 2007. Zircon ages of the metavolcanic rocks and metagranites of the Ollo de Sapo Domain in central Spain: implications for the Neoproterozoic to Early Palaeozoic evolution of Iberia. Geological Magazine London 144(6), 963.

Munhá, J., 1979. Blue Amphiboles, Metamorphic Regime and Plate Tectonic Modelling in the Iberian Pyrite Belt. Contributions to Mineralogy and Petrology 69, 279-289.

Munhá, J., 1983. Hercynian magmatism in the Iberian Pyrite Belt. In: Sousa, M.J.L., Oliveira, J.T. (Eds.), The Carboniferous of Portugal, Memorias Serviço Geológico de Portugal 29, 39-81.

Murphy, J.B., Eguiluz, L., Zulauf, G., 2002. Cadomian Orogens, peri-Gondwanan correlatives and Laurentia-Baltica connections. Tectonophysics 352, 1-9.

Murphy, J.B., Quesada, C., Gutiérrez-Alonso, G., Johnston, S.J., Weil, A., 2016. Reconciling competing models for the tectono-stratigraphic zonation of the Variscan orogen in Western Europe. Tectonophysics 681, 209-219.

Nance, R.D., Gutiérrez-Alonso, G., Keppie, J.D., Linnemann, U., Murphy, J.B., 2010. Evolution of the Rheic Ocean. Gondwana Research 17, 194-222.

Nance, R.D., Gutiérrez-Alonso, G., Keppie, J.D., Linnemann, U., Murphy, J.B., Quesada, C., Strachan, R.A., Woodcock, N.H., 2012. A brief history of the Rheic Ocean. Geoscience Frontiers 3,125-135. doi: 10.1016/j.gsf.2011.11.008.

Oliveira, J.T., 1990. The South Portuguese Zone. Stratigraphy and Synsedimentary Tectonism. In: Dallmeyer, R.D., Martínez García, E. (eds.), Pre-Mesozoic Geology of Iberia. Springer Verlag, Berlin, 334-347.

Oliveira, J.T., Pereira, E., 1992. Carta Geológica de Portugal, na escala de 1:500 000, Serviços Geológicos de Portugal.

Oliveira, J.T., Cunha, T.A., Streel, M., Vanguestaine, M., 1986. Dating the Horta da Torre Formation, a New Lithostratigraphic Unit of the Ferreira-Ficalho Group, South Portuguese Zone: geological consequences. Comun. Serv. Geol. Portugal 72, 129-135.

Oliveira, J.T., Relvas, J.M.R.S., Pereira, Z., Munhá, J., Matos, J.X., Barriga, F.J.A.S., Rosa, C.J., 2006. O Complexo Vulcano-Sedimentar de Toca da Moura-Cabrela (Zona de Ossa-Morena); Evoluçao tectono-estratigráfica e mineralizaçoes associadas. In: Días, R., Araújo, A., Terrinha, P., Kullberg, J.C. (Eds.), Geologia de Portugal no contexto da Iberia, Univ. Évora, Évora, 181-193.

Onézime, J., Charvet, J., Faure, M., Chauvet, A., Panis, D., 2002. Structural evolution of the southernmost segment of the West European Variscides: the South Portuguese Zone (SW Iberia). Journal of Structural Geology 24(3), 451-468.

Onézime, J., Charvet, J., Faure, M., Bourdier, J. L., Chauvet, A., 2003. A new geodynamic interpretation for the South Portuguese Zone (SW Iberia) and the Iberian Pyrite Belt genesis. Tectonics 22(4).

Ordóñez-Casado, B., 1998. Geochronological studies of the Pre-Mesozoic basement of the Iberian Massif: the Ossa-Morena Zone and the Allochthonous Complexes within the Central Iberian Zone. Ph.D. Thesis, ETH Zurich, 235 p.

Ordóñez-Casado, B., Martin-Izard, A., García-Nieto, J., 2008. SHRIMP-zircon U–Pb dating of the Ni–Cu–PGE mineralized Aguablanca gabbro and Santa Olalla granodiorite: Confirmation of an Early Carboniferous metallogenic epoch in the Variscan Massif of the Iberian Peninsula. Ore Geology Reviews 34, 343–353. doi: 10.1016/j.oregeorev.2008.03.002.

Ortega Gironés, E., González Lodeiro, F., 1986. La discordancia intra-Alcudiense en el dominio meridional de la Zona Centroibérica. Breviora Geológica Astúrica 27, 27-32.

Palero, F.J., 1993. Tectónica pre-hercínica de las series infraordovícicas del anticlinal de Alcudia y la discordancia intraprecámbrica en su parte oriental (sector meridional de la Zona Centroibérica). Boletín Geológio y Minero 104, 227-242.

Palomeras, I., Carbonell, R., Flecha, I., Simancas, J.F., Ayarza, P., Matas, J., Martínez Poyatos, D., Azor, A., González Lodeiro, F., Perez-Estaún, A., 2009. Nature of the lithosphere across the Variscan orogen of SW Iberia: Dense wide-angle seismic reflection data. Journal of Geophysical Research-Solid Earth, 114(B2).

Pastor-Galán, D., Groenewegen, T., Brouwer, D., Krijgsman, W., Dekkers, M.J., 2015. One or two oroclines in the Variscan orogen of Iberia? Implications for Pangea amalgamation. Geology 43(6), 527-530. doi: 10.1130/g36701.1.

Pedro, J., Araújo, A., Fonseca, P., Tassinari, C., Ribeiro, A., 2010. Geochemistry and U-Pb Zircon Age of the Internal Ossa-Morena Zone Ophiolite Sequences: A Remnant of Rheic Ocean in SW Iberia. Ofioliti, 35(2), 117-130.

Pereira, M.F., Chichorro, M., Linnemann, U., Eguiluz, L., Silva, J.B., 2006. Inherited arc signature in Ediacaran and Early Cambrian basins of the Ossa-Morena Zone (Iberian Massif, Portugal): Paleogeographic link with European and North African Cadomian correlatives. Precambrian Research 144, 297-315. doi: 10.1016/j.precamres.2005.11.011.

Pereira, M.F., Chichorro, M., Williams, I.S., Silva, J.B., Fernández, C., Díaz-Azpiroz, M., Aparaiz, A., Castro, C., 2009. Variscan intra-orogenic extensional tectonics in the Ossa-Morena Zone (Évora-Aracena-Lora del Río metamorphic belt, SW Iberian Massif): SHRIMP zircon U-Th-Pb geochronology. In: Murphy, J.B., Keppie, J.D., Hynes, A.J. (Eds.), Ancient Orogens and Modern Analogues. Geological Society, London, Special Publications 327, 215-237. doi: 10.1144/SP327.11.

Pereira, M.F., Apraiz, A., Chichorro, M., Silva, J.B., Armstrong, R.A., 2010. Exhumation of high pressure rocks in northern Gondwana during the Early Carboniferous (Coimbra-Cordoba shear zone, SW Iberian Massif): tectonothermal analysis and U-Th-Pb SHRIMP in-situ zircon geochronology. Gondwana Research 17, 440-460.

Pereira, M.F., Chichorro, M., Silva, J.B., Ordóñez-Casado, B., Lee J.K.W., Williams, I.S., 2012. Early carboniferous wrenching, exhumation of high-grade metamorphic rocks and basin instability in SW Iberia: Constraints derived from structural geology and U-Pb and $^{40}Ar/^{39}Ar$ geochronology. Tectonophysics 558, 28-44.

Pereira, M.F., Castro, A., Fernández, C., 2015a. The inception of a Paleotethyan magmatic arc in Iberia. Geoscience Frontiers 6, 297-306. doi: 10.1016/j.gsf.2014.02.006.

Pereira, M.F., Chichorro, M., Moita, P., Santos, J.F., Solá, A.M.R., Williams, I.S., Silva, J.B., Armstrong, R.A., 2015b. The multistage crystallization of zircon in calc‑alkalinegranitoids:

U–Pb age constraints on the timing of Variscantectonic activity in SW Iberia. International Journal of Earth Sciences 104, 1167–1183. doi: 10.1007/s00531-015-1149-3.

Pereira, Z., Piçarra, J.M., Oliveira, J.T., 1999. Lower Devonian Palynomorphs from the Barrancos region, Ossa-Morena Zone, Portugal. Bolletino della Società Paleontologica Italiana 38(2-3), 239-245.

Pereira, Z., Matos, J., Fernandes, P., Oliveira, J.T., 2008. Palynostratigraphy and systematic palynology of the Devonian and Carboniferous successions of the South Portuguese Zone, PORTUGAL. Memórias Geológicas do Instituto Nacional de Engenharia, Tecnologia e Inovaçao 34, Lisboa.

Pérez-Estaún, A., Pulgar, J., Álvarez-Marrón, J., ESCI-N Group, 1995. Crustal structure of the Cantabrian Zone: seismic image of a Variscan foreland thrust and fold belt (NW Spain). Revista de la Sociedad Geológica de España 8, 307-319.

Piçarra, J.M., 1998. First Devonian graptolites from Portugal. In: Gutiérrez-Marco, J.C., Rábano, I. (Eds.) Proceedings 6th International Graptolite Conference (GWG-IPA) & 1998 Field Meeting, IUGS Subcomission on Silurian Stratigraphy. Temas Geológico-Mineros ITGE, 23, 242-243.

Pin, C., Liñán, E., Pascual, E., Donaire, T., Valenzuela, A., 2002. Late Neoproterozoic crustal growth in the European Variscides: Nd isotope and geochemical evidence from the Sierra de Córdoba Andesites (Ossa-Morena Zone, Southern Spain). Tectonophysics 352, 133-151.

Pin, C., Fonseca, P.E., Paquette, J.L., Castro, P., Matte, P., 2008. The ca. 350 Ma Beja Igneous Complex: A record of transcurrent slab break-off in the Southern Iberia Variscan Belt? Tectonophysics 461(1-4), 356-377.

Ponce, C., Simancas, J.F., Azor, A., Martínez Poyatos, D.J., Booth-Rea, G., Expósito, I., 2012. Metamorphism and kinematics of the early deformation in the Variscan suture of SW Iberia. Journal of Metamorphic Geology 30(7), 625-638.

Quesada, C., 1990. Precambrian successions in SW Iberia: their relationship to Cadomian orogenic events. In: D'Lemos, R.S., Strachan, R.A., Topley, C.G. (Eds.), The Cadomian Orogeny. Special Publication of the Geological Society of London 51, 353-362.

Quesada, C., 1991. Geological constraints on the Paleozoic tectonic evolution of tectonostratigraphic terranes in the Iberian Massif. Tectonophysics 185, 225-245.

Quesada, C., Dallmeyer, R.D., 1994. Tectonothermal evolutionof the Badajoz-Córdoba shear zone (SW Iberia): characteristics and ^{40}Ar/^{39}Ar mineral age constraints. Tectonophysics 231, 195-213.

Quesada, C., Fonseca, P.E., Munhá, J., Oliveira, J.T., Ribeiro, A., 1994. The Beja-Acebuches Ophiolite (Southern Iberia Variscan fold belt): geological characterization and significance. Boletín Geológico Minero 105, 3-49.

Ribeiro, A., Quesada, C., Dallmeyer, R.D., 1990. Geodynamic evolution of the Iberian Massif. In: Dallmeyer, R.D., Martínez García, E. (Eds.), Pre-Mesozoic Geology of Iberia. Springer Berlin Heidelberg, 399-409.

Ribeiro, A., Dias R., Silva, B., 1995. Genesis of the Ibero-Armorican arc. Geodinamica Acta 8, 173-184.

Ribeiro, A., Munhá, J., Dias, R., Mateus, A., Pereira, E., Ribeiro, L., Fonseca, P., Araújo, A., Oliveira, T., Romao, J., Chaminé, H., Coke, C., Pedro, J., 2007. Geodynamic evolution of the SW Europe Variscides, Tectonics 26, TC6009.

Ribeiro, A., Munhá, J., Fonseca, P.E., Araujo, A., Pedro, J.C., Mateus, A., Tassinari, C., Machado, G., Jesus, A., 2010. Variscan ophiolite belts in the Ossa-Morena Zone (Southwest Iberia): Geological characterization and geodynamic significance. Gondwana Research 17(2-3), 408-421.

Rocha, R., Pereira, Z., Araújo, A., 2010. Novos dados bioestratigráficos (miosporos) na Formação de Terena- Implicações para a interpretação estrutural (Rio Ardila, Barrancos). VIII Congresso Nacional de Geologia de Portugal, Revista Electrónica de Ciências da Terra 17.

Rodríguez, J., Cosca, M.A., Gil Ibarguchi, J.I., Dallmeyer, R.D., 2003. Strain partitioning and preservation of $^{40}Ar/^{39}Ar$ ages during Variscan exhumation of a subducted crust (Malpica–Tui complex, NW Spain). Lithos 70 (3-4),111-139. doi: 10.1016/S0024-4937(03)00095-1.

Romeo, I., Capote, R., Tejero, R., Lunar, R., Quesada, C., 2006. Magma emplacement in transpression: The Santa Olalla Igneous Complex (Ossa-Morena Zone, SW Iberia). Journal of Structural Geology 28, 1821-1834. doi: 10.1016/j.jsg.2006.06.007.

Rosas, F.M., Marques, F.O., Ballèvre, M., Tassinari, C., 2008. Geodynamic evolution of the SW Variscides: Orogenic collapse shown by new tectonometamorphic and isotopic data from western Ossa-Morena Zone, SW Iberia. Tectonics 27, TC6008. doi:10.1029/2008TC002333.

Rubio Pascual, F.J., Matas J., Martín Parra, L.M., 2013. High-pressure metamorphism in the Early Variscan subduction complex of the SW Iberian Massif. Tectonophysics 592, 187-199.

San José, M.A., Herranz, P., Pieren, A.P., 2004. A review of the Ossa-Morena Zone and its limits. Implications for the definition of the Lusitan-Marianic Zone. Journal of Iberian Geology 30, 7-22.

Sánchez Carretero, R., Carracedo, M., Eguiluz, L., Garrote, A., Apalategui, O., 1989. El magmatismo calcoalcalino del Precámbrico terminal en la Zona de Ossa-Morena (Macizo Ibérico). Revista de la Sociedad Geológica de España 2, 7-21.

Sánchez Carretero, R., Eguiluz, L., Pascual, E., Carracedo, M., 1990. Ossa-Morena Zone: Igneous rocks. In: Dallmeyer, R.D., Martínez García, E. (Eds.), Pre-Mesozoic Geology of Iberia. Springer Berlin Heidelberg, 292-313.

Schermerhorn, J.L.G., 1971. An outline stratigraphy of the Pyrite Belt. Boletín Geológico Minero 82, 239-268.

Shelley, D., Bossière, G., 2000. A new model for the Hercynian Orogen of Gondwanan France and Iberia. Journal of Structural Geology 22(6), 757-776.

Sierra, S., Moreno, C., 2004. Cuenca Pérmica del Viar. In: Vera, J.A. (ed.), Geología de España. SGE-IGME, Madrid, 214-215.

Silva, J.B., Oliveira, J.T., Ribeiro, A., 1990. South Portuguese Zone, estructural outline. In: Dallmeyer, R.D., Martínez García, E. (Eds.), Pre-Mesozoic Geology of Iberia. Springer Verlag, Berlin, 348-362.

Simancas, J.F., 1983. Geología de la extremidad oriental de la Zona Sudportuguesa. Ph.D. Thesis, Universidad de Granada, 439 pp.

Simancas, J.F., 2004. Zona Sudportuguesa. In: Vera, J.A. (ed.), Geología de España. SGE-IGME, Madrid,199-201.

Simancas, J.F., Martínez Poyatos, D., Expósito, I., Azor, A., González Lodeiro, F., 2001. The structure of a major suture zone in the SW Iberian Massif: the Ossa-Morena/Central Iberian contact. Tectonophysics, 332(1-2), 295-308.

Simancas, J.F., González Lodeiro, F., Expósito, I., Azor, A., Martínez Poyatos, D., 2002. Opposite subduction polarities connected by transform faults in the Iberian Massif and western European Variscides. In: Martínez Catalán, J.R., Hatcher, R.D. Jr., Arenas, R., Díaz García F. (Eds.), Variscan-Appalachian dynamics: The building of the late Paleozoic basement. Boulder, Colorado, Geological Society of America Special Paper 364, 253-262.

Simancas, J.F., Carbonell, R., González Lodeiro, F., Pérez-Estaún, A., Juhlin, C., Ayarza, P., Kashubin, A., Azor, A., Martínez Poyatos, D., Almodóvar, G.R., Pascual, E., Sáez, R., Expósito, I., 2003. Crustal structure of the transpressional Variscan orogen of SW Iberia: SW Iberia deep seismic reflection profile (IBERSEIS). Tectonics 22(6). doi: 10.1029/2002TC001479.

Simancas, J.F., Expósito, I., Azor, A., Martínez Poyatos, D., González Lodeiro, F., 2004. From the Cadomian orogenesis to the Early Palaeozoic Variscan rifting in Southwest Iberia. Journal of Iberian Geology 30, 53-71.

Simancas, J.F., Tahiri, A., Azor, A., González Lodeiro, F., Martínez Poyatos, D., El Hadi, H., 2005. The tectonic frame of the Variscan-Alleghanian orogen in southern Europe and northern Africa. Tectonophysics 398, 181-198.

Simancas, J.F., Carbonell, R., González Lodeiro, F., Pérez Estaún, A., Juhlin, C., Ayarza, P., Kashubin, A., Azor, A., Martínez Poyatos, D., Sáez, R., Almodóvar, G.R., Pascual, E., Flecha, I., Martí, D., 2006. Transpressional collision tectonics and mantle plume dynamics: the Variscides of southwestern Iberia. Geological Society, London, Memoirs, 32(1), 345-354.

Simancas, J.F., Ayarza, P., Azor, A., Carbonell, R., Martínez Poyatos, D., Pérez-Estaún, A., González Lodeiro, F., 2013. A seismic geotraverse across the Iberian Variscides: Orogenic shortening, collisional magmatism and orocline development. Tectonics 32, 1-16. doi: 10.1002/tect.20035.

Simancas, J.F., Azor, A., Martínez Poyatos, D., Expósito, I., Pérez-Cáceres, I., González Lodeiro, F., 2016. Comment on "The Late Devonian Variscan suture of the Iberian Massif: A correlation of high-pressure belts in NW and SW Iberia. Tectonophysics 654, 96-100" by R. Fernández and R. Arenas. Tectonophysics 666, 281-284. doi: 10.1016/j.tecto.2015.07.040.

Talavera, C., Martínez Poyatos, D., González Lodeiro, F., 2015. SHRIMP U-Pb geochronological constraints on the timing of the intra-Alcudian (Cadomian) angular unconformity in the Central Iberian Zone (Iberian Massif, Spain). International Journal of Earth Sciences (Geol Rundsch) 104(7), 1739-1757. doi: 10.1007/s00531-015-1171-5.

Thiéblemont, D., Pascual, E., Stein, G., 1998. Magmatism in the Iberian Pyrite Belt: petrological constraints on a metallogenic model. Mineralium Deposita 33, 98-110.

Valenzuela, A., Donaire T., Pin C., Toscano M., Hamilton, M.A., Pascual, E., 2011. Geochemistry and U-Pb dating of felsic volcanic rocks in the Riotinto-Nerva unit, Iberian Pyrite Belt,

Spain: crustal thinning, progressive crustal melting and massive sulphide genesis. Journal of the Geological Society, London 168(3), 717-731.

Vauchez, A., 1975. Tectoniques tangeantielles superposées dans la segment hercynien Sud-bérique: Les nappes et pliscouchés de la region d'Alconchel-Fregenal de la Sierra (Badajoz). Boletín Geológico y Minero 86, 573-580.

Weil, A.B., Van der Voo, R., Van der Pluijm, B.A., Parés, J.M., 2000. The formation of an orocline by multiphase deformation: a paleomagnetic investingation of the Cantabria-Asturias Arc (northern Spain). Journal of Structural Geology 22, 735-756. doi: 10.1016/S0191-8141(99)00188-1.

Weil, A.B., Van der Voo, R., Van der Pluijm, B.A., 2001. Oroclinal bending and evidence against the Pangea megashear: The Cantabria-Asturias arc (northern Spain). Geology 29, 991-994.

Weil, A.B., Gutiérrez-Alonso, G., Johnston, S.T., Pastor-Galán, D., 2013. Kinematic constraints on buckling a lithospheric-scale orocline along the northern margin of Gondwana: A geologic synthesis. Tectonophysics 582, 25-49. doi: 10.1016/j.tecto.2012.10.006.

Chapter II

Pre-Variscan paleogeography of SW Iberian terranes

The main purpose of this chapter is to explore the paleogeography of SW Iberia through the significance of inherited detrital zircon data. This objective is split into two issues: (i) to test the Avalonian affinity of the South Portuguese Zone and the Sehoul Block in NW Morocco (including a robust new dataset) and (ii) to propose a late Precambrian to Paleozoic paleogeography of north Gondwana through a compilation of new and published pre-Cryogenian inherited zircon data.

Testing the Avalonian affinity of the South Portuguese Zone and the Neoproterozoic evolution of SW Iberia through detrital zircon populations

Irene Pérez-Cáceres[1], David Martínez Poyatos[1], José Fernando Simancas[1], and Antonio Azor[1].

1 Departamento de Geodinámica, Facultad de Ciencias, Universidad de Granada, Campus de Fuentenueva s/n, 18071 Granada, Spain.

Abstract

New SHRIMP U-Pb geochronogical data on detrital zircons from the South Portuguese Zone (SPZ) in SW Iberia and the Sehoul Block in northwest Morocco are provided, aimed at deciphering the presumed Avalonian affinity of these two regions. Despite the limitation imposed by the absence of Ordovician-Silurian rocks in outcrop, indirect support for an Avalonian affinity comes from the presence of Mesoproterozoic ($\approx$1 and 1.3–1.7 Ga) and Silurian-Early Devonian ($\approx$400 Ma) zircons in sediments of the SPZ. Moreover, the Ribeira de Limas formation of the Pulo do Lobo belt (northern SPZ) shows the same zircon pattern (dominated by a 580–630Ma population) and tectonic deformation as the Ronquillo formation in the inner SPZ, thus challenging the classical interpretation of the Pulo do Lobo belt as exotic with respect to the SPZ. On the contrary, the Horta da Torre formation, cropping out just south of the Ossa-Morena Zone/SPZ boundary, is the only element that can be considered exotic from a sedimentary perspective, due to presence of $\approx$1 and 1.4–1.6 Ga zircon populations. Finally, a close similarity in detrital zircon content has been found between the Santa Iría (upper Pulo do Lobo rocks) and PQ formations, both featuring a missing Variscan volcanic arc denoted by a population at 365–375 Ma. Regarding the Sehoul Block, its Caledonian tectonic imprint strongly supports an Avalonian derivation, although the zircon spectrum of its Cambrian sediments is dominated by Cadomian/Pan-African ages (560–605 Ma). On a broader scale, we have explored the Neoproterozoic evolution of SW Iberia through a synthesis of available published detrital zircon data. The difference in Proterozoic zircon inheritance between Ossa-Morena and Central Iberian samples (and their central European correlatives) is highlighted and explained in terms of right-lateral transcurrent tectonics along a northern Gondwana late Cadomian subduction zone.

Keywords

U-Pb SHRIMP on detrital zircon

Pulo do Lobo belt

Variscan-Alleghanian orogen

Avalonia

Pan-African/Cadomian orogeny

Keypoints

Detrital zircons support the Avalonian affinity of the South Portuguese Zone.

The Pulo do Lobo belt is not an exotic terrane.

Cadomian displacements determine the vicinity of the SW Iberian terranes.

1. Introduction

In clastic sedimentary rocks, the physical and chemical endurance of detrital zircon makes it a long-lasting survivor of weathering, erosion and sedimentary transport, collectively retaining memories of the primary igneous crystallization ages, as well as the ages of metamorphism of exhumed and eroded crustal rocks. These features, together with the availability of fast and reliable analytical methods (ID-TIMS, LA-ICPMS, SHRIMP), have been a major boost for using the age of detrital inherited zircon populations as tracers of the sources of sedimentary rocks and, indirectly, to perform paleogeographic reconstructions (e.g., Friedl et al., 2000; Fedo et al., 2003; Linnemann et al., 2004). Moreover, xenocrystic zircon grains -and the ages of zircon cores- in igneous rocks provide some constraints on the underlying basement (e.g., Barrie et al., 2002; Zeck et al., 2004; Montero et al., 2007; Braid et al., 2012). However, studies of detrital zircon still entail remarkable uncertainties regarding how zircon grains are separated and analyzed and how age distributions are compared (e.g., Gehrels, 2012). Apart from these flaws, the interpretation of detrital zircon age populations in sedimentary rocks also has some intrinsic limitations (e.g., Sircombe and Freeman, 1999; Fedo et al., 2003; Moecher and Samson, 2006; Zimmerman et al., 2015). The most important of these limitations is the simple assumption in paleogeographic reconstructions that clastic sediments are primary detritus, i.e., they derive directly from metamorphic or igneous sources, thus precluding the fact that most clastic grains have a polycyclic history (e.g., Leeder, 1982; Andersen et al., 2016). As an additional tool for paleogeographic/paleotectonic studies, whole-rock Nd and zircon Hf isotopic data have been used to discriminate between possible basements (e.g., Linnemann et al., 2004; Murphy et al., 2006; Bea et al., 2010; Albert et al., 2015; Cambeses, 2015; Henderson et al., 2016).

A number of Gondwana-derived terranes (Ganderia, Avalonia s. str., Meguma, Carolina, Armorica, Florida) were apparently involved in the Paleozoic terrane amalgamation previous to the closure of the Rheic ocean that led to the Variscan and Appalachian orogenies (e.g. Cocks and Torsvik, 2011; Linnemann et al., 2012). A good number of studies based on detrital zircon age distribution have dealt with the paleogeography of these terranes (e.g., Friedl et al., 2000; Linnemann et al., 2004; Murphy et al, 2004; Gerdes and Zeh, 2006), being many of these studies focused on the Variscan orogen in northwest Iberia (Fernández-Suárez et al., 2002, 2003, 2014; Gutiérrez-Alonso et al., 2003; Díez Fernández et al., 2010; Pastor-Galán et al., 2013; Albert et al., 2015; Henderson et al., 2016) and central-southwest Iberia (Bea et al., 2010; Braid et al., 2011; Talavera et al., 2012; Dinis et al., 2012; Pereira et al., 2012a, 2012b, 2014; Rodrigues et al., 2015; Cambeses, 2015). The main question addressed by these studies on inherited zircon populations has been the so-called Gondwanan or Avalonian affinity of the Iberian terranes, in order to discriminate their continental basements and drift histories. In this regard, Gondwanan affinity means location at/or very close to the margin of Gondwana during the entire Paleozoic (e.g., Matte, 2001; Nysaether et al., 2002; Nance et al., 2010; Stampfli et al., 2013), while Avalonian affinity denotes terranes that drifted from NW Gondwana in the Late Cambrian (opening of the Rheic ocean; Cocks and Fortey, 2009), collided with Baltica at latemost Ordovician time (Tornquist ocean closure) and docked to Laurentia in the middle Silurian (closure of the Iapetus ocean followed by the Caledonian orogeny) (e.g. Cocks and Torsvik,

2011; Linnemann et al., 2012). Taking into account the still undefined status of some of the Gondwanan-derived terranes, in this paper we consider Avalonia as a composite microplate including terranes such as Meguma, which probably formed the southernmost part of the 'Avalonia Terrane Assemblage' (Murphy, 2007; Waldron et al., 2011). Avalonia crops out in eastern North-America (Avalon Peninsula of Newfoundland, Maritime Provinces of Canada and the eastern US seaboard as far south as Massachusetts) and western Europe (Wales and Bravant massifs, and maybe the southwesternmost Iberian Massif). Potential source zircon populations (direct or recycled) in Avalonian rocks include Paleoproterozoic grains (≈2.0 Ga zircons formed during the Eburnean orogeny in North Gondwana), Mesoproterozoic (1.6−1.0 Ga zircons derived from Amazonia), Stenian-Tonian (≈1.0 Ga zircons derived from a Grenvillian type crust), Cryogenian-Ediacaran (0.7−0.54 Ga zircons formed during the Cadomian and Pan-African orogenic belts), and Paleozoic (0.5−0.4 Ga zircons formed during the Taconic, Caledonian and Acadian orogenies by docking of the Avalonian fragments to Laurrusia).

The Neoproterozoic location of Avalonia is thought to be westwards of the Gondwanan terranes, their respective basements might be rather different (Murphy et al., 2000 and 2006), i.e., the crustal basement of Avalonian terranes probably includes ≈1.0 and 1.3−1.7 Ga Amazonian components, while Gondwanan terranes must be dominated by a ≈2.0 Ga West African component, with or without a subordinate population of ≈1.0 Ga (e.g., Bea et al., 2010; Henderson et al., 2016). Meaningful and frequent ages of inherited zircon populations in the latest Precambrian and Paleozoic rocks of Iberia are the following: i) Paleoproterozoic zircons (≈2 Ga) that point to an ultimate provenance from the West African Craton or the Saharan Metacraton; ii) Mesoproterozoic zircons (≈1 Ga) coming from either Amazonian (Fernández-Suárez et al., 2002; Gutiérrez-Alonso et al., 2005) or Arabian-Nubian basements (Bea et al., 2010); iii) Late Neoproterozoic zircons (≈0.6 Ga) that provide evidence for a Cadomian volcanic arc at the northern Gondwana margin (Murphy et al., 2002); iv) Early Paleozoic zircons (≈0.5−0.4 Ga), interpreted as derived from pre-Variscan rift-related magmatism and/or from Caledonian-Appalachian igneous rocks; and v) Late Devonian zircons (≈380−360 Ma), attributed to a cryptic Rheic volcanic arc in SW Iberia (Pereira et al., 2012a). According to these data, most Iberian Variscan zones have a confirmed Gondwanan affinity, already suggested drawing on different geological-paleontological bases (e.g., Gutiérrez-Marco et al., 2002). Thus, the Gondwana realm would include the basal units of the Galicia-Tras-os-Montes Zone (GTOMZ), the autochthonous zones of northern and central Iberia (Cantabrian Zone, CZ; West Asturian-Leonese Zone, WALZ; and Central Iberian Zone, CIZ), and the Ossa-Morena Zone (OMZ) to the south (Fig. 2.1). As for the SPZ basement, several authors have proposed that this terrane could have been part of Avalonia, particularly representing the Meguma terrane (e.g., Braid et al., 2012; Pereira et al., 2016).
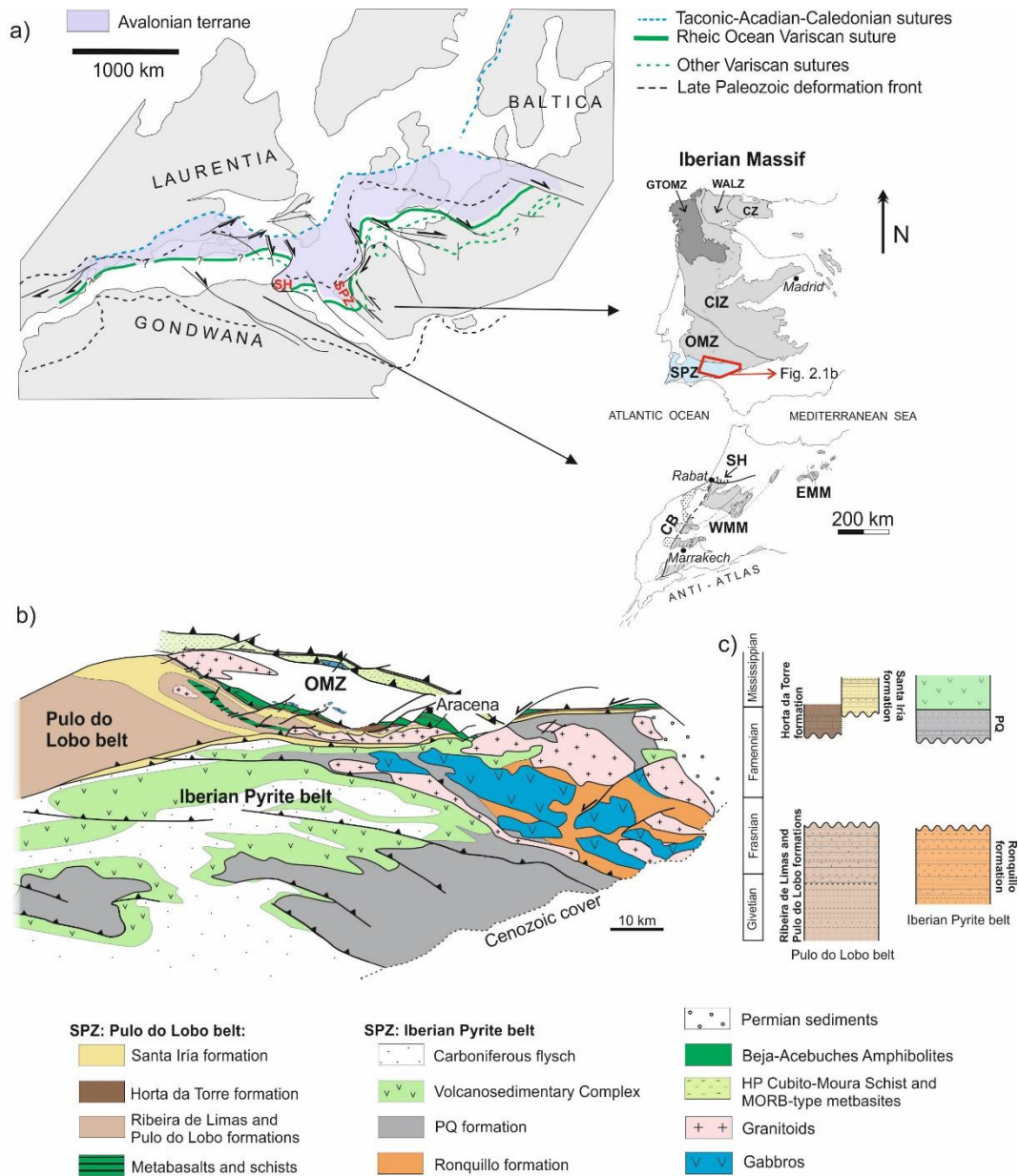
Figure 2.1. a) Reconstruction of the Variscan/Alleghanian frame at late Carboniferous time and geological sketches of the Iberian Massif and the Moroccan Variscides. CZ (Cantabrian Zone), WALZ (West Asturian-Leonese Zone), GTOMZ (Galicia Tras-os-Montes Zone), CIZ (Central Iberian Zone), OMZ (Ossa-Morena Zone), SPZ (South Portuguese Zone), SH (Sehoul Block), CB (Coastal Block), WMM (Western Morocco Meseta), EMM (Eastern Morocco Meseta). b) Geological map of the eastern SPZ. c) Stratigraphy of the SPZ.

Despite the wealth of available data on Iberian terranes, important questions remain open, such as: i) their location along the Gondwana margin during late Neoproterozoic times (e.g., Gutiérrez-Alonso et al., 2003; Bea et al., 2010; Cambeses, 2015); ii) the Avalonian or Gondwanan affinity of the upper allochthonous units of the GTOMZ (e.g., Martínez Catalán et al., 1997; Fernández-Suárez et al., 2003; Albert et al., 2015; Henderson et al., 2016; and iii) the Avalonian affinity proposed for the South Portuguese Zone (SPZ) (e.g., Simancas et al., 2005 and references therein). This paper mainly deals with the nature and

paleogeographic location of the SPZ, as well as its relationships with the neighboring OMZ, CIZ and NW Moroccan Variscides. To do so, we report new SHRIMP U-Pb geochronological data on detrital zircon populations from Devonian-Carboniferous clastic units of the Pulo do Lobo belt located in the northernmost SPZ, and from Devonian clastic units cropping out in the Iberian Pyrite belt, inside the SPZ, as well as from Cambrian sandstones of the Sehoul Block located in northwest Morocco (Fig. 2.1). At this respect, the Sehoul Block has been suggested to derive from Avalonia, (Simancas et al., 2005; Tahiri et al., 2010). Altogether, our new data and previously published data let us to undertake a well-supported discussion on late Neoproterozoic and Paleozoic paleogeography of SW Iberian and NW African Variscan terranes.

2. Geological setting

The Iberian Massif constitutes a nearly complete section of the Late Paleozoic Variscan-Alleghanian orogen (Fig. 2.1a), which forms a double orocline (e.g., Martínez Catalán, 2011 and 2012; Shaw et al, 2014; Murphy et al., 2016). Tectono-stratigraphic correlations across the orocline have proven difficult. However, a number of zones have been differentiated based on stratigraphic and tectono-metamorphic criteria. In NW Iberia and from east to west, the CZ, WALZ and CIZ represent the Paleozoic margin of Gondwana, from a more external position in the orogen (CZ) to the hinterland (WALZ and CIZ) (e.g., Pérez-Estaún et al., 1988; Martínez Catalán et al., 1997). The westernmost zone is the GTOMZ, which is entirely allochthonous over the CIZ (Fig. 2.1a) and represents a thick tectonic pile of continental and oceanic units. The rootless suture contained in this zone (defined by ophiolitic units) is generally attributed to the closure of the Rheic Ocean (e.g., Martínez Catalán et al., 1997), though alternative interpretations have been proposed more recently (e.g., Arenas et al., 2014).

The CIZ is the largest zone, extending from NW to SW Iberia (Fig. 2.1a). It is composed of Neoproterozoic metamorphic rocks unconformably overlain by Paleozoic metasedimentary rocks and lower Paleozoic metavolcanics. Lower Paleozoic orthogneisses are also abundant, though the vast majority of igneous rocks correspond to late Carboniferous undeformed granitoids. In northern Iberia, the CIZ shows continuity with the WALZ and CZ, the latter showing characteristics of an external foreland zone. In southwest Iberia, the CIZ is separated from the OMZ by a crustal-scale shear zone (Burg et al., 1981; Azor et al., 1994), which has been interpreted as a suture contact produced by the closure of a narrow Early Paleozoic ocean (Simancas et al., 2001; Gómez-Pugnaire et al., 2003). The OMZ is composed by late Precambrian and Paleozoic metasediments, as well as a good number of Cambrian-Ordovician metaigneous rocks featuring a rifting event that occurred at the northern margin of Gondwana. Furthermore, lower Carboniferous sediments and magmatism characterize the OMZ and southernmost CIZ attesting a transtensional event (Simancas et al., 2006; Pereira et al., 2009).

Southwards, the boundary between the OMZ and the SPZ has been generally interpreted as the suture of the Rheic Ocean (e.g., Crespo-Blanc and Orozco, 1988; Fonseca and Ribeiro, 1993; Simancas et al., 2003), an oceanic domain that was presumably closed in Devonian times (e.g., Araujo et al., 2005; Ponce et al., 2012). However, the Beja-Acebuches

ophiolitic rocks cropping out at this boundary have yielded an Early Carboniferous protolith age (Azor et al., 2008 and 2009), which compels a reassessment of the evolution of this tectonic boundary. At present, the only evidence for the Rheic suture at the OMZ/SPZ boundary is the presence of an allochthonous complex with eclogites, high-pressure schists and MORB-type metabasites north of the OMZ/SPZ contact (the so-called Cubito-Moura unit; Fig. 2.1; Fonseca et al., 1999; Araujo et al., 2005; Ponce et al., 2012). Accordingly, this boundary is a cryptic Rheic suture, strongly obliterated by Mississippian mafic intrusions and transpressional collisional deformation (Pérez-Cáceres et al., 2015). Whether or not the Rheic suture in SW Iberia continues in the allochtonous ophiolites of NW Iberia is currently an open question (Martínez Catalán et al., 1997; Arenas et al., 2014). Further east, the SPZ is usually correlated with the Rheno-Hercynian zone of central Europe, thus assuming an external position for it within the Variscan realm (Franke, 2000).

The SW Iberian Variscides (southernmost CIZ and OMZ) also contain some imprint of the Cadomian Late Precambrian orogeny. This imprint mostly consists of a widespread calc-alkaline Ediacaran arc-related magmatism in the OMZ and southernmost CIZ (e.g., Bandrés et al., 2004). In the southernmost CIZ, low-grade metamorphism and a foliation of Ediacaran age have been locally preserved (Blatrix and Burg, 1981; Dallmeyer and Quesada, 1992).

2.1. Tectono-stratigraphic framework of the South Portuguese Zone

The SPZ is the southernmost zone of the Iberian Massif, being characterized by the absence of outcropping pre-Middle Devonian rocks (Fig. 2.1b–c). Most of the samples studied in this work belong to the metasediments of the Pulo do Lobo belt, which constitutes the northernmost SPZ. The central SPZ is known as the Iberian Pyrite belt, whose Devonian metasedimentary formations have also been sampled. Finally, Upper Carboniferous flysch deposits dominate the southern SPZ.

The Pulo do Lobo belt consists of a group of clastic low-grade metasedimentary formations (Fig. 2.1c). The lowermost formation is the Pulo do Lobo formation s. str. and it is made up of black phyllites with abundant quartz veins. Gradually upwards, quartz-sandstone intercalations define the Ribeira de Limas formation, which contains lower Frasnian palynomorphs (Pereira et al., 2008). These two formations show the same three-phase deformation and have been interpreted as a pre-Carboniferous accretionary prism related to the subduction and closure of the Rheic Ocean; this interpretation is entirely based on the presence of intercalated metabasalts with MORB geochemical signature (e.g., Eden and Andrews, 1990; Oliveira, 1990). However, available radiometric ages point to an Early Carboniferous age for the metabasalt protoliths (Dahn et al., 2014; Pérez-Cáceres et al., 2015).

The upper formations in the Pulo do Lobo belt (Horta da Torre and Santa Iría) unconformably overlie the lower ones and are only affected by two deformation phases, instead of the three phases in the lower formations (Pérez-Cáceres et al., 2015). The Horta da Torre formation is composed of slates and mature quartzites, while the Santa Iría

formation is made up of slates and greywackes. Both formations contain upper Frasnian to upper Famennian palynomorphs (Pereira et al., 2008), though the youngest clastic zircons suggest an early Mississippian age for the Santa Iría formation (Fig. 2.1c; Braid et al., 2011; this work). The Horta da Torre formation has been locally named "Alájar mélange" (Eden and Andrews, 1990; Braid et al., 2011) due to a low-grade left-lateral shearing that dismembered the quartzitic beds into lenses. U-Pb zircon dating of igneous felsic rocks affected by this shearing has yielded an age of 337 Ma, thus constraining this deformation to be younger than this age (Pérez-Cáceres et al., 2015).

South of the Pulo do Lobo belt, the Iberian Pyrite belt is characterized by the presence of a Tournaisian volcanosedimentary complex with associated sulphide deposits, covered by a Visean flysch (Oliveira, 1990). Underlying the volcanosedimentary complex, two Devonian formations have been distinguished: the upper one corresponds to the Late Devonian PQ formation (Phyllite-Quartzite group; Schermerhorn, 1971; Pereira et al., 2008), made up of phyllites, cross-laminated quartzwackes and quartzites; the lower one is the Ronquillo formation (Simancas, 1983), which is made up of phyllites and metasandstones. The Ronquillo formation recorded polyphase deformation and is unconformably overlain by the PQ formation (Fig. 2.1c).

2.2. The Moroccan Variscides

The Moroccan Variscides (Michard et al., 2010) can be subdivided into the Eastern Meseta, the Western Meseta and the Coastal Block (Fig. 2.1a). To the south, the Moroccan Variscides exhibit a transition to the West African Craton through the Anti-Atlas domain. The facies of Silurian-Early Devonian sedimentary rocks of the Eastern Meseta are different from those in the Western Meseta, while the Late Devonian-Early Carboniferous is represented in both mesetas by similar clastic sedimentation with interbedded volcanic rocks. As regards deformation, the intensity is greater and the age is older in the Eastern Meseta (Late Devonian), compared to the Western Meseta (Carboniferous). The Coastal Block, separated from the Western Meseta by a fault striking NNE−SSW, is rather similar to the Western Meseta in stratigraphy but it shows very weak deformation.

The Sehoul Block (Fig. 2.1a) crops out along the northern margin of the Western Moroccan Meseta, is rather small in extent, and is dominated by metasedimentary Cambrian rocks intruded by early Variscan granitoids (367 Ma; Tahiri et al., 2010). The Sehoul Block thrust to the south onto the Western Meseta and has been interpreted as a fragment of Avalonia (Fig. 2.1a; Simancas et al., 2005) because the main deformation and metamorphism affecting its metasedimentary rocks is Caledonian in age (Michard et al., 2010; Tahiri et al., 2010). In this work, we have also analyzed the detrital zircon content of several Sehoul Cambrian metasandstones.

3. Samples and methods

Detrital zircons from 25 samples have been dated by U-Pb at the Ibersims SHRIMP laboratory of the University of Granada. From the obtained mineral extract, an average of 90 hand-picked zircon grains per sample were randomly selected in size, aspect and color, in order to characterize representative zircon populations. The geographic location of the samples (Appendix 1), microphotographs under cross-polarized light of selected samples and cathodoluminiscence images of representative zircon grains (Appendix 2), sample processing and detailed analytical procedures (Appendix 3), data sets (Appendix 4) and Wetherill plots (Appendix 5) are provided as supplementary information. The studied zircon grains show variable sizes, ranging between 50 and 300 μm. Most of the zircon grains are colorless or show yellowish to brownish color. The morphology is diverse, varying from elongate subidiomorphic, through stubby, to rounded shapes. Cathodoluminiscence images show different types of internal morphologies: most crystals display rounded core and rim, the latter exhibiting irregular concentric growth zoning, though euhedral oscillatory and longitudinal zoning have also been observed.

Three formations have been sampled and analyzed from the Pulo do Lobo belt:

-       Samples PLB-63, PLB-78, PLB-83 and PLB-90 belong to the Ribeira de Limas formation. These samples were collected from deformed metasandstones mainly composed of quartz, feldspar and minor mica. Zircons are rounded and medium-sized (≈100 μm), with the exception of sample PLB-63 that shows bigger grains (≈150 μm).

-       Samples PLB-28, PLB-53, PLB-68, PLB-69 and PLB-94 belong to the Horta da Torre formation, and were collected just south of the Beja-Acebuches Amphibolites (Fig. 2.1b). The zircons were separated from foliated metaquartzite beds. Zircon grains are smaller (<100 μm) and more rounded than in the other formations of the Pulo do Lobo belt.

-       Samples PLB-50, PLB-67, PLB-72 and PLB-75 belong to the Santa Iría formation. These samples were collected from deformed metagreywackes composed of quartz, feldspar and micas. Zircons grains are up to 200 μm and subidiomorphic, showing internal subeuhedral rims.

Two formations have been analyzed from the Iberian Pyrite belt:

-       Samples RNQ-04, RNQ-07, RNQ-08 and RNQ-09 are polyphase deformed metasandstones from the Ronquillo formation, with quartz and micas as dominant minerals. Zircons show variable size (60−150 μm) and shape, most of them being subidiomorph and elongated.

-       Samples RNQ-01 and RNQ-02 belong to the PQ formation. They correspond to fine-grained weakly deformed metagreywackes intercalated with slates. Zircons show variety in size and aspect, but most of them are ≈100 μm, broken and rounded.

Samples SH-01, SH-02, SH-03, SH-04, SH-05 and SH-06 are from deformed Cambrian metasandstones of the Sehoul Block in northwestern Morocco. They are mainly composed of quartz and minor mica. Except samples SH-01 and SH-02 that show subidiomorphic and bigger grains, zircons from these rocks are ≈100 μm, rounded and broken.

4. Results

4.1. Ribeira de Limas formation

We analyzed 349 zircon grains, rejecting 34 due to age discordance >10%.

The highest peak in all of the samples of the Ribeira de Limas formation corresponds to late Neoproterozoic ages at 580−620 Ma summing up to 62% of the zircon content (Fig. 2.2). A second important population spreads around 2.0 Ga (27% of zircon ages), while a few grains have yielded ages between 1.0 and 2.0 Ga. Sample PLB-78 exhibits a minor but distinctive youngest peak at 400 Ma.

Figure 2.2. a−d) Combined distribution histogram and relative probability plots of U-Pb detrital zircon concordant ages for the Ribeira de Limas formation samples. e) Percentages of zircon age populations represented on a circular plot. UTM coordinates of the samples: PLB-63 (4194680 N, 618285 E), PLB-78 (4194726 N, 658262 E), PLB-83 (4189514 N, 657768 E), PLB-90 (4188826 N, 669869 E).

4.2. Horta da Torre formation

A total of 462 zircons from five samples were analyzed, though 22 were rejected because age discordance exceeded 10%.

The most outstanding feature of the distribution of zircon ages is the presence of well-defined Mesoproterozoic populations with peaks at ≈1.0 Ga and ≈1.4–1.6 Ga, though ages spread between 1.0 and 2.0 Ga. The 2.0 Ga population is only well represented in samples PLB-28 and PLB-69. As a whole, 42% of the total zircon content is Mesoproterozoic and 27% Paleoproterozoic (Fig. 2.3). A dominant population at ≈580 Ma appears in samples PLB-28 and PLB-69, but not in the other three samples. Finally, a minor but distinctive population at ≈450 Ma exists in samples PLB-53, PLB-68 and PLB-94.
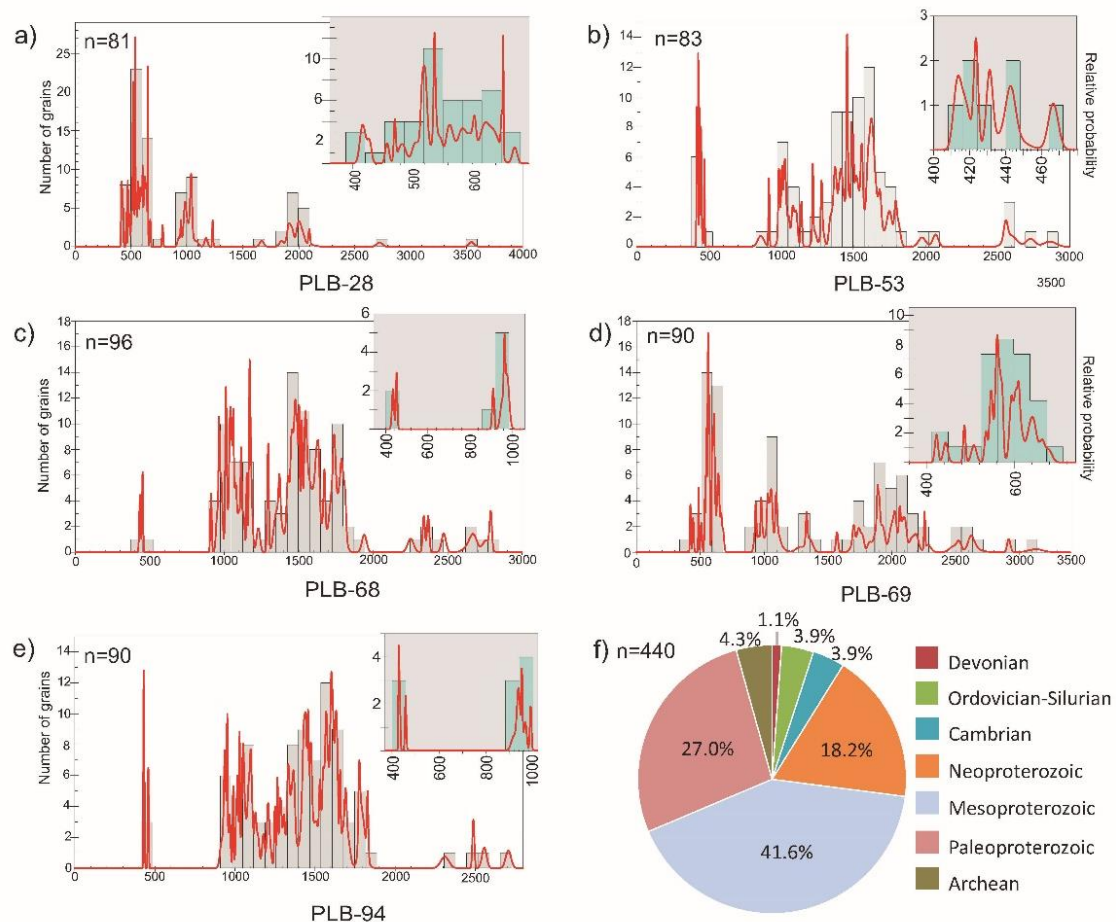
Figure 2.3. a–e) Combined distribution histogram and relative probability plots of U-Pb detrital zircon concordant ages for the Horta da Torre formation samples. f) Percentages of zircon age populations represented on a circular plot. UTM coordinates of the samples: PLB-28 (4192584 N, 706352 E), PLB-53 (4194647 N, 691935 E), PLB-68 (4192328 N, 699255 E), PLB-69 (4193766N, 694421 E), PLB-94 (4194928 N, 689520 E).

4.3. Santa Iría formation

We analyzed a total of 338 zircon grains, though 27 grains were discarded due to age discordance >10%. PLB-67 is the sample with highest number of discordant zircons.

The most outstanding feature of the zircon data in the Santa Iría formation is its youngest population, which is Late Devonian-Early Carboniferous and constitutes up to 40% of zircon content. The higher peak is Late Devonian (365−375 Ma), with a second important population at late Neoproterozoic (605−620 Ma) and minor Mesoproterozoic and Paleoproterozoic populations (Fig. 2.4).
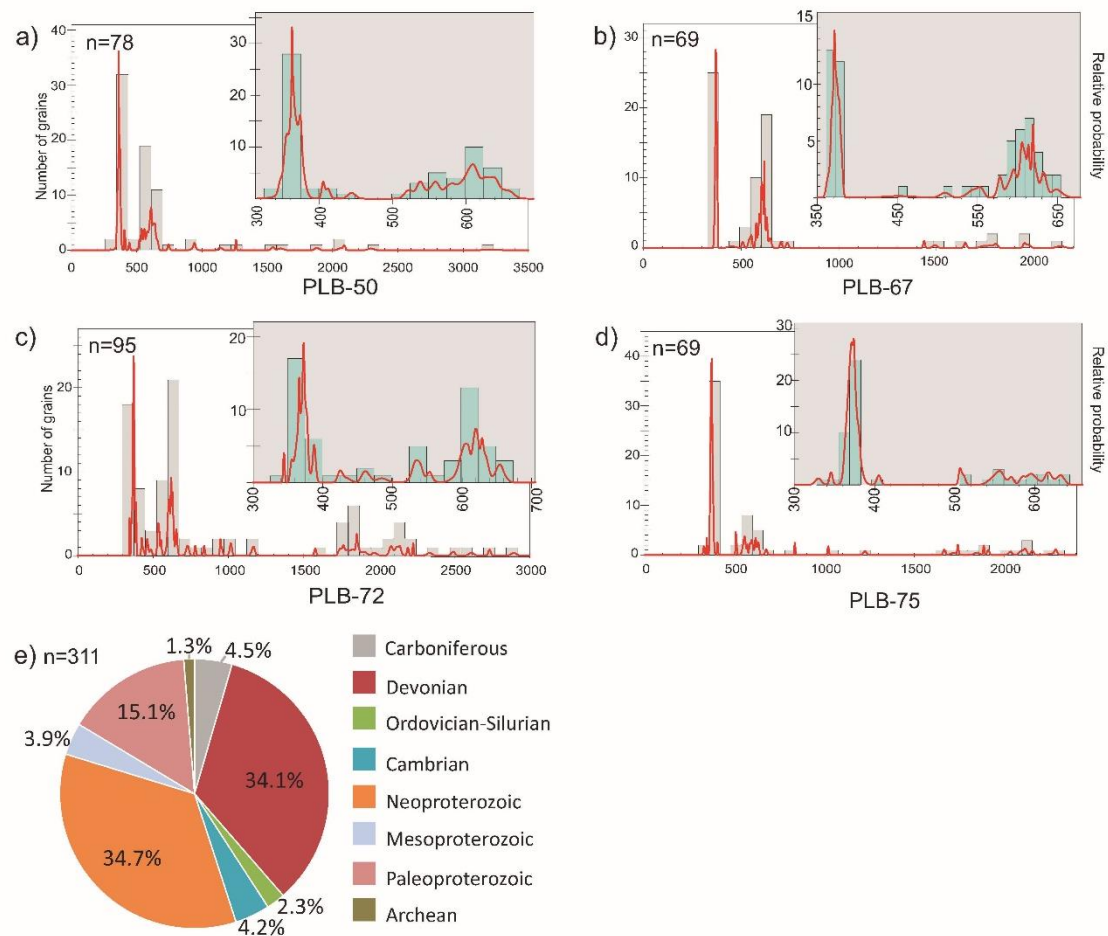
Figure 2.4. a−d) Combined distribution histogram and relative probability plots of U-Pb detrital zircon concordant ages for the Santa Iría formation samples. e) Percentages of zircon age populations represented on a circular plot. UTM coordinates of the samples: PLB-50 (4194335 N, 688125 E), PLB-67 (4199914 N, 650293 E), PLB-72 (4201977 N, 656925 E), PLB-75 (4200151 N, 657820 E).

4.4. Ronquillo formation

We analyzed a total of 342 zircons, having rejected 48 analyses due to age discordance >10%.

This formation has a dominant late Neoproterozoic - early Cambrian zircon population (58% of total zircon content), with peaks at different ages between 608 and 630 Ma, plus a secondary population at 540 Ma in the case of sample RNQ-9 (Fig. 2.5). The younger zircons depict a minor but distinctive peak at 400−410 Ma. Other minor populations spread around 2.0 Ga (dominant) and 1.0 Ga (subordinate).
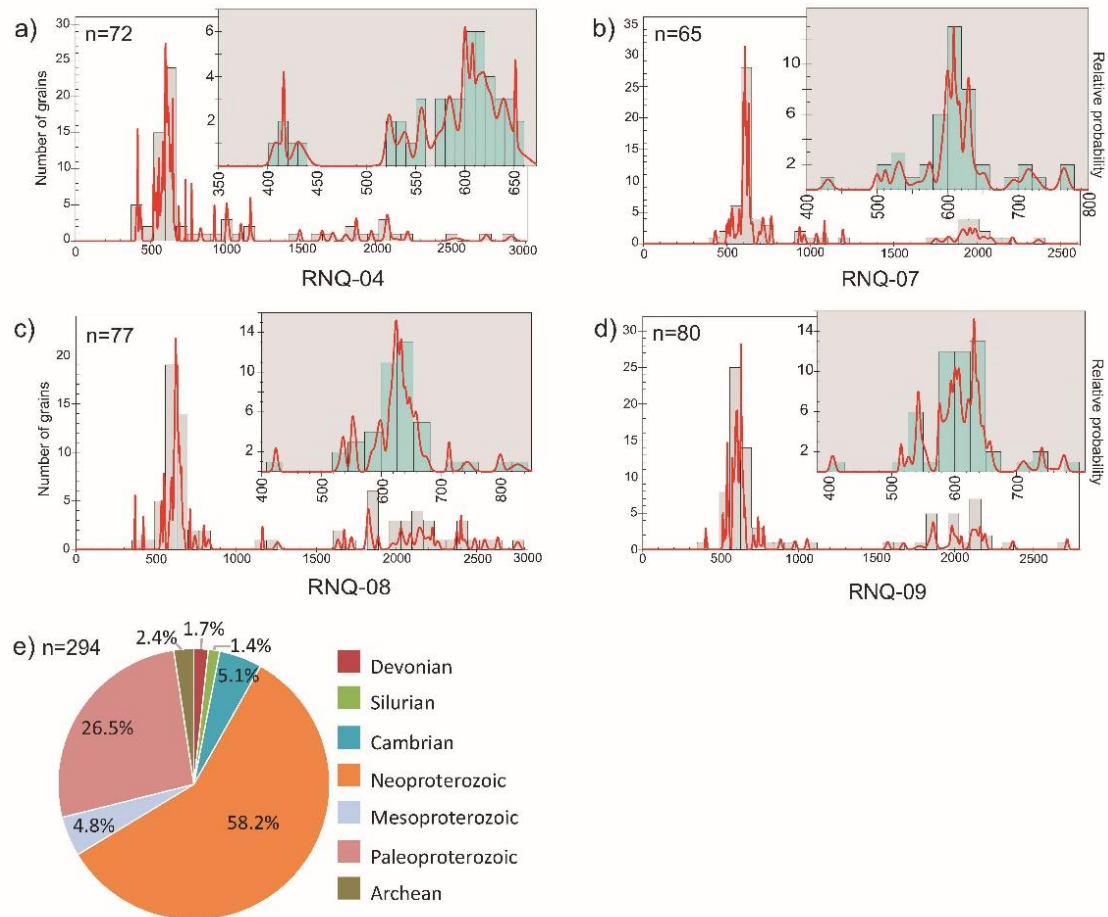
Figure 2.5. a–d) Combined distribution histogram and relative probability plots of U-Pb detrital zircon concordant ages for the Ronquillo formation samples. e) Percentages of zircon age populations represented on a circular plot. UTM coordinates of the samples: RNQ-04 (4173911 N, 748396 E), RNQ-07 (4178836 N, 750683 E), RNQ-08 (4180265 N, 748779 E), RNQ-09 (4161615 N, 757880 E).

4.5. PQ formation

We analyzed a total of 137 zircon grains, though 11 were discarded due to age discordance >10%.

The PQ metasandstones contain up to 25% of Devonian zircons, which constitute a well-defined peak at 366-375 Ma. The other main population, representing almost half of the total zircon content, is late Neoproterozoic (617−626 Ma). Finally, some grains are Paleoproterozoic, spreading around 2.0 Ga. (Fig. 2.6).

4.6. Sehoul Cambrian metasandstones

We analyzed 528 zircon grains from six samples, though 67 ages have been rejected due to age discordance >10%.

The Sehoul metasandstones have yielded a detrital zircon spectrum characterized by a dominant late Neoproterozoic peak at 560–605 Ma (76%). A few dispersed grains at around 1.0 Ga, a minor peak at around 2.0 Ga and a few ages older than 2.0 Ga complete the zircon data set (Fig. 2.7).
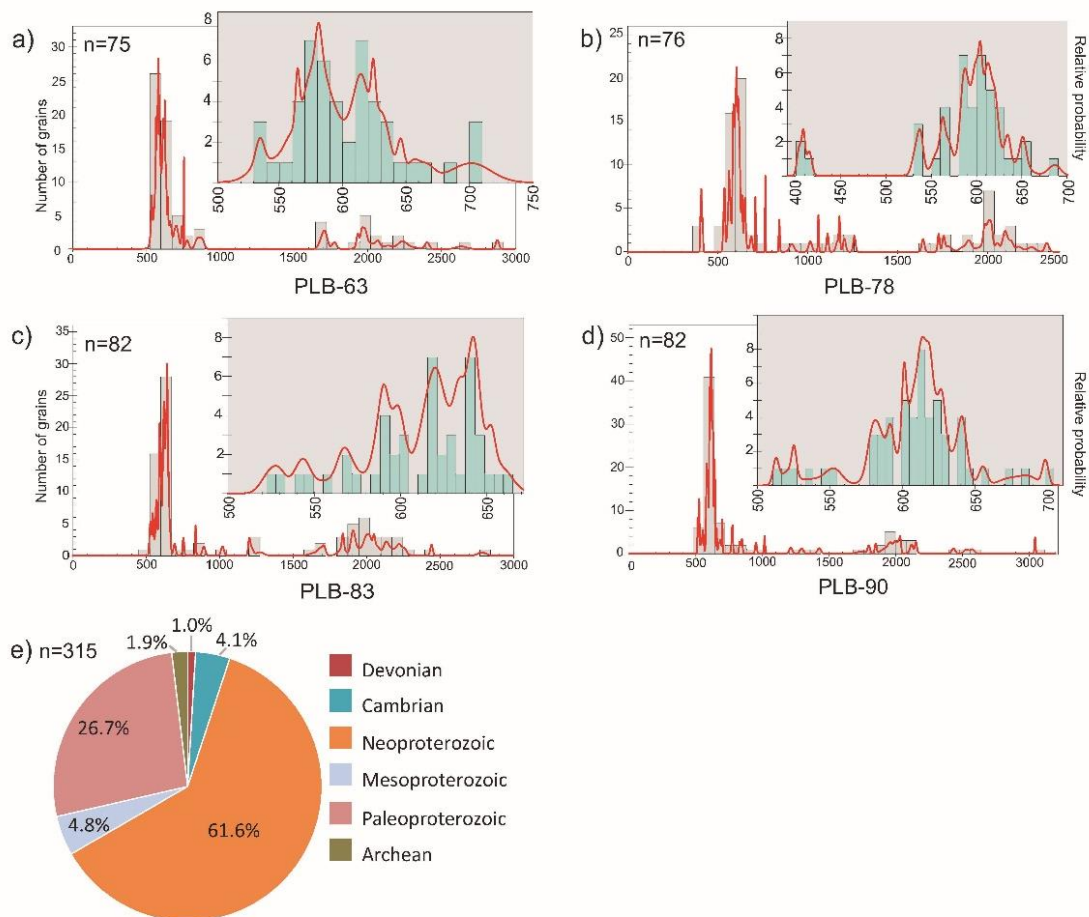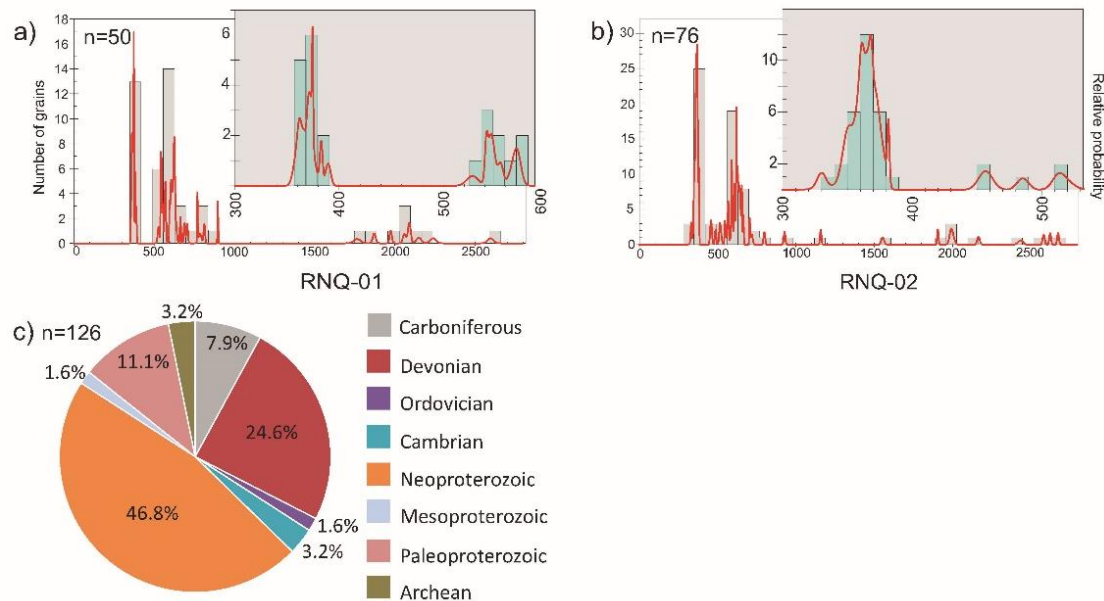

Figure 2.6. a–b) Combined distribution histogram and relative probability plots of U-Pb detrital zircon concordant ages for the PQ formation samples. c) Percentages of zircon age populations represented on a circular plot. UTM coordinates of the samples: RNQ-01 (4171762 N, 750852 E), RNQ-02 (4171618 N, 750726 E).

5. Interpretation of detrital zircon populations

5.1. Ribeira de Limas formation

The main 580-620 Ma population represents the dominant influence of the Cadomian/Pan-African arc-magmatism as a source of the Ribeira de Limas sediments (Fig. 2.2). The Paleoproterozoic zircon population at around 2.0 Ga indicates a Gondwanan signature, with zircons ultimately coming from the West African Craton. The younger peak at 400 Ma in sample PLB-78 constrains the maximum depositional age, which is compatible with the Frasnian age indicated by pollen data (Pereira et al., 2008). We interpret that the 400 Ma zircons may derive from a Caledonian-Appalachian igneous source.

Braid et al. (2011) considered the Alájar quartzites (Horta da Torre formation) equivalent to the Pulo do Lobo and Ribeira de Limas formations. However, the Horta da Torre rocks are definitely younger and generally less deformed than the Pulo do Lobo and Ribeira de

Limas ones. The confusion may derive from the locally intense ductile-to-brittle shear zone of Carboniferous age that affected the quartzites and phyllites of the Horta da Torre formation, giving them a "mélange" and polydeformed appearance at some outcrops (Pérez-Cáceres et al., 2015). Furthermore, the detrital zircon data of the Ribeira de Limas formation show a very different pattern: unlike the Avalonian signature of the Horta da Torre formation, our zircon data show a dominant influence of Gondwanan sources in the Ribeira de Limas formation, even though a Caledonian-Appalachian source has been detected in one sample (PLB-78).
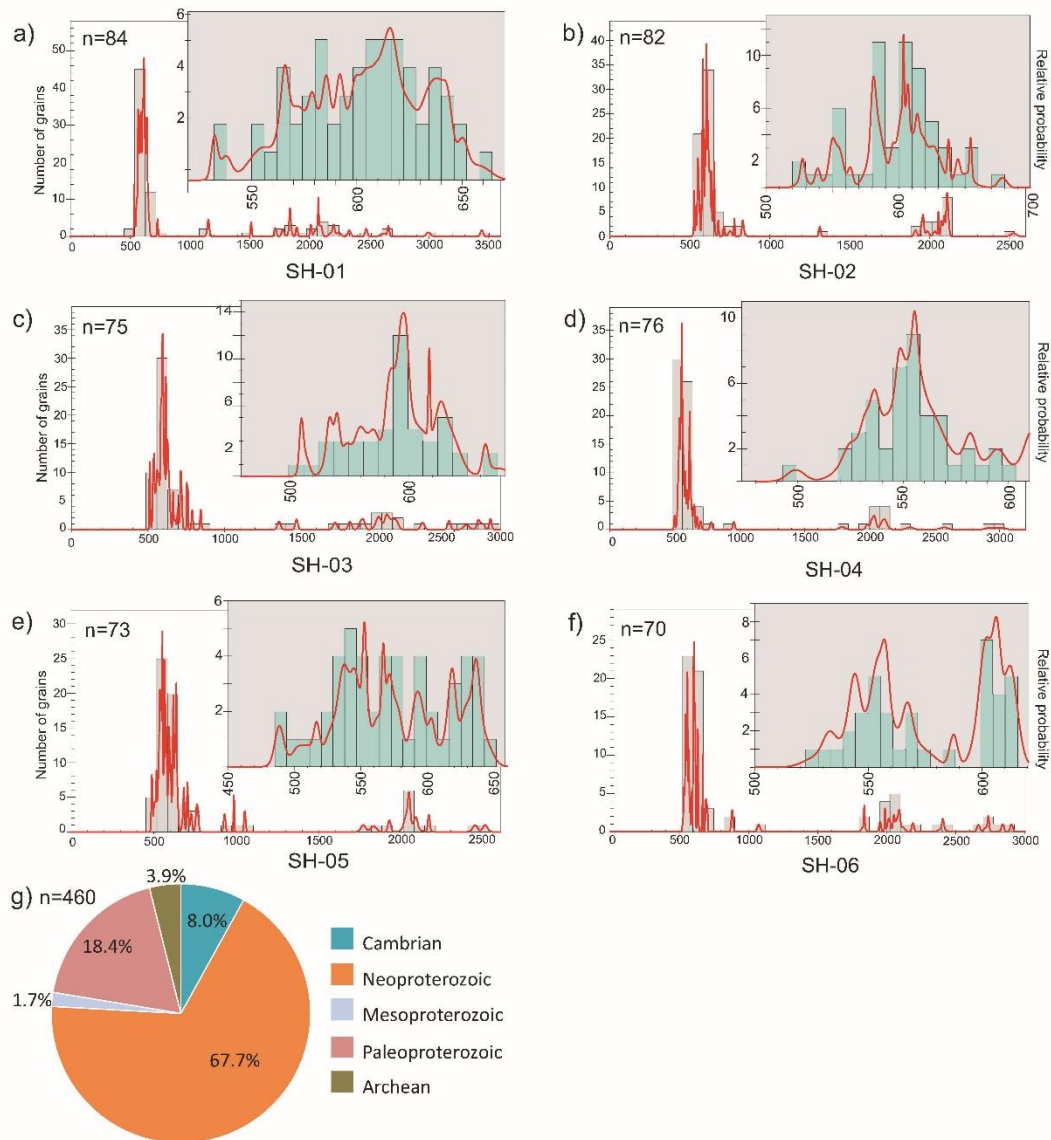
Figure 2.7. a–f) Combined distribution histogram and relative probability plots of U-Pb detrital zircon concordant ages for the Sehoul Block samples. g) Percentages of zircon age populations represented on a circular plot. UTM coordinates of the samples: SH-01 (3757730 N, 707964 E), SH-02 (3757806 N, 707956 E), SH-03 (3757858 N, 707951 E), SH-04 (3751232 N, 732226 E), SH-05 (3751232 N, 732226 E), SH-06 (3751222 N, 732110 E).

5.2. Horta da Torre formation

Our sampling of the Horta da Torre formation tests and complements previous data reported by Braid et al. (2011) from quartzites of the "Alájar mélange" (equivalent to our Horta da Torre formation). Thus, a robust data set is now available for this unit, which reveals three main features (Fig. 2.3):

i) The Paleoproterozoic and Mesoproterozoic record suggests either direct derivation from primary igneous sources or derivation from intermediate sedimentary sources containing zircons of those ages. This latter possibility might be preferable in view of the mature sands (orthoquartzites) constituting the Horta da Torre formation and the rounded shape and small size of most of the zircons, which favor a polycyclic origin. In any case, the abundance of varied Mesoproterozoic zircon populations (mainly at ≈1 and 1.4–1.6 Ga) suggests an Avalonian origin with ultimate Amazonian-Baltican sources. Regarding the ≈2.0 Ga zircons, they are usually interpreted as derived from the West African Craton, though zircons with this age in the Horta da Torre formation are less abundant compared with most inherited zircon populations in Iberia.

ii) The ≈580 Ma zircon population unequivocally represented in some samples, but nonexistent in others, may have a Cadomian and/or Pan-African derivation. Thus, the Cadomian influence on the composition of the Horta da Torre formation seems to have been intermittent.

iii) The 440–450 Ma zircon population may have been derived from a Caledonian-Appalachian source, thus giving additional support to the proximity of an Avalonian realm.

Braid et al. (2011) showed that the inherited zircon pattern of the Horta da Torre formation (Devonian in age) in SW Iberia is strikingly similar to the one of Silurian sandstones in the Southern Uplands (British Caledonides), which, in turn, might be taken as an indication of relative proximity between these two regions. This is not necessarily the case, since the compared rocks have different ages and thus the younger formation (Horta da Torre) might have been formed by recycling of rocks similar to those exposed in the Southern Uplands. Whatever the case, the Horta da Torre formation stands out unequivocally as reflecting dominant detrital sources located in a nearby Caledonian-Appalachian region at Late Devonian time.

5.3. Santa Iría formation

The main Devonian peak at 365–375 Ma may attest the existence of a cryptic Variscan volcanic arc, as suggested by Pereira et al. (2012a) (Fig. 2.4). However, a very minor younger population at ≈345 Ma sets the maximum depositional age for this formation, as also shown by the data reported by Braid et al. (2011). Thus, the Late Famennian palynomorph age determined for the Santa Iría metagreywackes (Pereira et al., 2008) is not compatible with detrital zircon data, which suggest instead a younger (Tournaisian?) age and, hence, pollen reworking. The zircon population at 605–620 Ma indicates erosion of a Cadomian/Pan-African magmatic arc. Finally, Mesoproterozoic and Paleoproterozoic sources have a minor and variable representation in the Santa Iría metagreywackes.

5.4. Ronquillo formation

According to the data given above, the maximum depositional age of this formation is 400 Ma, thus being compatible with the Givetian-lower Frasnian pollen-based age (Fig. 2.5; González et al., 2004). The source of these younger zircons may have been Caledonian-Appalachian igneous outcrops. As in most of the studied samples, the most abundant zircon population is late Neoproterozoic (608–630 Ma), pointing again to the Cadomian/Pan-African rocks as the main sedimentary source. Minor zircon populations of varied Mesoproterozoic and Paleoproterozoic age exist, the latter being usually dominant. Thus, both West African Craton (dominant) and Amazonian-Baltican rocks can be invoked as subordinate (direct or recycled via intermediate sediments) sources. Regarding regional correlations, the Ronquillo formation (inner SPZ) has the same detrital zircon content as the Ribeira de Limas formation (Pulo do Lobo belt in the northern SPZ). This fact, together with their similar age, lithology and deformation, allow us to correlate the Ronquillo and Ribeira de Limas formations on a firm basis.

5.5. PQ formation

The few younger zircons in the range 350–360 Ma in this formation are compatible with palynomorph data favouring a Late Famennian age (Fig. 2.6; Pereira et al., 2008). The late Neoproterozoic population is once again the dominant one, thus suggesting that Cadomian/Pan-African igneous rocks should have been the main source of sediments. The ≈2.0 Ga Paleoproterozoic zircon population, which presumably comes from the West African Craton, is minor in our samples, while Mesoproterozoic zircons are almost lacking.

5.6. Sehoul Cambrian metasandstones

The age of the youngest zircons (500–550 Ma) is compatible with the paleontological Middle Cambrian age of these rocks (Fig. 2.7). Nevertheless, the main population of inherited zircons is latest Neoproterozoic (550–630 Ma), once again indicating the main contribution of the Cadomian/Pan-African arc-magmatism as source of sediments. Regarding older sources, the Sehoul metasediments were dominantly influenced by the West African Craton (2.0 Ga). Thus, at Cambrian time, the Sehoul crust would have been attached to the Gondwana border, not far from its second source of zircons, the West African Craton. The Amazonian sources were either still farther or the sedimentary transport system was not favourable to bring Mesoproterozoic zircons into the Sehoul basin.

6. Discussion

6.1. Paleogeography and tectonic significance of the South Portuguese Zone

The lack of outcrops older than Devonian in the SPZ is a serious limitation that prevents direct stratigraphic and paleontological comparisons with other Variscan terranes, being at the same time an important constraint for inherited zircon analyses. In this regard, the

Ordovician-Silurian time-span corresponds to the drift apart of Avalonia from the Gondwana margin (e.g., Nysaether et al., 2002), yet the detritus arriving to the SPZ at that time is unknown. Thus, the presumed separation of the SPZ crust from the border of Gondwana, becoming part of the Avalonia microplate, cannot be properly tested through inherited zircon analysis in the SPZ. Detrital zircons in Ordovician-Devonian sediments from autochthonous northern Iberia provide with interesting information on the Gondwanan sources for that period (Pastor-Galán et al., 2013; Gutiérrez-Alonso et al., 2015). Unfortunately, these data are not relevant regarding the Avalonia wandering. Despite the limitations, inherited zircons in the SPZ still provide with some interesting arguments, as discussed below.

6.1.1. The basement of the South Portuguese Zone

The ages of xenocrystic zircons and inherited zircon cores from Variscan igneous rocks of the SPZ are scarce and include Mesoproterozoic (Amazonian?), late Neoproterozoic (Cadomian), Cambrian-Ordovician (rifting at the margin of Gondwana?) and Silurian (Caledonian-Appalachian?) (Barrie et al., 2002; Rosa et al., 2009), which collectively suggest an Avalonian affinity. According to these data, Paleoproterozoic zircons (≈2 Ga) are absent in the SPZ basement, in contrast to their prominent presence in other Iberian terranes, including the Devonian-Carboniferous cover of the SPZ. However and due to the scarce number of data, the apparent absence of ≈2.0 Ga in the SPZ basement is a suggestive but weak argument (Fedo et al., 2003). In addition, xenocrystic zircons can be affected by several factors such as nature of melting reactions, zircon dissolution kinetics in melts, etc. (Watson and Harrison, 1983; Bea and Montero, 2013).

The εNd model ages of the SPZ basement (0.9−1.2 Ga) are significantly younger than the exposed upper crust (0.8−1.8 Ga) (Braid et al., 2012). These contrasting model ages can be connected with the difference between zircon ages in basement and cover, suggesting that the Devonian-Carboniferous sediments may mainly derive from erosion of a Gondwanan crust, such as the one forming the neighboring OMZ (see section 6.2).

6.1.2. The outcropping sedimentary cover

Detrital zircon age populations in the sedimentary cover of the SPZ should be interpreted in terms of a composite terrane (Avalonia) that was close to or colliding with the Gondwana margin or peri-Gondwanan terranes at Middle Devonian-Carboniferous times. Accordingly, detrital sources of both Gondwana and Avalonia might be contributors to the Devonian-Carboniferous sediments of the SPZ. Despite the above, a number of interesting features can be denoted (Fig. 2.8):

    i) Considered as a whole, the SPZ Devonian-Carboniferous metasediments contain both Paleoproterozoic (usually dominant) and Mesoproterozoic zircons, though in minor quantities.

    ii) In a few Upper Devonian metasandstones (Horta da Torre formation; Fig. 2.8a), zircon populations of ≈1 Ga and between 1 and 2 Ga are very abundant, thus supporting

that a nearby Avalonian-type foreland was occasionally an important source of detritus at Devonian time. Furthermore, the zircon grains of this formation are smaller and more rounded than those from the other formations sampled, which suggest either long sedimentary transport or recycling of an older sedimentary unit.

iii) Late Neoproterozoic detrital zircons constitute the dominant population in most samples, due to the presumed great volume of the Cadomian/Pan-African igneous rocks and the close position of that magmatic arc to the northern border of Gondwana.

iv) Proximity of the SPZ basin to the Caledonian-Appalachian orogenic regions at Middle-Late Devonian time is inferred from the presence of small amounts of Silurian-earliest Devonian zircons in some samples of the Pulo do Lobo (Ribeira de Limas formation) and Ronquillo metasediments. Silurian zircons are abundant in the Horta da Torre formation (Figs. 2.3 and 2.8a) and have also been reported in PQ rocks (Pereira et al., 2012a). The additional presence of Mesoproterozoic zircons in the Horta da Torre formation suggests it to be the only one in the SPZ that can be really considered "exotic" in a sedimentary sense. Quite the opposite, the "exotic" interpretation that has been given to the lower formations of the Pulo do Lobo belt (Pulo do Lobo and Ribeira de Limas formations; Eden, 1991; Braid et al., 2011) cannot be sustained. Actually, based of zircon content, lithology and deformation, the Ribeira de Limas formation correlates well with the Ronquillo formation that crops out in the inner SPZ (Fig. 2.8b). This argument adds to the Early Carboniferous age of the metabasalts included in these rocks (Dahn et al., 2014; Pérez-Cáceres et al., 2015), thus questioning the interpretation of this unit as a Rheic-related (Silurian-Devonian) accretionary prism. The alternative proposal that the Rheic Ocean could have remained open until Mississippian times (e.g., Murphy et al., 2016) can be discarded, since collisional Devonian structures have been recognized in the southernmost OMZ (e.g., Fonseca and Ribeiro, 1993; Araújo et al., 2005; Ponce et al., 2012; Pérez-Cáceres et al., 2015).

v) A distinctive zircon population of early Variscan age (365-375 Ma) appears in the Upper Devonian lowermost Carboniferous rocks of the PQ and Santa Iría formations (Figs. 2.4, 2.6 and 2.8c). This population, which has also been reported in the coeval Tercenas formation at southernmost Portugal, points to a new source of detritus that likely corresponds to a missed magmatic Variscan arc (Pereira et al., 2012a). The same inherited zircon ages (365-375 Ma) are also present in the Upper Visean flysch of South Portugal (Pereira et al., 2014). Accordingly and considering the decline of this eo-Variscan population during the Late Carboniferous (see below), we hypothesize that the Variscan arc underwent its most intense erosion at late Famennian-late Visean times. Furthermore, the presence of a few 375-365 Ma and 1 Ga zircons in post-Paleozoic samples of SW Iberia has been interpreted as derived from either an authoctonous source (the above referred magmatic arc) or an exotic source (accretion of Meguma to Laurentia) (Dinis et al., 2016; Pereira et al., 2016).

vi) The Carboniferous flysch of the SPZ was fed from variable source of sediments (Pereira et al., 2012a and 2014; Rodrigues et al., 2015). Actually, early Variscan inherited zircons are dominant, though all of the range of meaningful ages has been reported: Caledonian-Appalachian, Cadomian/Pan-African, Mesoproterozoic and Paleoproterozoic

(Pereira et al., 2014, Rodrigues et al., 2015). These features point to the existence of a significant relief composed by a complex variety of rock units in the framework of the evolving Variscan collision.

vii) Finally, it is worth mentioning the zircon record in the late Carboniferous Buçaco basin, located north of the SPZ but next to the right-lateral Porto-Tomar shear zone, i.e., allegedly adjacent to docked Avalonian crust (Simancas et al., 2005). In this basin, coarse-grained beds mostly contain Pan-African and some Paleoproterozoic zircons, while sandy sediments show a high proportion of Mesoproterozoic and Paleozoic ages (Dinis et al., 2012). This scenario strongly suggests that an Avalonian-type crust (source of the Mesoproterozoic zircons) should have existed west of the Porto-Tomar fault. By restoring the dextral movement of the Porto-Tomar shear zone (Ribeiro et al. 1980), the crust currently west of the Buçaco basin shifts southwards to a position close to the SPZ, thus providing additional support to the Avalonian affinity of the SPZ.

To sum up, despite the lack at outcrop of Ordovician-Silurian rocks that could give direct support to the drift of the SPZ away from the border of Gondwana, there are indirect evidence on its Avalonian affinity. First, scarce xenocrystic zircons and εNd model ages suggest an Avalonian-type basement. Second and more important, among the variety of sedimentary sources suggested by detrital zircons there is unambiguous evidence of Caledonian-Appalachian sources close to the Devonian-Carboniferous SPZ basin.

6.1.3. The Sehoul Block in northern Morocco

The Caledonian-Appalachian deformation of the Sehoul Block relates this crustal area to Avalonia. However, the Sehoul Cambrian rocks contain a record of inherited zircons that is dominated by Gondwanan sources (Figs. 2.7 and 2.8d). The omnipresent Cadomian/Pan-African zircons tell us simply about the location of the Sehoul crust still attached to the Gondwana edge at Cambrian time. The Sehoul Block may have been located relatively close to its second source of zircons, namely the West African Craton, though a possible polycyclic derivation of zircons might complicate the paleogeographic picture. Apparently, the Amazonian sources would be farther at Cambrian time, yet the possibility that the sedimentary drainage was particularly unfavorable cannot be discarded. Finally, a particular feature of the Sehoul block is the presence of 367 Ma-old granitoids (Tahiri et al., 2010) that seem to be the only representation at current outcrop of the early Variscan volcanic arc witnessed by inherited zircons in the Santa Iría and PQ formations of the SPZ.

6.2. Cadomian/Pan-African tectonic frame of SW Iberia

The latest Neoproterozoic-Cambrian metasediments of the OMZ always exhibit Neoproterozoic and Paleoproterozoic detrital zircon populations, with a Mesoproterozoic gap (Fernández-Suárez et al., 2002; Pereira et al., 2012b; Cambeses, 2015) that suggests an ultimate source (polycyclic or direct) from the West African Craton. This distribution also indicates, as in most samples of Iberia, a strong detrital input from Cadomian/Pan-African igneous sources. Actually, the oldest magmatism that crops out in the OMZ belongs itself to the Cadomian/Pan-African orogen (Ordóñez-Casado, 1998; Bandrés et al., 2004).

The inherited zircons in Late Neoproterozoic-Early Paleozoic metasedimentary and igneous rocks of the CIZ exhibit Paleoproterozoic and Mesoproterozoic populations (Zeck et al., 2004; Bea et al., 2010; Abalos et al., 2012; Talavera et al., 2012; Fernández-Suárez et al., 2014; Shaw et al., 2014). The influence of these two types of Proterozoic sources is distinctive with respect to the OMZ and might correspond to a different position of these two continental pieces at the Gondwana border.
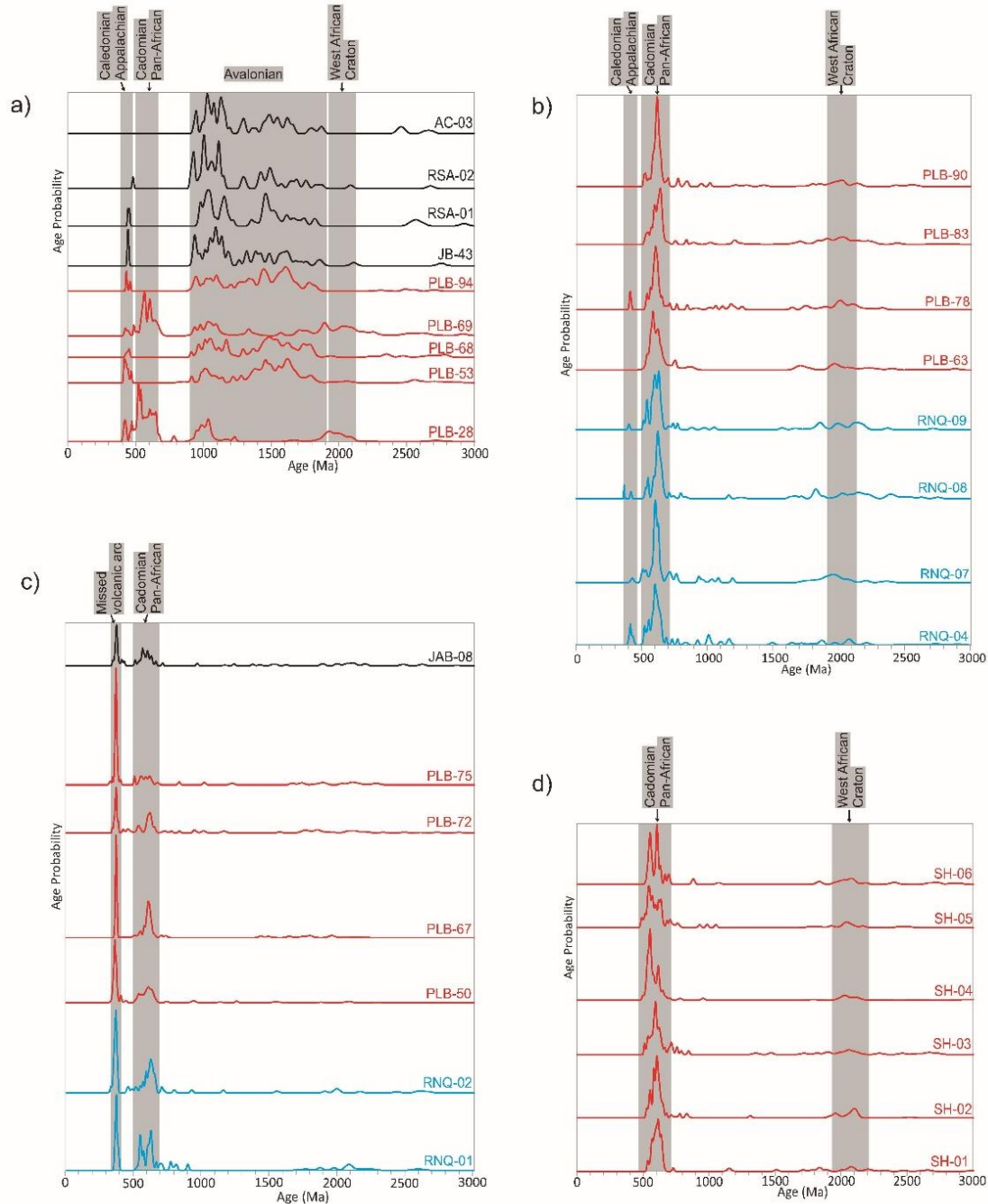
Figure 2.8. Comparative relative probability plots of U-Pb detrital zircon concordant ages for the different formations studied: (a) Samples in this study (red) and Braid et al. (2011) samples (black) of the Horta da Torre formation. (b) Samples of the Ronquillo formation (blue) and the Ribeira de Limas formation (red). (c) Samples of the PQ formation (blue) and the Santa Iría formation (red: this study; black: data from Braid et al., 2011). (d) Samples of the Sehoul Block (Moroccan Meseta). Our preferred interpretation of the main populations is indicated.

According to the above evidence, the OMZ would have been located at Neoproterozoic times close to the Eburnean Craton of West Africa, either at the border of the craton itself or at a short distance to the east in front of the Tuareg (Hoggar) shield, as favored by Cambeses (2015). As for the CIZ, the presence of a subordinate Mesoproterozoic zircon population indicates the contribution of a new sedimentary source, which has been persuasively located by Bea et al. (2010) at northeast Africa (Arabian-Nubian shield). Thus, the CIZ would have been located at Neoproterozoic time to the east of the OMZ.

A more detailed observation specifies that the Variscan boundaries between these two Iberian zones do not exactly match their detrital zircon difference: in SW Iberia the samples without Mesoproterozoic population appear not only in the OMZ but also some distance north of the OMZ/CIZ suture-like boundary. Our preferred interpretation is that inherited zircons mark a major contact of the Cadomian/Pan-African orogen, which juxtaposed a Cadomian terrane with single West-African influx to another one receiving also the influx of a ≈1 Ga Arabian-Nubian source (Bea et al., 2010) (Fig. 2.9). Actually, the suspicion of a major late Neoproterozoic contact hidden underneath the Carboniferous sediments of the so-called Pedroches basin can also be sustained on the ground of differences in the late Neoproterozoic sequences, i.e., the "Serie Negra" in the OMZ and southernmost CIZ versus the "Alcudian-Schist Greywacke Complex" to the north in the remaining CIZ (e.g., Valladares et al., 2002). Interestingly, the deformational and metamorphic imprint of the Andean-type Cadomian orogeny is elusive in most of southwest and central Iberia, the only clear Cadomian foliation and metamorphism having been found in outcrops close to that suspected major tectonic contact (Blatrix and Burg, 1981; Dallmeyer and Quesada, 1992; see discussion in Simancas et al., 2004).

According to the above and the available data on inherited zircon populations and basement outcrops from northern Africa to central Europe, we propose the schematic Cadomian/Pan-African tectonic frame shown in Fig. 2.9. To do so, we have plotted the available data on the Variscan tectonic frame discussed by Simancas et al. (2005) (Fig. 2.9 and references therein).

As shown in Fig. 2.9, the Iberian OMZ and the Saxo-Thuringian Zone in central Europe are distinctive with respect to their neighboring terranes by the presence in late Neoproterozoic-Cambrian sediments of ≈2.0 Ga detrital zircons, accompanied by a very minor ≈1 Ga population. In contrast, the CIZ and similar terranes in central Europe show inherited zircons of both ≈1.0 and ≈2.0 Ga. On the other hand, the late Neoproterozoic Pan-African suture bounding the West African Craton has been depicted in Fig. 2.10a-b converging obliquely with the Cadomian subduction boundary, based on a number of geological milestones. In the Anti-Atlas region of southern Morocco, the Pan-African orogeny consists of separate Neoproterozoic orogenic events closely related in space (Hefferan et al., 2014); the most spectacular exposure of the Pan-African suture is the Bou Azzer ophiolite, whose structure, kinematics and age of the obduction-collision (630−580 Ma) are well determined (El Hadi et al., 2010 and references therein). This suture must continue WNW before being dextrally displaced by the South Meseta Fault Zone (Michard et al., 2010). North of this fault, the continuity of the Pan-African suture through the Moroccan Variscides is uncertain, though it must be located east of the Rehamna massif

where the ≈2.0 Ga West African basement has been detected (Fig. 2.9; Dostal et al., 2005; Pereira et al., 2015). Further northwards, West African basements have been detected at the Galicia Bank off-shore NW Iberia (Avigad et al., 2012; Guerrot et al., 1989; Gardien et al., 2000) and at the so-called "Cadomian Domain" of the Cherbourg-Trégor region in NW France (Dercourt, 1997; Inglis et al., 2004). Overlying the West African basement, the Cadomian Domain of NW France is made up of tectonically bounded Neoproterozoic units (Chantraine et al., 2001), one of them being strikingly similar to the "Serie Negra" of SW Iberia. Moreover, the inherited zircon pattern age in these Neoproterozoic rocks is quite similar to the OMZ one (and the southernmost CIZ border) in SW Iberia (Fernández-Suárez et al., 2002; Strachan et al., 2014). In NW France, the Pan-African collisional belt would have been already merged into the Cadomian subduction orogen (Figs. 2.9 and 2.10). We suggest that the southern boundary of this particular domain was in essence a late Cadomian dextral fault zone imposed on the Pan-African/Cadomian orogenic belt, which served to approach West African and East African domains. To the west, this major Cadomian fault would have continued in the suspected tectonic contact hidden underneath the Pedroches Carboniferous basin, while in Morocco it might correspond to the eastern boundary of the Coastal Block (Michard et al., 2010). Our tentative interpretation (Fig. 2.10) is that blocking of the Pan-African collision gave way to a kinematics dominated by oblique convergence along the Cadomian subduction zone, which, in turn, partitioned into frontal shortening (subduction) and dextral strike-slip displacement of the magmatic arc.

Our paleogeographic Neoproterozoic reconstruction places the SPZ crust along the Gondwana margin, but west of the OMZ and CIZ, thus having an Avalonian-type basement (Murphy et al., 2006). On the contrary, most of the CIZ would have been located far to the east, receiving a mixed detrital influence from the Saharan Craton and the Arabian-Nubian Craton (Bea et al., 2010). In-between the SPZ and the big part of the CIZ, the OMZ plus the southernmost CIZ would have received significant detrital influence from the West African Craton, but not from eastern sources (Saharan and Arabian-Nubian cratons). The Pan-African suture that crops out at Bou Azzer runs through the Moroccan Meseta to SW Iberia (hidden below the Pedroches Basin, immediately north of the OMZ/CIZ boundary), and the Cherbourg-Trégor region (NW France), meeting the Cadomian subduction magmatic arc. At late Neoproterozoic time, tectonic slivering might have characterized the northern Gondwana margin (Fig. 2.10b), involving right-lateral displacements that juxtaposed the crustal piece formed by the OMZ plus southernmost CIZ to the crustal domain constituted by most of the CIZ and northern Iberia.

The subsequent Early Paleozoic rifting at the margin of Gondwana marks the onset of the Variscan cycle and gave way to a wide separation (Rheic Ocean) of the Avalonian terranes (SPZ in SW Iberia). At the same time, the OMZ terrane would have been drifted apart from the Gondwana margin to form a narrow ocean (Fig. 2.10c). On a broad orogenic scale, Murphy et al. (2006) argued that the site of initial rifting of the Rheic Ocean coincides with a Neoproterozoic suture responsible for the accretion of the Avalonian terranes to the cratonic border of Gondwana. Regarding the OMZ, its Early Paleozoic rifting seems to have taken place close to -but not coincident with- the main Cadomian boundary in SW Iberia, i.e., the Cadomian boundary is thought to be hidden under the

Pedroches Carboniferous basin, while the current OMZ/CIZ Variscan boundary (the suture of the Early Paleozoic rifting) crops out to the south (Burg et al., 1981; Azor et al., 1994) (Fig. 2.10d).

Zircon data: *(1) Guerrot et al. (1989); (2) Zeck and Whitehouse (1999); (3) Friedl et al. (2000); (4) Fernández-Suárez et al. (2000); (5) Fernández-Suárez et al. (2002); (6) De la Rosa et al. (2002); (7) Barrie et al. (2002); (8) Gutiérrez-Alonso et al. (2003); (9) Fernández-Suárez et al. (2003); (10) Linnemann et al. (2004); (11) Inglis et al. (2004); (12) Mingram et al. (2004); (13) Zeck et al. (2004); (14) Gutiérrez-Alonso et al. (2005); (15) Dostal et al. (2005); (16) Moecher et al. (2006); (17) Gerdes and Zeh (2006); (18) Linnemann et al. (2008); (19) Rosa et al. (2009); (20) Bea et al. (2010); (21) Abati et al. (2010); (22) Díez Fernández et al. (2010); (23) Braid et al. (2011); (24) Pereira et al. (2011); (25) Abalos et al. (2012); (26) Avigad et al. (2012); (27) Dinis et al. (2012); (28) Pereira et al. (2012a); (29) Talavera et al. (2012); (30) Braid et al. (2012); (31) Pastor-Galán et al. (2013); (32) Fernández-Suárez et al. (2014); (33) Linneman et al. (2014); (34) Pereira et al. (2014); (35) Fernández-Suárez et al. (2014); (36) Strachan et al.(2014); (37) Albert et al. (2015); (38) Orejana et al.(2015);(39) Pereira et al. (2015); (40) Rodrigues et al. (2015); (41) Cambeses (2015); (42) Margalef et al. (2016); (P) Pérez-Cáceres et al. (this paper).*

Figure 2.9. Summary of published ages of Proterozoic inherited zircons in Neoproterozoic and Paleozoic rocks plotted on a late Paleozoic Variscan/Alleghanian frame. Only inherited Paleo- and Mesoproterozoic zircons are considered, differentiating between samples with only Paleoproterozoic zircons and samples that also contain Mesoproterozoic zircons. WA (West African Craton basement), EA (East African Saharan and Nubian-Arabian craton basements), SPZ (South Portuguese Zone), SH (Sehoul Block).

7. Conclusions

1) The Avalonian affinity of the SPZ cannot unambiguously be tested drawing on inherited detrital zircons because the rocks attesting the drifting away from Gondwana (Ordovician-Silurian) do not crop out. Nevertheless, inherited zircons still provide with a number of arguments in favor of that hypothesis:

i.   Scarce xenocrystic zircons in granitoids and acid volcanic rocks of the SPZ show a composite ≈2.0 and ≈1.0 Ga cratonic provenance, with apparent dominance of the ≈1.0 Ga population. Despite the weakness of this evidence, it points however to an Avalonian basement.
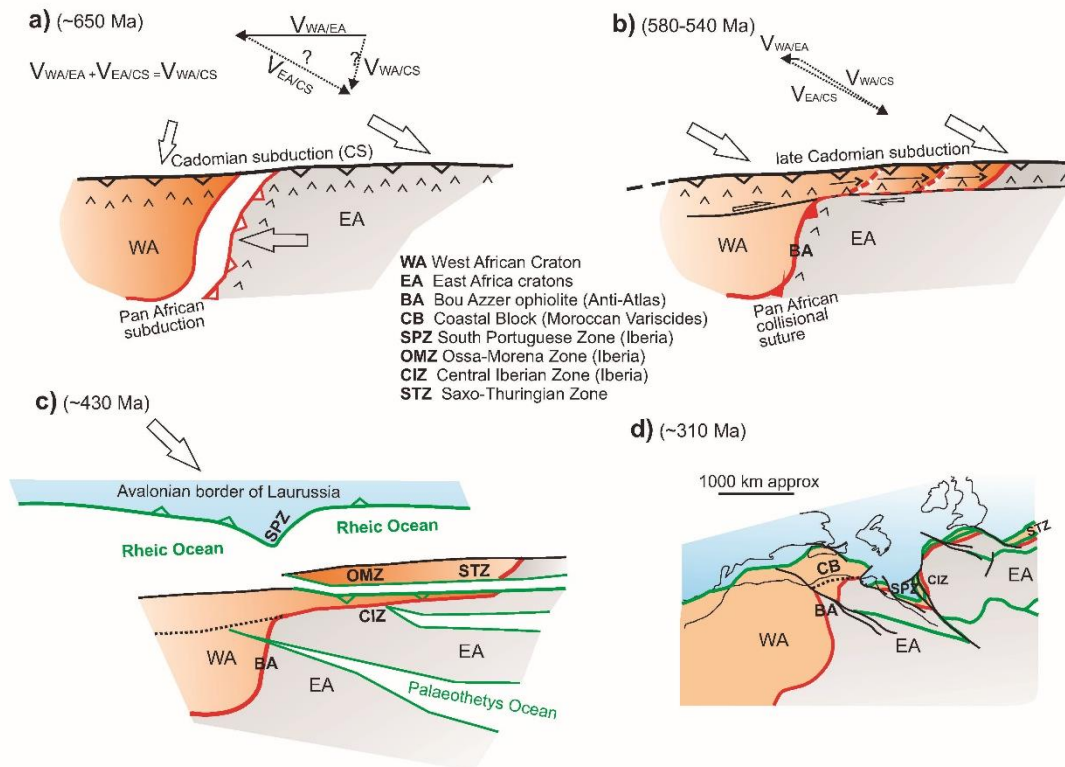
Figure 2.10. Sketch with the proposed large-scale tectonic/paleogeographic evolution of northern Gondwana from Neoproterozoic to Carboniferous times. The vectors (V) refer to relative displacements between plates.

ii.   Exceptional but plentiful presence of ≈1.0 Ga (and between 1.3 and 1.7 Ga) detrital zircons in the Horta da Torre formation at the northern SPZ prove its proximity at Late Devonian time to an Amazonian-Baltican sediment source (Avalonian foreland). The proximity of an Avalonian foreland (currently not visible at outcrop) is also inferred from the presence of ≈1.0 Ga detrital zircons in the Carboniferous flysch of the SPZ and the Late Carboniferous basin of Buçaco.

iii.   Recognition of ≈450 Ma detrital zircons in samples of the Horta da Torre and a minor population of ≈400 Ma in the Ribeira de Limas and Ronquillo formations also suggest that Caledonian-Appalachian sedimentary sources would not be too far at Middle-Late Devonian time.

2) The hypothesis of a missing (largely eroded) Variscan volcanic arc related to the Rheic subduction (Pereira et al., 2012a) is supported by zircon populations in the range 365−375 Ma found in samples of the PQ and Santa Iría formations (Late Devonian−Early Carboniferous), as well as in the flysch deposits of the SPZ (early-middle Carboniferous). Moreover, granitoids of 367 Ma are exposed in the Sehoul Block. However, despite the

presumed closeness of this Variscan arc for providing detritus, detrital zircons derived from it are always a subordinated population as compared to the one derived from the Late Neoproterozoic Cadomian/Pan-African arc. This latter arc could have been much more voluminous, since it has been the main source of detritus from Cambrian (e.g., the Sehoul rocks) to Carboniferous (SPZ) times.

3) The classical interpretation of the Pulo do Lobo belt at the northern SPZ as an exotic unit with respect to the SPZ must be reassessed. Actually, the Ribeira de Limas metasediments of the Pulo do Lobo belt are very similar in age, deformation and detrital zircon content to the Ronquillo formation that crops out in the inner SPZ. Interestingly, the Horta da Torre quartzitic formation that crops out just south of the OMZ/SPZ boundary is the only one in the SPZ that can be considered as "exotic" from a sedimentary point of view, exhibiting major influence of Mesoproterozoic and Caledonian-Appalachian (i.e., Avalonian-type) sources.

4) The observed difference in Proterozoic inherited zircons between Gondwanan regions with only Paleoproterozoic ages (the OMZ and southernmost CIZ in SW Iberia) and regions with both Paleo- and Mesoproterozoic ages (most of the CIZ) does not exactly match the Variscan suture that defines the OMZ/CIZ boundary (Fig. 2.9). This difference in Proterozoic zircon populations is interpreted as a major Cadomian/Pan-African tectonic contact laterally approaching West African and East African domains.

Acknowledgments

References

Abalos, B., Gil Ibarguchi, J.I., Sánchez-Lorda, M.E., Paquette, J.L., 2012. African/Amazonian Proterozoic correlations of Iberia: A detrital zircon U-Pb study of early Cambrian conglomerates from the Sierra de la Demanda (northern Spain). Tectonics 31, TC3003, doi: 10.1029/2011TC003041.

Albert, R., Arenas, R., Gerdes, A., Sánchez Martínez, S., Fernández-Suárez, J., Fuenlabrada, J.M., 2015. Provenance of the Variscan Upper Allochthon (Cabo Ortegal Complex, NW Iberian Massif). Gondwana Research 28, 1434-1448.

Andersen, T., Kristoffersen, M., Elburg, M., 2016. How far can we trust provenance and crustal evolution information from detrital zircons? A south African case study. Gondwana Reseach 34, 129-148.

Araújo, A., Fonseca, P., Munhá, J., Moita, P., Pedro, J., Ribeiro, A., 2005. The Moura Phyllonitic Complex: An accretionary complex related with obduction in the southern Iberia Variscan suture. Geodinamica Acta 18, 375-388.

Arenas, R., Sánchez Martínez, S., Gerdes, A., Albert, A., Díez Fernández, R., Andonaegui, P., 2014. Re-interpreting the Devonian ophiolites involved in the Variscan suture: U-Pb and Lu-Hf zircon data of the Moeche Ophiolite (Cabo Ortegal Complex, NW Iberia). International Journal of Earth Sciences 103, 1385-1402.

Avigad, D., Gerdes, A., Morag, N., Bechstädt, T., 2012. Coupled U-Pb-Hf of detrital zircons of Cambrian sandstones from Morocco and Sardinia: Implications for provenance and Precambrian crustal evolution of North Africa. Gondwana Research 21, 690-703, doi: 10.1016/j.gr.2011.06.005.

Azor, A., González Lodeiro, F., Simancas, J.F., 1994. Tectonic evolution of the boundary between the Central Iberian and Ossa-Morena zones (Variscan belt, southwest Spain). Tectonics 13, 45-61.

Azor, A., Rubatto, D., Simancas, J.F., González Lodeiro, F., Martínez Poyatos, D., Martín Parra, L.M., Matas, J., 2008. Rheic Ocean ophiolitic remnants in Southern Iberia questioned by SHRIMP U-Pb zircon ages on the Beja-Acebuches amphibolites, Tectonics, 27, TC5014, doi: 10.1029/2009TC002527.

Azor, A., Rubatto, D., Marchesi, C., Simancas, J.F., González Lodeiro, F., Martínez Poyatos, D., Martín Parra, L.M., Matas, J., 2009. Reply to comment by C. Pin and J. Rodríguez on "Rheic Ocean ophiolitic remnants in southern Iberia questioned by SHRIMP U-Pb zircon ages on the Beja-Acebuches amphibolites". Tectonics 28(5), TC5014, doi: 10.1029/2009TC002527.

Bandrés, A., Eguiluz, L., Pin, C., Paquette, J.L., Ordóñez-Casado, B., Le Fèvre, B., Ortega, L.A., Gil Ibaguchi, J.I., 2004. The northern Ossa-Morena Cadomian batholith (Iberian Massif): magmatic arc origin and early evolution. International Journal of Earth Sciences 93, 860-885.

Barrie, C.T., Amelin, Y., Pascual, E., 2002. U-Pb Geochronology of VMS mineralization in Iberian Pyrite Belt. Mineralium Deposita 37, 684-703.

Bea, F. and Montero, P., 2013. Diffusion-induced disturbances of the U-Pb isotope system in pre-magmatic zircon and their influence on SIMS dating. A numerical study. Chemical Geology 349-350, 1-17.

Bea, F., Montero, P., Talavera, C., Abu Anbar, M., Scarrow, J., Molina, J.F., Moreno, J.A., 2010. The palaeogeographic position of Central Iberia in Gondwana during the Ordovician: evidence from zircon geochronology and Nd isotopes. Terra Nova 22, 341-346, doi: 10.1111/j.1365-3121.2010.00957.

Blatrix, P., Burg, J.P., 1981. ^{40}Ar/^{39}Ar dates from the Sierra Morena (Southern Spain): Variscan metamorphism and Cadomian orogeny. Neues Jahrbuch für Mineralogie–Monatshefte 10, 470-478.

Braid, J.A., Murphy, J.B., Quesada, C., Mortensen, J., 2011. Tectonic escape of a crustal fragment during the closure of the Rheic Ocean: U-Pb detrital zircon data from the Late Palaeozoic Pulo do Lobo and South Portuguese zones, southern Iberia. Journal of the Geological Society of London 168, 383-392, doi: 10.1144/0016-76492010-104.

Braid, J.A., Murphy, J.B., Quesada, C., Bickerton, L., Mortensen, J., 2012. Probing the composition of unexposed basement, South Portuguese Zone, southern Iberia: implications for the connections between the Appalachian and Variscan orogens. Canadian Journal of Earth Sciences 49, 591-613, doi: 10.1139/E11-071.

Burg, J.P., Iglesias, M., Laurent, P., Matte, P., Ribeiro, A., 1981. Variscan intracontinental deformation: The Coimbra-Córdoba Shear zone (SW Iberian Peninsula). Tectonophysics 78, 161-177.

Cambeses, A., 2015. Ossa-Morena Zone Variscan "Calc-Alkaline" hybrid rocks: Interaction of mantle- and crustal-derived magmas as a result of intra-orogenic extension-related intraplating. Ph. D. Tesis, Universidad de Granada, 450 p.

Chantraine, J., Egal, E., Thiéblemont, D., Le Goff, E.L., Guerrot, C., Ballèvre, M., Guennoc, P., 2001. The Cadomian active margin (North Armorican Massif, France): a segment of the North Atlantic Pan African belt. Tectonophysics 331, 1-18.

Cocks, L.R.M., Torsvik, T.H., 2011. The Palaeozoic geography of Laurentia and western Laurussia: a stable craton with mobile margins. Earth-Science Reviews 106, 1–51.

Crespo-Blanc, A., Orozco, M., 1988. The southern Iberian shear zone: a major boundary in the Hercynian folded belt. Tectonophysics 148, 221-227.

Dahn, D.R.L., Braid, J.A., Murphy, J.B., Quesada, C., Dupuis, N., McFarlane, C.R.M., 2014. Geochemistry of the Peramora Melange and Pulo do Lobo schist: geochemical investigation and tectonic interpretation of mafic melange in the Pangean suture zone, Southern Iberia. International Journal of Earth Sciences 103, 1415-1431.

Dallmeyer, R.D., Quesada, C., 1992. Cadomian vs. Variscan evolution of the Ossa-Morena Zone (SW Iberia): field and $^{40}Ar/^{39}Ar$ mineral age constraints. Tectonophysics 216, 339-364.

Dercourt, J., 1997. Géologie et géodynamique de la France. Dunod, Paris, 320 p.

Díez Fernández, R., Martínez Catalán, J.R., Gerdes, A., Abati, J., Arenas, R., Fernández-Suárez, J., 2010. U-Pb ages of detrital zircons from the Basal allochthonous units of NW Iberia: Provenance and paleoposition on the northern margin of Gondwana during the Neoproterozoic and Paleozoic. Gondwana Research 18, 385-399, doi: 10.1016/j.gr.2009.12.006.

Dinis, P., Andersen, T., Machado, G., Guimaraes, F., 2012. Detrital zircon U-Pb ages of a late-Variscan Carboniferous succession associated with the Porto-Tomar shear zone (West Portugal): Provenance implications. Sedimentary Geology 273-274, 19-29, doi: 10.1016/j.sedgeo.2012.06.007.

Dinis, P.A., Dinis, J., Tassinari, C., Carter, A., Callapez, P., Morais, M., 2016. Detrital zircon geochronology of the Cretaceous succession from the Iberian Atlantic Margin: palaeogeographic implications. International Journal of Earth Sciences 105 (3), 727-745, doi: 10.1007/s00531-015-1221-z.

Dostal, J., Keppie, J.D., Hamilton, M.A., Aarab, E.M., Lefort, J.P., Murphy, B., 2005. Crustal xenoliths in Triassic lamprophyre dykes in western Morocco: tectonic implications for the Rheic Ocean suture. Geological Magazine 142, 159-172.

Eden, C.P., 1991. Tectonostratigraphic analysis of the northern extent of the oceanic exotic terrane, Northwestern Huelva Province, Spain. Ph. D. Thesis, University of Southhampton, 214 p.

Eden, C.P., Andrews, J.R., 1990. Middle to Upper Devonian mélanges in SW Spain and their relationship to the Meneage Formation in south Cornwall. Proceedings Ussher Society 7, 217-222.

El Hadi, H., Simancas, J.F., Martínez Poyatos, D., Azor, A., Tahiri, A., Montero, P., Fanning, C.M., Bea, F., González Lodeiro, F., 2010. Structural and geochronological contraints on the

evolution of the Bou Azzer Neoproterozoic ophiolite (Anti-Atlas, Morocco). Precambrian Research 182, 1-14, doi: 10.1016/j.precamres.2010.06.011.

Fedo, C.M., Sircombe, K.N., Rainbird, R.H., 2003. Detrital Zircon Analysis of the Sedimentary Record. Reviews in Mineralogy and Geochemistry 53, 277-303.

Fernández-Suárez, J., Gutiérrez-Alonso, G., Jeffries, T.E., 2002. The importance of along-margin terrane transport in northern Gondwana: insights from detrital zircon parentage in Neoproterozoic rocks from Iberia and Brittany. Earth and Planetary Science Letters 204, 75-88.

Fernández-Suárez, J., Díaz García, F., Jeffries, T.E., Arenas, R., Abati, J., 2003. Constraints on the provenance of the uppermost allochthonous terrane of the NW Iberian Massif: inferences from detrital zircon U-Pb ages. Terra Nova 15, 138-144, doi: 10.1046/j.1365-3121.2003.00479.

Fernández-Suárez, J., Gutiérrez-Alonso, G., Pastor-Galán, D., Hofmann, M., Murphy, J.B., Linnemann, U., 2014. The Ediacaran−Early Cambrian detrital zircon record of NW Iberia: possible sources and paleogeographic constraints. International Journal of Earth Sciences 103, 1335-1357.

Fonseca, P., Ribeiro, A., 1993. Tectonics of the Beja-Acebuches ophiolite - a major suture in the Iberian Variscan foldbelt. Geologische Rundschau 82, 440-447.

Fonseca, P., Munhá, J., Pedro, J., Rosas, F., Moita, P., Araujo, A., Leal, N., 1999. Variscan ophiolites and high-pressure metamorphism in southern Iberia. Ofioliti, 24, 259-268.

Franke, W., 2000. The mid-European segment of the Variscides: tectonostratigraphic units, terrane boundaries and plate tectonic evolution. Geological Society, London, Special Publications, 179, 35-61.

Friedl, G., Finger, F., McNaughton, N.J., Fletcher, I.R., 2000. Deducing the ancestry of terranes: SHRIMP evidence for South America-derived Gondwana fragments in central Europe. Geology 28, 1035-1038.

Gardien, V., Arnaud, N., Desmurs, L., 2000. Petrology and Ar-Ar dating of granulites from the Galicia Bank (Spain): African craton relics in Western Europe. Geodinamica Acta 13, 103-117.

Gehrels, G., 2012. Detrital zircon U-Pb geochronology: Current methods and new opportunities. In Busby, C., Azor, A. (Eds.), Tectonics of Sedimentary Basins: Recent Advances, p. 45-62. doi: 10.1002/9781444347166.ch2.

Gerdes, A., Zeh, A., 2006. Combined U-Pb and Hf isotope LA-(MC-)ICP-MS analyses of detrital zircons: Comparison with SHRIMP and new constraints for the provenance and age of an Armorican metasediment in Central Germany. Earth and Planetary Science Letters 249, 47-61.

Gómez-Pugnaire, M.T., Azor, A., Fernández Soler, J.M., and López Sánchez-Vizcaíno, V., 2003. The amphibolites from the Ossa-Morena/Central Iberian Variscan suture (southwestern Iberian Massif): Geochemistry and tectonic interpretation. Lithos, 68(1−2), 23-42, doi: 10.1016/S0024-4937(03)00018-5.

González, F., Moreno, C., López, M.J., Dino, R., Antonioli, L., 2004. Palinoestratigrafía del Grupo Pizarroso-cuarcítico del sector más oriental de la Faja Pirítica Ibérica, SO de España. Revista Española de Micropaleontología 36, 279-304.

Guerrot, C., Peucat, J.J., Capdevila, R., Dosso, L., 1989. Archean protoliths within Early Proterozoic granulitic crust of the west European Hercynian belt: Possible relics of the west African craton. Geology 17, 242-244.

Gutiérrez-Alonso, G., Fernández-Suárez, J., Jeffries, T., Jenner, G.A., Tubret, M.N., Cox, R., Jackson, S.E., 2003. Terrane acretion and dispersal in the northern Gondwana margin. An Early analogue of a long-lived active margin. Tectonophysics 365, 221-232, doi: 10.1016/S0040-1951(03)00023-4.

Gutiérrez-Alonso, G., Fernández-Suárez, J., Collins, A.S., Abad, I., Nieto, F., 2005. Amazon and Mesoproterozoic basement in the core of the Ibero-Armorican Arc: ^{40}Ar/^{39}Ar detrital mica ages complement the zircon's tale. Geology 33, 637-640, doi: 10.1130/G21485.1.

Gutiérrez-Alonso, G., Fernández-Suárez, J., Pastor-Galán, D., Johnston, S.T., Linnemann, U., Hofmann, M., Shaw, J., Colmenero, J.R., Hernández, P., 2015. Significance of detrital zircons in Siluro-Devonian rocks from Iberia. Journal of the Geological Society 172, 309-322.

Gutiérrez-Marco, J.C., Robardet., M., Rábano, I., Sarmiento, G.N., San José, M.A., Herranz, P., Pieren, A.P., 2002. Ordovician. Chapter 4. In: Gibbons, W., Moreno, T. (Eds.), The Geology of Spain. Geological Society, London. 31-49.

Hefferan, K., Soulaimani, A., Samson, S.D., Admou, H., Inglis, J., Saquaque, A., Latifa, C., Heywood, N., 2014. A Reconsideration of Pan African Orogenic Cycle in the Anti-Atlas Mountains, Morocco. Journal of African Earth Sciences 98, 34-46.

Henderson, B.J., Collins, W.J., Murphy, J.B., Gutiérrez-Alonso, G., Hand, M., 2016. Gondwanan basement terranes of the Variscan-Appalachian orogen: Baltican, Saharan and West African hafnium isotopic fingerprints in Avalonia, Iberia and the Armorican Terranes. Tectonophysics 681, 278-304.

Inglis, J.D., Samson, S.D., Lemos, R.S.D., Hamilton, M., 2004. U-Pb geochronological constraints on the tectonothermal evolution of the Paleoproterozoic basement of Cadomia, La Hague, NW France. Precambrian Research 134, 293-315.

Leeder, M.E., 1982. Sedimentology. George Allen & Unwin. London. 344 p.

Linnemann, U., McNaughton, N.J., Romer, R.L., Gehmlich, M., Drost, K., Tonk, C., 2004. West African provenance for Saxo-Thuringia (Bohemian Massif): Did Armorica ever leave pre-Pangean Gondwana? U/Pb-SHRIMP zircon evidence and the Nd-isotopic record. International Journal of Earth Sciences 93, 683-705.

Linnemann, U., Herbosch, A., Liégeois, J.P., Pin, C., Gärtner, A., Hofmann, M., 2012. The Cambrian to Devonian odyssey of the Brabant Massif within Avalonia: A review with new zircon ages, geochemistry, Sm-Nd isotopes, stratigraphy and palaeogeography. Earth-Science Reviews 112 (3-4), 126-154, doi: 10.1016/j.earscirev.2012.02.007.

Martínez Catalán, J.R., 2011. Are the oroclines of the Variscan belt related to late Variscan strike-slip tectonics? Terra Nova 23(4): 241-247.

Martínez Catalán, J.R., 2012. The Central Iberian arc, an orocline centered in the Iberian Massif and some implications for the Variscan belt. International Journal of Earth Sciences 101(5): 1299-1314.

Martínez Catalán, J.R., Arenas, R., Díaz García, F., Abati, J., 1997. Variscan accretionary complex of northwest Iberia: Terrane correlation and succession of tectonothermal events. Geology 25, 1103-1106.

Matte, P., 2001. The Variscan collage and orogeny (480-290 Ma) and the tectonic definition of the Armorica microplate: a review. Terra Nova 13, 122-128.

Michard, A., Soulaimani, A., Hoepffner, C., Ounaimi, H., Baidder, L., Rjimati, E.C., Saddiqi, O., 2010. The South-Western Branch of the Variscan Belt: Evidence from Morocco. Tectonophysics 492, 1-24.

Moecher, D.P., Samson, S.D., 2006. Differential zircon fertility of source terranes and natural bias in the detrital zircon record: Implications for sedimentary provenance analysis. Earth and Planetary Science Letters 247, 252-266, doi: 10.1016/j.epsl.2006.04.035.

Montero, P., Bea, F., González-Lodeiro, F., Talavera, C., Whitehouse, M.J., 2007. Zircon ages of the metavolcanic rocks and metagranites of the Ollo de Sapo Domain in central Spain: implications for the Neoproterozoic to Early Palaeozoic evolution of Iberia. Geological Magazine 144, 963-976, doi: 10.1017/S0016756807003858.

Murphy, J.B., 2007. Geological evolution of middle to late Paleozoic rocks in the Avalon terrane of northern mainland Nova Scotia, Canadian Appalachians: A record of tectonothermal activity along the northern margin of the Rheic Ocean in the Appalachian-Caledonide orogen. Geological Society of America, Special Paper 423, 413-435. doi: 10.1130/2007.2423(20).

Murphy, J.B., Stracham, R.A., Nance, R.D., Parker, K.D., Fowler, M.B., 2000. Proto-Avalonia: A 1.2−1.0 Ga tectonothermal event and constraints for the evolution of Rodinia. Geology 28, 1071-1074.

Murphy, J.B., Eguiluz, L., Zulauf, G., 2002. Cadomian Orogens, peri-Gondwanan correlatives and Laurentia-Baltica connections. Tectonophysics 352, 1-9.

Murphy, J.B., Fernández-Suárez, J., Keppie, J.D., Jeffries, T.E., 2004. Continuous rather than discrete Paleozoic histories for the Avalon and Meguma terranes based on detrital zircon data. Geology 32, 585-588, doi: 10.1130/G20351.1.

Murphy, J.B., Gutiérrez-Alonso, G., Nance, R.D., Fernández-Suárez, J., Keppie, J.D., Quesada, C., Strachan, R.A., Dostal, J., 2006. Origin of the Rheic Ocean: Rifting along a Neoproterozoic suture? Geology 34, 325-328.

Murphy, J.B., Quesada, C., Gutiérrez-Alonso, G., Johnston, S.J., Weil, A., 2016. Reconciling competing models for the tectono-stratigraphic zonation of the Variscan orogen in Western Europe. Tectonophysics 681, 209-219.

Nance, R.D., Gutiérrez-Alonso, G., Keppie, J.D., Linnemann, U., Murphy, J.B., 2010. Evolution of the Rheic Ocean. Gondwana research 17, 194-222.

Nysaether, E., Torsvik, T.H., Feist, R., Walderhaug, H.J., Eide, E.A., 2002. Ordovician palaeogeography with new palaeomagnetic data from the Montagne Noir (Southern France). Earth and Planetary Science Letters 203, 329-341.

Oliveira, J.T., 1990. The South Portuguese Zone. Stratigraphy and Synsedimentary Tectonism. In: Dallmeyer, R.D., Martínez-García, E., (Eds.), Pre-Mesozoic Geology of Iberia. Springer Verlag, Berlin, 334-347.

Ordóñez-Casado, B., 1998. Geochronological studies of the Pre-Mesozoic basement of the Iberian Massif: the Ossa-Morena Zone and the Allochthonous Complexes within the Central Iberian Zone. Ph.D. Thesis, ETH Zurich, 235 p.

Pastor-Galán, D., Gutiérrez-Alonso, G., Murphy, J.B., Fernández-Suárez, J., Hofman, M., Linnemann, U., 2013. Provenance analysis of the Paleozoic sequences of the northern Gondwana margin in NW Iberia: Passive margin to Variscan collision and orocline development. Gondwana Research 23, 1089-1103.

Pereira, M. F., Chichorro, M., Williams, I.S., Silva, J.B., Fernández, C., Díaz-Azpíroz, M., Apraiz, A., Castro, A., 2009. Variscan intra-orogenic extensional tectonics in the Ossa-Morena Zone (Évora-Aracena-Lora del Río metamorphic belt, SW Iberian Massif): SHRIMP zircon U-Th-Pb geochronology. Geological Society, London, Special Publications, 327(1), 215-237.

Pereira, M.F., Chichorro, M., Johnston, S.T., Gutiérrez-Alonso, G., Silva, J.B., Linnemann, U., Hofmann, M., Drost, K., 2012a. The missing Rheic Ocean magmatic arcs: Provenance analysis of Late Paleozoic sedimentary clastic rocks of SW Iberia. Gondwana Research 22, 882-891, doi: 10.1016/j.gr.2012.03.010.

Pereira, M.F., Solá, A.R., Chichorro, M., Lopes, L., Gerdes, A., Silva, J.B., 2012b. North-Gondwana assembly, break-up and paleogeography: U-Pb isotope evidence from detrital and igneous zircons of Ediacaran and Cambrian rocks of SW Iberia. Gondwana Research 22 (3–4), 866-881.

Pereira, M.F., Ribeiro, C., Vilallonga, F., Chichorro, M., Drost, K., Silva, J.B., Albardeiro, L., Hofmann, M., Linnemann, U., 2014. Variability over time in the sources of South Portuguese Zone turbidites: evidence of denudation of different crustal blocks during the assembly of Pangea. International Journal of Earth Sciences 103, 1453-1470, doi: 10.1007/s00531-013-0902-8.

Pereira, M.F., El Houicha, M., Chichorro, M., Armstrong, R., Jouhari, A., El Attari, A., Ennih, N., Silva, J.B., 2015. Evidence of a Paleoproterozoic basement in the Moroccan Variscan Belt (Rehamna Massif, Western Meseta). Precambrian Research 268, 61-73.

Pereira, M.F., Ribeiro, C., Gama, C., Drost, K., Chichorro, M., Vilallonga, F., Hofmann, M., Linnemann, U., 2016. Provenance of upper Triassic sandstone, southwest Iberia (Alentejo and Algarve basins): tracing variability in the sources. Int. J. Earth Sci. 1-15, doi: 10.1007/s00531-016-1295-2.

Pereira, Z., Matos, J., Fernandes, P., Oliveira, J.T., 2008. Palynostratigraphy and systematic palynology of the Devonian and Carboniferous successions of the South Portuguese Zone, PORTUGAL. Memórias Geológicas do Instituto Nacional de Engenharia, Tecnologia e Inovaçao 34, Lisboa.

Pérez-Cáceres, I., Martínez Poyatos, D., Simancas, J.F., Azor, A., 2015. The elusive nature of the Rheic Ocean in SW Iberia. Tectonics 34, 2429-2450, doi: 10.1002/2015TC003947.

Pérez-Estaún, A., Bastida, F., Alonso, J.L., Marquínez, J., Aller, J., Álvarez-Marrón, J., Marcos, A., Pulgar, J.A., 1988. A thin-skinned tectonics model for an arcuate fold and thrust belt: The Cantabrian Zone (Variscan Ibero-Armorican Arc). Tectonics 7, 517-537.

Ponce, C., Simancas, J.F., Azor, A., Martínez Poyatos, D., Booth-Rea, G., Expósito, I., 2012. Metamorphism and kinematics of the early deformation in the Variscan suture of SW Iberia. Journal of Metamorphic Geology, 30, 625-638.

Ribeiro, A., Pereira, E., Severo, L., 1980. Análise da deformaçao da zona de cisalhament Porto-Tomar na transversal de Oliveira de Azeméis, Comunicações dos Serviços Geológicos de Portugal, 66, 3-9.

Rodrigues, B., Chew, D.M., Jorge, R.C.G.S., Fernandes, P., Veiga-Pires, C., Oliveira, J.T., 2015. Detrital zircon geochronology of the Carboniferous Baixo Alentejo Flysch Group (South Portugal); constraints on the provenence and geodynamic evolution of the South Portuguese Zone. Journal of the Geological Society of London 172, 294-308, doi: 10.1144/jgs2013-084.

Rosa, D.R.N., Finch, A.A., Andersen, T., Inverno, C.M.C., 2009. U-Pb geochronology and Hf isotope ratios of magmatic zircons from the Iberian Pyrite Belt. Mineralogy and Petrology 95, 47-69.

Schermerhorn, J.L.G., 1971. An outline stratigraphy of the Pyrite Belt. Boletín Geológico Minero 82, 239-268.

Shaw, J., Gutierrez-Alonso, G., Johnston, S.T., Pastor-Galán, D., 2014. Provenance variability along the Early Ordovician north Gondwana margin: Paleogeographic and tectonic implications of U-Pb detrital zircon ages from the Armorican Quartzite of the Iberian Variscan belt. Geological Society of America Bulletin, 126(5–6), 702-719. doi: 10.1130/B30935.1.

Simancas, J.F., 1983. Geología de la extremidad oriental de la Zona Sudportuguesa. Ph.D. Thesis, Universidad de Granada. 439 p.

Simancas, J.F., Martínez Poyatos, D., Expósito, I., Azor, A., González Lodeiro, F., 2001. The structure of a major suture zone in the SW Iberian Massif: the Ossa-Morena/Central Iberian contact. Tectonophysics, 332(1-2), 295-308.

Simancas, J.F., Carbonell, R., González Lodeiro, F., Pérez-Estaún, A., Juhlin, C., Ayarza, P., Kashubin, A., Azor, A., Martínez Poyatos, D., Almodóvar, G.R., Pascual, E., Sáez, R., Expósito, I., 2003. Crustal structure of the transpressional Variscan orogen of SW Iberia: SW Iberia deep seismic reflection profile (IBERSEIS). Tectonics, 22(6), doi: 10.1029/2002TC001479.

Simancas, J.F., Expósito, I., Azor, A., Martínez Poyatos, D., González Lodeiro, F., 2004. From the Cadomian orogenesis to the Early Palaeozoic Variscan rifting in Southwest Iberia. Journal of Iberian Geology 30, 53-71.

Simancas, J.F., Tahiri, A., Azor, A., González Lodeiro, F., Martínez Poyatos, D., El Hadi, H., 2005. The tectonic frame of the Variscan-Alleghanian orogen in southern Europe and northern Africa. Tectonophysics 398, 181-198.

Simancas, J.F., Carbonell, R., González Lodeiro, F., Pérez Estaún, A., Juhlin, C., Ayarza, P., Kashubin, A., Azor, A., Martínez Poyatos, D., Sáez, R., Almodóvar, G.R., Pascual, E., Flecha, I., Martí, D., 2006. Transpressional collision tectonics and mantle plume dynamics: the Variscides of southwestern Iberia. Geological Society, London, Memoirs, 32(1), 345-354.

Sircombe, K.N., Freeman, M.J., 1999. Provenance of detrital zircons on the Western Australian coastline: implications for the geologic history of the Perth basin and denudation of the Yilgan craton. Geology 27, 879-882.

Stampfli, G.M., Hochard, C., Vérard, C., Wilhem, C., Von Raumer J., 2010. The formation of Pangea. Tectonophysics 593, 1-19.

Strachan, R.A., Linnemann, U., Jeffries, T., Drost, K., Ulrich, J., 2014. Armorican provenance for the mélange deposits below the Lizard ophiolite (Cornwall, UK): evidence for Devonian obduction of Cadomian and Lower Palaeozoic crust onto the southern margin of Avalonia. International Journal of Earth Sciences 103, 1359-1383.

Tahiri, A., Montero, P., El Hadi, H., Martínez Poyatos, D., Azor, A., Bea, F., Simancas, J.F., González Lodeiro, F., 2010. Geochronological data on the Rabat-Tiflet granitoids: Their bearing on the tectonics of the Moroccan Variscides. Journal of African Earth Sciences 57, 1-13.

Talavera, C., Montero, P., Martínez Poyatos, D., Williams, I.S., 2012. Ediacaran to Lower Ordovician age for rocks ascribed to the Schist-Graywacke Complex (Iberian Massif, Spain): Evidence from detrital zircon SHRIMP U-Pb geochronology. Gondwana Research 22, 928-942, doi: 10.1016/j.gr.2012.03.008.

Valladares, M.I., Barba, P., Ugidos, J.M., 2002. Precambrian. In: Gibbons, W., Moreno, T. (Eds.), The Geology of Spain, 7-16, Geological Society, London.

Waldron, J.W.F., Schofield, D.I., White, C.E., Barr, S.M., 2011. Cambrian successions of the Meguma Terrane, Nova Scotia, and Harlech Dome, North Wales: dispersed fragments of a peri-Gondwanan basin? Journal of the Geological Society 168, 83-98. doi: 10.1144/0016-76492010-068.

Watson, E.B., Harrison, T.M., 1983. Zircon saturation revisited: temperature and composition effects in a variety of crustal magma types. Earth and Planetary Science Letters 64, 295-304.

Zeck, H.P., Wingate, M.T.D., Pooley, G.D., Ugidos, J.M., 2004. A sequence of Pan-African and Hercynian Events Recorded in Zircons from an Orthogneiss from the Hercynian Belt of Western Central Iberia - an Ion Microprobe U-Pb Study. Journal of Petrology 45, 1613-1629, doi: 10.1093/petrology/egh026.

Zimmerman, U., Anderson, T., Madland, M.V., Larse, I.S., 2015. The role of U-Pb ages of detrital zircons in sedimentology-An alarming case study for the impact of sampling for provenance interpretation. Sedimentary Geology 320, 38-50.

Chapter III

Structure of the Ossa-Morena/South-Portuguese boundary

This chapter deals with the complex Variscan tectonothernal imprints at the boundary between the Ossa-Morena and South Portuguese zones, which have been responsible for the cryptic appearance of the Rheic Ocean suture in SW Iberia. New structural and geochronological data are reported to reinterpret the Beja-Acebuches and the Pulo do Lobo units and confirm the existence of an intracollisional transtensional stage that interrupted the Variscan collision at early Carboniferous time.

The structure of the boundary between the Ossa-Morena and South Portuguese zones has been studied in detail through structural mapping, with focus on the Beja-Acebuches amphibolites and the Pulo do Lobo unit. To do so, the geological maps of the Instituto Geológico y Minero de España (MAGNA series at 1:50.000-scale, sheets 915, 916, 917, 918, 919, 936, 937 and 938; Barranco et al., 1983; Apalategui et al., 1983, 1984, 1990; Jerez Mir and García Monzón, 1973; Gonzalo et al., 1978; Contreras and Santos, 1984; Navarro and Ramírez Copeiro del Villar, 1978) and the geological map of Portugal at 1:500.000-scale from the Serviços Geológicos de Portugal (Oliveira and Pereira, 1992) have been used as a starting point. Accordingly, a new geological map of this boundary is added as Appendix 8, with some enlarged sectors where the structural study was more detailed.

The elusive nature of the Rheic Ocean suture in SW Iberia

Irene Pérez-Cáceres[1], David Martínez Poyatos[1], José Fernando Simancas[1], and Antonio Azor[1].

1 Departamento de Geodinámica, Facultad de Ciencias, Universidad de Granada, Campus de Fuentenueva s/n, 18071 Granada, Spain.

Abstract

The Rheic Ocean suture resulted from pre-Carboniferous oceanic subduction followed by Late Devonian-Carboniferous Variscan collision. In SW Iberia, this suture has been classically located along the boundary between the Ossa-Morena and South Portuguese Zones based on the presence of three units: (i) a conspicuous metamafic unit (Beja-Acebuches) that crops out along this boundary and has been interpreted as a pre-Carboniferous Rheic Ocean ophiolite; (ii) a low-grade metasedimentary unit with minor mid-ocean ridge basalt-like lithologies (Pulo do Lobo unit), thought to represent a Rheic Ocean subduction-related accretionary prism; and (iii) the allochthonous Cubito-Moura unit that contains high-pressure and ophiolitic-like rocks. We report new structural and geochronological data that allow us to reinterpret the origin and internal structure of the Beja-Acebuches and the Pulo do Lobo units. Thus, both the Beja-Acebuches protoliths and the Pulo do Lobo metabasalts would have been formed in the context of an intracollisional extensional stage that interrupted the Variscan collision at early Carboniferous time, after the Rheic Ocean consumption, and the first continental collision. Later on, collision was resumed in an oblique left-lateral regime that gave way to coeval frontal (folds and thrusts) and lateral (shear zones and strike-slip faults) structures, with variable pressure-temperature conditions and space distribution along time. As a consequence of the superposition of transtension and complex transpression, the Rheic suture in SW Iberia has an obscure nearly cryptic appearance.

Keywords

Beja-Acebuches Unit

Peramora Mélange

Iberian Variscides

Pulo do Lobo unit

Left-lateral oblique collision

Keypoints

Variscan evolution of the Ossa-Morena/South Portuguese zone boundary.

Early carboniferous transtension and mafic magmatism in SW Iberia.

Transpression produced spatial and temporal strain partitioning in SW Iberia.

1. Introduction

The preorogenic paleogeography of continents and location of oceanic sutures involved in old collisional orogens are usually challenging to geologists. The main reason is the obscuring effect of superimposed collisional/transcurrent tectonothermal imprints, which may turn difficult the recognition of previous continent boundaries (e.g., Dewey, 1977; Schulmann et al., 2014). In this respect, the Late Paleozoic Variscan orogen in SW Iberia (Fig. 3.1) can be taken as an excellent example of complex and cryptic suture, where the supposed remnants of the Rheic Ocean are being continuously reinterpreted in the light of new structural and geochronological data.

This paper aims to offer a complete reinterpretation of the Variscan continental convergence in SW Iberia based on previous studies and new structural and geochronological data. First, we critically summarize the arguments leading to propose the boundary between the Ossa-Morena Zone (OMZ) and the South Portuguese Zone (SPZ) in SW Iberia as the site of obliteration of the Rheic Ocean lithosphere (Fig. 3.1). Then, we focus on the Variscan collisional tectonothermal imprints, which account for the progressive blurring of the features that characterize the OMZ/SPZ boundary as a suture.
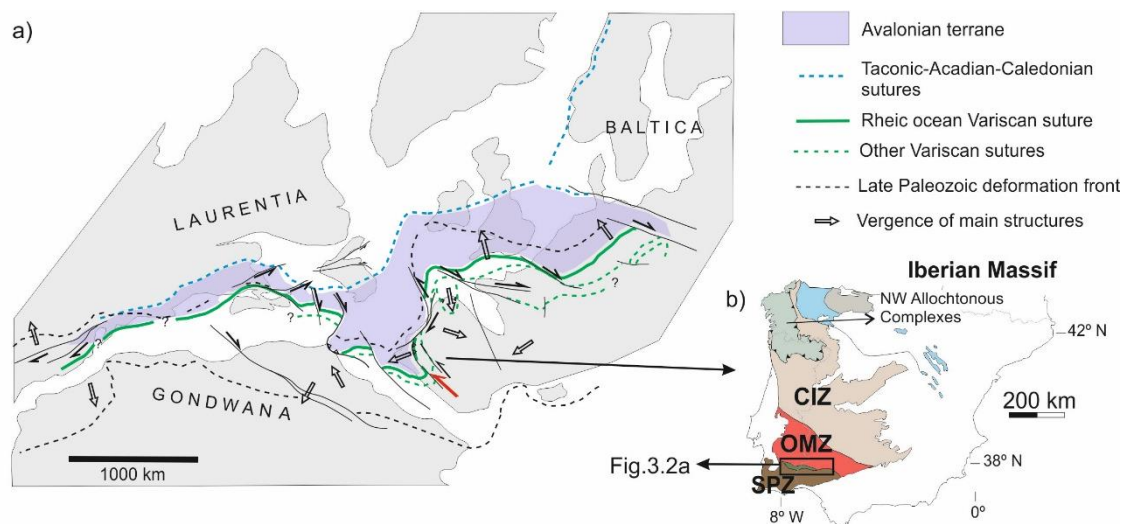
Figure 3.1. a) Reconstruction of the Variscan-Alleghanian orogenic frame at Late Carboniferous time (simplified from Simancas et al., 2005). The Avalonian continental fragment and the inferred Rheic Ocean and other second-order Variscan sutures are depicted. The SW Iberian (Rheic?) suture is hilighted in red. b) Geological subdivision of the Iberian Massif. CIZ: Central Iberian Zone, OMZ: Ossa-Morena Zone, SPZ: South Portuguese Zone.

2. Geological setting

Five geological units with different tectonometamorphic evolutions can be distinguished at the OMZ/SPZ boundary. All of these units run parallel to this collisional boundary (Fig. 3.2) and are introduced below from north to south:

(i) An allochthonous unit with mid-ocean ridge basalt (MORB)-featured metamafic rocks, eclogites and high-pressure metasediments, namely the Cubito-Moura unit, thrust onto the

southern OMZ (Fonseca et al., 1999; Araujo et al., 2005; Booth-Rea et al., 2006; Ponce et al., 2012).

(ii) The southernmost edge of the para-autochthonous OMZ: a 2–6 km-wide belt of high-temperature/low-pressure metamorphic rocks (gneisses, marbles, migmatites and amphibolites) and gabbros (Bard, 1977; Crespo-Blanc, 1991; Díaz Azpiroz et al., 2006).

(iii) The Beja-Acebuches (BA) unit: a conspicuous strip of metamafic rocks, from greenschists to metagabbros (locally ultramafic rocks), classically considered the suture boundary between the OMZ and the SPZ (e.g., Bard, 1977; Crespo-Blanc, 1991; Quesada et al., 1994; Díaz Azpiroz and Fernández, 2003). This unit crops out continuously along the boundary, with a maximum outcrop-width of 3.5 km.
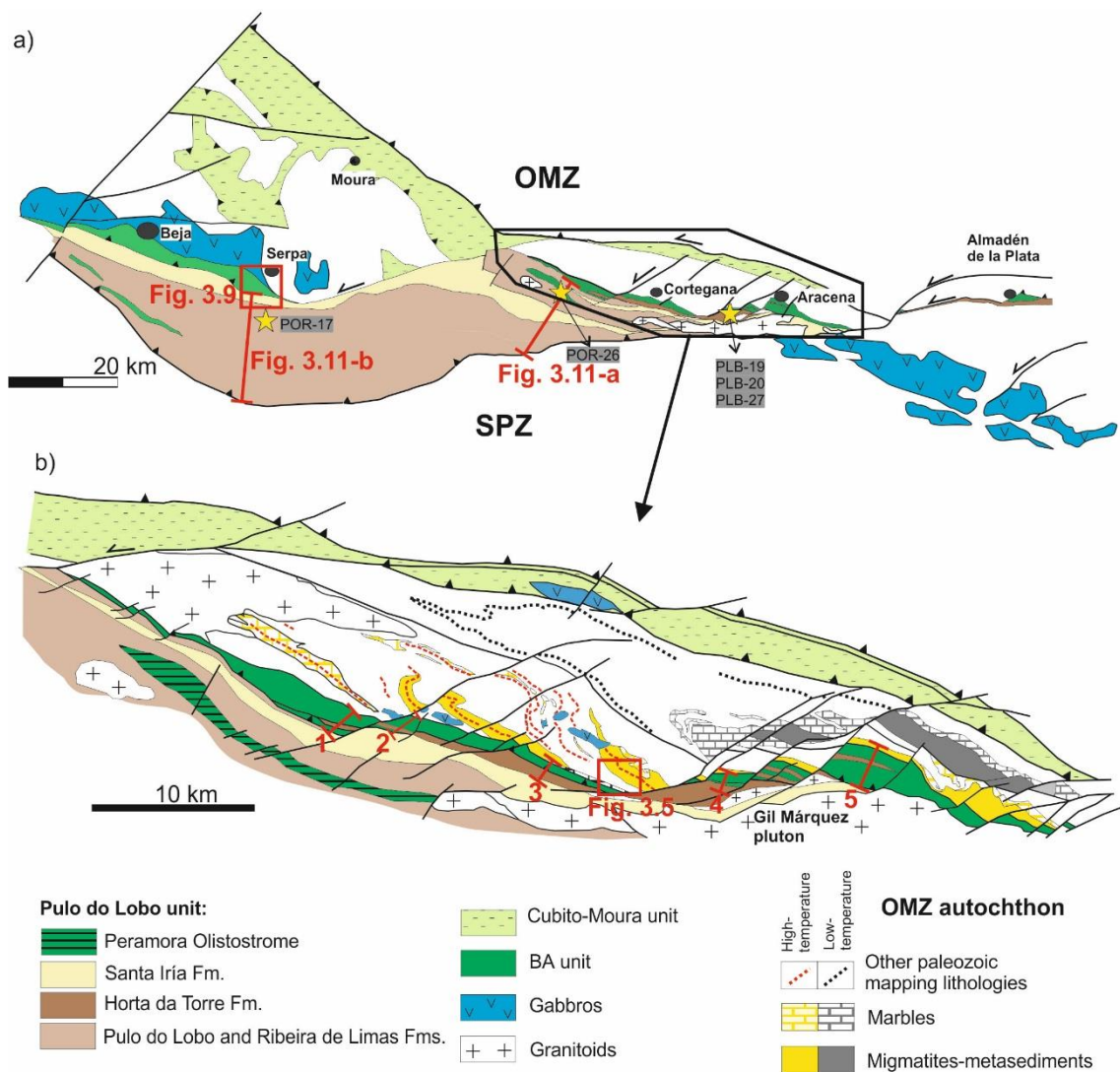
Figure 3.2. a) Schematic map of the OMZ/SPZ boundary showing the different units involved in the suture. Samples used for geochronology (yellow asterisks), as well as Figures 3.9 and 3.11 are located. b) Detailed geological map of the Aracena-Cortegana area. Figure 3.5 and cross-sections 1–5 in Figure 3.8 are located.

(iv) The Pulo do Lobo unit: a group of detrital low-grade metasedimentary formations cropping out extensively south of the BA unit. The lowermost formation (Pulo do Lobo Formation) is constituted by phyllites with abundant quartz veins. Gradually upwards, quartz-sandstone intercalations define the Ribeira de Limas Formation. These two lower formations have been said to represent a subduction-related accretionary prism (e.g., Eden and Andrews, 1990; Oliveira, 1990). The upper formations, namely Horta da Torre and Santa Iría, are constituted by dominant slates with quartzites and greywackes, respectively. They are Late Devonian-early Carboniferous in age (Pereira et al., 2007), and unconformably overlie the lower ones.

(v) The SPZ: a broad region made up of phyllites and quartz-sandstones (Upper Devonian), a volcano-sedimentary formation (Tournaisian-Lower Visean) and, at the top, a Flysch with slates and greywackes (Upper Visean-Bashkirian) (Oliveira, 1990).

3. The Rheic Ocean suture in the Iberian Variscides

The Rheic Ocean (McKerrow and Ziegler, 1972) was primarily defined drawing on paleomagnetic and paleontological data that led to detect two separated Paleozoic continents for the Ordovician-Devonian period: Laurussia (Laurentia/Baltica) and Gondwana (e.g., Cocks and Fortey, 1982, 1988; Livermore et al., 1985; Scotese et al., 1985; Scotese and Golonka, 1992; Cocks and Torsvik, 2002; Stampfli and Borel, 2002). It is broadly accepted that closure of the Rheic Ocean gave way to the Variscan-Alleghanian Orogeny that occurred in Devonian and Carboniferous times, and resulted in the assembly of Pangaea (e.g., Matte, 1991, 2001) (Fig. 3.1a). In the Iberian Variscides, the Rheic Ocean suture has been classically located at the Allochthonous Complexes on NW Iberia and at the OMZ/SPZ boundary in SW Iberia (Fig. 3.1b).

The nappe stack of NW Iberia can be viewed as two continental terranes separated by ophiolitic units, these latter being traditionally considered as Rheic Ocean remnants (Martínez Catalán et al., 1997; Díaz García et al., 1999; Arenas et al., 2007a, b). However, new isotopic data cast some doubt about the real meaning of these ophiolites, being actually interpreted as representing the suture of peri-Gondwanan terranes (Sánchez Martínez et al., 2011; Arenas et al., 2014). Whether or not the allochthonous ophiolites of NW Iberia represent the Rheic Ocean, their root does not outcrop in NW Iberia, thus being located somewhere to the west. By contrast, the autochthonous Rheic suture seems to crop out in SW Iberia, though very modified during the collisional evolution. Possible correlations between NW and SW Iberian ophiolites have been put forward (e.g., Ribeiro et al., 2007; Simancas et al., 2009; Díez Fernández and Arenas, 2015).

Two main tectonic contacts crop out in SW Iberia, bounding the OMZ to the north and south. To the north, the boundary between the OMZ and the Central Iberian zone (CIZ) has been interpreted as a second-order Variscan suture, i.e., the tectonic boundary between a terrane of Gondwanan affinity (OMZ) and the Gondwanan continent itself (CIZ) (Simancas et al., 2001; Gómez-Pugnaire et al., 2003). As already pointed out by Dewey (1977), sutures like this one are common complexities in continental convergent settings. We do not consider this boundary any more in this paper.

Direct evidences (paleomagnetic and/or paleontological data) to locate the Rheic Ocean suture along the OMZ/SPZ boundary are lacking, since pre-Late Devonian rocks do not crop out in the SPZ. Pioneer papers envisaged a main Variscan suture in SW Iberia based on simple geological pictures (Carvalho, 1972; Bard et al., 1973). A more refined tectonic scenario was arisen when the metamafic-ultramafic rocks cropping out along the OMZ/SPZ limit (the BA unit (Bard, 1977)) were interpreted as a Variscan ophiolite (Munhá et al., 1986; Crespo-Blanc, 1991; Fonseca and Ribeiro, 1993; Quesada et al., 1994; Castro et al., 1996) and the adjacent schists with minor MORB-like metabasalts (Pulo do Lobo unit) were interpreted as a subduction-related accretionary prism (Eden and Andrews, 1990; Silva et al., 1990; Eden, 1991; Braid et al., 2010; Ribeiro et al., 2010; Dahn et al., 2014). A third key element was the recognition of an allochthonous complex (the Cubito-Moura unit) resting onto the southern OMZ and including high-pressure schists, eclogites and MORB-like metamafic rocks (Fonseca et al., 1999; Araujo et al., 2005; Booth-Rea et al., 2006; Ponce et al., 2012). Thus, a tectonic scenario emerged in which the OMZ/SPZ boundary was identified with the Rheic Ocean suture, as featured by both rooted and allochthonous ophiolites, exhumed high-pressure rocks and an accretionary prism (e.g., Simancas et al., 2003). The obliteration of the Rheic Ocean lithosphere by subduction would have taken place in Devonian time, the latest Devonian and Carboniferous being a time of continental collision. Lacking arc-type subduction-related magmatism was the only unsatisfactory issue to complete the orogenic picture.

During the last years, significant data concerning the tectonic meaning of the OMZ/SPZ boundary have been published. First, the view of the BA unit as a Rheic Ocean ophiolite has been questioned after the very young age determined for its protholiths (≈340 Ma (Azor et al., 2008)). Thus, the BA unit could represent either a very late back-arc basin or a narrow Lower Carboniferous oceanic-like corridor. This latter would have developed in the same extensional context as the conspicuous sedimentary basins, rocks exhumation and magmatism of Early Carboniferous age recognized in most of SW Iberia (Simancas et al., 2003; Azor et al., 2008; Pereira et al., 2012b). This extensional event would have occurred between Devonian and Carboniferous compressional ones, and so it is viewed as intracollisional (see sections 4 and 5). Second, the MORB-like metabasalts (Giese and Buhn, 1993; Dahn et al., 2014) that appear in some sectors within the Pulo do Lobo phyllites have also yielded an Early Carboniferous age of 333-341 Ma (Dahn et al., 2014; this paper), thus invalidating their interpretation as tectonic slices of an accretionary prism related to the Rheic Ocean subduction.

According to the above arguments, the Cubito-Moura unit is perhaps the only real witness of Rheic Ocean subduction. This is supported by the following: (i) a preliminary Ordovician age (~480 Ma) for the protholihts of MORB-like metamafic rocks (six zircon U-Pb SHRIMP analyses from three rock samples) (Pedro et al., 2010), (ii) an Upper Devonian age (371 ± 17 Ma) for the high-pressure metamorphism (Sm/Nd whole rock-garnet isochron from an eclogite) (Moita et al., 2005), and (iii) the early development (Devonian?) of a relic tectonic fabric that has been related to the exhumation of the unit (Ponce et al., 2012), previous to the main Variscan (Devonian) collisional folds and thrusts.

Recent studies on zircon provenance and isotope geochemistry have brought a new wave in support of the OMZ/SPZ boundary as representing the suture of the Rheic Ocean.

These data favor an exotic character of the SPZ, akin to Avalonia instead of Gondwana (Braid et al., 2011, 2012; Pereira et al., 2014; Rodrigues et al., 2015). Finally, the awkward issue of the missing subduction-related magmatism has been slightly alleviated by the finding of detrital zircons of Devonian age, witnesses of unexposed (may be subducted) arc magmatism (Pereira et al., 2012a).

To conclude, despite the disclosure that the OMZ/SPZ boundary is much more complex than thought some years ago, it seems that its identification with the Rheic Ocean suture still holds.

4. Orogenic events preceding Carboniferous collision

We concentrate in this work on featuring the collisional Carboniferous deformation in SW Iberia, but it is imperative to start summarizing our current view on the previous Devonian collision stage and the intraorogenic extensional stage that interrupted the collisional history at early Carboniferous time.

4.1. Closing of the Rheic Ocean and Late Devonian collision

The first Variscan collisional stage is the consequence of the collision between Avalonia and Gondwana after the closing of the intervening Rheic Ocean. In SW Iberia, the SPZ is thought to represent a piece of Avalonia, while the OMZ and the Central Iberian Zone were part of the Gondwana margin (Fig. 3.1) (Simancas et al., 2005) (see section 3). The envisaged large-scale tectonic scenario is one with subduction of the OMZ continental margin below the SPZ just following the disappearance of the Rheic oceanic realm in Devonian time (Fig. 3.3a). As a result, uppermost Neoproterozoic and Lower Paleozoic rocks of the subducted OMZ cover scraped off its basement and formed a complex allochthonous unit constituted by exhumed eclogites and high-pressure metasediments together with ophiolite slices, called the Cubito-Moura unit, that emplaced onto the southern part of the OMZ (Fig. 3.3a) (Fonseca et al., 1999; Araujo et al., 2005). The metamorphic conditions of this early collisional stage were established based on tectonic fabrics and mineral assemblages preserved in metabasites (Fonseca et al., 1999; Rubio Pascual et al., 2013) and metapelites (Booth-Rea et al., 2006; Ponce et al., 2012). The kinematics of the exhumation, according to stretching lineations and tectonic fabrics preserved within early quartz veins, indicates oblique left-lateral convergence with top-to-the-ENE emplacement onto the OMZ (Ponce et al., 2012) (Fig. 3.3b). Later on, the Cubito-Moura unit was deformed by SW-vergent recumbent folds (Fig. 3.4). These folds have been correlated (Ponce et al., 2012) with the first structures that deform their relative OMZ-autochthon at low-grade conditions (Devonian kilometric-scale SW-vergent recumbent folds and thrusts) (Expósito et al., 2002).
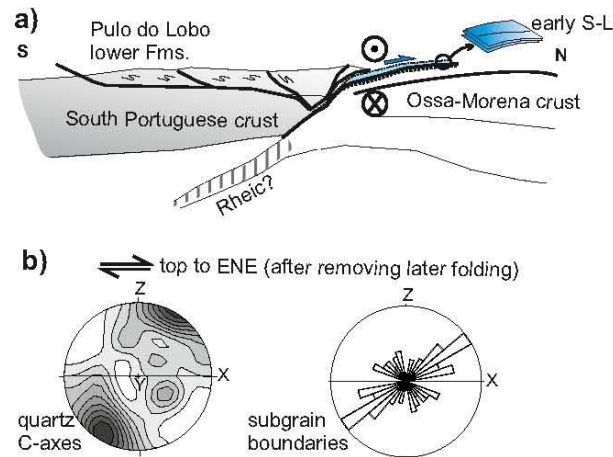
Figure 3.3. The early collisional (Devonian) stage after Ponce et al. (2012). a) Crustal sketch showing the exhumation of the allochthonous Cubito- Moura unit (high-pressure continental rocks and mafic Rheic? rocks) that generated a first recognizable S-L tectonic fabric. b) Kinematic analysis of S-L tectonic fabric indicating top-to-the-ENE sense of movement: a stereoplot of quartz C-axes orientation (equal-area, lower hemisphere projection) and a rose diagram of quartz subgrain boundaries.

4.2. Intraorogenic extensional stage

The definition of an intraorogenic extensional, likely transtensional, stage (Fig. 3.4) that temporarily interrupted the continental convergence in SW Iberia at early Carboniferous time is demonstrated by the following geological/geophysical features:

(i) Widespread Tournaisian-Visean sedimentary basins in the OMZ and the southern border of Central Iberian Zone filled in with slates, greywackes and basaltic flows, all of them lying unconformably over rocks previously folded in Devonian time (e.g., Simancas et al., 2001; Pereira et al., 2012b).

(ii) A great volume of volcanic rocks (basaltic and rhyolitic bimodal magmatism) in the SPZ, which evidences a Tournaisian-early Visean rifting stage (Schermerhorn, 1971; Munhá, 1983; Oliveira, 1990) dated at 355–345 Ma (Barrie et al., 2002; Dunning et al., 2002; Valenzuela et al., 2011).

(iii) Mantle-derived dioritic-gabbroic plutons (350–335 Ma) in the OMZ and the eastern part of the SPZ (Simancas, 1983; Pin et al., 2008; Cambeses et al., 2014).

(iv) The mafic magmatism represented by the BA unit (Azor et al., 2008).

(v) Mafic igneous rocks intruded in the middle crust of the OMZ and the upper crust of the SPZ, according to the interpretation of geophysical data provided by the IBERSEIS deep seismic profiles (Simancas et al., 2003; Schmelzbach et al., 2008; Palomeras et al., 2009).

Furthermore, new geochronological data on metavolcanic rocks located just south of the BA unit are reported in this work (see sections 5.2.3 and 5.3.1) and reinforce the

significance of this extensional event in SW Iberia. Possible geodynamic scenarios for this extension are discussed later.
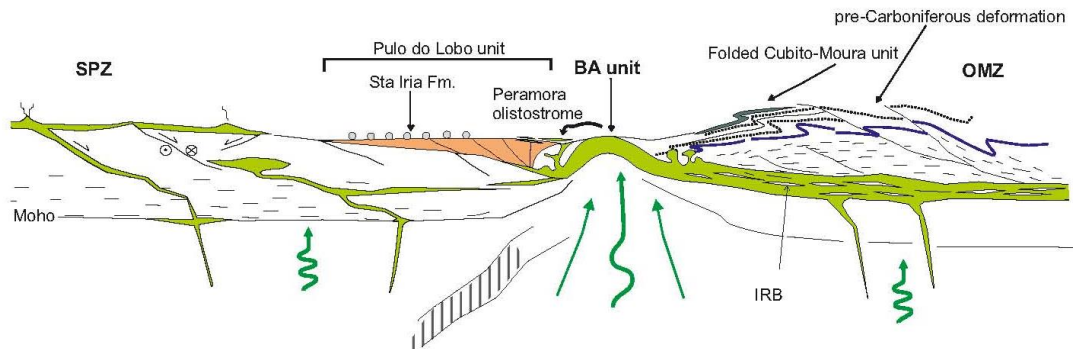
Figure 3.4. Sketch showing the early Carboniferous transtensional stage in SW Iberia. The BA unit formed as a proto-oceanic corridor located at the OMZ/SPZ boundary. Other suture-related units and the midcrustal IBERSEIS Reflective Body are represented. Acid and mafic igneous rocks of this age intruded in the OMZ and SPZ are depicted with green color.

5. Carboniferous transpressional collision

5.1. Deformation at the southernmost Ossa-Morena Zone

The southern edge of the OMZ just north of the BA unit is characterized by the outcrop of gabbros, anatectic granodiorites and high-temperature/low-pressure metamorphic rocks: migmatites, gneisses, marbles and amphibolites (Bard, 1977; Apalategui et al., 1984; Crespo-Blanc, 1991; Díaz Azpiroz et al., 2006) (Fig. 3.2b). This metamorphism is loosely dated in the range 345–330 Ma (Dallmeyer et al., 1993; Castro et al., 1999). These metamorphic rocks are stratigraphically equivalent to the "typical" OMZ Upper Proterozoic-Cambrian succession cropping out to the north and exhibiting low-grade metamorphism (Bard, 1977). The boundary between low- and high-grade metamorphic rocks is a north dipping poorly exposed fault.

The high-grade metamorphic band shows SW-vergent folds with a gneissic-migmatitic axial-plane foliation (Fig. 3.5). These folds trend NW-SE, being the axial traces oblique to the OMZ/SPZ boundary. Furthermore, they are arranged in-relay (Fig. 3.2b), thus suggesting to have been formed in a left-lateral transpressional tectonic regime. To the south, the folds are bounded by a 50–150 m wide band parallel to the OMZ/SPZ boundary and lithologically heterogeneous, made up of lenses of gneisses, amphibolites and marbles (the so-called "nivel de mezcla" by Crespo-Blanc (1991)). This band lacks kinematic criteria and we interpret it as a high-temperature shear zone giving way to a tectonic mélange by mingling of different lithologies (Fig. 3.5). Upright low-temperature folds are superposed onto the high-temperature ones, giving way to hook interference patterns on map (Fig. 3.2b and 3.5). Furthermore, there is at least a previous foliation, visible in restitic enclaves enclosed by the gneissic-migmatitic foliation (Fig. 3.6a) and witnessing the existence of pre-Carboniferous deformations in these rocks (Fig. 3.3).

Northwards the Carboniferous structure of the allochthonous Cubito-Moura unit and its relative low-grade OMZ-autochthon consists of NW-SE trending upright folds that crenulate the previous structures (Devonian SW-vergent recumbent folds and thrusts) (Expósito at al., 2002; Ponce et al., 2012).
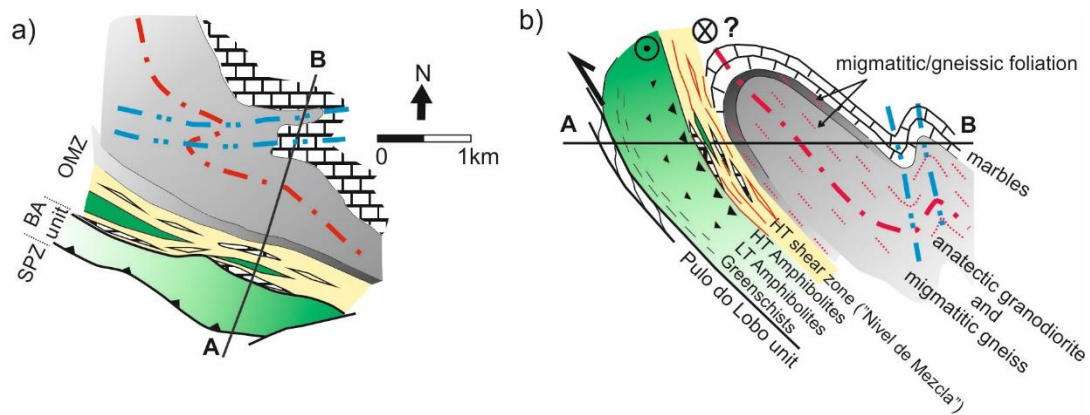
Figure 3.5. Deformation at the southernmost OMZ, near Santa Ana La Real (location in Figure 3.2b), showing high-temperature sin-metamorphic folds (in red) oblique to the OMZ-SPZ boundary. a) Schematic map. b) Cross-section.

5.2. Deformation of the Beja-Acebuches unit

5.2.1. Ductile shearing

The BA unit shows a penetrative foliation developed at varying conditions that evolved from granulite to greenschist facies, although amphibolite facies conditions are dominant. High-temperature amphibolites and granulites are coarse-grained and banded rocks (Fig. 3.6b-c), and sometimes a faint mineral lineation is perceptible (Fig. 3.6d). Low-temperature amphibolites and greenschists are fine-grained, mylonitic rocks with prominent stretching lineation (Fig. 3.6e) and abundant noncoaxial asymmetric microstructures, showing left-lateral kinematics (Fig. 3.6f). These fabrics attest high strain with dominant simple shear. The stereoplots in Fig. 3.7 show foliation and lineation orientation data in the BA unit (see also Crespo-Blanc (1991) and Díaz Azpiroz et al. (2004)).

Shearing at greenschist facies conditions gave way to a heterogeneous deformation, contrasting with the more homogeneous aspect of the deformation at higher temperatures. At outcrop scale, lozenges constituted by less deformed rocks are surrounded by highly sheared rocks (Fig. 3.6g). At larger scale, the cross-sections in Fig. 3.8 (Cortegana-Aracena area) illustrate how ramifications of the greenschist facies shear zones disrupt the BA unit into several minor bodies. Furthermore, centimetric- to metric-scale tight shear folds frequently appear, with variable axial orientation, though always contained in the foliation planes (Fig. 3.6h and 3.7).

Kinematic criteria are very scarce in high-temperature amphibolites, but abundant in low-temperature ones and greenschists, showing a consistent left-lateral component (Crespo-Blanc, 1991; Díaz Azpiroz and Fernández, 2005) (Fig. 3.6e-f). Overall, the kinematics of

the BA unit ductile shearing involves a thrust movement with strong left-lateral component.

Figure 3.6. a) Pre-Carboniferous relic foliation preserved in enclaves enclosed by the gneissic-migmatitic foliation in the southernmost OMZ. b) High-temperature tectonic layering in the BA unit. c) Tectonic banding (high-temperature amphibolite facies of the BA unit) suggesting original gabbros intruded by mafic dykes. d) High-temperature mineral lineation in the BA unit. e) Well-developed foliation and mineral stretching lineation in low-temperature (greenschists facies) amphibolites of the BA unit. f) Left-lateral asymmetric shear structures in feldspars (low-temperature amphibolites of the BA unit). g) Left-lateral shear deformation affecting quartz veins in the Pulo do Lobo Formation close to the contact with the BA unit. h) Asymmetric shear folds affecting greenschists of the BA unit. i) Porphyric (subvolcanic) texture in greenschists facies rocks of the BA unit. j) S0 sedimentary bedding and S1* foliation in the Sta. Iría Formation, folded by D2*. k) S1 folded within S2 centimetric-scale tectonic banding, in turn folded by D3 in the Pulo do Lobo Formation. l) Brittle faulting in quartzites of the Horta da Torre Formation.
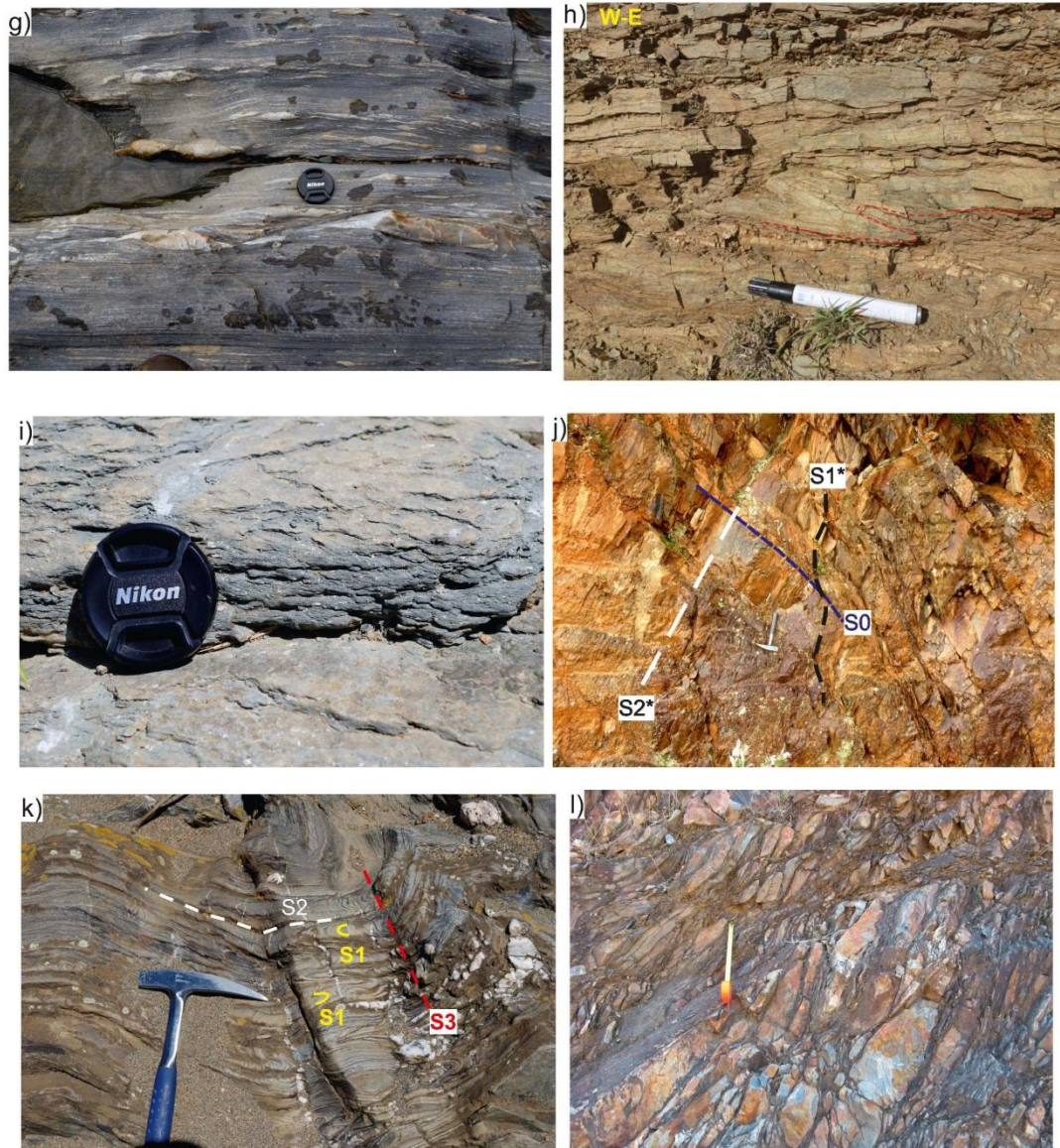
Figure 3.6 (continued).

5.2.2. Folds

In the western sector, some meta-ultramafic rocks crop out in the BA unit (Fonseca and Ribeiro, 1993), although amphibolites are dominant. Amphibolites alternate light and dark bands according to grain size and composition (Fig. 3.6d). This banding is in most cases interpreted as a result of shearing of gabbros intruded by mafic dykes. Furthermore, fine-grained amphibolites and greenschists derive from mafic subvolcanic rocks, as indicated by porphyritic textures (Fig. 3.6i). Thus, when the internal structure of the BA unit is taken into account (see below), it appears organized in a rock succession with ultramafic rocks, gabbros with dykes and subvolcanic rocks (Quesada et al., 1994), resembling an oceanic-like crust metamorphosed at high- to low-temperature facies.

In the eastern sector, banded amphibolites overlie amphibolites exhibiting subvolcanic textures, thus indicating that the BA unit is reversed in this sector. We interpret this

structural pattern as the overturned limb of a south-vergent regional-scale fold (Fig. 3.8), with an axis roughly parallel to the regional strike of the BA unit. This fold has been mapped, dismembered by left-lateral faults, in the western sector along the Guadiana River south of Quintos (Fig. 3.9). We refer to this fold as Quintos fold. The normal limb of the Quintos fold shows that the BA unit thrust northwards onto the OMZ southern border before folding (Fig. 3.8).
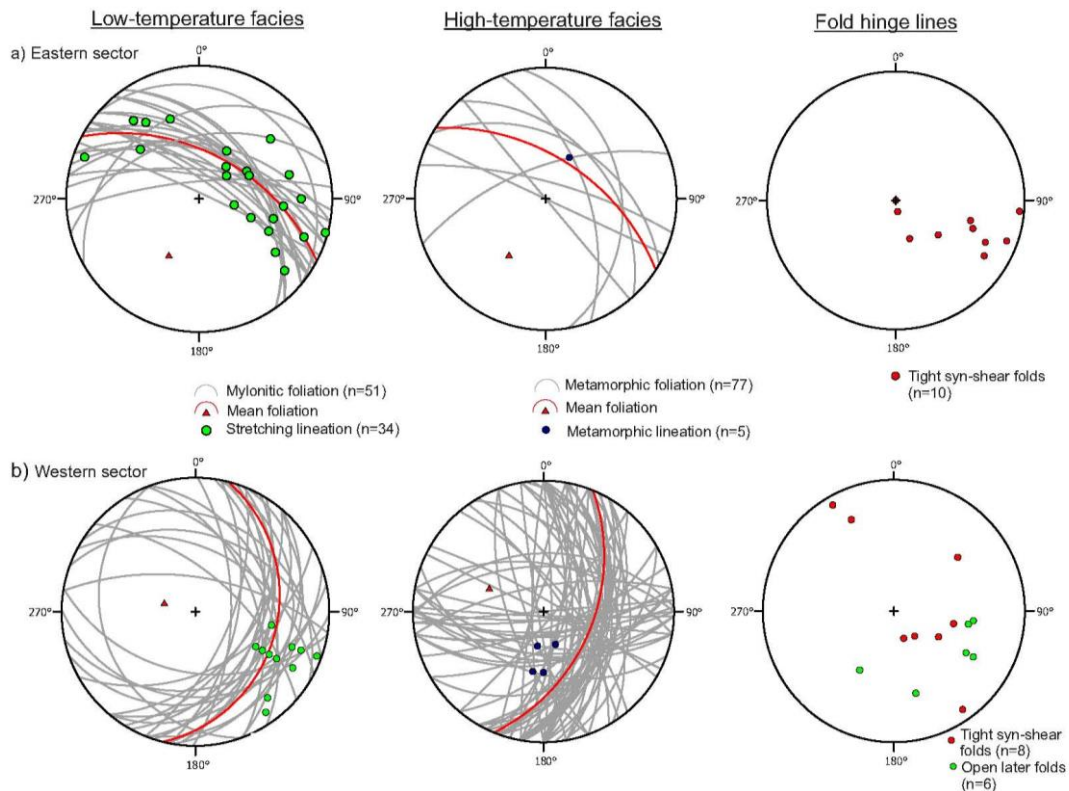
Figure 3.7. Structural data of the BA unit (equal-angle, lower hemisphere stereoplots), distinguishing low-temperature fabrics (mylonitic foliation and stretching lineation), high-temperature fabrics (metamorphic foliation and mineral lineation), and fold hinges. a) Eastern (Cortegana-Almadén de la Plata) sector. b) Western (Beja-Serpa) sector.

5.2.3. Age of the deformation

The age of the shearing in the BA unit is relatively well constrained. Thus, $^{40}Ar/^{39}Ar$ dating on hornblende concentrates from the high-temperature facies are slightly older than 340 Ma (Dallmeyer et al., 1993), and overlap with the $^{40}Ar/^{39}Ar$ and Rb/Sr ages obtained for the high-temperature metamorphism on the southern edge of the OMZ (345–330 Ma) (Castro et al., 1999). On the other hand, SHRIMP U-Pb data on zircons from amphibolites of the BA unit yielded protolith ages between 340 and 335 Ma (Azor et al., 2008).

The factual coincidence, within range, of protolith and high-temperature metamorphic ages of the BA unit, point to the interpretation that thrusting onto the southern edge of the

OMZ and left-lateral shearing began very shortly after the BA magmatic emplacement along the OMZ/SPZ suture, between 340 and 335 Ma. This age overlap also explains the concomitant high-temperature metamorphism of the southern OMZ. A thorough discussion of that issue was presented by Azor et al. (2008).
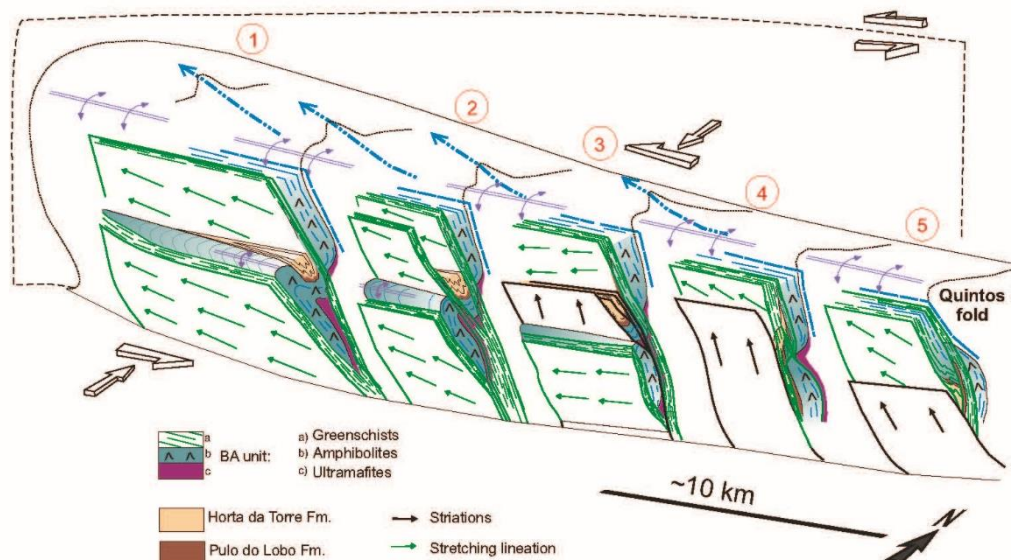
Figure 3.8. Detailed cross-sections of the overturned limb of the Quintos fold in the central sector (Aracena-Cortegana) of the BA unit, showing secondary folds and discrete low-temperature (greenschists facies) shear bands. See Figure 3.2b for location.

Additional geochronological data have been obtained just south of the BA unit (Fig. 3.2a), where a low-temperature shear zone affecting metasediments, greenschists and acid-intermediate metavolcanic rocks crops out. These metavolcanic rocks have been dated by SHRIMP U-Pb on zircons (see sample description, methodology and data set in appendix 4, 6 and 7), yielding protolith ages of 345 ± 5 Ma (sample PLB-19), 339 ± 2 Ma (sample PLB-20) and 337 ± 3 Ma (sample PLB-27) (Fig. 3.10a-c). The obtained ages provide maximum ages for the low-temperature shearing.

5.3. Deformation of the Pulo do Lobo unit

The overall structure and tectonic evolution of the Pulo do Lobo unit have been loosely treated in previous attempts. The structure of this unit has simply been described as an imbricated tectonic mélange (Eden and Andrews, 1990), a single-phase folded belt (Onézime et al., 2002), or an accretionary ensemble of compartmentalized tectonic domains dominated by different noncoaxial deformations (Braid et al., 2010). At outcrop scale, Fonseca (2005) described the existence of a polyphasic superposition of folding deformations.
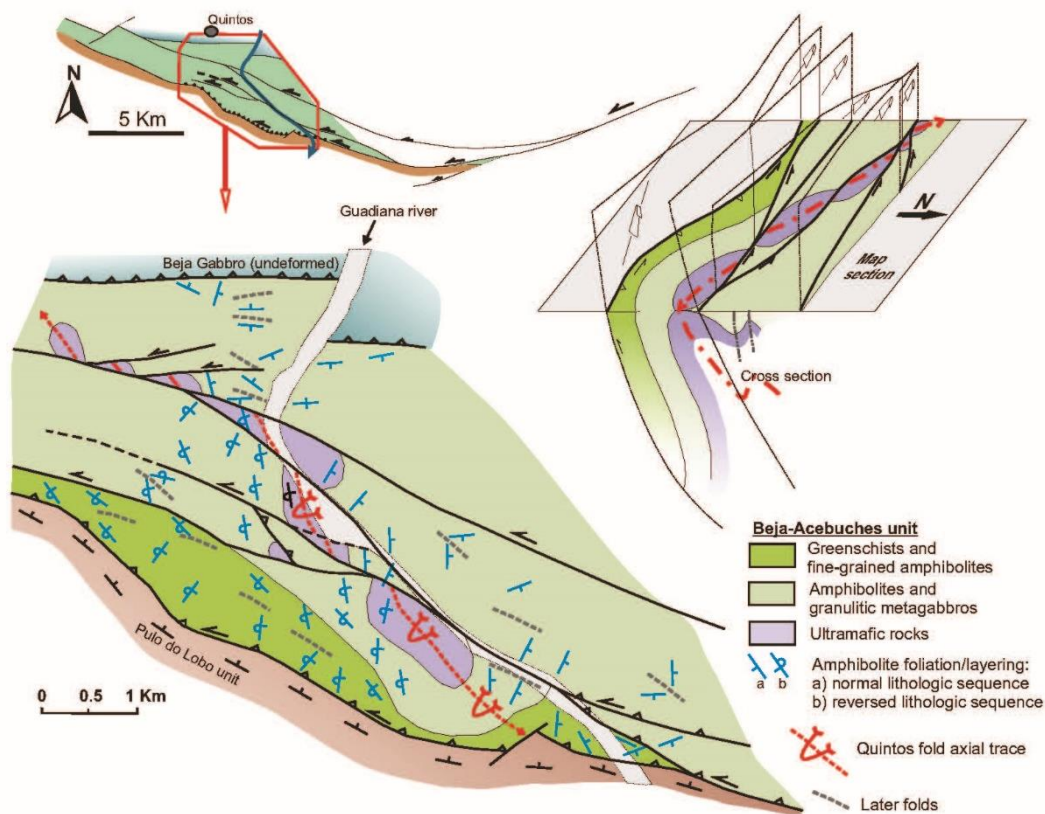
Figure 3.9. Structural map and 3-D interpretation of the BA unit in the Guadiana river area (location in Figure 3.2a). The lithological map is adapted from Fonseca (1989) in Quesada et al. (1994); small acid intrusive bodies are not represented.

The lower formations, Pulo do Lobo and Ribeira de Limas, are affected by three penetrative folding deformation phases (D1, D2 and D3), being unconformably covered by the upper formations (Horta da Torre and Santa Iría), where only the last two deformation phases are recorded (Fig. 3.6j). The metamorphic conditions did not exceed low-grade.

The age of the lower formations of the Pulo do Lobo unit is not precisely defined. Concerning the Ribeira de Limas Formation, early Frasnian palynomorph assemblages have been reported (Pereira et al., 2007), but the youngest detrital zircon population in these rocks is ≈360 Ma-old (Famennian) according to LA-ICPMS ages reported by Braid et al. (2011). The two upper formations contain Late Famennian pollen assemblages (Pereira et al., 2007), however the youngest detrital zircon population from the Santa Iría Formation indicates a maximum depositional age of 347 Ma (Late Tournasian) (Braid et al., 2011). We favor zircon ages in view of the published evidence of abundant reworked palynomorphs in nearby early Carboniferous basins. For instance, in the Toca da Moura basin, more than 90% of reworked palynomorphs have been reported (Lopes et al., 2014).
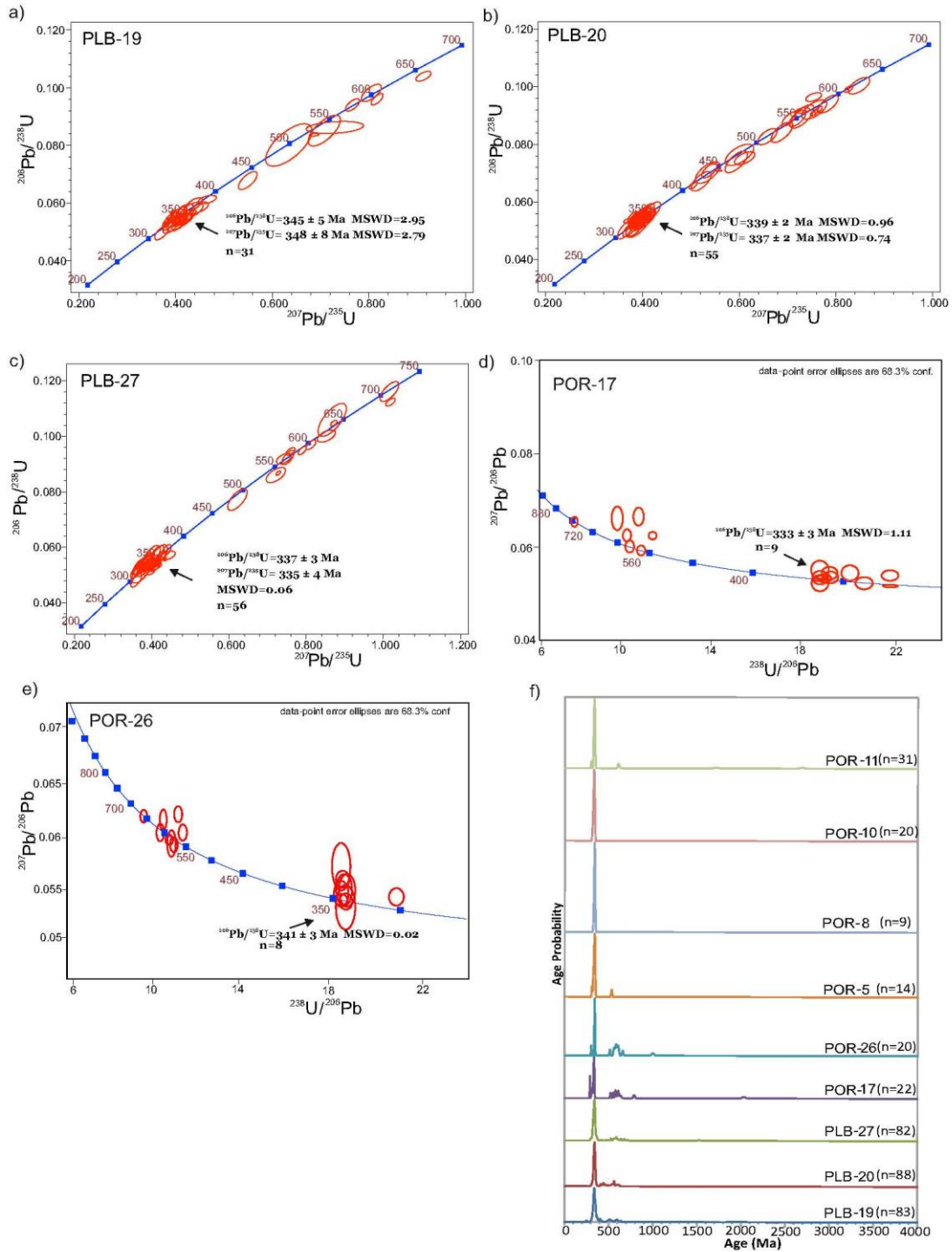
Figure 3.10. Concordia diagrams for the SHRIMP zircon U-Pb analyses of the studied samples (for location see Figure 2a). Sample description, methodology, and data set in the supporting information. Samples (a) PLB-19, (b) PLB-20, and (c) PLB-27 are represented according to Wetherill projection. Average ages are calculated from the analyses plotted as red ellipses. Samples (d) POR-17 and (e) POR-26 are plotted in Tera-Wasserburg diagrams. (f) Comparison of ages based on the Gehrels [2011] method between our new data and the ages published by Azor et al. [2008] for protolihts of the BA unit (samples POR-5, POR-8, POR-10, and POR-11). It shows a common age of around 340 Ma for the deformed metamafic rocks of the BA and Pulo do Lobo units.

The structure of the Pulo do Lobo unit is illustrated in cross-sections and stereoplots in Fig. 3.11. The first regional deformation phase (D1) is exclusively present in the two lower formations and consists in a relict foliation (S1) preserved inside the microlithons that define the second foliation (S2). Although the geometry of D1 structures cannot be restored, the angle between S1 and the S2 microlithons is usually high (Fig. 3.6k), thus suggesting a high angle between D1 and D2 axial planes.
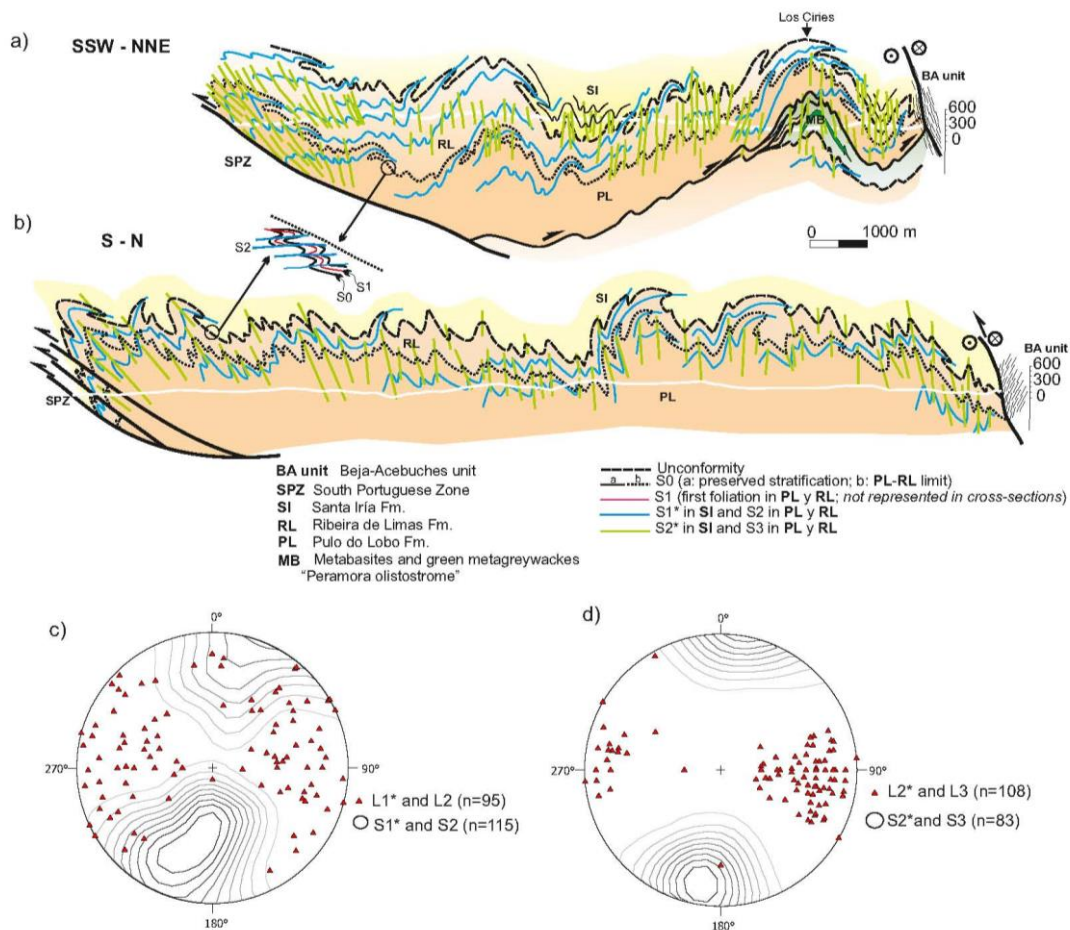
Figure 3.11. Cross-sections of the Pulo do Lobo unit at the (a) eastern (modified from Martínez Poza et al., 2012) and (b) western sectors (see Figure 3.2a for location). Structures corresponding to the three deformation phases are depicted. c) Stereoplot (equal-angle, lower hemisphere projection) of foliation (contours) and intersection lineation (including fold axes) for D2 and D1*. d) Idem for D3 and D2*.

The second regional deformation phase (D2 in the lower formations and D1* in the upper formations) is characterized by north-vergent folds, with an associated slaty cleavage in the upper formations (S1*) and a crenulation-dissolution cleavage (S2) in the lower formations. As a result, S2 commonly appears as a milimetric- to centimetric-scale tectonic banding (Fig. 3.6k) and constitutes the principal foliation at sample and outcrop scales.

The third regional deformation phase (D3 in the lower formations and D2* in the upper formations) was responsible for upright or slightly south-vergent folds with an associated spaced crenulation-dissolution cleavage (S3) or disjunctive cleavage (S2*) (Fig. 3.6j-k and

11). In the lower formations, there are numerous D3 metric-scale chevron folds, and in some cases crenulation-dissolution processes make S3 to appear as a characteristic decimetric- to metric-scale tectonic banding. Locally, south-vergent brittle thrusts formed during D3 too (Fig. 3.11).

D2 and D3 in the Pulo do Lobo unit resulted from the Carboniferous collision between OMZ and SPZ, being correlatable with the deformations affecting the southernmost OMZ and the BA unit. Thus, the northwards thrusting of the BA unit onto the southern OMZ can be correlated with D2, while the south-vergent folding of both the BA unit and the southernmost OMZ can be correlated with D3. As for D1 in the Pulo do Lobo unit, it might have occurred during the first episodes of the collision, probably in Late Devonian time.

5.3.1. The Peramora Mélange

At the eastern part of the Pulo do Lobo unit, in the core of a D3 antiform (Los Ciries antiform; Apalategui et al., (1983)) (Fig. 3.11a), lenticular levels of metamafic rocks with MORB affinity appear included in a green detrital matrix of mafic derivation (Eden, 1991; Dahn et al., 2014). These rocks show a penetrative foliation correlative with S2, and no relics of a previous foliation have been observed in the blocks or in their enclosing matrix. Both blocks and matrix appear metamorphosed at greenschist facies conditions and seem to be imbricated with the phyllites of the Pulo do Lobo Formation Up to now, they have been interpreted as a tectonic mélange (Peramora Mélange) related to the Rheic Ocean lithosphere subduction (see section 3). However, an Early Carboniferous zircon population has been reported from these metamafic rocks (Dahn et al., 2014), in agreement with the new data reported below.

Two metamafic samples (POR-17 and POR-26; Fig. 3.2a) have been dated by SHRIMP U-Pb on zircons (see sample description, methodology and data set in Appendix 4, 6 and 7), yielding, inherited grains aside, an early Carboniferous population. Nine analyses from sample POR-17 yield an age of 333 ± 3 Ma, while eight analyses from sample POR-26 yield an age of 341 ± 3 Ma (Fig. 3.10d-e).

Dahn et al. (2014) have reported U-Pb zircon data from several samples of the metamafic rocks (blocks and matrix) from the Peramora Mélange. Leaving aside inherited grains, these authors obtained an Early Carboniferous zircon population (seven analyses, the youngest being 333 Ma-old). Despite being >95 % concordant, Dahn et al. (2014) force the interpretation by considering zircons younger than 339 Ma as an artifact resulting from Pb-loss. For these authors, the "youngest permissible" zircon age is 341 ± 8 Ma for the mafic blocks. Whatever the case, their data agree with our own, i.e., both the metabasalt blocks and their enclosing matrix are Early Carboniferous.

In agreement with the Early Carboniferous ages, the pre-Carboniferous D1 event was apparently not recorded by the metamafic rocks (a relic S1 foliation has not been observed), contrary to the well-preserved S1 foliation in the surrounding metasediments of the Pulo do Lobo Formation (Fig. 3.6k). Obviously, the high competence of the mafic blocks might have inhibited the development of S1 foliation.

The interpretation of these Early Carboniferous ages entails a complete revision of the paleotectonic meaning attributed to the Pulo do Lobo unit. The classical interpretation of these rocks as a remnant of Rheic oceanic crust is untenable. Actually, these rocks could be chronologically equivalent to the Santa Iría Formation though with different lithology, the Peramora Mélange representing an olistostromic facies of mafic derivation (Fig. 3.4) (see discussion).

5.4. Deformation of the South Portuguese Zone

The SPZ is a south-vergent fold-and-thrust belt, resulting from the propagation to the foreland of the deformation that started at the OMZ/SPZ boundary (Fig. 3.12; (Simancas, 2004). Thus, deformation and metamorphism decrease southwards from the OMZ/SPZ boundary. The age of the migrating deformation is well constrained by the age of the preceding clastic Flysch, which is Upper Visean (≈330 Ma) in the north and Moscovian (≈310 Ma) at the southernmost corner of Portugal (Oliveira, 1990).
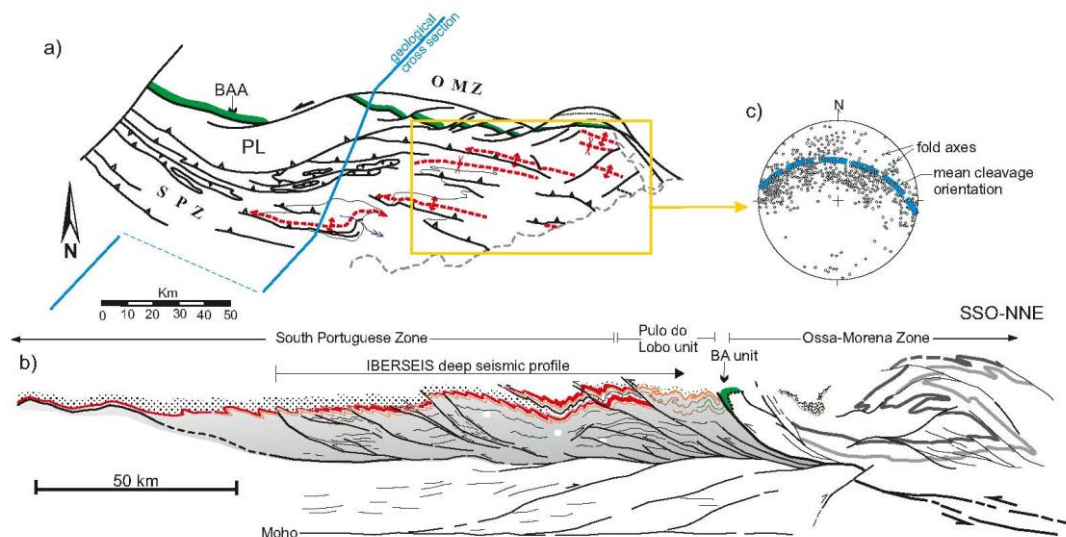
Figure 3.12. Schematic structural map of the (a) SPZ and (b) cross-section (modified from Simancas et al., 2003). c) Stereoplot (equal-angle, lower hemisphere projection) of structural data from the eastern part of the SPZ.

5.5. Left-lateral brittle faulting

The last Variscan structures affecting the OMZ/SPZ boundary are left-lateral strike-slip faults (Fig. 3.2 and 3.13a). There are two significant east-west large-scale low-angle faults with left-lateral slips of tens of kilometers. These two main faults divide the BA unit in three different lenticular portions, from east to west: Almadén de la Plata, Aracena-Cortegana and Serpa-Beja (Fig. 3.2a and 3.13). A set of shorter SW-NE faults cross cut the earlier ones and the BA unit at higher angles. All these faults feature the present-day map view of the OMZ/SPZ boundary (Fig. 3.2). This faulting occurred in the Pennsylvanian, with Lower Permian sediments (Broutin, 1981) sealing the faults.
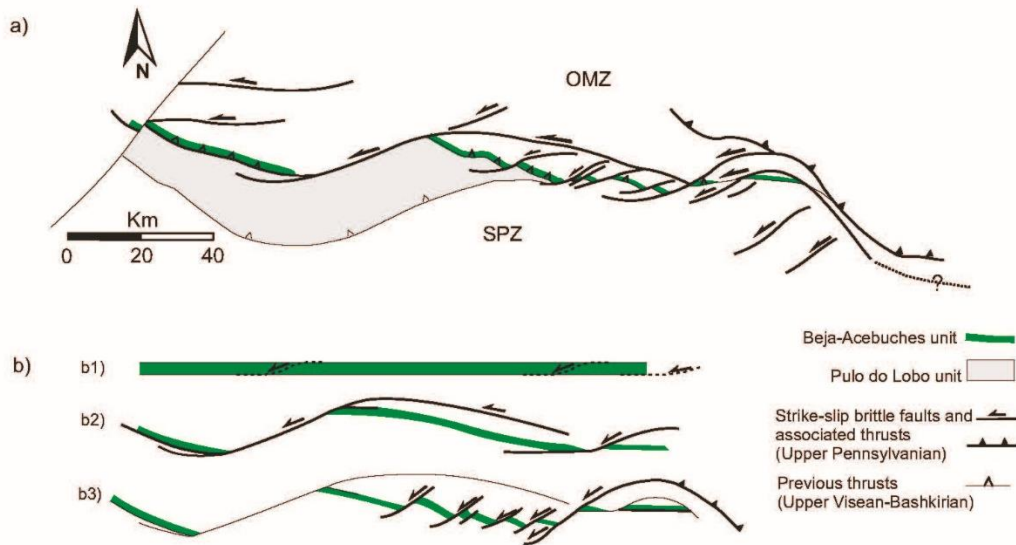
Figure 3.13. a) Schematic map of the main late Variscan faults affecting the OMZ-SPZ boundary. b) Evolutionary model with relative age and geometry of the left-lateral strike-slip faulting.

6. Discussion on the Carboniferous evolution

6.1. Early Carboniferous extensional tectonics

Extensional tectonics interrupted collision in SW Iberia as attested by a number of geological and geophysical features (see section 4.2). All of them coincide in a short time-span. At the scale of the OMZ/SPZ boundary, this early Carboniferous orogenic evolution resulted in a significant transformation of the previous suture contact, later on accentuated with the resuming of the collisional deformation (see next section). The intrusion/extrusion of the BA mafic rocks took place during the early Carboniferous along an elongated strip that coincides with the putative position of the former Rheic Ocean suture, south (present-day coordinates) of the allochthonous Cubito-Moura unit. Concerning the BA unit itself, its linear outcrop pattern, partial MORB geochemical signature, and lithologies that resemble an oceanic crust, point to a narrow oceanic domain formed during transient plate divergence (Fig. 3.4). The geodynamic scenario behind this tectonic setting is discussed below. Soon after its formation, either during the rifting stage (bulged swells or rift flanks) or at the beginning of the subsequent northwards obduction, the BA unit started to provide south-directed mafic-derived debris that were incorporated as olistostromes onto the Pulo do Lobo unit (Fig. 3.4).

The early Carboniferous rifting process would have been most likely transtensional considering the strong left-lateral component inferred all along the collisional history of the OMZ/SPZ boundary, from the Devonian (see section 4.1) to the Carboniferous (see next section). In this scenario, it is plausible to invoke a smooth variation in the large-scale kinematics from transpression to transtension. The geodynamic scenario behind this transtensional and magmatic event is unclear. The geochemical signature of the early Carboniferous mafic magmatism in SW Iberia is very diverse (Munhá, 1983; Quesada et al., 1994; Armendáriz et al., 2008; Pin et al., 2008; Cambeses, 2015) and does not support by

itself any specific tectonic setting. Some authors have proposed the influence of an anomalous sub-lithospheric mantle, may be a mantle plume, as the reason for this event, taking into account its broad extent all along SW Iberia (Simancas et al., 2006) and neighboring regions of Canada (Dessureau et al., 2000; Murphy and Keppie, 2005). Other authors have suggested a tectonic scenario related to the break-off of the Rheic Ocean subducted slab (Pin et al., 2008). A back-arc setting has been also suggested based on the geochemical signature of the BA unit (e.g., Quesada et al., 1994), as in other Central European Variscan massifs (Faure et al., 2009). However, in SW Iberia, extension affects both sides of the putative suture and, according to our regional knowledge, subduccion at this boundary would have ended prior to early Carboniferous time.

6.2. Carboniferous renewed oblique collision

After the short-lived early Carboniferous transtensional stage, collision was resumed in the SW Iberian Variscides keeping the left-lateral oblique component until the end of the Variscan orogeny. The evolutionary model that we present in the following paragraphs is based on the previous knowledge of the OMZ/SPZ boundary, together with the new structural and geochronological data presented in this paper. In detail, the strain was uniformly distributed in some stages, while in others it was heterogeneously partitioned through the development of discrete shear zones where the lateral component was accumulated. In general, the deformation propagated southwards from the OMZ to the SPZ.

6.2.1. Stage A: Obduction of the Beja-Acebuches unit

The overlap between available magmatic and metamorphic ages in the BA unit (at ≈340 Ma) cannot be but an indication that deformation started just after intrusion. The first consequence of the resumed compression was the obduction of the BA unit. Once the Quintos fold is restored, the BA unit appears superposed northwards onto the OMZ border (Fig. 3.14), as previously depicted Fonseca and Ribeiro (1993). Kinematic criteria related to this thrusting have not been preserved and, therefore, the precise emplacement vector is unknown. According to Figueiras et al. (2002), mineralogical and textural relics of this event have been observed at the base of the BA unit, pointing to granulite-facies conditions. The high heat flow necessary to achieve granulite facies is favored by the local context: a hot (just formed) BA unit obducting onto a domain (the southern border of the OMZ) that at that time was at high-temperature metamorphic conditions too (see next section).

South of the BA unit, the Pulo do Lobo unit also shows structures that can be reasonably linked to the northwards emplacement of the BA unit. Thus, north-vergent folds that represent the second deformation in the lower formations (Pulo do Lobo and Ribeira de Limas) and the first one in the upper formations (Santa Iría and Horta da Torre) have been described (see section 5.3). Both, age and vergence of this deformation favor its correlation with the northwards thrusting of the BA unit (Fig. 3.14a). We also attribute to this event

the imbrications of the Pulo do Lobo phyllites with the mafic-derived olistostromes that crop out in the Ciries antiform (Fig. 3.11a and 3.15a).
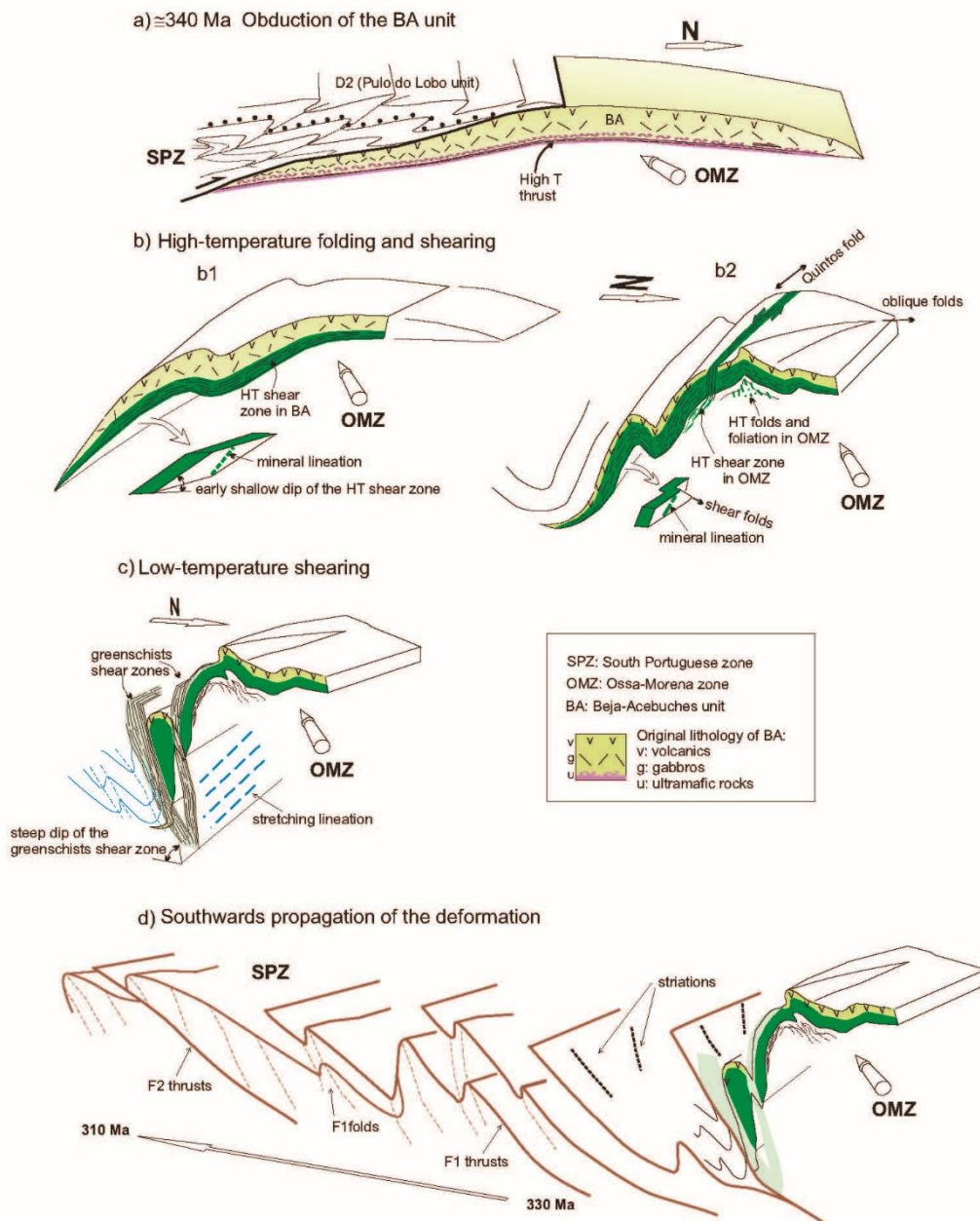
Figure 3.14. (a–d) Evolutionary model of the BA unit during the Carboniferous transpression. See text for further explanations.

6.2.2 Stage B: High-temperature folding and shearing

In this stage (Fig. 3.14b and 3.15b) the rocks of the BA unit were deformed by ductile shearing coeval to the development of the south-vergent Quintos fold. The metamorphic conditions in the shear zone and in the underlying OMZ rocks were at low-pressure and

granulite to high-temperature amphibolite facies conditions, revealing a very high thermal gradient in the upper crust (Bard, 1977; Castro et al., 1996). This type of metamorphism can be explained only as regional contact metamorphism originated by significant volumes of mafic magmas intruding the upper crust (Wickham and Oxburgh, 1987; De Yoreo et al., 1991; Annen and Sparks, 2002). In our case, the source for the inferred high heat flow was most probably the widespread mafic magmatism generated in the context of the preceding transtensional stage (see sections 4.2 and 6.1).

At present, the Quintos fold has an asymmetric close geometry with an overturned southern limb, although during its nascent stage it would have an open geometry as depicted in Fig. 3.14b1. Thus, we interpret it as a buckling fold that accumulated most of the shortening component, while the lateral component was concentrated in the shear zone.

Below the northern limb of the Quintos fold, syn-metamorphic SW-vergent folds have been described affecting high-grade gneisses and marbles of the southernmost OMZ (see section 5.1). These folds are arranged in-relay and strike NW-SE, i.e., oblique to the OMZ/SPZ boundary (Fig. 3.2b and 3.4b2). To the south, they end in a narrow high-temperature shear zone (Fig. 3.5). Thus, in-relay arrangement and obliquity to the shear zone, suggest that these folds formed in a left-lateral tectonic regime coeval with the high-temperature shearing.

6.2.3. Stage C: Low-temperature shearing

This stage is characterized by shear deformation of the BA unit at low-temperature amphibolite to greenschist conditions. By progressive tightening of the Quintos fold, its southern limb reached a high dip, becoming a subvertical anisotropy that concentrated the deformation. Thus, a net of anastomosed discrete shear zones were developed (Fig. 3.14c). The concentration of low-temperature deformation along discrete shear zones allowed the previous high-temperature tectonic fabric to be preserved at wide sectors of the BA unit. Besides the main ductile shear zones shown in Fig. 3.8, there are outcrop scale shear bands enclosing less deformed amphibolite lozenges. The pitch of the stretching lineation in these low-temperature shear zones is generally low (0–45°) towards the east or SE (Fig. 3.7). The kinematic indicators are abundant and consistently indicate oblique left-lateral movement (Fig. 3.6e-f).

6.2.4. Stage D: Southwards propagation of deformation

Low-temperature shearing in the southern limb of the Quintos fold probably ceased when deformation propagated to the Pulo do Lobo unit (D3 folds) and to the still undeformed SPZ, developing a foreland fold and thrust belt (Fig. 3.14d). In this stage, the deformation was distributed at local scale between folds and brittle faults, with thrust displacements prevailing over left-lateral ones. The intensity of deformation decreased and migrated southwards (Fig. 3.12b). In the Pulo do Lobo unit, recent geochronological dating of deformed and undeformed lithologies of the Gil Márquez pluton (Fig. 3.15c) provides a

possible 345–335 Ma range for the age of this deformation (Gladney et al., 2014). A further constraint is given by our new geochronological data on metavolcanic rocks affected by low-temperature shearing (345 ± 5 Ma, 339 ± 2 Ma, and 337 ± 3 Ma; see section 5.2.3). Accordingly, the age of this deformation in the Pulo do Lobo unit can be tightly constrained between 337 and 335 Ma. Deformation reached the southernmost SPZ in Moscovian time (≈310 Ma; Oliveira (1990)). By that time, left-lateral strike-slip faults concentrated at the OMZ/SPZ boundary (Fig. 3.13 and 3.15c). Thus, transpressive deformation was heterogeneous again, concentrating lateral displacements on brittle faults along the OMZ/SPZ boundary, and shortening on folds and thrusts in the southwestern SPZ.
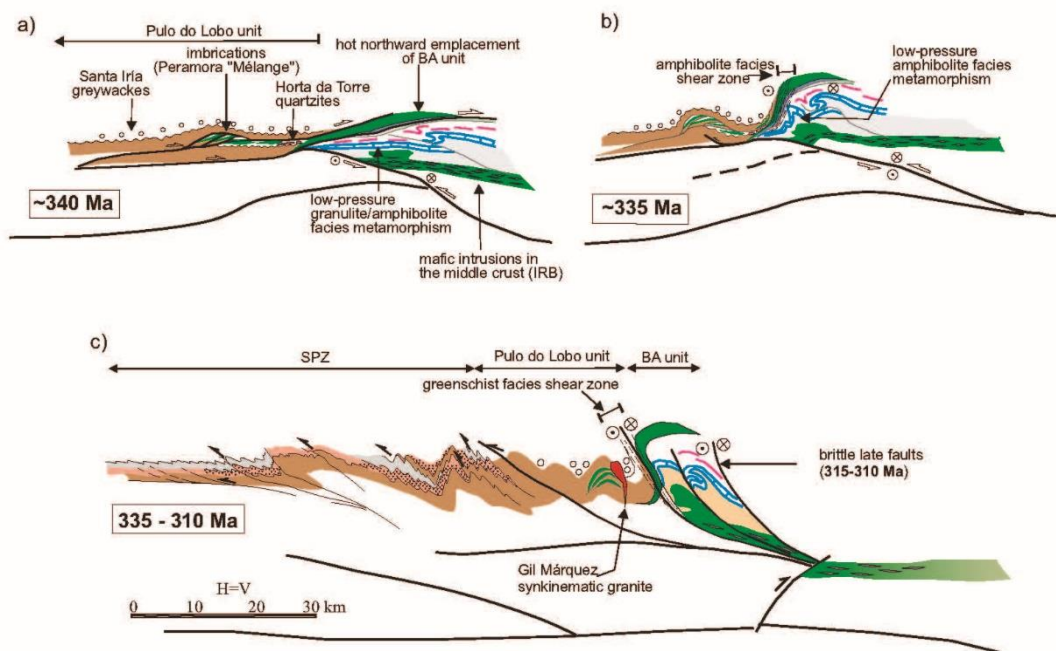
Figure 3.15. (a–c) Evolutionary model of southern Iberia from Middle-Late Devonian to Late Carboniferous. See text for further explanations.

7. Conclusions

We have established for the first time the internal structure of the BA unit, which is essential to decipher the tectonic evolution of the OMZ/SPZ boundary. This unit is affected by a kilometric-scale south-vergent close syn-metamorphic fold that is a main constraint for both geometry and kinematics of the Carboniferous collision.

The structure of the Pulo do Lobo, another key unit of the OMZ/SPZ boundary, has also been determined in this paper for the first time. Our structural analysis has firmly established the relationships between the upper (Carboniferous) and lower (Devonian) formations of this unit and their respective structural evolutions.

The Peramora Mélange has been completely reinterpreted, based on our structural analysis and recent dating (including our own geochronological data) of the mafic rocks. Thus,

instead of a Devonian subduction-related mélange, it is now considered an early Carboniferous, mafic-derived olistostrome, tectonically imbricated with the Devonian Pulo do Lobo phyllites.

The new structural and geochronological data reported in this paper, together with other robust information gained in the last years, lead us to significantly modify several key topics in the evolution of the OMZ/SPZ suture boundary. This evolution involves the following events:

(i) In Late Devonian time, after the Rheic Ocean closure, the southern continental margin of the OMZ was subducted under the SPZ. The subducted rocks were affected by high-pressure metamorphism and then exhumed along with ophiolitic (Rheic Ocean?) rocks in an oblique compressive tectonic regime with left-lateral component.

(ii) A contrasting intracollisional stage dominated by transtension and mafic magmatism occurred in early Carboniferous time, including the BA unit and the Peramora mafic olistostromes. Thus, this stage had outstanding effects on the Rheic suture in SW Iberia, contributing to obscure its recognition.

(iii) The tectonic regime turned again into compression from late Missisippian to end Carboniferous times. The deformation was complex and dominated again by left-lateral transpression. It involved the following events at the OMZ/SPZ boundary (Fig. 3.15): (1) Closing of the BA proto-oceanic domain and thrusting onto the southern continental edge of the OMZ; (2) high-temperature left-lateral ductile shearing and large-scale folding; (3) low-temperature ductile shearing; (4) southwards propagation of the deformation through the SPZ; and final concentration of deformation along the OMZ/SPZ boundary as left-lateral brittle faulting. All these events further contributed to conceal the primary OMZ/SPZ suture.

References

Annen, C., and R. S. J. Sparks (2002), Effects of repetitive emplacement of basaltic intrusions on thermal evolution and melt generation in the crust, Earth and Planetary Science Letters, 203, 937-955.

Apalategui, O., E. Barranco, F. Contreras, M. Delgado and F. J. Roldán (1983), Hoja 916, Aroche, Mapa Geológico de España a escala 1:50000, Inst. Geológico y Minero de España, Madrid.

Apalategui, O., F. Contreras and L. Eguiluz (1984), Hoja 917, Aracena, Mapa Geológico de España a escala 1:50000, Inst. Geológico y Minero de España, Madrid.

Apalategui, O., E. Barranco, F. Contreras, M. Delgado and F. J. Roldán (1990), Hoja 918, Santa Olalla de Cala, Mapa Geológico de España a escala 1:50000, Inst. Geológico y Minero de España, Madrid.

Araujo, A., P. Fonseca, J. Munhá, P. Moita, J. Pedro and A. Ribeiro (2005), The Moura Phyllonitic Complex: An accretionary complex related with obduction in the southern Iberia Variscan suture, Geod. Acta, 18(5), 375-388.

Arenas, R., J. R. Martínez Catalán, S. Sánchez Martínez, F. Díaz García, J. Abati, J. Fernández-Suárez, P. Andonaegui, and J. Gómez-Barreiro (2007a), Paleozoic ophiolites in the Variscan suture of Galicia (northwest Spain): Distribution, characteristics and meaning, in 4-D Framework of Continental Crust, Mem., vol. 200, edited by R. D. Hatcher Jr. et al., pp. 425–444, Geol. Soc. of Am, Boulder, Colo.

Arenas, R., J. R. Martínez Catalán, S. Sánchez Martínez, J. Fernández-Suárez, P. Andonaegui, J. A. Pearce and F. Corfu (2007b), The Vila de Cruces Ophiolite: A remnant of the early Rheic Ocean in the Variscan suture of Galicia (NW Iberian Massif), Journal of Geology, 115, 129-148.

Arenas, R., S. Sánchez Martínez, A. Gerdes, R. Albert, R. Díez Fernández and P. Andonaegui (2014), Re-interpreting the Devonian ophiolites involved in the Variscan suture: U–Pb and Lu–Hf zircon data of the Moeche Ophiolite. International Journal of Earth Sciences (Geol Rundsch), 103(5), 1-18.

Armendáriz, M., R. López-Guijarro, C. Quesada, C. Pin and F. Bellido (2008), Genesis and evolution of a syn-orogenic basin in transpression: Insights from petrography, geochemistry and Sm–Nd systematics in the Variscan Pedroches basin (Mississippian, SW Iberia), Tectonophysics, 461, 395-413.

Azor, A., D. Rubatto, J. F. Simancas, J.F. González Lodeiro, D. Martínez Poyatos, L. M. Martín Parra and J. Matas (2008), Rheic Ocean ophiolitic remnants in Southern Iberia questioned by SHRIMP U-Pb zircon ages on the Beja-Acebuches amphibolites, Tectonics, 27, TC5014, doi: 10.1029/2009TC002527.

Barranco, E., F. Contreras and F. J. Roldán (1983), Hoja 915, Rosal de la Frontera, Mapa Geológico de España a escala 1:50000, Inst. Geológico y Minero de España, Madrid.

Bard, J.P., R. Capdevila, P. Matte and A. Ribeiro (1973), Geotectonic model for the Iberian Variscan Orogen. Nature Physical Science, 241, 50-52.

Bard, J. P. (1977), Signification tectonique des métatholeites d'affinité abyssale de la ceinture de basse pression d'Aracena (Huelva, Espagne), Bulletin de la Société géologique de France, 19, 385-393.

Barrie, C. T., Y. Amelin and E. Pascual (2002), U-Pb geochronology of VMS mineralization in the Iberian Pyrite Belt, Mineralium Deposita, 37(8), 684-703.

Booth-Rea, G., J. F. Simancas, A. Azor, J. M. Azañón, F. Gonzalez Lodeiro and P. Fonseca (2006), HP-LT Variscan metamorphism in the Cubito-Moura schists (Ossa-Morena Zone, southern Iberia), Comptes Rendus Geoscience, 338(16), 1260-1267.

Braid, J. A., J. B. Murphy and C. Quesada (2010), Structural analysis of an accretionary prism in a continental collisional setting, the Late Paleozoic Pulo do Lobo Zone, Southern Iberia, Gondwana Research, 17(2-3), 422-439.

Braid, J. A., J. B. Murphy, C. Quesada and J. Mortensen (2011), Tectonic escape of a crustal fragment during the closure of the Rheic Ocean: U-Pb detrital zircon data from the Late Palaeozoic Pulo do Lobo and South Portuguese zones, southern Iberia, Journal of the Geological Society, London, 168(2), 383-392.

Braid, J. A., J. B. Murphy, C. Quesada, L. Bickerton and J. Mortensen (2012), Probing the composition of unexposed basement, South Portuguese Zone, southern Iberia: implications for the connections between the Appalachian and Variscan orogens. Canadian Journal of Earth Sciences, 49(4), 591-613.

Broutin, J. (1981), Etude paléobotanique et palynologique du passage Carbonifére-Permien dans les bassins continentaux du Sud-Est de la Zone d'Ossa-Morena (environs de Guadacanal, Espagne du Sud). Implications paléogéographiques et stratigraphiques. Ph. D. Thesis, Université Pierre et Marie Curie, Paris, 234 pp.

Cambeses, A. (2015), Ossa-Morena Zone Variscan 'calc-alkaline' hybrid rocks: interaction of mantle- and crustal-derived magmas as a result of intra-orogenic extension-related intraplating. Ph. D. Thesis, Universidad de Granada, 450 pp.

Cambeses, A., J. Scarrow, H., P. Montero, J. F. Molina and J.A. Moreno (2014), SHRIMP U–Pb zircon dating of the Valencia del Ventoso plutonic complex, Ossa-Morena Zone, SW Iberia: Early Carboniferous intra-orogenic extension-related 'calc-alkaline' magmatism, Gondwana Research, 21(4), 887-900.

Carvalho, D. (1972), The metallogenetic consequences of plate tectonics and the upper Paleozoic evolution of southern Portugal, Estudos Notas e Trabalhos S.F.M., 20 (3-4), 297-320.

Castro, A., C. Fernández, J. D. De la Rosa, I. Moreno Ventas and G. Rogers (1996), Significance of MORB-derived amphibolites from the Aracena metamorphic belt, southwest Spain, Journal of Petrology, 37(2), 235-260.

Castro, A., C. Fernández, H. El-Hmidi, M. El-Biad, M. Díaz, J. de la Rosa and F. Stuart (1999), Age constraints to the relationships between magmatism, metamorphism and tectonism in the Aracena metamorphic belt, southern Spain, International Journal of Earth Sciences, 88(1), 26-37.

Cocks, L. R. M., and R. A. Fortey (1982), Faunal evidence for oceanic separations in the Palaeozoic of Britain. Journal of the Geological Society, London, 139, 465-78.

Cocks, L. R. M., and R. A. Fortey (1988), Lower Palaeozoic facies and faunas around Gondwana, in Gondwana and Tethys, edited by M.G. Audley-Charles and A. Hallam, Geological Society, London, Memoirs, 37, 183-200.

Cocks, L. R. M., and T.H. Torsvik (2002), Earth Geography from 500 to 400 million years ago: a faunal and palaeomagnetic review, Journal of the Geological Society, London, 159, 631-644.

Contreras, F. and A. Santos (1984), Hoja 937, El cerro de Andévalo, Mapa Geológico de España a escala 1:50000, Inst. Geológico y Minero de España, Madrid.

Crespo-Blanc, A. (1991), Evolución geotectónica del contacto entre la zona de Ossa-Morena y la zona Surportuguesa en las sierras de Aracena y Aroche (Macizo Ibérico Meridional): Un

contacto mayor en la cadena Hercínica Europea. Ph. D. Thesis, Universidad de Granada, 327 pp.

Dahn, D. R. L., J. A. Braid, J. B. Murphy, C. Quesada, N. Dupuis, and C. R. M. McFarlane (2014), Geochemistry of the Peramora Melange and Pulo do Lobo schist: geochemical investigation and tectonic interpretation of mafic melange in the Pangean suture zone, Southern Iberia, International Journal Earth Sciences, 103(5), 1415-1431.

Dallmeyer, R. D., P. E. Fonseca, C. Quesada, and A. Ribeiro (1993), ^{40}Ar/^{39}Ar Mineral Age Constraints for the Tectonothermal Evolution of a Variscan Suture in Southwest Iberia, Tectonophysics, 222(2), 177-194.

Dessureau, G., D. J. W. Piper and G. Pe-Piper (2000), Geochemical evolution of earliest Carboniferous continental tholeiitic basalts along a crustal-scale shear zone, southwestern Maritimes basin, eastern Canada, Lithos, 50(1-3), 27-50.

Dewey, J. F. (1977), Suture zone complexities - Review, Tectonophysics, 40(1-2), 53-67.

De Yoreo, J. J., D. R. Lux and C. V. Guidotti (1991), Thermal modeling in low-pressure/high-temperature metamorphic belts, Tectonophysics, 188, 209-238.

Díaz Azpiroz, M., and C. Fernández (2003), Characterization of tectono-metamorphic events using crystal size distribution (CSD) diagrams. A case study from the Acebuches metabasites (SW Spain), Journal of Structural Geology, 25(6), 935-947.

Díaz Azpiroz, M., A. Castro, C. Fernández, S. López, J. C. Fernández Caliani and I. Moreno-Ventas (2004), The contact between the Ossa-Morena and the South Portuguese zones: Characteristics and significance of the Aracena metamorphic belt, in its central sector between Aroche and Aracena (Huelva), Journal of Iberian Geology, 30, 23-51.

Díaz Azpiroz, M., and C. Fernández (2005), Kinematic analysis of the southern Iberian shear zone and tectonic evolution of the Acebuches metabasites (SW Variscan Iberian Massif), Tectonics, 24, TC3010, doi: 10.1029/2004TC001682.

Díaz Azpiroz, M., C. Fernández, A. Castro and M. El-Biad (2006), Tectonometamorphic evolution of the Aracena metamorphic belt (SW Spain) resulting from ridge-trench interaction during Variscan plate convergence, Tectonics, 25, TC1001, doi: 10.1029/2004TC001742.

Díaz García, F., R. Arenas, J. R. Martínez Catalán, J. González del Tanago and G. R. Dunning (1999), Tectonic evolution of the Careón ophiolites (northwest Spain): A remnant of oceanic lithosphere in the Variscan belt, Journal of Geology, 107, 587-605.

Díez Fernández, R. and R. Arenas (2015), The Late Devonian Variscan suture of the Iberian Massif: A correlation of high-pressure belts in NW and SW Iberia, Tectonophysics, 654, 96-100.

Dunning, G. R., A. Díez Montes, J. Matas, L. M. Martín Parra, J. Almarza and M. Donaire (2002), Geocronología U/Pb del volcanismo ácido y granitoides de la Faja Pirítica Ibérica (Zona Surportuguesa), Geogaceta, 32, 127-130.

Eden, C., and J. Andrews (1990), Middle to upper Devonian melanges in SW Spain and their relationship to the Meneage formation in south Cornwall, Proceedings of the Ussher Society, 7, 217-222.

Eden, C. P. (1991), Tectonostratigraphic analysis of the northern extent of the oceanic exotic terrane, Northwestern Huelva Province, Spain. Ph. D. Thesis, University of Southhampton, 214 pp.

Expósito, I., J. F. Simancas, F. González Lodeiro, A. Azor and D. J. Martínez Poyatos (2002), Estructura de la mitad septentrional de la zona de Ossa-Morena: Deformación en el bloque inferior de un cabalgamiento cortical de evolución compleja, Revista de la Sociedad Geológica de España, 15, 3-14.

Faure, M., J. M. Lardeaux and P. Ledru (2009), A review of the pre-Permian geology of the Variscan French Massif Central, Comptes Rendus Geoscience, 341, 202-213.

Fonseca, P., and A. Ribeiro (1993), Tectonics of the Beja-Acebuches Ophiolite - a Major Suture in the Iberian Variscan Foldbelt, Geologische Rundschau, 82(3), 440-447.

Fonseca, P., J. Munhá, J. Pedro, F. Rosas, P. Moita, A. Araujo and N. Leal (1999), Variscan ophiolites and high-pressure metamorphism in southern Iberia, Ofioliti, 24(2), 259-268.

Fonseca, P. E. (2005), O terreno acrecionário do Pulo do Lobo: implicações geodinâmicas da sutura com a Zona de Ossa-Morena (SW da Cadeia Varisca Ibérica), Cadernos do Laboratorio Xeolóxico de Laxe, 30, 213-222.

Fonseca, P. E. (1989), Estudo de um segmento da sutura da Cadeia Varisca Ibéacuterica: Serpa - Pulo do Lobo, PhD thesis, Dep. Geologia da FCUL, Lisbon.

Figueiras, J., A. Mateus, M. A. Goncalves, J. Waerenborgh and P. Fonseca (2002), Geodynamic evolution of the South Variscan Iberian Suture as recorded by mineral transformations, Geodinamica Acta, 15(1), 45-61.

Gehrels, G. (2011), Detrital Zircon U-Pb Geochronology: Current Methods and New Opportunities, in Tectonics of Sedimentary Basins: Recent Advances, edited by C. Busby and A. Azor, John Wiley, Chichester, U. K., doi: 10.1002/9781444347166.ch2.

Giese, U. and B. Bühn (1993), Early Paleozoic rifting and bimodal volcanism in the Ossa-Morena Zone of south-west Spain, Geologische Rundschau, 83, 143-160.

Gladney, E. R., J. A. Braid, J. B. Murphy, C. Quesada and C. R. M. McFarlane (2014), U-Pb geochronology and petrology of the late Paleozoic Gil Marquez pluton: magmatism in the Variscan suture zone, southern Iberia, during continental collision and the amalgamation of Pangea, International Journal of Earth Sciences, 103(5), 1433-1451.

Gómez-Pugnaire, M. T., A. Azor, J. M. Fernández-Soler and V. López Sánchez-Vizcaíno (2003), The amphibolites from the Ossa-Morena/Central Iberian Variscan suture (southwestern Iberian Massif): Geochemistry and tectonic interpretation, Lithos, 68, 23-42.

Gonzalo, F., J. Locutura, A. Sánchez and F. Vázquez (1978), Hoja 936, Paymogo, Mapa Geológico de España a escala 1:50000, Inst. Geológico y Minero de España, Madrid.

Jerez Mir, F. and G. García Monzón (1973), Hoja 919, Almadén de la Plata, Mapa Geológico de España a escala 1:50000, Inst. Geológico y Minero de España, Madrid.

Livermore, R. A., A. G. Smith and J. C. Briden (1985), Paleomagnetic Constraints on the Distribution of Continents in the Late Silurian and Early Devonian, Philosophical Transactions of the Royal Society of London Series B-Biological Sciences, 309 (1138), 29-56.

Lopes, G., Z. Pereira, P. Fernandes, R. Wicander, J. X. Matos, D. Rosa and J. T. Oliveira (2014), The significance of reworked palynomorphs (middle Cambrian to Tournaisian) in the Visean Toca da Moura Complex (South Portugal). Implications for the geodynamic evolution of Ossa Morena Zone, Review of Palaeobotany and Palynology, 200, 1-23.

Martínez Catalán, J. R., R. Arenas, F. Díaz García and J. Abati (1997), Variscan accretionary complex of northwest Iberia: Terrane correlation and succession of tectonothermal events. Geology, 25, 1103-1106.

Martínez Poza, A. I., D. J. Martínez Poyatos, J. F. Simancas and A. Azor (2012), La estructura varisca de la Unidad del Pulo do Lobo (SO del Macizo Ibérico) en las transversales de Aroche y Rosal de la Frontera (Huelva), Geogaceta, 52, 21-24.

Matte, P. (1991), Accretionary history and crustal evolution of the Variscan Belt in western Europe, Tectonophysics, 196, 309-339.

Matte, P. (2001), The Variscan collage and orogeny (480-290 Ma) and the tectonic definition of the Armorica microplate: a review, Terra Nova, 13, 122-128.

McKerrow, W. S., and A. M. Ziegler, (1972), Paleozoic oceans, Nature, 240, 92-94.

Moita, P., J. Munhá, P. E. Fonseca, C. C. G. Tassinari, A. Araújo and T. Palácios (2005), Phase equilibria and geochronology of Ossa-Morena eclogites, VIII Congreso de Geoquímica dos Países de Língua Portuguesa, Universidade de Aveiro, Aveiro, Portugal, 463-466.

Munhá, J. (1983), Hercynian magmatism in the Iberian Pyrite Belt, in The Carboniferous of Portugal, edited by M. J. L. Sousa and J. T. Oliveira, Mem. Serv. Geol. Portugal, 29, 39-81.

Munhá, J., J. T. Oliveira, A. Ribeiro, V. Oliveira, C. Quesada and R. Kerrich (1986), Beja-Acebuches ophiolite, characterization and geodynamic significance, Maleo, 2, 31.

Murphy, J. B., and J. D. Keppie (2005), The Acadian Orogeny in the northern Appalachians, International Geology Review, 47, 663-687.

Navarro, D. and J. Ramírez Copeiro del Villar (1978), Hoja 938, Nerva, Mapa Geológico de España a escala 1:50000, Inst. Geológico y Minero de España, Madrid.

Oliveira, J. T. (1990), Part VI: South Portuguese Zone, stratigraphy and synsedimentary tectonism, in Pre-Mesozoic Geology of Iberia, edited by R. D. Dallmeyer and E. Martínez García, Springer, 334-347.

Oliveira, J. T. and E. Pereira (1992), Carta Geológica de Portugal, na escala de 1:500 000, Seviços Geológicos de Portugal.

Onézime, J., J. Charvet, M. Faure, A. Chauvet and D. Panis (2002), Structural evolution of the southernmost segment of the West European Variscides: the South Portuguese Zone (SW Iberia), Journal of Structural Geology, 24(3), 451-468.

Palomeras, I., R. Carbonell, I. Flecha, F. Simancas, P. Ayarza, J. Matas, D. Martínez Poyatos, A. Azor, F. González Lodeiro and A. Perez-Estaún (2009), Nature of the lithosphere across the Variscan orogen of SW Iberia: Dense wide-angle seismic reflection data, Journal of Geophysical Research-Solid Earth, 114(B2).

Pedro, J., A. Araujo, P. Fonseca, C. Tassinari and A. Ribeiro (2010), Geochemistry and U-Pb Zircon Age of the Internal Ossa-Morena Zone Ophiolite Sequences: A Remnant of Rheic Ocean in SW Iberia, Ofioliti, 35(2), 117-130.

Pereira, M. F., M. Chichorro, S. T. Johnston, G. Gutiérrez-Alonso, J. B. Silva, U. Linnemann, M. Hofmann and K. Drost (2012a), The missing Rheic Ocean magmatic arcs: Provenance analysis of Late Paleozoic sedimentary clastic rocks of SW Iberia, Gondwana Research, 22(3-4), 882-891.

Pereira, M. F., M. Chichorro, J. B. Silva, B. Ordóñez-Casado, J. K. W. Lee and I. S. Williams (2012b), Early carboniferous wrenching, exhumation of high-grade metamorphic rocks and basin instability in SW Iberia: Constraints derived from structural geology and U-Pb and $^{40}Ar/^{39}Ar$ geochronology, Tectonophysics, 558, 28-44.

Pereira, M.F., C. Ribeiro, F. Vilallonga, M. Chichorro, K. Drost, J. B. Silva, L. Albardeiro, M. Hofmann and U. Linnemann (2014), Variability over time in the sources of South Portuguese Zone turbidites: evidence of denudation of different crustal blocks during the assembly of Pangaea, International Journal of Earth Sciences (Geol Rundsch), 103, 1453-1470.

Pereira, Z., J. Matos, P. Fernandes and J. T. Oliveira (2007), Devonian and Carboniferous palynostratigraphy of the South Portuguese Zone, Portugal – An overview, Comunicações Geológicas, 94, 53-79.

Pin, C., P. E. Fonseca, J. L. Paquette, P. Castro and P. Matte (2008), The ca. 350 Ma Beja Igneous Complex: A record of transcurrent slab break-off in the Southern Iberia Variscan Belt?, Tectonophysics, 461(1-4), 356-377.

Ponce, C., J. F. Simancas, A. Azor, D. J. Martínez Poyatos, G. Booth-Rea and I. Expósito (2012), Metamorphism and kinematics of the early deformation in the Variscan suture of SW Iberia, Journal of Metamorphic Geology, 30(7), 625-638.

Quesada, C., P. E. Fonseca, J. Munhá, J. T. Oliveira and A. Ribeiro (1994), The Beja–Acebuches Ophiolite (Southern Iberia Variscan fold belt): geological characterization and significance, Boletín Geológico Minero, 105, 3-49.

Ribeiro, A., J. Munhá, R. Dias, A. Mateus, E. Pereira, L. Ribeiro, P. Fonseca, A. Araújo, T. Oliveira, J. Romao, H. Chaminé, C. Coke and J. Pedro (2007), Geodynamic evolution of the SW Europe Variscides, Tectonics, 26, TC6009.

Ribeiro, A., J. Munhá, P. E. Fonseca, A. Araujo, J. C. Pedro, A. Mateus, C. Tassinari, G. Machado and A. Jesus (2010), Variscan ophiolite belts in the Ossa-Morena Zone (Southwest Iberia): Geological characterization and geodynamic significance, Gondwana Research, 17(2-3), 408-421.

Rodrigues, B., D. M. Chew, R. C. G. S. Jorge, P. Fernandes, C. Veiga-Pires and J. T. Oliveira (2015), Detrital zircon geochronology of the Carboniferous Baixo Alentejo Flysch Group (South Portugal); constraints on the provenance and geodynamic evolution of the South Portuguese Zone, Journal of the Geological Society, London, 2013-2084.

Rubio Pascual, F. J., J. Matas and L. M. Martín Parra (2013), High-pressure metamorphism in the Early Variscan subduction complex of the SW Iberian Massif, Tectonophysics, 592, 187-199.

Sánchez Martínez, S., R. Arenas, A. Gerdes, P. Castiñeiras, A. Potrel and J. Fernández-Suárez (2011), Isotope geochemistry and revised geochronology of the Purrido Ophiolite (Cabo Ortegal Complex, NW Iberian Massif): Devonian magmatism with mixed sources and involved Mesoproterozoic basement. Journal of the Geological Society, London, 168, 733-750.

Schermerhorn, J. L. G. (1971), An outline stratigraphy of the Pyrite Belt, Boletín Geológico Minero, 82, 239-268.

Schmelzbach, C., J. F. Simancas, C. Juhlin and R. Carbonell (2008), Seismic reflection imaging over the south Portuguese zone fold-and-thrust belt, SW Iberia, Journal of Geophysical Research-Solid Earth, 113(B8).

Schulmann, K., O. Lexa, V. Janoušek, J. M. Lardeaux and J. B. Edel (2014), Anatomy of a diffuse cryptic suture zone: An example from the Bohemian Massif, European Variscides. Geology, 42(4), 275-278.

Scotese, C. R., R. Vandervoo and S. F. Barrett (1985), Silurian and Devonian Base Maps, Philosophical Transactions of the Royal Society of London Series B-Biological Sciences, 309(1138), 57-77.

Scotese, C.R., and J. Golonka (1992), Paleogeographic Atlas, PALEOMAP Progress Report 20-0692, 34 pp, Department of Geology, University of Texas at Arlington.

Silva, J. B., J. T. Oliveira and A. Ribeiro (1990), South Portuguese Zone, estructural outline, in Pre-Mesozoic Geology of Iberia, edited by R. D. Dallmeyer, E. Martínez García, Springer, Berlin, Germany, 348-362.

Simancas, J. F. (1983), Geología de la Extremidad Oriental de la Zona Sudportuguesa, Ph. D. Thesis, Universidad de Granada, 439 pp.

Simancas, J. F., D. Martínez Poyatos, I. Expósito, A. Azor and F. González Lodeiro (2001), The structure of a major suture zone in the SW Iberian Massif: the Ossa-Morena/Central Iberian contact, Tectonophysics, 332(1-2), 295-308.

Simancas, J. F., R. Carbonell, F. González Lodeiro, A. Pérez-Estaún, C. Juhlin, P. Ayarza, A. Kashubin, A. Azor, D. Martínez Poyatos, G. R. Almodóvar, E. Pascual, R. Sáez and I. Expósito (2003), Crustal structure of the transpressional Variscan orogen of SW Iberia: SW Iberia deep seismic reflection profile (IBERSEIS), Tectonics, 22(6), 1062.

Simancas, J. F. (2004), Zona Sudportuguesa, in Geología de España, edited by J. A. Vera, 199-201, SGE-IGME, Madrid, Spain.

Simancas, J. F., A. Tahiri, A. Azor, F. González Lodeiro, D. J. Martínez Poyatos and H. El Hadi (2005), The tectonic frame of the Variscan-Alleghanian orogen in southern Europe and northern Africa, Tectonophysics, 398(3-4), 181-198.

Simancas, J. F., R. Carbonell, F. González Lodeiro, A. Pérez-Estaún, C. Juhlin, P. Ayarza, A. Kashubin, A. Azor, D. J. Martínez Poyatos, R. Sáez, G. R. Almodóvar, R. Pascual, I. Flecha and D. Martí (2006), Transpressional collision tectonics and mantle plume dynamics, in The Variscides of southwestern Iberia, edited by D. G. Gee and R. A. Stephenson, Geological Society, London, Memoirs, 32, 345-354.

Simancas, J. F., A. Azor, D. Martínez Poyatos, A. Tahiri, H. El Hadi, F. González Lodeiro, A. Pérez-Estaún and R. Carbonell (2009), Tectonic relationships of Southwest Iberia with the allochthons of Northwest Iberia and the Moroccan Variscides, Comptes Rendus Geoscience, 341(2-3), 103-113.

Stampfli, G. M., and G. D. Borel (2002), A plate tectonic model for the Paleozoic and Mesozoic constrained by dynamic plate boundaries and restored synthetic oceanic isochrones, Earth and Planetary Science Letters, 196, 17-33.

Valenzuela, A., T. Donaire, C. Pin, M. Toscano, M. A. Hamilton and E. Pascual (2011), Geochemistry and U-Pb dating of felsic volcanic rocks in the Riotinto-Nerva unit, Iberian

Pyrite Belt, Spain: crustal thinning, progressive crustal melting and massive sulphide genesis, Journal of the Geological Society, London, 168(3), 717-731.

Wickham, S. M., and E. R. Oxburgh (1987), Low-pressure regional metamorphism in the Pyrenees and its implications for the thermal evolution of rifted continental crust, Philosophical transactions of the Royal Society of London Series A-Mathematical Physical and Engineering Sciences, 321, 219-242.

Chapter IV

Metamorphism of the Pulo do Lobo unit

The metamorphism of the Pulo do Lobo unit is described in this chapter. To this end, three different and complementary methodologies have been applied. The new results reported here contribute to the knowledge of the metamorphic conditions of the Pulo do Lobo unit in relation to its deformation. Furthermore, the results are compared in order to assess the reliability of the different methods applied.

Multidisciplinary study of the low-grade metamorphism of the Pulo do Lobo metasedimentary belt (SW Iberian Variscides)

Irene Pérez-Cáceres[1], David Martínez Poyatos[1], Olivier Vidal[2], Olivier Beyssac[3], Fernando Nieto[4], José Fernando Simancas[1], and Antonio Azor[1].

1 Departamento de Geodinámica, Facultad de Ciencias, Universidad de Granada, Campus de Fuentenueva s/n, 18071 Granada, Spain.

2 Institut de Sciences de la Terre (ISTerre), CNRS-University of Grenoble 1, 1381 rue de la Piscine, 38041 Grenoble, France.

3 Institut de Minéralogie et de Physique des Milieux Condensés (IMPMC), CNRS-Université Pierre et Marie Curie, Case Courrier 115, 4 place Jussieu, 75005 Paris, France.

4 Departamento de Mineralogía y Petrología, IACT, Facultad de Ciencias, Universidad de Granada-CSIC, Campus de Fuentenueva s/n, 18071 Granada, Spain.

Abstract

The Pulo do Lobo belt is one of the units related to the orogenic suture between the Ossa-Morena and the South Portuguese zones in the SW Iberian Variscides. This unit has been classically interpreted as a Rheic subduction-related accretionary prism formed during the pre-Carboniferous convergence and eventual collision between the South Portuguese Zone (part of Avalonia) and the Ossa-Morena Zone (peri-Gondwanan terrane). Before resuming the collision that dominated late Carboniferous time, a Mississippian transtensional event took place, with extensive magmatism that in the Pulo do Lobo belt is represented by discrete mafic intrusions in the dominant metapelites. Three methodologies have been applied to the Devonian/Carboniferous phyllites and slates of the Pulo do Lobo belt in order to study their poorly known low-grade metamorphic evolution. X-Ray diffraction (XRD) was used to specify the mineralogy and to measure crystallographic parameters (illite crystallinity and white mica b-cell dimension). Compositional maps of selected samples were obtained from electron probe microanalysis, and processed with the XmapTools software to produce mineralogical maps and chlorite geothermometric

calculations through thermodynamic modeling. Raman spectrometry of carbonaceous matter (RSCM) was used to obtain peak temperatures.

The microstructural study evidences the existence of two phyllosilicate growth events at the chlorite zone, the main one (M1) related to the development of a Devonian foliation S1, and a minor one (M2) associated with a crenulation cleavage (S2) developed at middle/upper Carboniferous time. M1 entered well into epizone (greenschist facies) conditions (≈400-500 °C), as indicated by illite crystallinity, RSCM and relic chlorite core thermometry. A number of evidences suggest chlorite retrogression after M1, thus precluding the use of the muscovite/chlorite thermobarometer, which in fact shows thermodynamic disequilibrium. M2 conditions were of lower temperature, in accordance with the unconformity that separates the Devonian and Carboniferous formations of the Pulo do Lobo belt, reaching the anchizone/epizone boundary (≈300-330 °C, as derived from illite crystallinity and RSCM thermometry). Regarding the metamorphic pressure, the data are very homogeneous (very low celadonite content in muscovite and low values of white mica *b*-cell dimension), being compatible with a low-pressure gradient, which, in turn, is unexpected in a subduction-related accretionary prism.

Keywords

Pulo do Lobo metapelites

Low-grade metamorphism

Low-pressure gradient

X-Ray diffraction

Chlorite thermometry

Raman spectroscopy of carbonaceous matter

Highlights

Three different methods (X-Ray diffraction, EPMA, RSCM) to study the metamorphism of the Pulo do Lobo metapelites.

Devonian metamorphism entered epizone conditions.

Carboniferous metamorphism reached the anchizone/epizone boundary.

The inferred low-pressure gradient is incompatible with a subduction-related accretionary prism.

1. Introduction

The knowledge of temperature and pressure conditions reached by the different units stacked hinterlands of orogens helps to better interpret their tectonometamorphic evolution (e.g., Goffé and Velde, 1984; Smith, 1984; Goffé and Chopin, 1986; Jolivet et al., 1994; Gutiérrez-Alonso and Nieto, 1996; Bousquet et al., 2008; Lanari et al., 2012). Moreover, the application of diverse geothermometric and/or geobarometric methods and the comparison between the obtained results, lead to a more accurate interpretation (e.g., Vidal et al., 2006; Ali, 2010; Lanari et al., 2012). The varied results derived from different methodologies may also allow the characterization of superposed tectonometamorphic events, thus improving the knowledge of the P-T paths and their tectonic significance.

The metamorphism in the Iberian Variscides has been mostly studied in intensely metamorphosed rocks, in order to characterize high-grade events and obtain the P-T-t paths of suture-related units (e.g., Gil Ibarguchi et al., 1990; Abalos et al., 1991; Escuder Viruete et al., 1994; Barbero et al., 1995; Martínez Catalán et al., 1996; Arenas et al., 1997; Azor and Ballèvre, 1997; Fonseca et al., 1999; Díaz Azpiroz et al., 2006; Rosas et al., 2008; Pereira et al., 2010; Ponce et al., 2012; López-Carmona et al., 2013; Martínez Catalán et al., 2014). The low- to very low-grade units have received much less attention (e.g., Martínez Catalán, 1985; Bastida et al., 1986, 2002; López Munguira et al., 1991; Gutiérrez-Alonso and Nieto, 1996; Abad et al., 2001, 2002, 2003; Martínez Poyatos et al., 2001; Nieto et al., 2005; Vázquez et al., 2007), mostly due to the scarcity of appropriate robust methodologies to apply in these kind of rocks. Despite the difficulties, obtaining new results from low-grade rocks is of capital importance in order to understand the tectonometamorphic evolution of some key units of the Iberian Variscides.

In this work, three different methodologies are applied to the metapelites of the Pulo do Lobo belt, a suture-related low-grade unit in SW Iberia (Fig. 4.1), aiming to better constrain its tectonometamorphic evolution and significance. To do so, a number of samples were analyzed with: (i) X-Ray Diffraction (XRD) in order to identify the significant mineralogy not easily recognizable with optical microscopy (fine-grained muscovite, paragonite, mixed-layer phyllosilicates, etc.) and measure crystallographic parameters (illite crystallinity and b-cell dimension); (ii) Compositional maps derived from electron probe microanalysis (EPMA) and thermodynamic modeling through chlorite chemistry; and (iii) Raman spectrometry of carbonaceous matter (RSCM) to stablish peak temperatures. Finally, as well as providing with new data and interpretation about the metamorphism of the Pulo do Lobo belt, the comparison between the results obtained by the different applied methodologies allows a discussion on their reliability and sensitivity to different geological processes.

2. Geological setting

The SW of Iberia resulted, in the frame of the Variscan/Alleghanian orogeny, as from the Devonian-Carboniferous left-lateral oblique collision of three terranes represented, from north to south, by the Central Iberian Zone (CIZ), the Ossa-Morena Zone (OMZ) and the external South Portuguese Zone (SPZ) (Fig. 4.1a). The boundaries between these terranes

are considered as orogenic sutures (Pérez-Cáceres et al., 2016, and references therein). Besides the dominant left-lateral kinematics, SW Iberia also attests Mississippian synorogenic sedimentary basins, widespread mafic magmatism and high-temperature metamorphic areas, which altogether reveal an intracollisional transtensional stage (Simancas et al., 2003, 2006; Pereira et al., 2012).

The OMZ is commonly interpreted as a continental piece that drifted from the CIZ (i.e., north Gondwana) in early Paleozoic times (Matte, 2001). Both zones are composed by Ediacaran to Carboniferous sedimentary successions mostly affected by Variscan NW-SE trending folds and regional low-grade metamorphism. The OMZ/CIZ suture (Badajoz-Córdoba Shear Zone) includes early Paleozoic amphibolites with oceanic affinity, Late Devonian eclogite relicts and intense high- to low-grade left-lateral shear imprint (Burg et al., 1981; Abalos et al., 1991; Azor et al., 1994; Ordóñez-Casado, 1998; López Sánchez-Vizcaíno et al., 2003; Pereira et al., 2010). In the southern OMZ, an autochthonous high-temperature metamorphic area (Évora-Aracena) is composed of gabbros, anatectic granodiorites and high-temperature/low-pressure metamorphic rocks (Bard, 1977; Crespo-Blanc, 1991; Díaz Azpiroz et al., 2006; Pereira et al., 2009). These rocks show a gneissic-migmatitic foliation (dated as 345-330 Ma; Dallmeyer et al., 1993; Castro et al., 1999) associated with SW-vergent folds, and a relic foliation is also observed in restitic enclaves.

The SPZ is a continental piece considered as a fragment of Avalonia (Pérez-Cáceres et al., 2017 and references therein). The OMZ/SPZ boundary is represented by the well-known Beja-Acebuches Amphibolites (Fig. 4.1b), a narrow strip of metamafic rocks that resemble a dismembered ophiolitic succession (from greenschists to metagabbros and locally ultramafic rocks) (e.g., Bard, 1977; Crespo-Blanc, 1991; Quesada et al., 1994). This boundary was interpreted as a Variscan suture of the Rheic Ocean that separated Avalonia/Laurrusia and Gondwana during Ordovician to Devonian times (Munhá et al., 1986; Crespo-Blanc, 1991; Fonseca and Ribeiro, 1993; Quesada et al., 1994; Castro et al., 1996), though this idea was reconsidered based on the Mississippian age of the mafic protholits (≈340 Ma; Azor et al., 2008). Actually, the Beja-Acebuches unit is better interpreted as an outstanting part of the early Carboniferous intraorogenic, lithospheric-scale transtensional and magmatic episode that here obscures the previous suture-related features of the OMZ/SPZ boundary (Pérez-Cáceres et al., 2015 and references therein). The rocks of the Beja-Acebuches Amphibolites were affected by a left-lateral ductile shearing occurred at granulite to greenschist facies conditions, though amphibolite facies conditions were dominant (e.g., Quesada et al., 1994; Castro et al., 1996; Castro et al., 1999; Díaz Azpiroz et al., 2006). This metamorphism has been dated in 345-330 Ma (Dallmeyer et al., 1993; Castro et al., 1999), thus suggesting that it started very shortly after the magmatic emplacement.

The allochthonous Cubito-Moura unit (Fonseca et al., 1999; Araújo et al., 2005; Rosas et al., 2008; Pérez-Cáceres et al., 2015) was emplaced onto the southern OMZ border (Fig. 4.1b) with a left-lateral top-to-the-ENE kinematics (Ponce et al., 2012). This unit contains Ediacaran-Lower Paleozoic continental and Ordovician (≈480 Ma as preliminar protholith age; Pedro et al., 2010) MORB-featured mafic rocks transformed into high-pressure blueschists and eclogites at ≈370 Ma, according to a preliminar Sm-Nd dating (Moita et al., 2005). Apart from the characterization of eclogites and blue-schists, the high-pressure

metamorphism has also been studied by using white mica and chlorite (and chloritoid pseudomorphs) mineral equilibria (Booth-Rea et al., 2006; Ponce et al., 2012; Rubio Pascual et al., 2013), which yielded conditions of 1 GPa at 450 °C during in the first deformation phase and 0.8 to 0.5 GPa at 450 °C during the second one. According to Ponce et al. (2012), the high-pressure rocks would belong to a subducted portion of the southern border of the OMZ, while the metamafic rocks would represent Rheic Ocean slivers scrapped off and exhumed during the early Variscan collision with the SPZ.
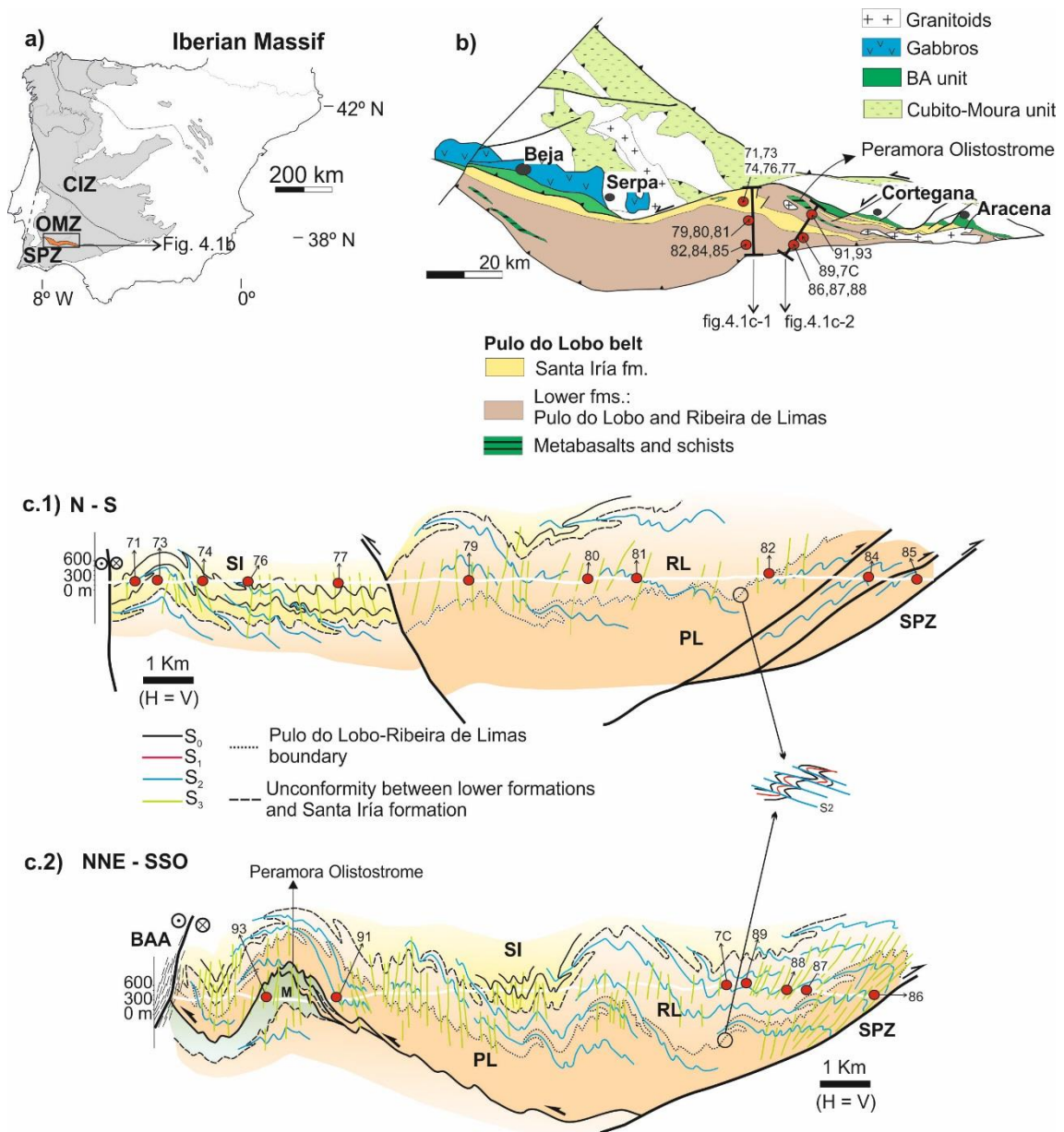
Figure 4.1. a) Geological subdivision of the Iberian Massif. OMZ: Ossa-Morena Zone, SPZ: South Portuguese Zone, CIZ: Central Iberian Zone. b) Geological map of the Pulo do Lobo belt and other units related to the OMZ/SPZ boundary. c.1-2) Geological cross-sections of the Pulo do Lobo belt (see b for location) (modified from Martínez Poza et al., 2012 and Pérez-Cáceres et al., 2015). Numbered red circles in b-c locate the samples studied. BAA: Beja-Acebuches amphibolites, M: metabasalts, PL: Pulo do Lobo formation, RL: Ribeira de Limas formation, SI: Santa Iría formation.

South of the Beja-Acebuches Amphibolites, low- to very low-grade successions crop out in the SPZ: Devonian siliciclastics, earliest Carboniferous volcanosedimentary successions, and a south-migrating Carboniferous flysch that represents the foreland of the Variscan orogen (e.g., Oliveira et al., 1990). The SPZ can be divided, from north to south, into the Pulo do Lobo belt (see below), the Iberian Pyrite belt (that includes massive sulphide deposits) and the Carboniferous flysch. The deformation in the SPZ consists in a south- to southwest-vergent fold and thrust belt with decreasing strain intensity and age southwards (Oliveira et al., 1990; Simancas, 2004). The metamorphic grade also decreases southwards, from epizone to diagenesis, through the SPZ (Munhá, 1990; Abad et al., 2001).

2.1. Pulo do Lobo belt

Besides the Beja-Acebuches and Cubito-Moura units, a third key element related to the OMZ/SPZ suture is the Pulo do Lobo belt, which crops out just south of this boundary and represents the northernmost SPZ (Fig. 4.1b). The Pulo do Lobo belt constitutes a refolded structure involving low-grade Devonian-Carboniferous sedimentary formations. These formations are, from base to top (Fig. 4.1b-c):

(i) The Pulo do Lobo formation (s. str.) is constituted by a continuous series from satin black and grey to light brown phyllites, fine-grained schists, and minor intercalations of quartz sandstones (Fig. 4.2a). The presence of abundant segregated quartz veins (pre- to post-folds) is common. Fossils have not been found in this formation, tough it is stratigraphically below the Ribeira de Limas formation (see below). For that reason, the Pulo do Lobo formation must be older than lower Frasnian, probably Givetian in age.

(ii) The Ribeira de Limas formation is constituted by phyllites and slates with thin beds of quartz sandstones and arkoses (Fig. 4.2b). The presence of palynomorphs has enabled to date this formation as upper Givetian-early Frasnian (Pereira et al., 2008). The contact between the Pulo do Lobo and Ribeira de Limas formations is gradual, with a progressive increase of sandstones and a decrease of black slates upwards. For that reason, distinguishing between both formations near the contact is sometimes difficult. Consequently, we refer to the Pulo do Lobo and Ribeira de Limas formations as the lower formations of the Pulo do Lobo belt. Furthermore, these lower formations share the same structure consisting in three fold-related foliations, which contrasts with the upper formation with only two foliations (Fig. 4.2a-b; Pérez-Cáceres et al., 2015). The first foliation of the lower formations (S1) is preserved inside microlithons of the second foliation (S2); usually, the angle between these two foliations is high. S2 is the main foliation and consists in a crenulation-dissolution cleavage that frequently appears as a milimetric- to centimetric-spaced tectonic banding. This foliation is related to north-vergent folds. The third foliation (S3) is a spaced crenulation-dissolution cleavage that sometimes develops a characteristic decimetric to metric tectonic banding. S3 is related to upright to slightly south-vergent folds.

(iii) The Santa Iría formation is composed by alternating beds of slates and greywackes (Fig. 4.2c). The greywacke beds show normal grading and erosive base. Paleontological and palynostatigraphic studies suggest an Upper Frasnian to Upper Famennian age for this

formation (Pereira et al., 2008). However, an early Carboniferous age is much plausible, since more than 90% of the palynomorphs correspond to reworked material (Lopes et al., 2014) and the younger detrital zircon populations are early Carboniferous (Braid et al., 2011; Pérez-Cáceres et al., 2017). The Santa Iría formation only shows two foliations, correlative with the last two deformation phases of the lower formations. Therefore, an unconformity between them is inferred, which also agrees with the age and flysch character of the Santa Iría formation (Pérez-Cáceres et al., 2015). S2 is observed as a penetrative slaty cleavage, while S3 is a disjunctive crenulation cleavage.

According to the evolutionary model proposed by Pérez-Cáceres et al. (2015), the two main foliations S2 and S3 in the Pulo do Lobo belt resulted from the middle/upper Carboniferous collision between the OMZ and SPZ. Thus, the northward hot obduction of the Beja-Acebuches Amphibolites onto the southern OMZ can be correlated with the north-vergent folds (D2) of the Pulo do Lobo belt. Subsequent reversal of the regional vergence produced the D3 folds, which also correlate with the upright- to south-vergent folding of the Beja-Acebuches Amphibolites. The first foliation S1 in the Pulo do Lobo belt might have occurred during the vanishing stages of Rheic Ocean subduction and/or the starting Variscan collision, probably at Late Devonian time.

The Pulo do Lobo belt contains some decimetric- to metric-scale lenticular bodies of metamafic rocks with MORB affinity intercalated with the phyllites of the Pulo do Lobo formation, resembling a tectonic mélange (the so-called Peramora Mélange; Fig. 4.1b-c; Apalategui et al., 1983; Eden, 1991; Dahn et al., 2014). Based on this aspect and on the supposedly Rheic Ocean derived greenschists, the Pulo do Lobo belt has been classically interpreted as a pre-collisional subduction-related accretionary prism (Eden and Andrews, 1990; Silva et al., 1990; Eden, 1991; Braid et al., 2010; Ribeiro et al., 2010; Dahn et al., 2014). However, the recently obtained Mississippian U/Pb zircon ages from the metamafic rocks (Dahn et al., 2014; Pérez-Cáceres et al., 2015) make difficult to maintain such hypothesis. More properly, they can be interpreted as mafic intrusions/extrusions in the frame of the intracollisional transtensional magmatic event that prevailed in SW Iberia during the Mississippian. The metamafic rocks display a main foliation (equivalent to the S2 of the enveloping metasediments) developed at loosely constrained greenschist facies conditions. These rocks would have been imbricated with the Pulo do Lobo metasediments during D2 (Peramora Olistostrome; Pérez-Cáceres et al., 2015). Furthermore, if following the classical interpretation of a subduction-related accretionary mélange, other features typical of modern subduction systems should be expected, such as slices of oceanic slab-derived lithologies (varied metaigneous lithologies and also deep ocean bottom metasediments), arc-derived volcanoclastics..., or high-pressure metamorphic gradient remnants of partial subduction/exhumation in an accretionary wedge (e.g., Platt, 1986; Ernst, 2005). At this respect, Rubio Pascual et al. (2013) have recognized some rhomboidal aggregates of epidote porfiroblasts, interpreted as remnants of lawsonite pseudomorphs, in the Pulo do Lobo mafic schists. Our multidisciplinary metamorphic study of the Pulo do Lobo metasediments adds with new data concerning this topic.

To sum up, the SW Iberian Variscides are characterized by a complex tectonometamorphic evolution marked by the collision between three Paleozoic continental terranes. The most intense metamorphism concentrates in these suture contacts, though it varies from

greenschist to granulite facies conditions. Late Devonian high-pressure rocks represent the remnants of early subduction/collision zones (e.g., CIZ/OMZ boundary and Cubito-Moura unit). Furthermore, the widespread Mississippian mafic magmatism and extension in SW Iberia attest to a regional, locally intense, thermal imprint before the final middle/upper Carboniferous continental collision.

3. Samples and analytical methods

Eighteen samples were collected from well-exposed outcrops of phyllosilicate-rich detrital rocks of the Pulo do Lobo belt along two north-south transects perpendicular to the structural trend. Five samples belong to the Santa Iría formation (unconformable upper formation) and thirteen to the lower formations (location of samples are in the map and cross-sections of Fig. 4.1b-c). As a whole, the samples were selected in clean outcrops far from faults and joints, free of alteration effects, and were taken as homogeneous as possible. Sampling design was intended to collect representative sites, both of the overall stratigraphic succession and along the two transects. We also aimed to characterize the unconformity between the lower and upper formations from a metamorphic point of view, since aspect crystallinity at hand specimen seems to be lower in the Santa Iría formation. Some samples from the lowermost Pulo do Lobo formation were collected not far from the metabasite lenses of the Peramora Mélange.

Before analysis, samples were examined under the optical microscope and SEM for overall mineralogy, deformation and minerals/foliations relationships. All the samples correspond to slates or phyllites with phyllosilicates smaller than 500 μm, and they are composed by variable quartz + white mica ± chlorite ± feldspar ± ore and accessory minerals (Fig. 4.2d-f). The lower formations show three foliations (S1, S2, S3; Fig. 4.2a-b, d-e), while the Santa Iría formation is affected only by the last two (S2, S3; Fig. 4.2c, f). Moreover, samples from the Santa Iría formation have much smaller grain-size and apparently less crystallinity (Fig. 4.2f). The first foliation S1 is defined by the bigger micas and chlorites (Fig. 4.2d-e), being folded by microscopic to centimetric tight folds of the second deformation phase (Fig. 4.2a-b, d-e). The second foliation S2 is the main foliation at outcrop (Fig. 4.2a-c), but the development of phyllosilicates (mostly white mica) is lesser than during D1. The third foliation S3 is much less penetrative (Fig. 4.2a-c) and does not develop phyllosilicates. Large detrital phyllosilicate clasts have not been observed.

3.1. X-Ray diffraction

Sample preparation and analysis by XRD were done in the laboratories of the Department of Mineralogy and Petrology of the University of Granada (Spain). After washing and cleaning of patinas and oxides, samples were crushed to a <2 mm fraction. The <2-μm fractions were separated by repeated extraction of supernatant liquid after centrifugation, according to the Stokes' law. Oriented aggregates were prepared by sedimentation on glass slides of whole-rock and <2 μm fractions (the latter aims to minimize the content of detrital micas non-re-equilibrated during very low-grade metamorphism, which are generally larger than 2 μm). Samples were also treated with ethylene glycol (EGC) to

identify illite/smectite or chlorite/smectite mixed-layers on the basis of their expansibility. Samples were analyzed using a PANalytical X'Pert Pro powder diffractometer equipped with an X'Celerator detector, CuKα radiation, operated at 45 kV and 40mA, Ni filter and 0.25° divergence slit. The resulting diffraction diagrams were examined to extract information on mineralogy based on their characteristic reflections and white mica crystal data.

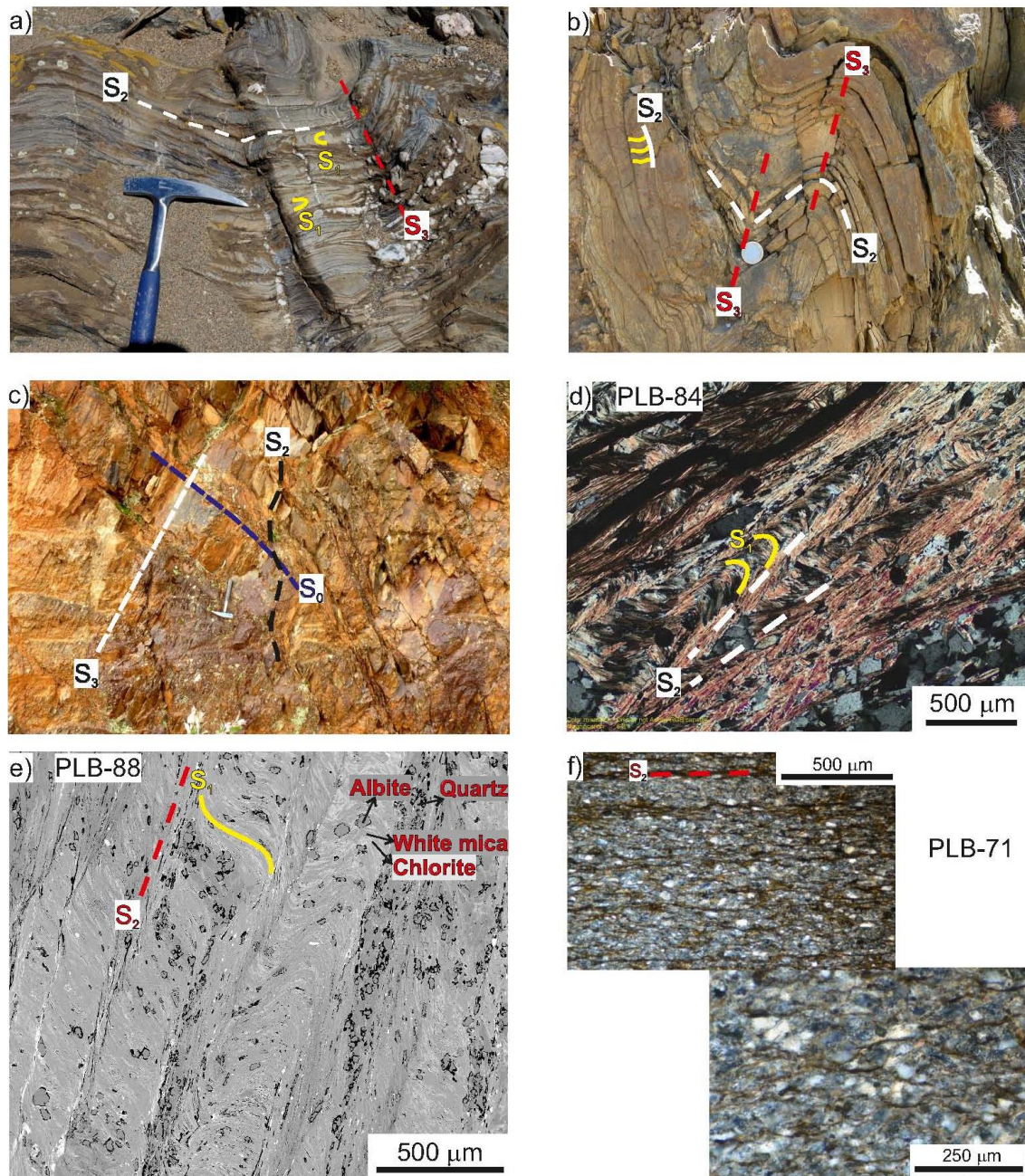Figure 4.2. Images of the Pulo do Lobo rocks illustrating deformation at outcrop scale: a) Pulo do Lobo formation, b) Ribeira de Limas formation, c) Santa Iría formation. Microphotographs of thin-section: d) Cross-polarized light image of sample PLB-84 (Pulo do Lobo formation), e) SEM-BSE image of sample PLB-88 (Ribeira de Limas formation), f) Cross-polarized light image of sample PLB-71 (Santa Iría formation).

The Illite "Crystallinity" index (Kübler Index; KI; Kübler, 1968) is the classical and most frequent indicator used in metapelitic rocks affected by very low-grade metamorphism (anchizone and low-epizone conditions). The KI is based on the measurement of the full peak-width of K-white mica at half maximum intensity, expressed as Δ°2θ of the Bragg angle. Preparation of samples and experimental conditions were carried out according to IGCP 294 IC Working Group recommendations (Kisch, 1991). A step increment of 0.008° 2θ and a counting time of 52 s/step were used in the diffractometer. The KI has been measured in all the samples for both the 5 and 10 Å reflection peaks of K-white mica in order to identify possible effects of other overlapping phases on the mica 10Å peak (Nieto and Sánchez-Navas, 1994; Battaglia et al., 2004). Some XRD traces showing complex mixture of mixed-layered minerals were decomposed with the MacDiff software (Petschick, 2004). The KI values obtained (x) have been recalculated to the crystallinity index standard (CIS values; y) according to the equation y=0.972x + 0.1096 (R2 = 0.942), obtained in the laboratory using the international standards of Warr and Rice (1994). The lower and upper boundaries of the anchizone in the CIS scale are 0.52 and 0.32 °2θ, respectively (Warr and Ferreiro Mähnlmann, 2015). The thermal range for the anchizone is c. 200-300 °C, though the KI cannot be considered as a true geothermometer (Frey, 1987; Kisch, 1987).

The *b*-cell dimension is used to characterize the metamorphic pressure gradient at the time of formation/recrystallization of the white mica, because it depends quite exclusively on the phengite substitution. Guidotti and Sassi (1986) stablished that *b* values lower than 9.000 Å are typical of low-pressure facies conditions, while *b* values higher than 9.040 Å are related to rather high-pressure facies metamorphism. The *b*-cell parameter of white mica was obtained from the (060) reflection peak measured on polished rock-slices cut normal to the sample main foliation. For all the measurements, quartz reflection at 59.96 °2θ from each sample was used as an internal standard.

3.2. EPMA-derived X-Ray compositional maps and chlorite thermometry

From all of the samples collected, three carbon-coated polished thin-sections were selected according to the larger grain size of phyllosilicate abundance, previously examined by optical microscope and SEM. The selected samples (PLB-84, PLB-88 and PLB-93) belong to the lower formations of the Pulo do Lobo belt (Fig. 4.2d-e). The Santa Iría samples cannot be studied due to the tiny grain size of the slaty minerals (commonly less than 3 μm); even in the samples studied, the small grain size has been a limitation for analysis.

X-Ray compositional maps and accurate spot analyses were performed on a JEOL JXA-8230 electron probe microanalyzer (EPMA) at the Institut des Sciences de la Terre (ISTerre) in Grenoble (France), according to the analytical procedure proposed by De Andrade et al. (2006) and Lanari et al. (2014). The data acquisition was made in Wavelength dispersive spectrometry mode (WDS). Ten elements (Si, Ca, Al, K, Mn, Na, P, Ti, Fe and Mg) were analyzed using five WD spectrometers: TAP crystal for Si and Al, PETL for Ti and P, TAPH for Na and Mg, PETH for K and Ca, and LIFH for Mn and Fe. The standardization was made using certified natural minerals and synthetic oxides: Wollastonite (Si, Ca), Corundum (Al), Orthoclase (K), Rhodonite (Mn), Albite (Na),

Apatite (P), Rutile (Ti), Hematite (Fe), and Periclase (Mg). The X-Ray maps were obtained by adding successive adjacent profiles. Beam current of 100 nA and beam size spot (focused) were used. The step (pixel) size was 1 μm and Dwel time was 200-300 msec per pixel. Spot analyses were obtained along the profiles within the mapping areas. Operating conditions for spot analyses were 15 kV accelerating voltage, 12 nA beam current and beam size spot (focused). The on-peak counting time was 30 sec for each element and 30 sec for two background measurements at both sides of the peak. The ZAF correction procedure was applied. The internal standards were orthoclase and/or chromium-augite (Jarosewich et al., 1980) and were run (3 points on each standard) after each profile in order to monitor instrumental drift and to estimate analytical accuracy. Drift correction was made, if necessary, using the corresponding regression equation.

After analyzing the three samples in the microprobe, the obtained X-Ray maps were processed with XMapTools, which is a MATLAB©-based graphical user interface program to estimate the pressure-temperature conditions of crystallization of minerals in metamorphic rocks (Lanari et al., 2014). The compositional maps can be standardized with the spot analyses measured along the profiles. External functions are provided and used to plot mineral compositions into binary and ternary diagrams (interface modules *Chem2D and Triplot3*D), and to estimate pressure-temperature conditions using published empirical and semi-empirical thermobarometers. In our work, temperature maps have been calculated on the basis of the chlorite thermometers of Cathelineau (1988) and Lanari et al. (2014).

Chlorite and white mica are good minerals for thermobarometric estimations because they present several chemical substitutions controlled by the equilibrium conditions (mainly pressure and temperature) that can be modeled by using a set of different end-members (Vidal et al., 2001, 2005, 2006; Parra et al., 2002; Dubacq et al., 2010). Unfortunately, the composition of phyllosilicates in our samples does not reflect chemical equilibrium between chlorite and white mica, thus precluding the use of these paired minerals as a geothermobarometer. Nevertherless, we have extracted representative chlorite oxide compositions from XMapTools in order to estimate temperatures based on the five chlorite end-members: Mg-amesite ($Si_2Al_4Mg_4O_{10}(OH)_8$), Fe-amesite ($Si_2Al_4Fe_4O_{10}(OH)_8$), daphnite ($Si_3Al_2Fe_5O_{10}(OH)_8$), clinochlore ($Si_3Al_2Mg_5O_{10}(OH)_8$) and sudoite ($Si_3Al_4Mg_2\square_1O_{10}(OH)_8$). The three main substitutions that occur in chlorite are $FeMg_{-1}$, Tschermak and di/trioctahedral substitutions, which can be modeled with the corresponding end-members (e.g., Vidal et al., 2005). Chlorite shows Al^{IV} increase and vacancy decrease at increasing temperature (e.g., Cathelineau and Nieva, 1985; Cathelineau, 1988; Vidal et al., 2001). The multiequilibrium approach of Vidal et al. (2005 and 2006) proposes a coeval estimate of Fe^{3+} content in chlorite and equilibrium temperature at a given pressure. The position of these equilibria depends on chlorite end-member, quartz and water activities. In this work, temperatures and XFe^{3+} of chlorite were estimated by considering water activity equal to 1, and 5 kbar as the maximum pressure according to the approximate estimation from the metamorphic facies (Rubio-Pascual et al., 2013). According to Vidal et al. (2005 and 2006), thermodynamic equilibrium is obtained when, considering the minimum Fe^{3+} proportion, the temperature difference between the four used equilibria is less than 30 °C (Lanari et al., 2012 and references therein).

3.3. Raman Spectroscopy of carbonaceous matter

A number of studies in the Alpine and Variscan belts have shown that Raman spectroscopy of carbonaceous matter (RSCM) is a useful tool to characterize its degree of graphitization, i.e., the temperature-dependent grade of organization from organic matter to graphite during metamorphism (e.g., Beyssac et al., 2002a, b, 2004, 2016; Lahfid et al., 2010; Souche et al., 2012; Delchini et al., 2016). These works have shown that the RSCM geothermometer can be applied to determine peak temperature attained by a rock-sample, because the structural transformation of its CM is a prograde and irreversible process that equilibrates at maximum temperature reached during the thermal history of the sample.

In this work, twelve thin-sections were selected by the aspect and quantity of CM, previously examined by optical microscopy (e.g., Fig. 4.3a). From them, ten samples were finally analyzed: eight samples belong to the lower formations (Pulo do Lobo and Ribeira de Limas formations), while two belong to the Santa Iría formation. Polished thin sections cut perpendicularly to the foliation were analyzed at the Institut de Minéralogie et de Physique des Milieux Condensés of the University Pierre et Marie Curie in Paris (France). We followed closely the analytical procedure described by Beyssac et al. (2002a, b; 2003). More than 15 Raman spectra (e.g., Fig. 4.3b-c) were obtained for each sample using a Renishaw InVIA Reflex microspectrometer equiped with a 514 nm Spectra Physics argon laser under circular polarization. The laser was focused by a DMLM Leica microscope, and laser power was set to around 1 mW at the sample surface. The Rayleigh diffusion was eliminated by edge filters, and the entrance slit was closed down to 10-15 μm to achieve nearly confocal configuration. The signal was dispersed using an 1800 g/mm grating and finally analyzed by a Peltier cooled RENCAM CCD detector. The recorded spectral window was large, from 700 to 2000 cm^{-1}. Before each session, the spectrometer was calibrated with a silicon standard. CM was systematically analyzed behind a transparent adjacent mineral, generally quartz or white mica oriented along S1. Spectra were processed with the software Peakfit.

Very disordered CM Raman spectra of very low-grade metamorphic rocks (<330 °C) are significantly different from those of more structurally evolved CM of higher metamorphic grade rocks. For higher temperature rocks (330-650 °C), Beyssac et al. (2002a) established a correlation between the temperature and the CM Raman ratio parameter R2 [defined as R2=D1/(G+D1+D2), where G is the area of a single main spectral band around 1580 cm^{-1} that corresponds to the Raman spectrum of perfect graphite, and D1 and D2 are the areas of minor bands at ≈1350 cm^{-1} and ≈1620 cm^{-1}, respectively, that correspond to disorganized CM] (e.g., Fig. 4.3b). The R2 parameter is temperature- dependent through the equation T (°C) = -45R2 + 641. R2 ranges from 0 to 0.7 and is inversely proportional to the temperature, which varies from 330 to 650 °C ± 10-15 °C (Beyssac et al., 2004). The relative error on temperature is due to uncertainties of the petrological data used for calibration. This procedure was used for the samples from the lower formations of the Pulo do Lobo belt (e.g., Fig. 4.3a-b).

For lower temperature rocks (<330 °C), the spectrum is more complex and composed by the graphite G band that overlaps with the D2 band (≈1620 cm^{-1}), D1 band (≈1350 cm^{-1}), plus D3 (≈1500 cm^{-1}) and D4 (≈1200 cm^{-1}) bands (e.g., Fig. 4.3c) (Sadezky et al., 2005).
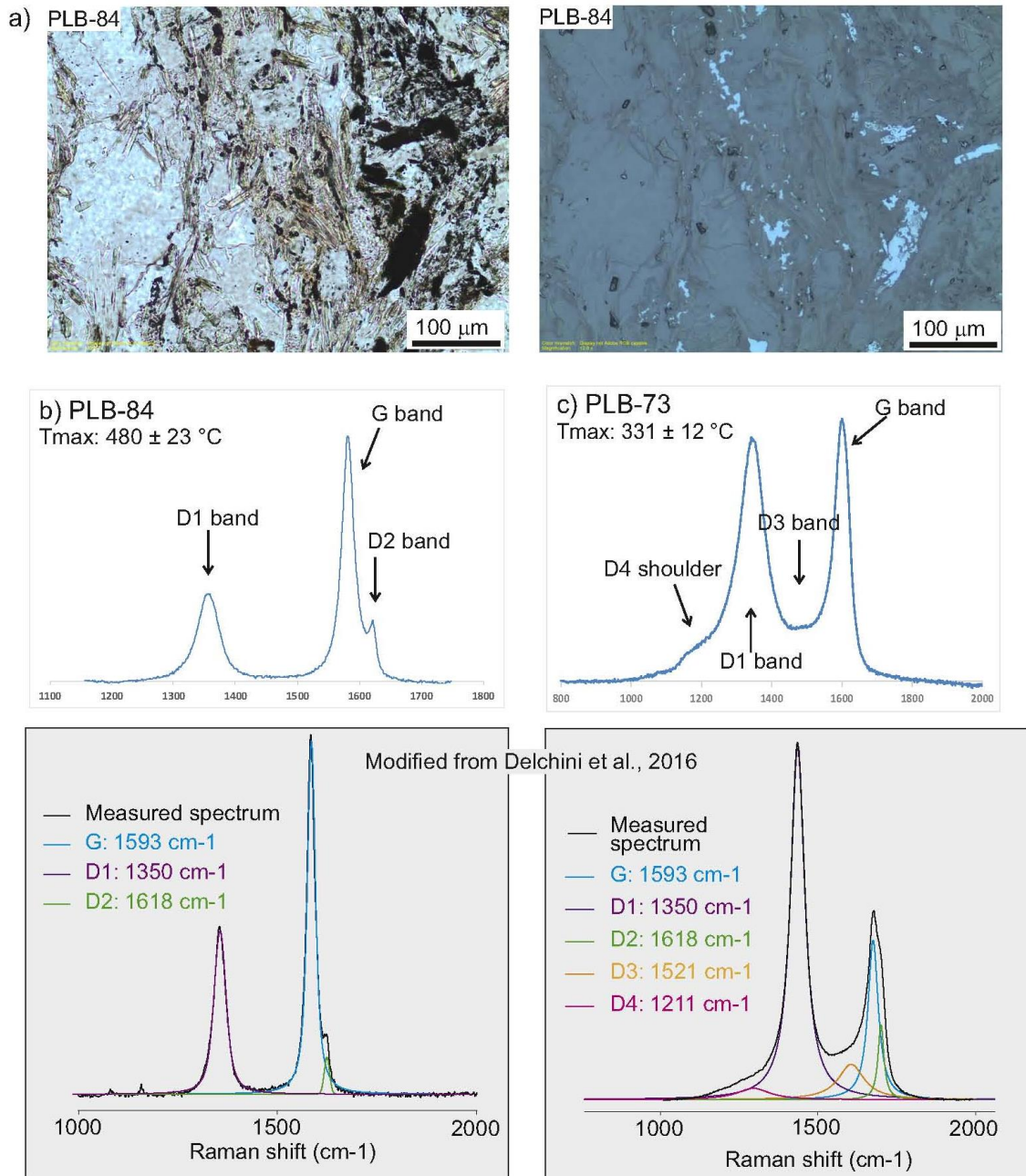
Figure 4.3. a) Microphotographs showing carbonaceous matter in sample PLB-84 (Pulo do Lobo formation): transmitted light (left image) and reflected light (right image). Spots for analysis with Raman Spectroscopy have been selected in the opaque anisotropic material located behind transparent minerals (quartz or mica). b) Example of a high-temperature spectrum of RSCM in sample PLB-84 (up), and an example taken from Delchini et al. (2016) (down) for comparison of the spectral bands. c) Example of a low-temperature spectrum of RSCM in sample PLB-73 (up), and an example taken from Delchini et al. (2016) (down) for comparison of the spectral bands.

There are two area ratios (RA) that relate the evolution of the Raman spectrum with increasing metamorphic grade: RA1 = (D1 + D4) / (D1 + D2 + D3 + D4 + G) and RA2 = (D1 + D4) / (D2 + D3 + G) (Lahfid et al., 2010). These two ratios progressively increase with the metamorphic grade and can be used as quantitative estimates of the

degree of graphitization in very low-grade metasediments. According to Lahfid et al. (2010), the relationship between the area ratios and the temperature is RA1 = 0.0008T + 0.3758 and RA2 = 0.0045T + 0.27. This procedure was used for the samples from the Santa Iría formation (e.g., Fig. 4.3c).

4. Results

4.1. X-Ray diffraction

The mineralogy and crystal parameters obtained from the 18 samples of the Pulo do Lobo belt are summarized in Table 4.1. The results obtained from the whole-rock and the <2 μm fractions are very similar, which suggests that the influence of detrital micas non-re-equilibrated during metamorphism is negligible.

The mineralogy of the samples is relatively simple: Qz + Ms + Chl ± Pg ± C/S. The slates of the Santa Iría formation have quartz, muscovite and chlorite, with chlorite/smectite interlayers (C/S) in some samples. In the lower formations, besides quartz and muscovite, chlorite is present in almost all of the samples, paragonite appears in most of them, and chlorite/smectite interlayers are occasional.

Table 4.1. Samples and results obtained by XRD (<2 μm fraction) and average RSCM thermometry. Mineral abbreviations according to Whitney & Evans (2010). Qz: Quartz; Ms: Muscovite; Chl: Chlorite; Pg: paragonite; C/S: chlorite-smectite mixed layers. Std Dv: standard deviation.

Formation	Sample PLB-	UTM coordinates		Mineralogy	CIS Ms (10 Å)	b (Å)	d_{001} (Å)	T_{max} (°C) RSCM	
		X	Y	Qz + Ms +		Ms	Ms	Mean	Std Dv
Santa Iría (upper formation)	71	656571	4202532	Chl	0.32	8.991	9.995	316	15
	73	656937	4201969	Chl	0.33	8.996	9.997	329	12
	74	657683	4201284	Chl + C/S	0.27	8.999	10.001	-	
	76	657817	4200264	Chl	0.29	8.997	9.997	-	
	77	658462	4197940	Chl + C/S	0.28	8.998	9.995	-	
lower fomations	79	658244	4194716	Chl + Pg	0.27	8.995	9.993	424	28
	80	657370	4194128	Chl	0.27	9.001	9.988	-	
	81	657412	4191653	Chl + Pg + C/S	0.29	-	9.988	-	
	82	657768	4189514	Chl + Pg	0.26	8.995	9.986	532	28
	84 (map 2)	657448	4186921	Chl + Pg + C/S	0.28	8.994	9.988	481	24
	85	658363	4185606	Chl + Pg	0.24	8.996	9.996	-	
	86	669833	4186562	Pg + C/S	0.25	8.993	9.986	-	
	87	669676	4187664	Chl + Pg	0.25	8.998	9.986	471	24
	88 (map 1)	669708	4187924	Chl + Pg	0.23	8.997	9.990	465	20
	89	669869	4188826	Chl	0.28	8.996	9.993	418	12
	91	674526	4196530	Chl + Pg	0.25	9.000	9.995	-	
	93 (map 3)	674985	4196974	Chl + Pg	0.23	9.002	9.990	495	23
	7C	669881	4188776	-	-	8.993	-	458	17

The CIS values measured in the 10 Å peak of white mica of the <2 µm fraction are shown in Table 4.1. Values of the Santa Iría samples (n=5) range from 0.27 to 0.33 $\Delta°2\theta$, the mean value being 0.30 (standard deviation 0.02). As for the lower formations (n=12), CIS values range from 0.23 to 0.29, the mean value being 0.26 (standard deviation 0.02). The CIS values measured in the 5 Å peak are very similar to those of the 10 Å peak.

The measured *b*-cell parameter of white mica varies in a close range around 9 Å (8.991-9.002). Mean value is 8.995 (standard deviation 0.003) for the Santa Iría formation samples, and 8.997 (standard deviation 0.003) for the samples of the lower formations.

4.2. X-ray compositional maps and chlorite thermometry

Three X-Ray maps from thin sections of samples PLB-84, 88 and 93 (Fig. 4.4a) were obtained and processed with XMapTools. The distribution of major elements allowed identifying a number of minerals: white mica, chlorite, some albite porphyroblasts, and ilmenite and rutile (or iron oxides product of oxidation) as accessory minerals (Fig. 4.4b). Although quartz is abundant in all of the samples, the zoomed selected areas for X-ray mapping (composed mostly by phyllosilicates) do not contain quartz. White mica is abundant along both S1 and S2 foliations (Fig. 4.2d-e and 4.4b). Chlorite is found mostly along S1 and is very scarce and small-sized along S2 (Fig. 4.2e and 4.4b), with the exception of sample PLB-93 where chlorite is similar in both foliation domains (Fig. 4.4b).

Mapped compositions of white mica and chlorite are plotted in the ternary diagrams of Figure 4.5. The composition of white mica is similar in the three maps. White mica is close to muscovite, with 25% of pyrophyllite and very scarce celadonite content (Fig. 4.5a). The micas present low degree of Na substitution and low phengitic component, being near to the muscovite end-member. These results agree well with the XRD information (Table 1): low *b*-cell parameter and high d_{001}.

The compositions of chlorite are different depending on the map, but all of them have in common ≈50% clinoclore + daphnite and ≈50% amesite + sudoite (Fig. 4.5b). Chlorites of sample PLB-88 are poor in amesite, those of PLB-84 reveal variable solid solution between amesite and sudoite, and those of PLB-93 are poor in sudoite.

Following the semi-empirical relationship between Al^{IV} chlorite content and temperature (Cathelineau, 1988), temperature maps of chlorite have been obtained (Fig. 4.4c). Temperatures range from 100 to 450 °C in samples PLB-88 and PLB-84, being higher in sample PLB-93 (300-600 °C) (Fig. 4.4c). Tiny chlorites developed along S2 show lower temperatures than the larger and more abundant chlorites along S1, with the exception of sample PLB-93. Furthermore, in the three samples some large chlorites oriented along S1 show high-temperature relic cores (350-450 °C in samples PLB-88 and PLB-84, and 400-500 °C in sample PLB-93; see white insets in Fig. 4.4). Similar maps have been obtained for the chlorites, which show equilibrium when using the more recent geothermometer of Lanari et al. (2014), though the calculated temperatures are ≈100 °C lower (Fig. 4.4d).
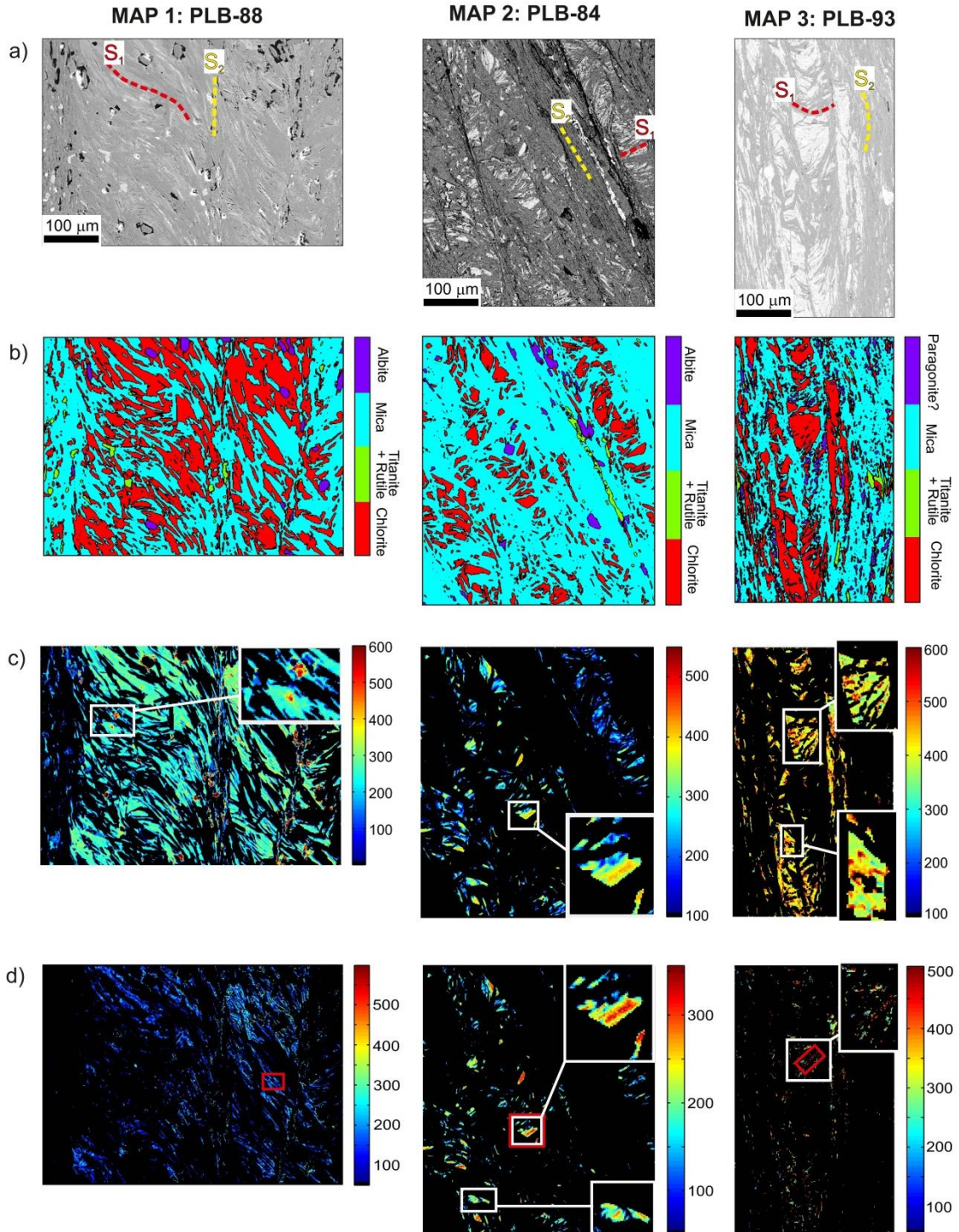
Figure 4.4. X-Ray maps of the three selected samples analyzed by EPMA and XMapTools. The samples belong to the lower formations of the Pulo do Lobo belt (sample PLB-88: Ribeira de Limas formation; samples PLB-84 and PLB-93: Pulo do Lobo formation; the latter [PLB-93] is close to Carboniferous igneous intrusions). a) EPMA BSE photographs. b) Mineralogy maps. c) Temperature maps of chlorite using the Cathelineau (1988) geothermometer. d) Temperature maps of chlorite using the Lanari et al. (2014) geothermometer. White squares show selected areas illustrating higher-temperature chlorite cores. Red squares show the selected areas used for chlorite-quartz-water geothermometric calculations (after Vidal et al., 2006) shown in Fig. 4.6.

A homogeneous area of representative chlorites in an S1 microlithon was selected from each map (see red insets in Fig. 4.4d). The corresponding chlorite compositions were exported into oxide weight percentages and introduced in the chlorite-quartz-water equilibria for geothermometric calculations (Vidal et al., 2005, 2006). The calculated temperatures (Fig. 4.6) average 150-250 °C, with the exception of sample PLB-93 where they are ≈100 °C higher.
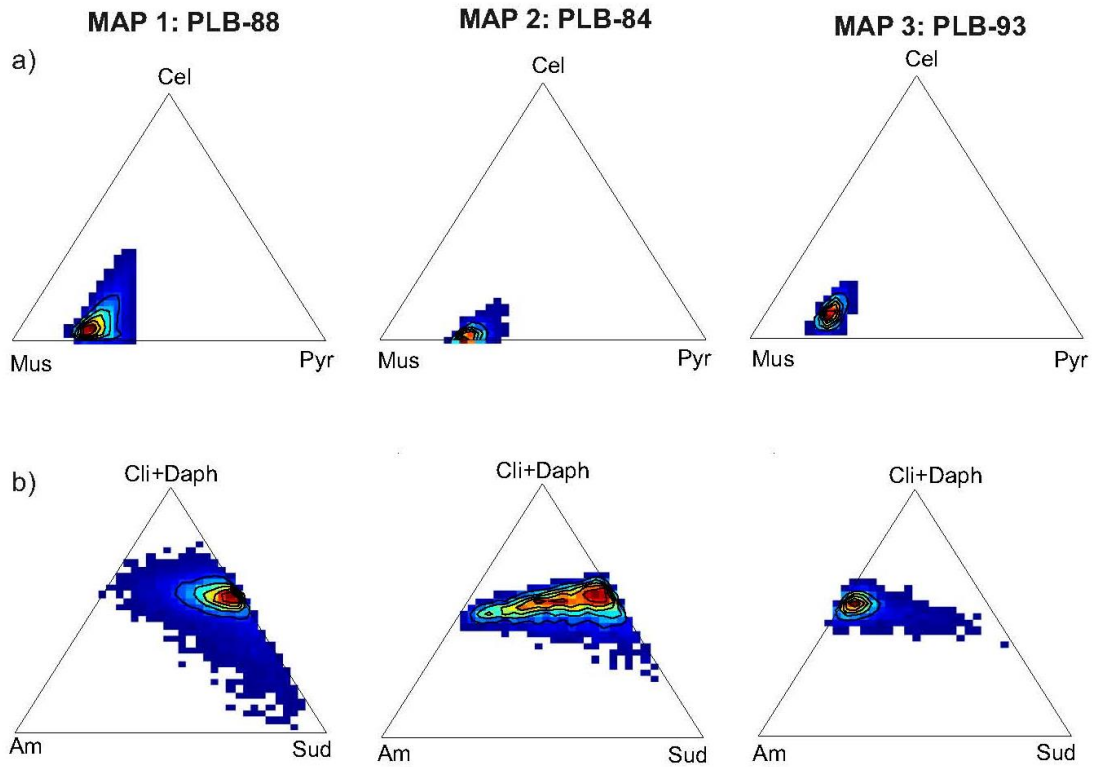
Figure 4.5. Ternary plots of all the analyzed white micas (a) (Cel: celadonite, Mus: muscovite, Pyr: pyrophyllite) and chlorite (b) (Cli+Daph: clinochlore + daphnite, Am: amesite, Sud: sudoite) plotted with the XmapTools TriPlot3D module.
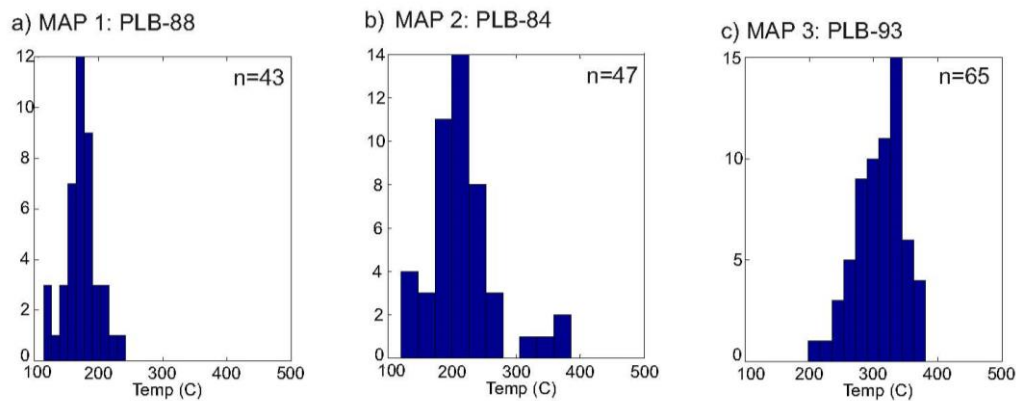

Figure 4.6. Histograms of the temperatures obtained using the chlorite-quartz-water geothermometer (Vidal et al., 2006) on selected representative S1 chlorites (see red squares in Fig. 4.4d for location).

4.3. RSCM thermometry

The ratio parameters and corresponding maximum temperatures obtained from all the spectra analyzed (15-20 per sample) are shown in tables 4.2 (eight samples from the lower formations) and 4.3 (two samples from the Santa Iría formation). The Raman spectra were decomposed into bands following the fitting procedure proposed in Beyssac et al. (2002a) and distinguishing the lower formations (high-temperature Raman spectra; ratio parameter R2) from the Santa Iría formation (low-temperature Raman spectra; ratio parameters RA1 and RA2). The average temperatures for the lower formations range from 420 to 530 °C, with a mean value of 468 °C (standard deviation of 35). The highest temperatures are found in samples PLB-82 (530 °C) and PLB-93 (495 °C), while the remaining ones do not exceed 480 °C. As for the Santa Iría formation, temperatures are lower (315-330 °C) (Table 4.1).

Table 4.2. R2 parameter values and calculated maximum temperatures from all the Raman Spectra (RS) of CM analyzed in samples from the lower formations. Std Dv: standard deviation. Std Err: standard error (calculated as the standard deviation divided by $\sqrt{n}$).

RS (n=19)	R2	T_{max} (°C)	RS (n=15)	R2	T_{max} (°C)	RS (n=18)	R2	T_{max} (°C)	RS (n=15)	R2	T_{max} (°C)
Mean	0.489	424	Mean	0.246	532	Mean	0.360	481	Mean	0.382	471
Std Dv	0.064	28	Std Dv	0.063	28	Std Dv	0.053	24	Std Dv	0.054	24
Std Err		7	Std Err		7	Std Err		6	Std Err		6
PLB-79-10	0.520	409	PLB-82-1	0.255	527	PLB-84-1	0.371	476	PLB-87-1	0.268	522
PLB-79-11	0.507	415	PLB-82-10	0.255	528	PLB-84-12	0.405	461	PLB-87-10	0.363	480
PLB-79-12	0.495	421	PLB-82-11	0.229	539	PLB-84-13	0.351	485	PLB-87-13	0.455	438
PLB-79-13	0.522	409	PLB-82-12	0.220	543	PLB-84-14	0.392	466	PLB-87-15	0.423	453
PLB-79-14	0.501	418	PLB-82-16	0.142	578	PLB-84-15	0.413	457	PLB-87-16	0.370	476
PLB-79-15	0.528	406	PLB-82-19	0.203	550	PLB-84-16	0.303	506	PLB-87-18	0.388	468
PLB-79-16	0.513	413	PLB-82-2	0.228	539	PLB-84-17	0.446	443	PLB-87-19	0.445	443
PLB-79-17	0.490	423	PLB-82-20	0.189	557	PLB-84-18	0.328	495	PLB-87-2	0.304	506
PLB-79-19	0.548	397	PLB-82-21	0.157	571	PLB-84-19	0.418	455	PLB-87-20	0.465	434
PLB-79-2	0.351	485	PLB-82-22	0.273	520	PLB-84-2	0.264	524	PLB-87-21	0.381	472
PLB-79-20	0.513	413	PLB-82-23	0.314	501	PLB-84-20	0.319	499	PLB-87-22	0.362	480
PLB-79-21	0.584	381	PLB-82-24	0.359	481	PLB-84-21	0.299	508	PLB-87-24	0.363	479
PLB-79-22	0.496	420	PLB-82-25	0.338	491	PLB-84-3	0.347	487	PLB-87-7	0.393	466
PLB-79-3	0.504	417	PLB-82-7	0.298	509	PLB-84-5	0.306	505	PLB-87-8	0.345	487
PLB-79-4	0.404	461	PLB-82-8	0.229	539	PLB-84-6	0.444	443	PLB-87-9	0.403	462
PLB-79-5	0.371	476				PLB-84-7	0.389	468			
PLB-79-6	0.414	457				PLB-84-8	0.331	494			
PLB-79-8	0.446	442				PLB-84-9	0.353	484			
PLB-79-9	0.576	385									

RS (n=21)	R2	T$_{max}$ (°C)	RS (n=19)	R2	T$_{max}$ (°C)	RS (n=19)	R2	T$_{max}$ (°C)	RS (n=20)	R2	T$_{max}$ (°C)
Mean	0.396	465	Mean	0.502	418	Mean	0.329	495	Mean	0.411	458
Std Dv	0.044	20	Std Dv	0.027	12	Std Dv	0.052	23	Std Dv	0.039	17
Std Err		4	Std Err		3	Std Err		5	Std Err		4
PLB-88-1	0.339	490	PLB-89-31	0.542	400	PLB-93-1	0.225	541	PLB-7C-10	0.453	439
PLB-88-10	0.387	469	PLB-89-32	0.459	437	PLB-93-10	0.306	505	PLB-7C-11	0.373	475
PLB-88-11	0.451	440	PLB-89-33	0.506	416	PLB-93-11	0.319	499	PLB-7C-12	0.460	436
PLB-88-12	0.398	464	PLB-89-34	0.456	438	PLB-93-12	0.329	494	PLB-7C-13	0.409	459
PLB-88-13	0.346	487	PLB-89-35	0.476	429	PLB-93-13	0.403	462	PLB-7C-14	0.442	444
PLB-88-14	0.402	462	PLB-89-36	0.498	419	PLB-93-14	0.224	541	PLB-7C-15	0.346	487
PLB-88-15	0.377	473	PLB-89-37	0.531	405	PLB-93-15	0.323	497	PLB-7C-16	0.491	422
PLB-88-16	0.391	467	PLB-89-38	0.498	419	PLB-93-16	0.367	478	PLB-7C-17	0.415	456
PLB-88-17	0.399	463	PLB-89-39	0.505	416	PLB-93-17	0.343	488	PLB-7C-18	0.405	461
PLB-88-18	0.411	458	PLB-89-40	0.513	413	PLB-93-18	0.363	480	PLB-7C-19	0.354	483
PLB-88-19	0.405	461	PLB-89-41	0.491	423	PLB-93-19	0.368	477	PLB-7C-2	0.414	457
PLB-88-2	0.363	480	PLB-89-42	0.504	417	PLB-93-20	0.361	480	PLB-7C-20	0.431	449
PLB-88-20	0.500	419	PLB-89-43	0.508	415	PLB-93-3	0.322	498	PLB-7C-21	0.389	468
PLB-88-21	0.391	467	PLB-89-44	0.504	417	PLB-93-4	0.285	514	PLB-7C-22	0.405	461
PLB-88-3	0.354	484	PLB-89-45	0.473	430	PLB-93-5	0.270	521	PLB-7C-3	0.391	467
PLB-88-4	0.353	484	PLB-89-46	0.555	394	PLB-93-6	0.419	455	PLB-7C-4	0.479	428
PLB-88-5	0.478	428	PLB-89-47	0.539	401	PLB-93-7	0.368	477	PLB-7C-6	0.410	459
PLB-88-6	0.363	479	PLB-89-48	0.488	424	PLB-93-8	0.341	489	PLB-7C-7	0.392	467
PLB-88-7	0.387	469	PLB-89-49	0.492	422	PLB-93-9	0.318	500	PLB-7C-8	0.376	473
PLB-88-8	0.360	481							PLB-7C-9	0.385	470
PLB-88-9	0.461	436									

Table 4.3. RA1 and RA2 parameter values and calculated maximum temperatures from all the Raman Spectra (RS) of CM analyzed in samples from the Santa Iría formation. Std Dv: standard deviation. Std Err: standard error (calculated as the standard deviation divided by $\sqrt{n}$).

RS (n=17)	RA1	T$_{max}$ (°C)	RA2	T$_{max}$ (°C)	RS (n=16)	RA1	T$_{max}$ (°C)	RA2	T$_{max}$ (°C)
Mean	0.629	316	1.696	317	Mean	0.638	327	1.761	331
Std Dv	0.009	12	0.067	15	Std Dv	0.007	9	0.053	12
Std Err		3		4	Std Err		1		3
PLB71-39	0.634	323	1.731	325	PLB73-1	0.631	319	1.712	321
PLB71-41	0.605	286	1.531	280	PLB73-14	0.630	318	1.701	318
PLB71-42	0.634	323	1.733	325	PLB73-17	0.628	316	1.691	316
PLB71-43	0.636	326	1.750	329	PLB73-20	0.633	321	1.724	323
PLB71-44	0.633	322	1.726	324	PLB73-21	0.636	325	1.748	328
PLB71-45	0.630	317	1.699	318	PLB73-22	0.629	317	1.696	317
PLB71-46	0.640	330	1.779	335	PLB73-23	0.641	332	1.786	337
PLB71-47	0.628	315	1.689	315	PLB73-24	0.637	327	1.756	330
PLB71-48	0.638	327	1.759	331	PLB73-25	0.633	322	1.725	323
PLB71-49	0.614	298	1.592	294	PLB73-26	0.633	321	1.724	323
PLB71-50	0.636	325	1.747	328	PLB73-27	0.643	335	1.805	341
PLB71-52	0.623	309	1.654	308	PLB73-28	0.648	341	1.844	350
PLB71-53	0.633	322	1.728	324	PLB73-29	0.645	337	1.820	344
PLB71-54	0.637	326	1.753	330	PLB73-30	0.643	334	1.800	340
PLB71-55	0.622	308	1.648	306	PLB73-31	0.644	335	1.806	341
PLB71-56	0.626	313	1.674	312	PLB73-6	0.648	340	1.837	348
PLB71-57	0.620	305	1.630	302					

5. Interpretation and discussion

5.1. Deformation/metamorphism relationships

The obtained analytical results have to be interpreted in the context of the Variscan evolution of the Pulo do Lobo belt. As described above, two regional deformational events D1 and D2 gave way to the development of foliations (Devonian S1 and Carboniferous S2) accompanied by metamorphic phyllosilicate growth (M1 and M2). The textural observations evidence that in most samples of the lower formations M1 was the main crystallization event, developing abundant and large-sized white mica and chlorite in S1 microlithons, while M2 gave way to small-sized white mica (e.g., Fig. 4.2e and map 1 in Fig. 4.4). On the other hand, in polydeformed low-grade rocks it is common that previously grown minerals simply rotate, without reequilibrating, towards a new foliation developed at lower-grade conditions. This can be the case of the white micas that define S2 in some samples (e.g., Fig. 4.2d), which, in turn, is not contradictory with the similar chemical composition of S1 and S2 micas (Fig. 4.5a). As shown in our samples, S1 is variably crenulated by D2, so that M1 minerals are variably rotated towards S2. Consequently, the metamorphic data obtained from the samples of the lower formations will be ascribed to D1-M1. Sample PLB-93 might represent an exception, since its slightly higher temperature might be due to nearby intrusions. At this respect, it is important to note the Mississippian transtensional event (basins development and abundant mafic magmatism) that took place between D1 and D2. The characterization of M2 can be done by studying the samples from the Santa Iría formation, which are only affected by S2 accompanied by tiny phyllosilicate growth (Fig. 4.2f).

5.2. First tectonothermal event (Devonian M1)

The mineral association detected (Qz + Ab + Ms + Chl ± Pg ± C/S) is compatible with very low- to low-grade metamorphism. White mica crystallinity values (0.23-0.29 $\Delta°2\theta$; average 0.26) are always in the range of the epizone (low-grade or greeschists facies; > 300 °C; Frey, 1987; Kisch, 1987), in accordance with the values reported by Abad et al. (2001). Nevertheless, both the values of KI, still far from 0.20 $\Delta°2\theta$, and their variability, suggests that temperature was not high enough as to stabilize a highly crystalline white mica at high epizone conditions. This is in agreement with the low Na content of K-micas coexisting with paragonite, meaning a very-low temperature position in the muscovite-paragonite solvus for natural quasibinary Pg-Ms pairs (Guidotti et al., 1994). By contrast, the maximum temperatures obtained with RSCM geothermometry are relatively high (420-530 °C; average 470 °C), thus suggesting rather higher-grade conditions (very high epizone or even medium-grade) that should have prompted the formation of minerals like biotite or garnet. The absence of such minerals can be explained by growth inhibition due to Na-excess in the rocks studied, as evidenced by the presence of albite and paragonite. The discrepancy between white mica crystallinity and RSCM geothermometry can be explained in terms of the higher sensibility of the CM to fast reequilibrium at peak temperature, especially during a short-time thermal event; in such situation, the silicate minerals will not reequilibrate because they would require more time to complete the metamorphic reactions (Beyssac et al., 2002a). At this respect, the Mississippian intrusions subsequent to M1 in the

Pulo do Lobo formation could have exerted a fast and locally intense thermal imprint that influenced CM but not the crystalchemistry of silicates. This difference between reaction progress of inorganic and organic materials was also reported by Abad et al. (2014) in metapelites and metagreywackes of the SPZ in contact with the Monchique Pluton.

The composition of paired chlorite and white mica was used to calculate pressure and temperature (according to Vidal et al., 2006) but the variety of results obtained reflects chemical disequilibrium, precluding their use as a geothermobarometer. The temperatures calculated by using chlorite geothermometers (Vidal et al., 2006; Lanari et al., 2014) are very low: 150-250 °C for samples PLB-88 and PLB-84, and 250-350 °C for sample PLB-93 (Figs. 4d and 6). The slightly higher temperature of sample PLB-93 (as inferred by its highest white mica crystallinity of 0.23 $\Delta°2\theta$, high RSCM temperature of 495 °C, high-temperature (amesite-rich) chlorite and higher chlorite thermometry) can be explained by its nearness to metric-scale mafic igneous bodies of the Peramora Mélange (located at ≈200 m to the south) and/or to a granite stock (located at ≈5 km to the west) (Fig. 4.1b). The long-distance thermal influence of plutonic intrusions on low-grade rocks located as far as 10 km has been evidenced (e.g., Merriman and Frey, 1999; Martínez Poyatos et al., 2001).

Chlorite temperatures are very low as compared with XRD and RSCM data, and can thus be interpreted as the result of variable chlorite retrogression. The existence of retrograde chlorite is in accordance with (i) the chemical disequilibrium showed by the white mica/chlorite geothermobarometer, (ii) the presence of chlorite/smectite mixed layers, (iii) the higher temperature relic cores preserved in large chlorites defining S1 (Fig. 4.4c-d), and (iv) the previously reported XRD and TEM data of chlorite retrogradated to smectite and corrensite in the Pulo do Lobo (see fig. 1 in Nieto et al., 2005). Vidal et al (2006, 2016) showed that the existence of chlorites of different compositions, crystallized at different temperatures and times of the low-grade metamorphic evolution, is the usual scenario and, hence, the definition of a single temperature and pressure is impossible and it cannot be restricted to the peak temperature conditions. The maximum temperature showed by chlorite relic cores is 350-450 °C, which is more in accordance with the conditions estimated for M1 by XRD and RSCM data.

5.3. Second tectonothermal event (middle/upper Carboniferous M2)

The mineralogy of the Santa Iría samples (Qz + Ms + Chl ± C/S) is compatible with very low- to low-grade conditions. The white mica crystallinity values (0.27-0.33 $\Delta°2\theta$; average 0.30) belong to the lower epizone, very close to the boundary with the anchizone (≈300 °C; Frey, 1987; Kisch, 1987). The temperature calculated by RSCM in two samples (315 and 330 °C) is compatible with the XRD data.

Our metamorphic data corroborate the existence of an unconformity between the lower and upper formations of the Pulo do Lobo belt (Pérez-Cáceres et al., 2015), in accordance with the different apparent crystallinities observed at hand specimen and thin section. Thus, the lower formations record a Devonian tectonothermal event that reached epizone or greenschist facies conditions (M1 with generalized phyllosilicate growth at temperatures as high as 450 °C), while the overlying upper formation records a middle/upper

Carboniferous tectonothermal event close to the anchizone/epizone boundary (M2 with tiny phyllosilicate growth at temperatures $\approx$300-330 °C). Obviously, M2 also affected somehow the lower formations, being, at lest in part, the responsible of the observed retrogression of M1 chlorite.

5.4. Pressure gradient

The obtained *b*-cell parameter values of white mica (in a short range between 8.991-9.002 Å; average 8.996; standard deviation 0.003) are very similar in the lower and upper formations of the Pulo do Lobo belt. The *b* parameter is consistently homogeneous and reflects very low phengite substitution in the mica, as expected at a low-pressure metamorphic gradient, near the intermediate pressure gradient boundary (Guidotti and Sassi, 1986). Our results coincide with the previous work of Abad et al. (2001).

The chemistry of white mica is very homogeneous through the studied samples (Fig. 4.5a). The composition is close to muscovite and very poor in celadonite component, as expected for micas formed at low-pressure gradients, in agreement with the low *b*-cell parameters. In the case of high or medium pressure conditions, a continuous trend of micas compositions would be found reflecting the decompression conditions after the pressure climax and the *b*-cell parameter represent an average value of the range of mica compositions found in the sample (Abad et al, 2003). Contrarily, for low-pressure conditions, the overall range of pressure is very short, micas present a composition near to the muscovitic end-member and the *b*-cell parameter is low and similar among the various samples, as it is the case in the Pulo do Lobo samples (Table 1).

The above data do not support the interpretation of the Pulo do Lobo belt as a subduction-related accretionary prism (Eden and Andrews, 1990; Silva et al., 1990; Eden, 1991; Braid et al., 2010; Ribeiro et al., 2010; Dahn et al., 2014), where high- to very-high pressure gradients are expected (e.g., Platt, 1986; Ernst, 2005). In fact, most of the geological data concerning the Pulo do Lobo belt do not support such interpretation (see section 2.1). The only feature that would evidence a high-pressure gradient is the interpretation of some rhomboidal aggregates of epidote porfiroblasts as the remnants of supposed lawsonite pseudomorphs previous to S2 in some samples of Pulo do Lobo mafic schists (Rubio Pascual et al., 2013), but no analytical data have been presented to support the lawsonite-precursor character (e.g. electron microscopy data showing remnants of the precursor, as it is usual in such textural relationships).

6. Conclusions

Eighteen metapelites from the Pulo do Lobo belt have been studied to characterize their Variscan low- to very low-grade metamorphism. XRD provided with mineral content and white mica crystal chemical data (illite crystallinity and *b*-cell parameter). EPMA provided with high-resolution compositional maps that allowed mineral mapping and chlorite thermodynamic calculations through XmapTools. Finally, Raman spectroscopy allowed maximum temperature estimations based on the structural organization of the carbonaceous matter.

The microstructural analysis of the samples of the lower formations (Devonian Pulo do Lobo and Ribeira de Limas) shows the existence of two superposed tectonothermal events with associated foliation and phyllosilicate growth (S1-M1 and S2-M2). M2 was less intense, being the only event that affected the overlying Carboniferous Santa Iría formation. The regional geology also shows that a Mississippian thermal (magmatic-derived) event occurred in-between.

M1 and M2 correspond to the chlorite zone, but M1 clearly entered the epizone (greenschists facies with temperatures up to ≈450 °C), while M2 did not exceed the anchizone-epizone boundary (≈300 °C).

In the lower formations, the temperatures obtained from RSCM reach 530 °C and seem to overestimate M1 conditions as compared to other methods. The discrepancy can be explained by the higher sensibility of CM to quickly reequilibrate at maximum temperatures that could have occurred during the Mississippian thermal event. Furthermore, the Na-excess in the samples from the lower formations (evidenced by the presence of albite and paragonite), could have inhibited the growth of index minerals such as biotite or garnet), or alternatively the metamorphic conditions necessary for their genesis could have not been reached).

Thermodynamic disequilibrium between white mica and chlorite has precluded their use for geothermobarometry, and a variety of data (including the existence of relic high-temperature chlorite cores, the presence of chlorite/smectite mixed layers, or the very-low temperatures calculated with chlorite geothermometers) indicate chlorite retrogression after M1 metamorphic climax.

The low-pressure conditions derived from white mica indicators (very poor in celadonite component and very low b-cell values) are incompatible with the high-pressure metamorphic gradient expected in a subduction-related accretionary wedge, which has been the classical interpretation of the Pulo do Lobo belt.

Acknowledgements

References

Abad, I., Mata, M.P., Nieto, F., Velilla, N., 2001. The phyllosilicates in diagenetic-metamorphic rocks of the South Portuguese Zone, southwestern Portugal. The Canadian Mineralogist 39(6), 1571-1589.

Abad, I., Nieto, F., Velilla, N., 2002. Chemical and textural characterisation of diagenetic to low-grade metamorphic phyllosilicates in turbidite sandstones of the South Portuguese Zone: A comparison between metapelites and sandstones. Schweizerische Mineralogische und Petrographische Mitteilungen 82(2), 303-324.

Abad, I., Nieto, F., Gutiérrez-Alonso, G., 2003. Textural and chemical changes in slate-forming phyllosilicates across the external-internal zones transition in the low-grade metamorphic belt of the NW Iberian Variscan Chain. Swiss Bulletin of Mineralogy and Petrology 83(1), 63-80.

Abad, Nieto, F., Velilla, N., Suárez-Ruiz, 2014. Metamorphic evidences from the Monchique pluton (South Portugal): Contact metamorphism vs regional metamorphism under very low-grade conditions. Revista de la Sociedad Geológica de España 27(1): 337-350.

Abalos, B., Gil Ibarguchi, J.I., Eguiluz, L., 1991. Cadomian subduction/collision and Variscan transpression in the Badajoz-Córdoba shear belt, southwest Spain. Tectonophysics 199, 51-72.

Ali, A., 2010. The tectono-metamorphic evolution of the Balcooma Metamorphic Group, north-eastern Australia: a multidisciplinary approach. Journal of Metamorphic Geology 28(4), 397-422.

Apalategui, O., Barranco, E., Contreras, F., Delgado, M., Roldán, F. J., 1983. Hoja 916, Aroche, Mapa Geológico de España a escala 1:50000, Inst. Geológico y Minero de España, Madrid.

Araújo, A., Fonseca, P., Munhá, J., Moita, P., Pedro, J., Ribeiro, A., 2005. The Moura Phyllonitic Complex: an accretionary complex related with obduction in the southern Iberia Variscan suture. Geodinamica Acta 18, 375-388.

Arenas, R., Abati, J., Martínez Catalán, J.R., García, F. D., Pascual, F.R., 1997. PT evolution of eclogites from the Agualada Unit (Ordenes Complex, northwest Iberian Massif, Spain): Implications for crustal subduction. Lithos 40(2), 221-242.

Azor, A., Ballèvre, M., 1997. Low-pressure metamorphism in the Sierra Albarrana area (Variscan belt, Iberian massif). Journal of Petrology 38(1), 35-64.

Azor, A., González Lodeiro, F., Simancas, J.F., 1994. Tectonic evolution of the boundary between the Central Iberian and Ossa-Morena zones (Variscan Belt, southwest Spain). Tectonics 13, 45-61.

Azor, A., Rubatto, D., Simancas, J.F., González Lodeiro, F., Martínez Poyatos, D., Martín Parra L.M., Matas, J., 2008. Rheic Ocean ophiolitic remnants in Southern Iberia questioned by SHRIMP U-Pb zircon ages on the Beja-Acebuches amphibolites. Tectonics 27(5).

Barbero, L., 1995. Granulite-facies metamorphism in the Anatectic Complex of Toledo, Spain: late Hercynian tectonic evolution by crustal extension. Journal of the Geological Society 152(2), 365-382.

Bard, J.P., 1977. Signification tectonique des métatholeites d'anité abyssale de la ceinture de base pression d'Aracena (Huelva, Espagne). Bulletin de la Société Géologique de France, 19, 385-393.

Bastida, F., Martínez-Catalán, J.R., Pulgar, J.A., 1986. Structural, metamorphic and magmatic history of the Mondoñedo nappe (Hercynian belt, NW Spain). Journal of Structural Geology 8(3-4), 415-430.

Bastida, F., Brime, C., García-López, S. Aller, J., Valin, M.L., Sanz-López, J., 2002. Tectono-thermal evolution of the Cantabrian Zone (NW Spain). In: Palaeozoic conodonts from northern

Spain, edited by S. García López and F. Bastida, Instituto Geológico y Minero de España, Cuadernos del Museo Geominero, 1, 105-123, Madrid. ISBN: 84-7840-446-5

Battaglia, S., Leoni, L., Sartori, F., 2004. The Kübler index in late diagenetic to low-grade metamorphic pelites: a critical comparison of data from 10 Å and 5 Å peaks. Clays and Clay Minerals 52(1), 85-105.

Beyssac, O., Goffé, B., Chopin, C., Rouzaud, J.N., 2002a. Raman spectra of carbonaceous material in metasediments: a newgeothermometer. Journal of Metamorphic Geology 20, 859-871, doi: 10.1046/j.1525-1314.2002.00408.x.

Beyssac, O., Rouzaud, J.-N., Goffé, B., Brunet, F., Chopin, C., 2002b. Graphitization in a high-pressure, lowtemperature metamorphic gradient: a Raman microspectroscopy and HRTEM study. Contrib. Mineral. Petrol. 143, 19-31.

Beyssac, O., Goffé, B., Petitet, J.P., Froigneux, E., Rouzaud, J.N., 2003. On the characterization of disordered and heterogeneous carbonaceous materials using Raman spectroscopy. Spectrochim. Acta A Mol. Biomol. Spectrosc. 59, 2267-2276.

Beyssac, O., Bollinger, L., Avouac, J.P., Goffé, B., 2004. Thermal metamorphism in the lesser Himalaya of Nepal determined from Raman spectroscopy of carbonaceous material. Earth and Planetary Science Letters 225, 233-241, doi: 10.1016/j.epsl.2004.05.023.

Beyssac, O., Cox, S.C., Vry, J., Herman, F., 2016. Peak metamorphic temperature and thermal history of the Southern Alps (New Zealand). Tectonophysics 676, 229-249.

Booth-Rea, G., Simancas, J.F., Azor, A., Azañón, J.M., Gonzalez Lodeiro, F., Fonseca, P., 2006. HP-LT Variscan metamorphism in the Cubito-Moura schists (Ossa-Morena Zone, southern Iberia). Comptes Rendus Geoscience 338(16), 1260-1267.

Bousquet, R., Oberha, R., Goffé, B., Wiederkehr, M., Koller, F., Schmid, S.M., Schuster, R., Engi, M., Berger, A., Martinotti, G., 2008. Metamorphism of metasediments at the scale of an orogen: a key to the tertiary geodynamic evolution of the Alps. Geological Society, London, Special Publications 298, 393-411.

Braid, J.A., Murphy, J.B., Quesada, C., 2010. Structural analysis of an accretionary prism in a continental collisional setting, the Late Paleozoic Pulo do Lobo Zone, Southern Iberia, Gondwana Research 17(2-3), 422-439.

Burg, J.P., Iglesias, M., Laurent, P., Matte, P., Ribeiro, A., 1981. Variscan intracontinental deformation: the Coimbra-Córdoba Shear zone (SW Iberian Peninsula). Tectonophysics 78, 161-177.

Castro, A., Fernández, C., De la Rosa, J.D., Moreno Ventas, I., Rogers, G., 1996. Significance of MORB-derived amphibolites from the Aracena metamorphic belt, southwest Spain. Journal of Petrology 37(2), 235-260.

Castro, A., Fernández, C., El-Hmidi, H., El-Biad, M., Díaz, M., De la Rosa, J., Stuart, F., 1999. Age constraints to the relationships between magmatism, metamorphism and tectonism in the Aracena metamorphic belt, southern Spain. Int. J. Earth Sci. 88(1), 26-37.

Cathelineau, M., 1988. Cation site occupancy in chlorites and illites as a function of temperature. Clay Minerals 23, 471-485.

Cathelineau, M., Nieva, D., 1985. A chlorite solid solution geothermometer the Los Azufres (Mexico) geothermal system. Contrib. Mineral Petrol. 91(3), 235-244.

Crespo-Blanc, A., 1991. Evolución geotectónica del contacto entre la zona de Ossa-Morena y la zona Surportuguesa en las sierras de Aracena y Aroche (Macizo Ibérico Meridional): Un contacto mayor en la cadena Hercínica Europea. Ph.D. Thesis, Univ. de Granada, 327 pp.

Dahn, D.R.L., Braid, J.A., Murphy, J.B., Quesada, C., Dupuis, N., McFarlane C.R.M., 2014. Geochemistry of the Peramora Melange and Pulo do Lobo schist: Geochemical investigation and tectonic interpretation of mafic melange in the Pangean suture zone, Southern Iberia. Int. J. Earth Sci. 103(5), 1415-1431.

Dallmeyer, R.D., Fonseca, P.E., Quesada, C., Ribeiro, A., 1993. $^{40}Ar/^{39}Ar$ mineral age constraints for the tectonothermal evolution of a variscan suture in Southwest Iberia. Tectonophysics 222, 177-194.

De Andrade, V., Vidal, O., Lewin, E., O'Brien, P., Agard, P., 2006. Quantification of electron microprobe compositional maps of rock thin sections: an optimized method and examples. Journal of Metamorphic Geology 24(7), 655-668.

Delchini, S., Lahfid, A., Plunder, A., Michard, A., 2016. Applicability of the RSCM geothermometry approach in a complex tectono-metamorphic context: The Jebilet massif case study (Variscan Belt, Morocco). Lithos 256, 1-12.

Díaz Azpiroz, M., Fernández, C., Castro, A., El-Biad, M., 2006. Tectonometamorphic evolution of the Aracena metamorphic belt (SW Spain) resulting from ridge-trench interaction during Variscan plate convergence. Tectonics 25(1).

Dubacq, B., Vidal, O., De Andrade, V., 2010. Dehydration of dioctahedral aluminous phyllosilicates: thermodynamic modelling and implication for thermobarometric estimates. Contrib. Mineral Petrol. 159, 159-174.

Eden, C.P., 1991. Tectonostratigraphic analysis of the northern extent of the oceanic exotic terrane, Northwestern Huelva Province, Spain. Ph. D. Thesis, Univ. of Southhampton, 214 pp.

Eden, C., Andrews, J., 1990. Middle to upper Devonian melanges in SW Spain and their relationship to the Meneage formation in south Cornwall. Proc. Ussher Soc. 7, 217-222.

Ernst, W.G., 2005. Alpine and Pacific styles of Phanerozoic mountain building: subduction‑zone petrogenesis of continental crust. Terra Nova 17(2), 165-188.

Escuder Viruete, J., Arenas, R., Martínez Catalán, J.R., 1994. Tectonothermal evolution associated with Variscan crustal extension in the Tormes gneiss dome (NW Salamanca, Iberian Massif, Spain). Tectonophysics 238(1-4), 117-138.

Fonseca, P., Ribeiro, A., 1993. Tectonics of the Beja-Acebuches ophiolite - a major suture in the Iberian variscan foldbelt. Geol. Rundsch. 82, 440-447.

Fonseca, P., Munhá, J., Pedro, J., Rosas, F., Moita, P., Araujo, A., Leal, N., 1999. Variscan ophiolites and high-pressure metamorphism in southern Iberia. Ofioliti 24, 259-268.

Frey, M., 1987. Very low-grade metamorphism of clastic sedimentary rocks. In: Low temperature metamorphism, edited by M. Frey, Blackie, Glasgow, 9-58.

Goffé, B., Chopin, C., 1986. High-pressure metamorphism in the Western Alps: zoneography of metapelites, chronology and consequences. Schweizerische Mineralogische und Petrographische Mitteilungen 66(1-2), 41-52.

Goffé, B., Velde, B., 1984. Contrasted metamorphic evolutions in thrusted cover units of the Briançonnais zone (French Alps): A model for the conservation of HP-LT metamorphic mineral assemblages. Earth and Planetary Science Letters 68(2), 351-360.

Guidotti, C.V., Sassi, F.P., 1986. Classification and correlation of metamorphic facies series by means of muscovite b data from low-grade metapelites. Neues Jahrbuch fur Mineralogie-Abhandlungen 153, 363-380.

Guidotti, C.V., Sassi, F.P., Blencoe, J.G., Selverstone, J., 1994. The paragonite–muscovite solvus: I. P-T-X limits derived from the Na – K compositions of natural, quasibinary paragonite-muscovite pairs. Geoch. Cosmochim. Acta, 58, 2269–2275.

Gutiérrez-Alonso, G., Nieto, F., 1996. White-mica'crystallinity', finite strain and cleavage development across a large Variscan structure, NW Spain. Journal of the Geological Society 153(2), 287-299.

Gil Ibarguchi, J., Mendia, M., Girardeau, J., Peucat, J.J., 1990. Petrology of eclogites and clinopyroxene-garnet metabasites from the Cabo Ortegal Complex (northwestern Spain). Lithos 25(1-3), 133-162.

Jarosewich, E.J., Nelen, J.A., Norberg, J.A., 1980. Reference samples for electron microprobe analysis: Geostandards Newsletter 4, 43-47.

Jolivet, L., Daniel, J.M., Truffert, C., Goffé, B., 1994. Exhumation of deep crustal metamorphic rocks and crustal extension in arc and back-arc regions. Lithos 33(1-3), 3-30.

Kisch, H.J., 1987. Correlation between indicators of very low-grade metamorphism. In: Low temperature metamorphism, edited by M. Frey, Blackie, Glasgow, 227-300.

Kisch, H.J., 1991. Illite crystallinity: recommendations on sample preparation, X-ray diffraction settings, and interlaboratory samples. Journal of Metamorphic Geology 9, 665–670.

Kübler, B., 1968. Evaluation quantitative du metamorphisme par la cristallinite de l'Illite. Bull. Centres Rech. Pau-SNPA 2, 385-397.

Lahfid, A., Beyssac, O., Deville, E., Negro, F., Chopin, C., Goffé, B., 2010. Evolution of the Raman spectrum of carbonaceous material in low-grade metasediments of the Glarus Alps (Switzerland). Terra Nova 22, 354-360, doi: 10.1111/j.1365-3121.2010.00956.x.

Lanari, P., Guillot, S., Schwartz, S., Vidal, O., Tricart, P., Riel, N., Beyssac, O., 2012. Diachronous evolution of the alpine continental subduction wedge: evidence from P-T estimates in the Briançonnais Zone houillère (France-Western Alps). Journal of Geodynamics 56-57, 39-54.

Lanari, P., Vidal, O., De Andrade, V., Dubacq, B., Lewin, E., Grosch, E.G., Schwartz, S., 2014. XMapTools: A MATLAB©-based program for electron microprobe X-Ray image processing and geothermobarometry. Computers & Geosciences 62, 227-240.

Lopes, G., Pereira, Z., Fernandes, P., Wicander, R., Matos, J.X., Rosa, D., Oliveira, J.T., 2014. The significance of reworked palynomorphs (middle Cambrian to Tournaisian) in the Visean Toca da Moura Complex (South Portugal). Implications for the geodynamic evolution of Ossa Morena Zone. Rev. Palaeobot. Palynol. 200, 1-23.

López-Carmona, A., Pitra, P., Abati, J., 2013. Blueschist-facies metapelites from the Malpica-Tui Unit (NW Iberian Massif): phase equilibria modelling and H2O and Fe2O3 influence in high-pressure assemblages. Journal of Metamorphic Geology 31(3), 263-280.

López Munguira, A., Nieto, F., Pardo, E. S., Velilla, N., 1991. The composition of phyllosilicates in Precambrian, low-grademetamorphic, clastic rocks from the Southern Hesperian Massif (Spain) used as an indicator to metamorphic conditions. Precambrian Research 53(3-4), 267-279.

López Sánchez-Vizcaíno, V., Gómez Pugnaire, M.T., Azor, A., Fernández Soler, J.M., 2003. Phase diagram sections applied to amphibolites: a case study from the Ossa-Morena/Central Iberian Variscan suture (Southwestern Iberian Massif). Lithos 68, 1-21.

Martínez Catalán, J.R., 1985. Estratigrafía y estructura del Domo de Lugo:(Sector Oeste de la Zona Asturoccidental-leonesa). Corpus Geol. Gallaeacie (2º Serie), 2, 1-291.

Martínez Catalán, J.R., Arenas, R., Díaz García, F., Rubio Pascual, F.J., Abati, J., Marquínez, J., 1996. Variscan exhumation of a subducted Paleozoic continental margin: the basal units of the Ordenes Complex, Galicia, NW Spain. Tectonics 15(1), 106-121.

Martínez Catalán, J.R., Rubio Pascual, F.J., Díez Montes, A., Díez Fernández, R., Gómez Barreiro, J., Dias Da Silva, Í., González Clavijo, E., Ayarza, P., Alcock, J.E., 2014. The late Variscan HT/LP metamorphic event in NW and Central Iberia: relationships to crustal thickening, extension, orocline development and crustal evolution. Geological Society, London, Special Publications 405(1), 225-247.

Martínez Poyatos, D., Nieto, F., Azor, A., Simancas, J.F., 2001. Relationships between very low-grade metamorphism and tectonic deformation: Examples from the southern Central Iberian Zone (Iberian Massif, Variscan Belt). Journal of the Geological Society 158, 953-968, doi: 10.1144/0016-764900-206.

Matte, P., 2001. The Variscan collage and orogeny (480-290 Ma) and the tectonic definition of the Armorica microplate: A review. Terra Nova 13, 122-128.

Merriman, R.J., Frey, M., 1999. Patterns of very low-grade metamorphism in metapelitic rocks. In: "Low-grade metamorphism", M. Frey, D. Robinson (eds.), Blackwell, Oxford, 61–107.

Moita, P., Munhá, J., Fonseca, P., Pedro, J., Araújo, A., Tassinari, C., Palacios, T., 2005. Phase equilibria and geochronology of Ossa-Morena eclogites. Actas do XIV Semana de Gequímica / VIII Congresso de geoquímica dos Países de Língua Portuguesa, 2, 471-474.

Munhá, J., 1983. Hercynian magmatism in the Iberian Pyrite Belt. In: The Carboniferous of Portugal, edited by M.J.L. Sousa and J.T. Oliveira, Mem. Serv. Geol. Portugal, 29, 39-81.

Munhá, J., Oliveira, J.T., Ribeiro, A., Oliveira, V., Quesada, C., Kerrich, R., 1986. Beja-Acebuches ophiolite, characterization and geodynamic significance. Maleo 2, 31.

Munhá, J., 1990. Metamorphic evolution of the south Portuguese/Pulo do Lobo zone. In: Pre-Mesozoic Geology of Iberia, edited by R.D. Dallmeyer and E. Martínez García, Springer, Berlin, Germany, pp. 363-368.

Nieto, F., Mata, M.P., Bauluz, B., Giorgetti, G., Árkai, P., Peacor, D.R., 2005. Retrograde diagenesis, a widespread process on a regional scale. Clay Minerals 40(1), 93-104.

Nieto, F., Sánchez-Navas, A., 1994. A comparative XRD and TEM study of the physical meaning of the white mica «crystallinity» index. European Journal of Mineralogy 6(5), 611-621.

Oliveira, J.T., 1990: Part VI: South Portuguese Zone, stratigraphy and synsedimentary tectonism. In: Pre-Mesozoic Geology of Iberia, edited by R.D. Dallmeyer and E. Martínez García, Springer, Berlin, Germany, pp. 334-347.

Ordóñez-Casado, B., 1998. Geochronological studies of the Pre-Mesozoic basement of the Iberian Massif: the Ossa-Morena Zone and the Allochthonous Complexes within the Central Iberian Zone. Ph.D. Thesis, ETH Zurich, 235 pp.

Parra, T., Vidal, O., Agard, P., 2002. A thermodynamic model for Fe-Mg dioctahedral K White micas using data from phase-equilibrium experiments and natural pelitic assemblages. Contrib. Mineral Petrol. 143, 706-732.

Pedro, J., Araujo, A., Fonseca, P., Tassinari, C., Ribeiro, A., 2010. Geochemistry and U-Pb Zircon Age of the Internal Ossa-Morena Zone Ophiolite Sequences: A Remnant of Rheic Ocean in SW Iberia. Ofioliti 35(2), 117-130.

Pereira, M.F., Chichorro, M., Williams, I.S., Silva, J.B., Fernández, C., Díaz-Azpíroz, M., Apraiz, A., Castro, A., 2009. Variscan intra-orogenic extensional tectonics in the Ossa-Morena Zone (Évora-Aracena-Lora del Río metamorphic belt, SW Iberian Massif): SHRIMP zircon U-Th-Pb geochronology. Geological Society, London, Special Publications, 327(1), 215-237.

Pereira, M.F., Apraiz, A., Chichorro, M., Silva, J.B., Armstrong, R.A., 2010. Exhumation of high pressure rocks in northern Gondwana during the Early Carboniferous (Coimbra-Cordoba shear zone, SW Iberian Massif): tectonothermal analysis and U-Th-Pb SHRIMP in-situ zircon geochronology. Gondwana Research 17, 440-460.

Pereira, M.F., Chichorro, M., Silva, J.B., Ordóñez-Casado, B., Lee, J.K., Williams, I.S., 2012. Early carboniferous wrenching, exhumation of high-grade metamorphic rocks and basin instability in SW Iberia: constraints derived from structural geology and U-Pb and 40 Ar-39 Ar geochronology. Tectonophysics 558, 28-44.

Pereira, Z., Matos, J., Fernandes, P., Oliveira, J.T., 2008. Palynostratigraphy and systematic palynology of the Devonian and Carboniferous successions of the South Portuguese Zone, Portugal. Memórias Geológicas do Instituto Nacional de Engenharia, Tecnologia e Inovaçao 34, Lisboa.

Pérez-Cáceres, I., Martínez Poyatos, D., Simancas, J.F., Azor, A., 2015. The elusive nature of the Rheic Ocean in SW Iberia. Tectonics 34, 2429-2450, doi: 10.1002/2015TC003947.

Pérez-Cáceres, I., Simancas, J.F., Martínez Poyatos, D., Azor, A., 2016. Oblique collision and deformation partitioning in the SW Iberian Variscides. Solid Earth 7, 857-872, doi: 10.5194/se-7-857-2016.

Pérez-Cáceres, I., Martínez Poyatos, D., Simancas, J.F., Azor, A., 2017.Testing the Avalonian affinity of the South Portuguese Zone and the Neoproterozoic evolution of SW Iberia through detrital zircon populations. Gondwana Research 42C, 177-192, doi: 10.1016/j.gr.2016.10.010.

Petschick, R., 2004. MacDiff 4.2.5. Powder Diffraction Software, 61p.

Platt, J. P. (1986). Dynamics of orogenic wedges and the uplift of high-pressure metamorphic rocks. Geological Society of America Bulletin 97(9), 1037-1053.

Ponce, C., Simancas, J.F., Azor, A., Martínez Poyatos, D.J., Booth-Rea, G., Expósito, I., 2012. Metamorphism and kinematics of the early deformation in the Variscan suture of SW Iberia. Journal of Metamorphic Geology 30(7), 625-638.

Quesada, C., Fonseca, P.E., Munhá, J., Oliveira, J.T., Ribeiro, A., 1994. The Beja-Acebuches Ophiolite (Southern Iberia Variscan fold belt): geological characterization and significance. Boletín Geológico Minero 105, 3-49.

Ribeiro, A., Munhá, J., Fonseca, P.E., Araujo, A., Pedro, J.C., Mateus, A., Tassinari, C., Machado, G., Jesus, A., 2010. Variscan ophiolite belts in the Ossa-Morena Zone (Southwest Iberia): Geological characterization and geodynamic significance. Gondwana Research 17(2-3), 408-421.

Rosas, F.M., Marques, F.O., Ballèvre, M., Tassinari, C., 2008. Geodynamic evolution of the SW Variscides: orogenic collapse shown by new tectonometamorphic and isotopic data from western Ossa-Morena Zone, SW Iberia. Tectonics 27, TC6008.

Rubio Pascual, F.J., Matas J., Martín Parra, L.M., 2013. High-pressure metamorphism in the Early Variscan subduction complex of the SW Iberian Massif. Tectonophysics 592, 187-199.

Sadezky, A., Muckenhuber, H., Grothe, H., Niessner, R., Pöschl, U., 2005. Raman microspectroscopy of soot and related carbonaceous materials: spectral analysis and structural information. Carbon 43, 1731-1742.

Silva, J. B., Oliveira, J.T., Ribeiro, A., 1990. South Portuguese Zone, estructural outline. In: Pre-Mesozoic Geology of Iberia, edited by R.D. Dallmeyer and E. Martínez García, Springer, Berlin, Germany, pp. 348-362.

Simancas, J.F., Carbonell, R., Lodeiro, F.G., Pérez-Estaún, A., Juhlin, C., Ayarza, P., Kashubin, A., Azor, A., Martínez Poyatos, D., Almodóvar, G.R., Pascual, E., Sáez, R., Expósito, I., 2003. Crustal structure of the transpressional Variscan orogen of SW Iberia: SW Iberia deep seismic reflection profile (IBERSEIS). Tectonics 22(6), doi: 10.1029/2002TC001479.

Simancas, J.F., Expósito, I., Azor, A., Martínez Poyatos, D., González Lodeiro, F., 2004. From the Cadomian orogenesis to the Early Palaeozoic Variscan rifting in Southwest Iberia. Journal of Iberian Geology 30, 53-71.

Simancas, J.F., Carbonell, R., González Lodeiro, F., Pérez-Estaún, A., Juhlin, C., Ayarza, P., Kashubin, A., Azor A., Martínez Poyatos, D.J., Sáez, R., Almodóvar, G.R., Pascual R., Flecha, I., Martí, D., 2006. Transpressional collision tectonics and mantle plume dynamics: The Variscides of southwestern Iberia. Memoirs, Geol. Soc., 32(1) 345-354.

Smith, D.C., 1984. Coesite in clinopyroxene in the Caledonides and its implication for geodynamics. Nature 310, 641-644.

Souche, A., Beyssac, O., Andersen, T.B., 2012. Thermal structure of supra-detachment basins: a case study of the Devonian basins of western Norway. Journal of the Geological Society 169(4), 427-434.

Vázquez, M., Abad, I., Jiménez-Millán, J., Rocha, F.T., Fonseca, P.E., Chaminé, H.I., 2007. Prograde epizonal clay mineral assemblages and retrograde alteration in tectonic basins controlled by major strike-slip zones (W Iberian Variscan chain). Clay Minerals 42(1), 109-128.

Vidal, O., Parra, T., Trotet, F., 2001. A thermodynamic model for Fe-Mg aluminous chlorite using data from phase equilibrium experiments and natural pelitic assemblages in the 100-600 °C 1-25 kbar range. American Journal of Science 63, 557-592.

Vidal, O., Parra, T., Vieillard, P., 2005. Thermodynamic properties of the Tschermak solid solution in Fe-chlorite: application to natural examples and possible role of oxidation. American Mineralogist 90, 347-358.

Vidal, O., De Andrade, V., Lewin, E., Muñoz, M., Parra, T., Pascarelli, S., 2006.P-T-deformation-Fe3+/Fe2+ mapping at the thin section scale and comparison with XANES mapping. Application to a garnet-bearing metapelite from the Sambagawa metamorphic belt (Japan). Journal of Metamorphic Geology 24, 669-683.

Vidal, O., Lanari, P., Munoz, M., Bourdelle, F., De Andrade, V., 2016. Deciphering temperature, pressure and oxygen-activity conditions of chlorite formation. Clay Minerals 51(4), 615-633.

Warr, L.N., Rice, A.H.N., 1994. Inter-laboratory standardization and calibration of clay mineral crystallinity and crystallite size data. Journal of Metamorphic Geology 12, 141–152.

Warr, L.N., Ferreiro Mählmann, R., 2015. Recommendations for Kübler Index standardization. Clay Minerals 50(3), 283-286.

Whitney, D.L., Evans, B.W., 2010. Abbreviations for names of rock-forming minerals. American mineralogist 95(1), 185.

Chapter V

An assessment of the Variscan kinematics in SW Iberia

The geological data collected in this Thesis are added to those obtained by a long-term research in order to quantify the Variscan left-lateral transpressional displacements in SW Iberia. The essential deformational features of the different structural domains of SW Iberia have been summarized and adequate transpressional models have been applied to constrain the kinematic analysis. The left-lateral collisional evolution of SW Iberia is a particular feature of this transect of the Variscan orogen not properly considered in most of the large-scale tectonic reconstructions.

Oblique collision and deformation partitioning in the SW Iberian Variscides

Irene Pérez-Cáceres[1], José Fernando Simancas[1], David Martínez Poyatos[1], Antonio Azor[1], and Francisco González Lodeiro[1]

1 Departamento de Geodinámica, Facultad de Ciencias, Universidad de Granada, Campus de Fuentenueva s/n, 18071 Granada, Spain.

Abstract

Different transpressional scenarios have been proposed to relate kinematics and complex deformation patterns. We apply the most suitable of them to the Variscan orogeny in SW Iberia, which is characterized by a number of successive left-lateral transpressional structures developed in the Devonian to Carboniferous period. These structures resulted from the oblique convergence between three continental terranes (Central Iberian Zone, Ossa-Morena Zone and South Portuguese Zone), whose amalgamation gave way to both intense shearing at the suture-like contacts and transpressional deformation of the continental pieces in-between, thus showing strain partitioning in space and time. We have quantified the kinematics of the collisional convergence by using the available data on folding, shearing and faulting patterns, as well as tectonic fabrics and finite strain measurements. Given the uncertainties regarding the data and the boundary conditions modeled, our results must be considered as a semiquantitative approximation to the issue, though very significant from a regional point of view. The total collisional convergence surpasses 1000 km, most of them corresponding to left-lateral displacement parallel to terrane boundaries. The average vector of convergence is oriented E–W (present-day coordinates), thus reasserting the left-lateral oblique collision in SW Iberia, in contrast with the dextral component that prevailed elsewhere in the Variscan orogen. This particular kinematics of SW Iberia is understood in the context of an Avalonian plate salient currently represented by the South Portuguese Zone.

Keywords

Oblique collision

Transpressional deformation

SW Iberia Variscan kinematics

Rheic Ocean suture

Highlights

Variscan left-lateral transpression.

Spatial and temporal deformation partitioning in SW Iberia.

Displacement estimate and relative pre-collisional disposition of SW Iberian terranes.

1. Introduction

Oblique convergence/divergence between lithospheric plates or continental blocks are common tectonic scenarios, usually named transpression/transtension (Harland, 1971; Sanderson and Marchini, 1984). Strain resulting from transpression is usually modeled as a combination of a three-dimensional coaxial component and an orthogonal simple shear component (Tikoff and Fossen, 1999). Less frequently, oblique convergence has been modeled as a combination of two simple shears, with lateral (wrenching) and orthogonal (thrusting) kinematics (Ellis and Watkinson, 1988). The oblique convergence/divergence that characterizes transpression usually involves deformation partitioning into thin bands concentrating lateral displacements and broader domains concentrating orthogonal displacements (e.g., Holdsworth and Strachan, 1991; Tikoff and Teyssier, 1994).

Following the works by Sanderson and Marchini (1984) and Fossen and Tikoff (1993), many increasingly sophisticated models have been developed to analyze high-strain transpressional zones. A number of boundary conditions have been introduced, such as lateral extrusion (Dias and Ribeiro, 1994; Jones et al., 1997; Teyssier and Tikoff, 1999), inclined walls (Jones et al., 2004), oblique extrusion and/or oblique simple shear (Jiang and Williams, 1998; Lin et al., 1998; Czeck and Hudleston, 2003, 2004; Fernández and Díaz-Azpiroz, 2009), no slip at the boundaries with undeformed walls (Dutton, 1997; Robin and Cruden, 1994) and migrating boundaries (Jiang, 2007).

SW Iberia (Fig. 5.1) geological architecture resulted from a complex transpressional evolution during the Variscan collision in the Devonian to Carboniferous period (e.g., Pérez- Cáceres et al., 2015). This evolution involved the oblique convergence between three continental terranes, namely, from north to south, the Central Iberian Zone (CIZ), the Ossa-Morena Zone (OMZ) and the South Portuguese Zone (SPZ). These terranes show transpressional left-lateral kinematics with deformation partitioning (Burg et al., 1981; Matte, 1991; Crespo-Blanc, 1992; Azor, 1994; Quesada et al., 1994; Expósito et al., 2002; Silva and Pereira, 2004; Ponce et al., 2012), thus contrasting with the dextral component that characterizes most of the Variscan collision in other regions of the orogen (e.g., Shelley and Bossière, 2000).

This work aims to describe and approximately quantify the Variscan transpressional deformation in SW Iberia. We are particularly interested in evaluating the left-lateral component of the transpressional deformation, in order to achieve an approximate image of the relative position of the terranes involved in this oblique collision. To do so, the use of sophisticated transpressional models might not be justified, since these models demand stringent geological data hardly available for a large-scale tectonic analysis (e.g., Jiang and Williams, 1998; Fernández et al., 2013). For this reason, simple monoclinic-flow models (Dewey et al., 1999) and other approximate tools may yield regionally valuable approximations.
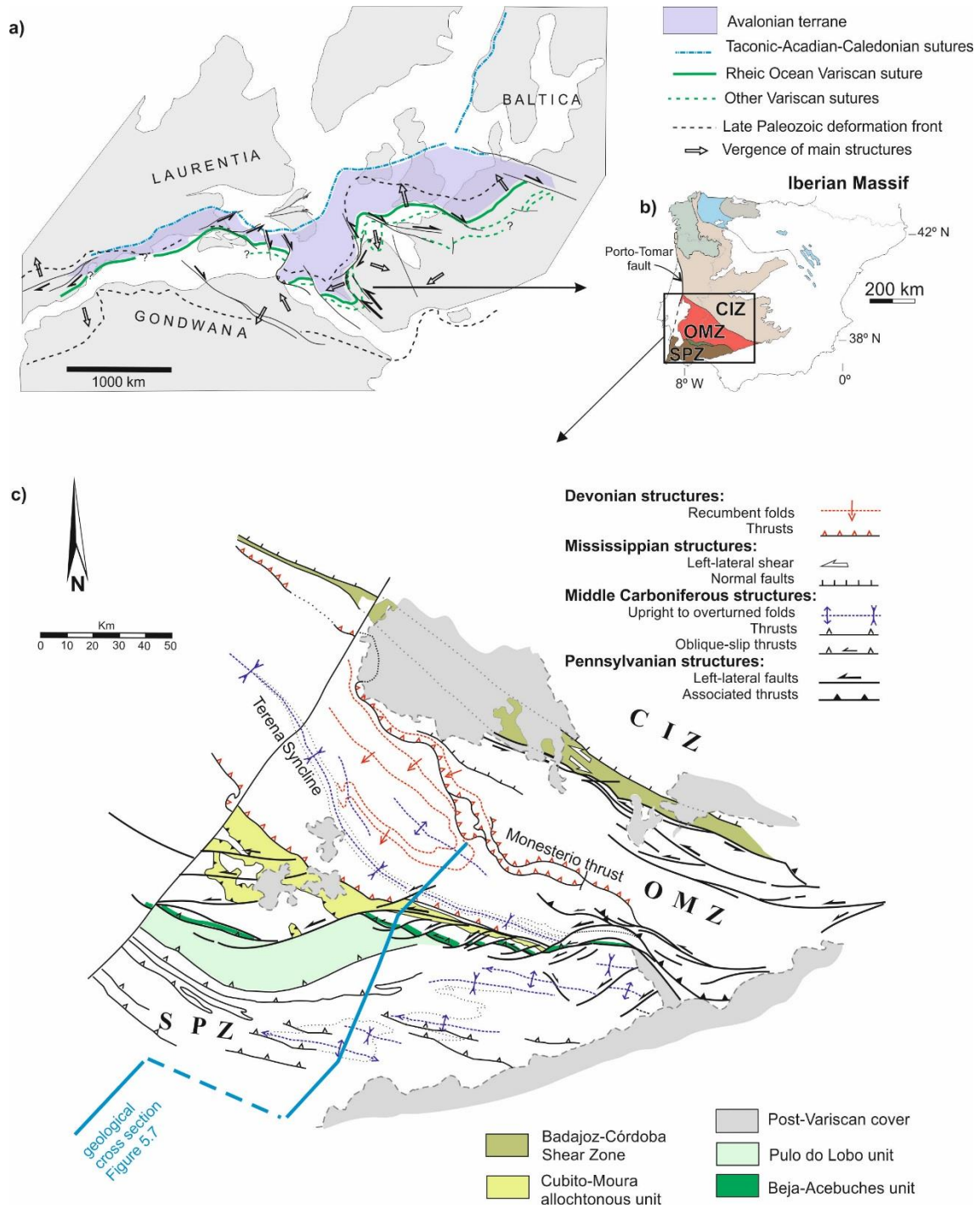
Figure 5.1. a) Reconstruction of the Variscan-Alleghanian orogen at the end of the Carboniferous simplified from Simancas et al. (2005). The Avalonian continental piece and the inferred Rheic Ocean and other second-order Variscan sutures are depicted. The SW Iberian left-lateral shear sutures are highlighted. b) Geological subdivision of the Iberian Massif. CIZ: Central Iberian Zone; OMZ: Ossa-Morena Zone; SPZ: South Portuguese Zone. c) Structural map of the SW Iberia showing the main units and the different Devonian and Carboniferous structures. The location of the cross-section in Fig. 5.7 is indicated.

2. Variscan events in SW Iberia

The Variscan/Alleghanian orogeny resulted from the closure of the Rheic Ocean that separated Avalonia and Gondwana during the Ordovician to Devonian period (Fig. 5.1a). The subsequent collision amalgamated these two continents along with intervening minor oceanic realms and micro-continents in-between (e.g., Matte, 1991, 2001; Murphy and Nance, 1991; Franke, 2000; Stampfli and Borel, 2002).

Prior to the Rheic Ocean formation, the arc-type Cadomian orogeny variedly overprinted the northern margin of Gondwana during the Ediacaran (e.g., Linnemann et al., 2014). In Iberia, this orogeny resulted in the development of thick synorogenic arc-related basins (e.g., in the CIZ; Rodríguez-Alonso et al., 2004) and calc-alkaline arc-related magmatism that concentrated in the OMZ and southernmost CIZ (Sánchez Carretero et al., 1990; Pin et al., 2002; Bandrés et al., 2004; Simancas et al., 2004).

As for the Variscan evolution, the boundaries between the CIZ, OMZ and SPZ terranes are considered as sutures (Fig. 5.1). The CIZ is a continental domain that formed part of northern Gondwana, while the OMZ is commonly interpreted as a continental piece that rifted (and drifted to some extent) from Gondwana (i.e., the CIZ) in the early Paleozoic (Matte, 2001; Robardet, 2002). Subsequent collision between these two terranes resulted in the suture unit known as Badajoz-Córdoba Shear Zone (BCSZ) or Central Unit (Fig. 5.1c) (Burg et al., 1981; Azor et al., 1994). The BCSZ includes some early Paleozoic amphibolites (Ordóñez-Casado, 1998) with a geochemical signature akin to oceanic crust (Gómez-Pugnaire et al., 2003). A first collisional stage is attested by eclogite relics in the BCSZ (1.6-1.7 GPa; Abalos et al., 1991; Azor, 1994; López Sánchez-Vizcaíno et al., 2003) and large-scale Devonian recumbent folds and thrusts in the colliding blocks (OMZ and southern CIZ; Simancas et al., 2001, and references therein). The eclogites were exhumed during the subsequent, latest Devonian to Early–Middle Mississippian intense ductile left-lateral shearing that characterizes the BCSZ (Burg et al., 1981), coeval to normal faulting, basin development and mafic magmatism at both sides of the BCSZ. Renewed Pennsylvanian compression is attested by upright folds and left-lateral strike-slip faults. Overall, the CIZ–OMZ boundary is interpreted as a Gondwana-related second-order suture of the Variscan orogen (e.g., Simancas et al., 2005).

The OMZ–SPZ boundary (Fig. 5.1) has been classically interpreted as the suture of the Rheic Ocean. This boundary is constituted by three units (Fig. 5.1c): (i) the Beja-Acebuches (BA hereafter) unit, metamorphosed mafic and ultramafic rocks that crop out all along this major contact (Munhá et al., 1986; Crespo-Blanc, 1991; Fonseca and Ribeiro, 1993; Quesada et al., 1994; Castro et al., 1996; Azor et al., 2008); (ii) the Pulo do Lobo unit, a low-grade metasedimentary unit with minor MORB-like metabasalts (Eden and Andrews, 1990; Silva et al., 1990; Eden, 1991; Braid et al., 2010; Dahn et al., 2014); and (iii) the allochthonous Cubito-Moura unit, which contains high-pressure and MORB-like rocks emplaced onto the OMZ border (Fonseca et al., 1999; Araújo et al., 2005; Ponce et al., 2012). Recent work including new structural and radiometric data has improved our knowledge on the significance of the Pulo do Lobo Unit, as well as on the geometry and timing of deformations affecting the OMZ–SPZ suture (Pérez-Cáceres et al., 2015), which is now viewed as a Rheic cryptic suture, blurred by Carboniferous tectonothermal imprints. Thus, the envisaged evolution of the OMZ–SPZ boundary can be summarized as follows (Fig. 5.2):

(i) Following Rheic Ocean consumption in Devonian period, the southern border of the OMZ partially subducted (high-pressure rocks). Some of the subducted rocks were later scrapped off along with Rheic Ocean rocks and emplaced (the allochthonous Cubito-Moura unit) onto the southern OMZ (Araújo et al., 2005; Fig. 5.2a). The kinematics of emplacement, recorded in an early stretching lineation, is top-to-the-ENE, which corresponds to a tectonic regime of oblique left-lateral convergence (Ponce et al., 2012).

(ii) An Early–Middle Mississippian transtensional event temporarily interrupted the convergence and created a very narrow aisle of oceanic-like crust (actually represented by the BA unit) just at the OMZ–SPZ boundary (Fig. 5.2b) (Azor et al., 2008). Moreover, ca. 340 Ma mafic and acid magmatism intruded/extruded at both sides of the oceanic strip.

(iii) Convergence was resumed immediately, giving way to northwards obduction of the BA unit, as well as north-verging folds and tectonic imbrications in the Pulo do Lobo unit (Pérez-Cáceres et al., 2015; Fig. 5.2c).

(iv) Subsequently, south-vergent transpressional structures developed (Fig. 5.2d). The BA unit was folded synchronously with left-lateral high-temperature shearing (Pérez-Cáceres et al., 2015), which evolved to greenschist facies conditions and concentrated in the southern part of the unit (Crespo-Blanc and Orozco, 1988; Quesada et al., 1994). Oblique convergence propagated southwards across the SPZ in the Pennsylvanian. At latemost Variscan orogeny period, left-lateral displacements newly focused on the OMZ–SPZ boundary as brittle strike-slip faults.

3. Deformation partitioning in SW Iberia

One of the most striking features of SW Iberia is the partitioning of bulk regional deformation into four well-defined domains, namely, from north to south: (i) CIZ–OMZ boundary, (ii) OMZ terrane, (iii) OMZ–SPZ boundary, and (iv) SPZ terrane (Fig. 5.1c).

The CIZ–OMZ boundary, marked by the BCSZ, shows a prominent *S-L* fabric with occasional *L*–type tectonites. The stretching lineation is subhorizontal and kinematic indicators indicate left-lateral displacement (Burg et al., 1981; Azor et al., 1994). Moreover left-lateral strike-slip faults developed in the Pennsylvanian period around this boundary. The OMZ records Devonian and Carboniferous compressional deformation events separated by a singular Mississippian transtensional stage. Both Devonian and Carboniferous folds and thrusts trend obliquely to the OMZ boundaries, suggesting a transpressional setting (Expósito, 2000; Expósito et al., 2002). The OMZ–SPZ boundary is underlined by the narrow belt of the BA unit, affected by left-lateral ductile shearing and strike-slip brittle faults (Bard, 1977; Crespo-Blanc and Orozco, 1988; Quesada et al., 1994; Díaz-Azpiroz and Fernández, 2005). Finally, the SPZ is a Carboniferous south-vergent fold-and-thrust belt (Oliveira, 1990; Simancas et al., 2003) with axial traces slightly oblique to the northern boundary of the terrane, thus featuring transpressional deformation (Simancas, 1986).
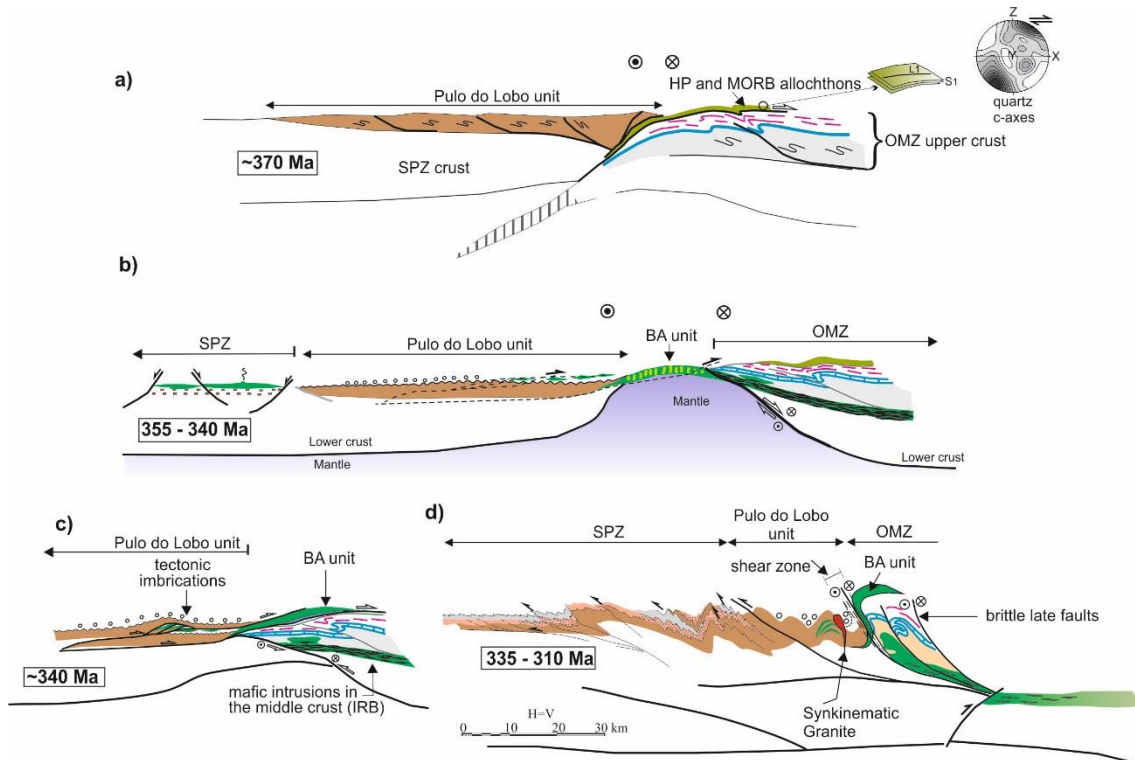
Figure 5.2. Evolutionary model for the OMZ–SPZ boundary from the Middle–Late Devonian to the Pennsylvanian proposed by Pérez-Cáceres et al. (2015). a) Closing of the Rheic Ocean and Late Devonian collision. b) Early Carboniferous intracollisional transtensional stage mainly represented by the metamafic BA unit. c) Carboniferous renewed oblique collision, producing the obduction of the BA unit onto the OMZ. d) High- to low-temperature folding and shearing of the BA unit and southwards propagation of the deformation. Notice that the left-lateral component of displacements, indicated by standard symbols, cannot be included in these cross-sections.

The brief description advanced above illustrates that ductile and brittle sinistral strike-slip shear bands characterize the CIZ–OMZ and OMZ–SPZ boundaries, while deformation inside the OMZ and SPZ terranes includes a significant component of orthogonal shortening. Deformation partitioning such as that displayed in SW Iberia is believed to be favored by low angles of plate convergence (Teyssier et al., 1995), but a more comprehensible kinematic analysis can be gained by analyzing deformation data in more detail. Our description will proceed from north to south, except for the displacements associated with late Variscan brittle faulting that will be considered jointly at the end.

4. Ductile shearing at the CIZ–OMZ boundary

The BCSZ is a NW–SE-trending band of highly deformed schists, gneisses, migmatites and amphibolites that constitutes the CIZ–OMZ boundary (Fig. 5.1c). It exhibits, consistently along 200 km of visible outcrop, an intense mylonitic S-L fabric (locally L fabric) with subhorizontal stretching lineation (pitch less than 15°) and left-lateral kinematics (Burg et al., 1981; Azor et al., 1994). The age of the ductile shearing in the BCSZ ranges from at least latest Devonian to Middle Mississippian, according to different, not fully consistent, metamorphic geochronological data: 340-330 (Ar/Ar on biotite) (Blatrix and Burg, 1981),

370-360 Ma (Ar/Ar on hornblende), 340-330 (Ar/Ar on muscovite) (Quesada and Dallmeyer 1994) and c. 340 (U/Pb on zircon) (Ordóñez-Casado, 1998; Pereira et al., 2010). In any case, textural evidence indicates that high-pressure metamorphism took place prior to that shearing, i.e., before the Late Devonian period. South of the BCSZ, the OMZ depicts pro-wedge Devonian SW-vergent folds and thrusts (Expósito et al., 2002); to the north, the southernmost CIZ shows conjugate retro-wedge NE-vergent Devonian folds (Martínez Poyatos, 1997; Simancas et al., 2001; Expósito et al., 2002).

The kinematics of the BCSZ is analyzed here in two different ways: (i) considering the recorded strain, in the light of the simple shear model; and (ii) considering a more complete, though poorly constrained, subduction–exhumation path.

(i) Simple shear in the BCSZ: the mylonitic fabric with subhorizontal stretching lineation, consistent all along 200 km of outcrop (Burg et al., 1981; Azor et al., 1994), suggests approximate monoclinic strain (Lin et al., 1998), and can be approximately analyzed by means of the strike-slip simple shear model. The finite strain in this shear zone can be roughly assessed from the very elongated shape of some orthogneissic bodies located inside the BCSZ (e.g., the Ribera del Fresno orthogneiss), which suggests X/Z ≈ 11 and γ ≈ 3 assuming simple shear. However, this is a rather conservative estimation, since these bodies are relatively rigid strain markers surrounded by schists. For this reason, we will take γ = 4 in the following calculation. The thickness of the BCSZ is another important parameter to take into account; the maximum outcropping thickness is 15 km, but the original one was probably greater (20-25 km) because late Variscan brittle faults abruptly cut and bound the ductile shear zone, as seen on the geological map (Fig. 5.1c) and in the seismic image (Simancas et al., 2003). Thus, considering an original thickness of 20-25 km and a mean shear strain γ = 4, a tentative left-lateral displacement of 80-100 km results. The transpression model of inclined walls (Jones et al., 2004) is another way to examine the BCSZ, since this crustal-scale shear zone has been seismically imaged dipping to the NE (Simancas et al., 2003). According to this transpression model, the subhorizontal stretching lineation would be only compatible with an angle of convergence less than 10°, i.e., the simple shear component should have been extremely dominant. Thus, the left-lateral displacement derived from this model does not differ significantly from the one obtained with the strike-slip simple shear model.

(ii) Two simple shear events during a subduction–exhumation path: besides left-lateral displacement, the movement between the CIZ and the OMZ must have included a dip-slip component of shearing, enabling first the burial and then the exhumation of the high-pressure rocks. Note, however, that the exhumation path has not resulted in a generalized L fabric, as it typically occurs under transtensional kinematics (e.g., Teyssier and Tikoff, 1999). For that reason, we use the double strike-slip and dip-slip shear model of Ellis and Watkinson (1988) in our estimates. According to this model and considering a shear zone dip of 45° (Fig. 2, curve 3 in Ellis and Watkinson, 1988), the subhorizontal stretching lineation that characterizes the BCSZ would indicate a convergence/divergence angle of 15-35°. We take 25° for our calculations in Fig. 5.3a; if the high-pressure rocks of the BCSZ reached depths of ≈ 55 km (1.6-1.7 GPa), then a left-lateral displacement of around 115 km is inferred during the exhumation of these rocks. If a similar calculation is considered for the previous burial path, the whole subduction/exhumation path would amount to ≈ 230 km of left-lateral displacement.

From the above estimations, a great discrepancy exists between the results of the two models considered: 80-100 km and 230 km, respectively. Actually, most or all of the shearing recorded in the BCSZ may correspond to the Carboniferous exhumation path (see above for the reported cooling metamorphic ages), thus explaining most of the difference. Anyway, because these calculations provide only a rough estimate, we will take an intermediate rather conservative value of ≈ 150 km for the whole ductile left-lateral displacement concentrated at the CIZ–OMZ boundary.
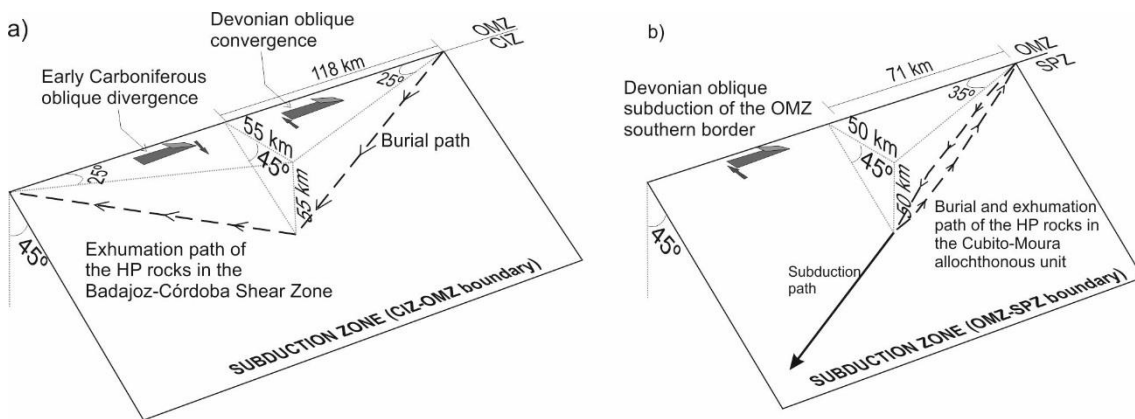
Figure 5.3. Simple models of burial and exhumation for the high-pressure rocks cropping out at the two collisional boundaries of the OMZ. a) CIZ–OMZ boundary. b) OMZ–SPZ boundary. See text for more explanations.

5. Deformation inside the OMZ

The OMZ records Devonian and Carboniferous compressional events (folds and thrusts), separated by the Early–Middle Mississippian transtensional stage (Pérez-Cáceres et al., 2015). The Devonian deformation gave way to SW-vergent recumbent folds and thrusts, while the Carboniferous one caused upright or slightly vergent folds and reverse faults (Fig. 5.1c). The two sets of folds have subparallel axes (Expósito et al., 2002); their axial traces trend oblique to the OMZ boundaries, depicting a z shape, in accordance with a left-lateral component of transpression increasing towards the borders (Fig. 5.1c). The Devonian tectonic fabric is S or S-L type, the stretching/mineral lineation is at high angles to the fold axes and the strain ellipsoids are generally oblate with very variable strain intensity (2.5 ≤ X/Z ≤ 9) and no significant areal change on the XZ section (Expósito, 2000). Regarding the Carboniferous tectonic fabric, it is generally planar with a steeply plunging X axis.

A continuous transpressional evolution has been suggested for the OMZ (Silva and Pereira, 2004) but there is no theoretical transpressional model that fits the complex and heterogeneous evolution of the OMZ. As a basic kinematic analysis, we propose the evolution schematically displayed in Fig. 5.4, which accounts for the following geometrical features: (i) the axial traces of the Carboniferous folds (as depicted by the Terena syncline) (Fig.1c) are smoothly curved, trending NNW-SSE at the central OMZ and WNW-ESE towards its borders; (ii) the Devonian folds and thrusts trend subparallel to the Carboniferous ones, though the Devonian axial surfaces are folded (type 3 interference fold pattern; Ramsay and Huber, 1987) (Fig. 5.1c); and (iii) the northern and southern

OMZ boundaries are not parallel (Fig. 5.1c), the obliquity having been enhanced during the Carboniferous transpression (Fig. 5.4c, d).

The Carboniferous shortening can be divided into the two stages shown in Figs. 4c and 5: (i) first, a set of folds formed due to SW-NE compression, its original orientation being preserved in the central OMZ (Fig. 5.5a); (ii) then, these folds rotated heterogeneously to reach a Z shape in map view, congruent with left-lateral transpression (Fig. 5.5b). These two stages are described below.

(i) The width of the central OMZ as measured perpendicular to the original trend of the Carboniferous folds is ≈ 150 km (Fig. 5.5a). As regards to the finite strain, the available data are insufficient for an accurate evaluation of shortening. Let us take a conservative shortening of ≈ 35 %, just enough to generate the axial-plane Carboniferous foliation observed in these rocks. Accordingly, a shortening of ≈ 80 km would have taken place perpendicular to the folds, which means, in turn, that the width of the OMZ just before Carboniferous folding would have been ≈ 230 km (150 + 80). Given the oblique orientation of the shortening direction with respect to the CIZ–OMZ boundary (50°; Figs. 4c and 5), the corresponding left-lateral component parallel to the CIZ–OMZ boundary is ≈ 55 km.

(ii) In the second stage, the trend of the Carboniferous folds rotated heterogeneously. This rotation can be modeled according to the transpressional equation of Fossen and Tikoff (1993), but the simpler equation $\cot\Phi' = \alpha \cot\Phi + \gamma$ of Sanderson and Marchini (1984) will be used here in view of our main interest in evaluating finite lateral displacements (Φ' and Φ are the final and original angles of the rotated line, α is the vertical stretch and γ is the shear strain parallel to the boundary). To analyze this deformation, the OMZ has been divided into five bands, each one characterized by a particular reorientation angle (Fig. 5.5b). As rotation is concentrated at the two boundaries of the OMZ (Fig. 5.4c) deformation must involve a dominant shear component; thus, we have tentatively assumed a modest value α-1 = 0.7 (α = 1.43) obtaining the following results.

- Band I (Φ' = 10°, Φ = 40°, width = 40 km) would have undergone a shear strain of γ = 4, which results in 160 km of left-lateral displacement.

- Band II (Φ' = 30°, Φ = 40°, width = 13 km) would have undergone approximately zero shear strain (only frontal shortening).

- Band III is considered to have preserved the original orientation.

- Band IV (Φ' = 30°, Φ = 50°, width = 17 km) would have undergone a shear strain of γ = 0.53, causing 9 km of left-lateral displacement.

- Finally, band V (Φ' = 15°, Φ = 50°, width = 23 km) is characterized by γ = 2.53 and a left-lateral displacement of 58 km.

Overall, these calculations based on the sinistral rotation of the Carboniferous folds amount to ≈ 225 km. Added to the 55 km of left-lateral displacement calculated above, the total left-lateral Carboniferous displacement would amount to ≈ 280 km. Notice that considering a simple shear model to explain these rotations, instead of a transpressional one, would result in a greater left-lateral component. On the contrary, a lower left-lateral component would result from considering rotations as due to orthogonal shortening, but this interpretation seems to be at odds with the observed increasing rotation towards the boundaries of the OMZ.
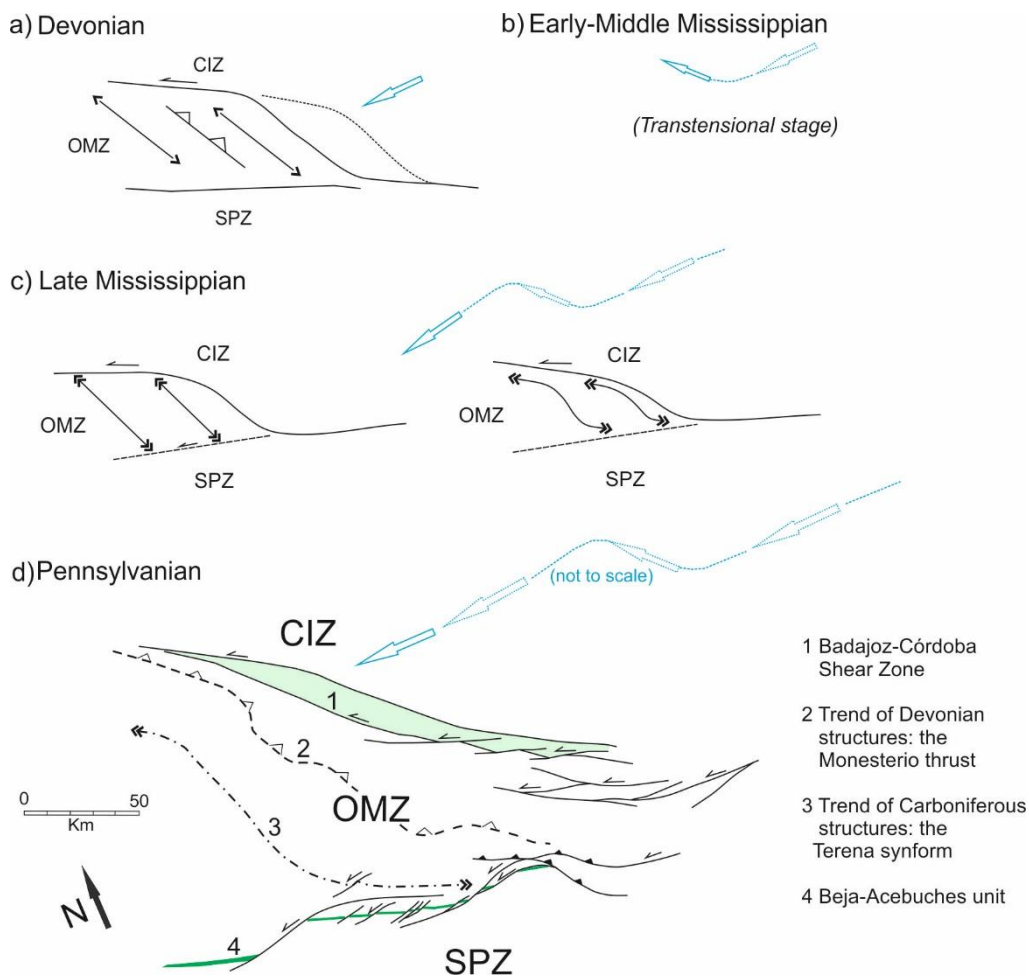
Figure 5.4. (a–d) Schematic evolutionary model of the deformations inside de OMZ from the Devonian to the Pennsylvanian period. See text for further explanations.

Devonian deformation in the OMZ can be analyzed taking into account the subparallelism of Devonian and Carboniferous fold axes (Fig. 5.4d). Like for the Carboniferous structures, we assume that the original trend of the Devonian structures is observed at the central part of the OMZ (40° with respect to the northern border of the OMZ). Devonian shortening would be perpendicular to this trend and, as said above, the width of the OMZ before Carboniferous deformation would be 230 km. On the other hand, an approximate mean strain ratio $X/Z \approx 5$ can be proposed from the available range of strain measures ($2.5 \leq X/Z \leq 9$; Expósito, 2000), which results in $Z = 0.44$ if the XZ area remained unchanged and a Devonian shortening of ≈ 290 km. Given the oblique orientation of the shortening direction with respect to the CIZ–OMZ boundary, the resulting left-lateral Devonian displacement would be ≈ 185 km, and the total left-lateral Devonian plus Carboniferous displacement would amount to ≈ 465 km. Note that a lower (conservative) mean strain $X/Z = 4$ yields substantially similar results: 230 km of Devonian shortening, of which 145 km is of Devonian left-lateral displacement, and then ≈ 425 km of total Devonian–Carboniferous left-lateral displacement. Finally, we have tested these results following a different approach, the shortening obtained from stratigraphic markers on the OMZ

geological cross-section (Simancas et al., 2003). On this ground, a transversal shortening of ≈ 57 % is estimated, which entails (for a 150 km-wide OMZ at present) a total shortening of ≈ 200 km and a left-lateral component of ≈ 130 km. Added to the left-lateral displacement inferred from the rotation of Carboniferous folds (≈ 225 km; see above), a total figure of ≈ 355 km is obtained; i.e., lower than the previous numbers of 465 and 425 km. Thus, despite the fact that our arguments are rather crude, a figure of ≈ 400 km can be a valuable approximation to the left-lateral displacement due to the Devonian and Carboniferous deformation inside the OMZ.
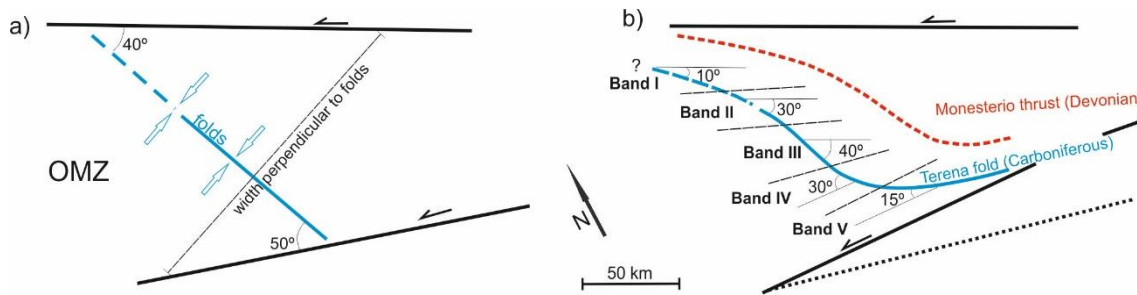
Figure 5.5. Stages of Carboniferous shortening inside the OMZ. a) NE–SW compression gave way to a set of upright folds. b) Folds rotation by heterogeneous left-lateral shearing. The five different bands considered to analyze the deformation are depicted.

6. Subduction/exhumation at the southern OMZ continental margin

In the Middle-Late Devonian times, the southern continental margin of the OMZ subducted under the SPZ, as witnessed by exhumed high-pressure metasedimentary rocks of the OMZ cover included in the allochthonous Cubito-Moura unit (Fig. 5.2a) (Fonseca et al., 1999; Araújo et al., 2005; Booth-Rea et al., 2006). The kinematics of this event can be gauged by the early stretching lineation developed during exhumation, which once restored later folds, trends ≈ N70°E and shows top-to-the-ENE sense of shearing (Ponce et al., 2012). This orientation forms an angle of ≈ 30° with the ≈ N100°E trend of the OMZ–SPZ boundary. Based on the model of thrust-and-wrench shearing parallel to a subduction zone, this orientation of the stretching lineation would correspond to a convergence angle of 45°–55°, depending on the dip of the subduction zone (curve 3 in Figs. 1 and 2 by Ellis and Watkinson, 1988). By contrast, the model of simple-inclined transpression (orthogonal shortening and strike-slip shearing with inclined walls) (Jones et al., 2004) suggests a more oblique convergence at an angle ≤ 20°. Since it is unclear which one of these two models fits better the SW Iberia tectonic scenario, we will take an intermediate convergence angle of 35° for the next tentative calculation.

A rough estimate of the left-lateral displacement between the SPZ and the OMZ during this stage can be proposed based on (i) a simple subduction–exhumation channel with opposite senses of burial and exhumation (Fig. 5.3b), (ii) a convergence angle of 35°, (iii) an intermediate dip of 45° for the subduction plane, and (iv) a maximum depth of ≈ 50 Km for the high-pressure rocks, corresponding to the maximum recorded pressure of 1.4 GPa in the Cubito-Moura unit (Fonseca et al., 1999; Ponce et al., 2012; Rubio Pascual et al., 2013). According to these assumptions, a simple calculation yields 71 km of lateral

displacement during burial and the same amount during exhumation, i.e., altogether ≈ 140 km of left-lateral displacement of the OMZ with respect to the SPZ during this Devonian event. The same line of reasoning results in 100 km and 270 km of left-lateral displacement for extreme convergence angles of 45° and 20°, respectively.

7. Emplacement of the Beja-Acebuches mafic/ultramafic belt

Along the OMZ–SPZ boundary, an intrusion of mafic and ultramafic rocks (the BA unit; Fig. 5.1c; Quesada et al., 1994) was emplaced during the transtensional stage that dominated all of SW Iberia during the earliest Carboniferous (Azor et al., 2008) (Fig. 5.2b). There are no kinematic indicators but an undefined left-lateral transtension is suggested in order to maintain the same lateral displacements as in the previous (see above) and subsequent (see below) convergent stages (Fig. 5.4). The lateral displacement due to this event has not been taken into account in our kinematic assessment.

8. Obductive thrust of the Beja-Acebuches unit

The convergence between the OMZ and the SPZ was resumed very soon after the formation of the BA unit. The renewed convergence resulted in hot obductive thrust of the BA unit onto the OMZ border (Fig. 5.2c) (Fonseca and Ribeiro, 1993; Pérez-Cáceres et al., 2015). As in the previous stage, the lack of kinematic indicators prevents from knowing the specific thrusting vector, presumably oblique to the OMZ–SPZ boundary.

9. Ductile shearing and folding at the OMZ–SPZ boundary

After the obductive thrust referred above, the convergent evolution became characterized by the interplay between large-scale folding and left-lateral shearing (Fig. 5.6) (Pérez-Cáceres et al., 2015).

The OMZ–SPZ boundary was affected by an E–W-trending south-vergent fold (Quintos fold) (Figs. 2d and 6). Coeval to the Quintos fold, ductile shearing came about concentrated in the BA unit, which evolved from high- to low-temperature (the so-called Southern Iberian shear zone; Crespo-Blanc and Orozco, 1988; Díaz-Azpiroz and Fernández, 2005; Fernández et al., 2013). The age of these deformations is constrained in the range 340-335 Ma (Late Visean), according to the available geochronological data (Dallmeyer et al., 1993; Castro et al., 1999).

The high-temperature rocks of the Southern Iberian shear zone (granulite and high-temperature amphibolite facies) are middle-grained and display foliation and compositional layering and, sometimes, mineral lineation. The low-temperature rocks (amphibolite and greenschist facies) are fine-grained and show a well-developed *S-L* mylonitic fabric with abundant microstructures indicating left-lateral shear sense (Crespo-Blanc, 1991; Díaz-Azpiroz and Fernández, 2005; Fernández et al., 2013). The pitch of the high-temperature mineral lineation is medium to high to the E–NE, while the stretching/mineral lineation in the low-temperature rocks has medium to low pitch angles to the E–SE.
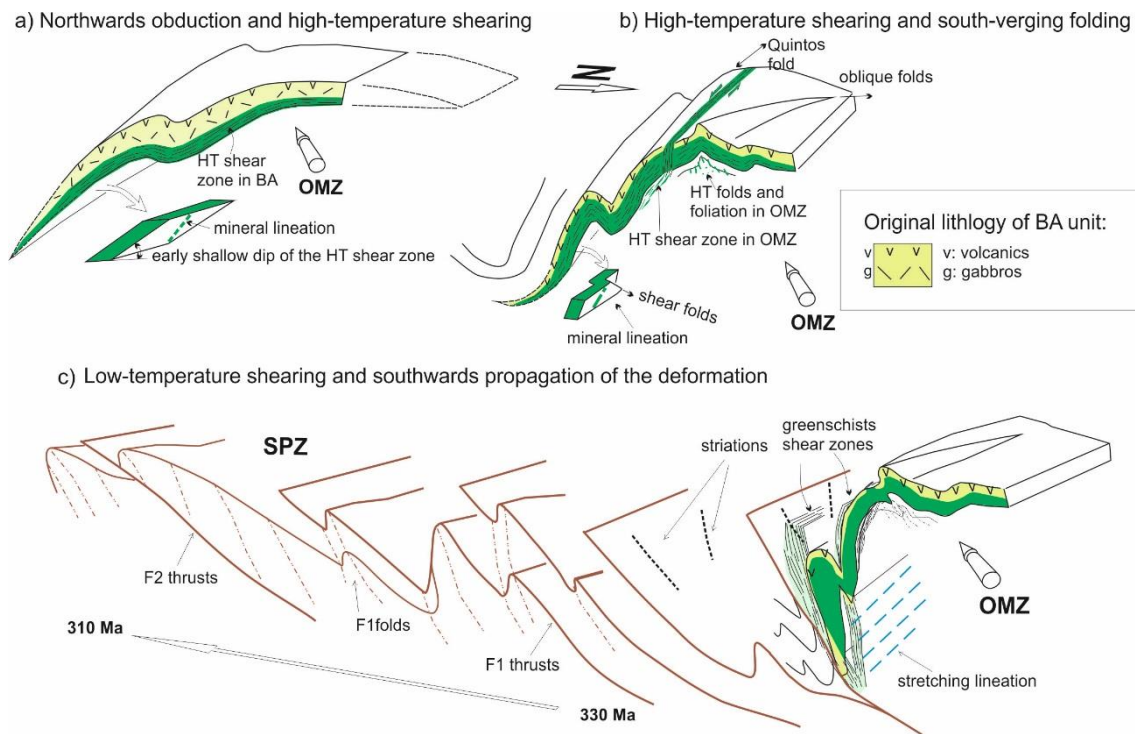
Figure 5.6. (a–c) Evolutionary model of the BA unit during the Carboniferous transpression, from northward obduction to southward propagation of the deformation. Modified from Pérez-Cáceres et al. (2015).

The evolution displayed in Fig. 5.6 (Pérez-Cáceres et al., 2015) indicates that the high-temperature fabric would have been developed when the shear zone had low dip, while the low-temperature one would have been formed in a steeper shear zone, as the Quintos fold was getting tighter. Accordingly, the transpression model of simple-inclined walls (Jones et al., 2004) provides with a possible explanation for the observed pitch variation: at an angle of convergence $\beta \approx 10°$ and a shortening S <0.2 (simple-shear-dominated transpressional zones), the model predicts pitch angles of 50°-60° when the dip of the shear zone is $20° \leq \delta \leq 30°$, and pitch angles of 10°-35° when the dip of the shear zone is $50° \leq \delta \leq 80°$.

Regardless of the transpression model considered, the left-lateral displacement due to the Southern Iberian shear zone cannot be accurately calculated. Assuming that the mafic layering corresponds to dykes intruded in gabbro (Quesada et al., 1994) and considering that layering and foliation are almost parallel, a $\gamma \geq 4$ can be proposed (simple shear). Considering that the maximum thickness of the BA unit is $\approx$ 2000 m across its ghost stratigraphy (metabasalts-gabbros-ultramafites), a plausible shear strain $\gamma = 5$ would correspond to a left-lateral displacement of only 10 km, which is a rather modest figure. Reasonably higher or lower values of γ would not result in greater regionally significant lateral displacements.

10. Deformation inside the SPZ

The SPZ is a fold-and-thrust belt made up of low-grade slates, metasandstones and metavolcanic rocks of Devonian to Carboniferous age (Fig. 5.7). The fold-and-thrust system is rooted in a detachment level located at the middle crust (IBERSEIS seismic

profile; Simancas et al., 2003). Deformation propagated southwards from the late Visean to Moscovian period (Oliveira, 1990). At the western part of the SPZ, its structural trend deviates from the common WNW-ESE trend, due to the influence of the N-S oriented Porto-Tomar dextral Fault (Ribeiro et al., 1980) (Fig. 5.1b). For this reason, we do not consider this western part in the following analysis.

Relevant features of the SPZ deformation include the following (Simancas, 1986) (i) The foliation trends N105°E and dips 50° to the north on average; (ii) The tectonic fabric is planar (S-tectonites), locally exhibiting a faint stretching lineation noticeable in pyroclastic rocks; S-L tectonites are observed only at localized thrust bands; (iii) When visible, the stretching lineation shows high-pitch angles of 65°-90°; (iv) Finite strain ellipsoids are oblate with the X axis always upright; (v) Folds axes display a remarkably variable plunging, with smooth curved hinges observed at outcrop (vi) Fold traces are slightly oblique clockwise with respect to the OMZ–SPZ boundary, thus suggesting left-lateral transpression.
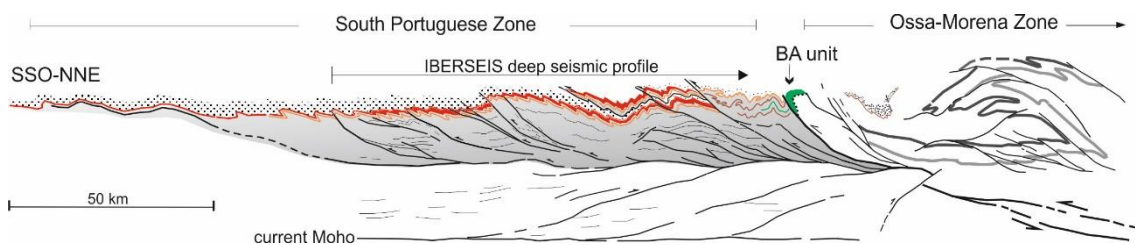
Figure 5.7. Schematic structural cross-section of the southern OMZ and SPZ (modified from Simancas et al., 2003). See Fig. 5.1c for location.

The deformation of the SPZ is partitioned into strain, buckle folds and thrusts at local scale, but considered as a whole it can be approximated to a bulk homogeneous deformation that can be analyzed in the light of a suitable transpressional model. In this respect, the northern wall of the SPZ transpressional zone is the currently steep Southern Iberian shear zone, the southern wall is loosely defined at the southernmost SPZ and the base of the transpressional zone is the mid-crustal detachment imaged in the IBERSEIS seismic section (Fig. 5.7). Furthermore, significant lateral escape of the deformed rock volume (Jones et al., 1997) can be rejected, since folds show smooth curved hinges. Finally, as the X finite strain axis roughly but consistently coincides with the dip direction, then the bulk strain symmetry may be considered approximately monoclinic (Lin et al., 1998, 1999). Thus, the boundary conditions of the SPZ fit reasonably well with those in the models of Sanderson and Marchini (1984), who factorized bulk strain into finite pure shearing followed by simple shearing, and Fossen and Tikoff (1993), who modeled simultaneous superposition of the strain components. The latter model is in general a more realistic way of modeling transpression, because in nature simultaneous superposition of shear components must be the rule. Nevertheless, the pure shear component probably diminishes as shortening increases, i.e., the ratio simple shear/pure shear would increase with increasing deformation, as it has been suggested for natural transpression zones (Dutton, 1997; Jiang, 2007). Actually, the evolution of the SPZ might have been of this type, as suggested by the fact that deformation ended with pure sinistral strike-slip faulting.

If this is the case, modeling natural deformation here by simultaneous superposition with constant simple shear/pure shear ratio is not obviously advantageous with respect to the finite factorization of pure shear followed by simple shear. Accordingly, we have modeled the bulk deformation of the SPZ as superposition of pure shear followed by simple shear (Sanderson and Marchini, 1984) the bulk shear strain thus obtained gives us the approximate value of the bulk left-lateral displacement (Fig. 5.8a).

Strain data from the SPZ have been projected in the finite strain grid of Sanderson and Marchini (1984) (Fig. 5.8b), suggesting a bulk transversal shortening of ≈ 40 % (α-1 ≈ 0.6) and a shear strain of γ ≈ 1 (bulk angular shear strain ψ = 45°). For the α-1 and γ values deduced above, the transpressional model used predicts that the long axis of the horizontal strain ellipse (map view) would be oriented at θ' = 18° with a vertical X strain axis, in reasonable agreement with the data (Fig. 5.8c). Thus, the bulk strain of the SPZ can be factorized into a transversal shortening of ≈ 40 % followed by a strike-slip shearing of γ ≈ 1 (ψ = 45°). Taking a ≈ 90 km width for the SPZ (excluding the less-deformed SW sector), that shear strain yields a left-lateral relative displacement of the OMZ with respect to the SPZ of ≈ 90 km. This finite strain factorization has been geometrically depicted in Fig. 5.8d. Modeling our data of the SPZ in terms of simultaneous superposition with constant simple shear/pure shear ratio (Fossen and Tikoff, 1993) does not yield significantly different results, but just a slightly higher bulk angular shear strain (ψ ≈ 50°).
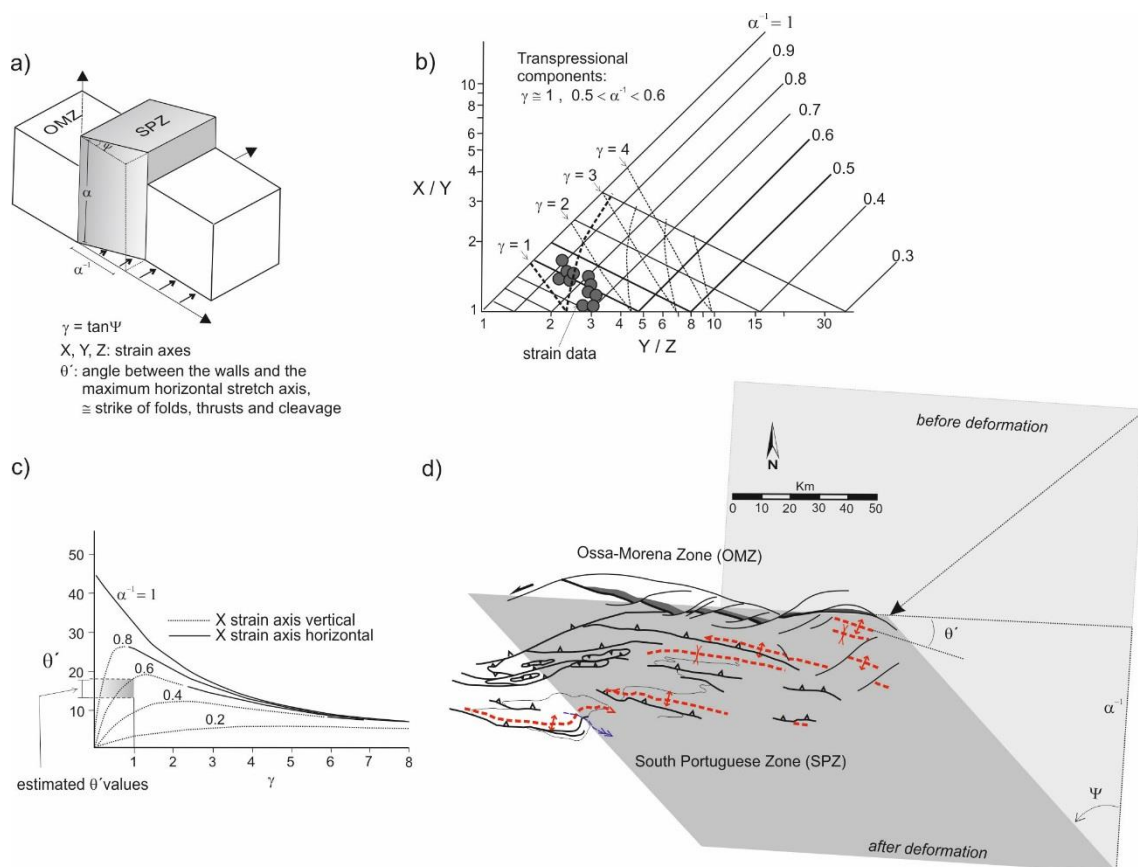
Figure 5.8. a) Transpressional model of Sanderson and Marchini (1984). b) Strain data from the SPZ suggest the values of shortening (α) and shearing (γ) according to this model. c) Angle between the boundary of the transpressional block and the maximum horizontal stretch axis, according to the estimated and values. d) Sketch of the eastern SPZ showing the transpressional deformation.

11. Brittle faulting

Left-lateral strike-slip faults characterize the late Variscan evolution of SW Iberia. These brittle structures concentrated at the northern and southerxn boundaries of the OMZ (Fig. 5.1c). The system of strike-slip faults at the CIZ–OMZ boundary was analyzed by Jackson and Sanderson (1992) based on a power-law distribution of fault displacements from outcrop to map scale. As a result, they evaluated 87 km of along-strike brittle displacement.

A well-organized left-lateral strike-slip fault system started to develop at the OMZ–SPZ boundary at Moscovian period, coeval with folding and thrusting deformation at the southwesternmost SPZ, as attested by syn-orogenic flysch deposits (Fig. 5.9; Oliveira, 1990). Two faulting stages can be differentiated (Simancas, 1983). First, two smoothly curved E–W oriented major faults divided the southernmost OMZ into three lens-shaped blocks, their summed slip accounting for 75 % (55-60 km) of the total slip of the left-lateral brittle faulting. These two faults concentrated the strike-slip component of the transpression, while simultaneous orthogonal shortening occurred at the southwesternmost SPZ (Carrapateira thrust; Ribeiro and Silva, 1983). The second faulting stage is characterized by a set of en échelon NE–SW shorter faults summing ≈ 20 km of slip. Thus, the total strike-slip of all the faults amounts to 80 km. This brittle shearing just preceded the attachment of the SPZ to the OMZ.
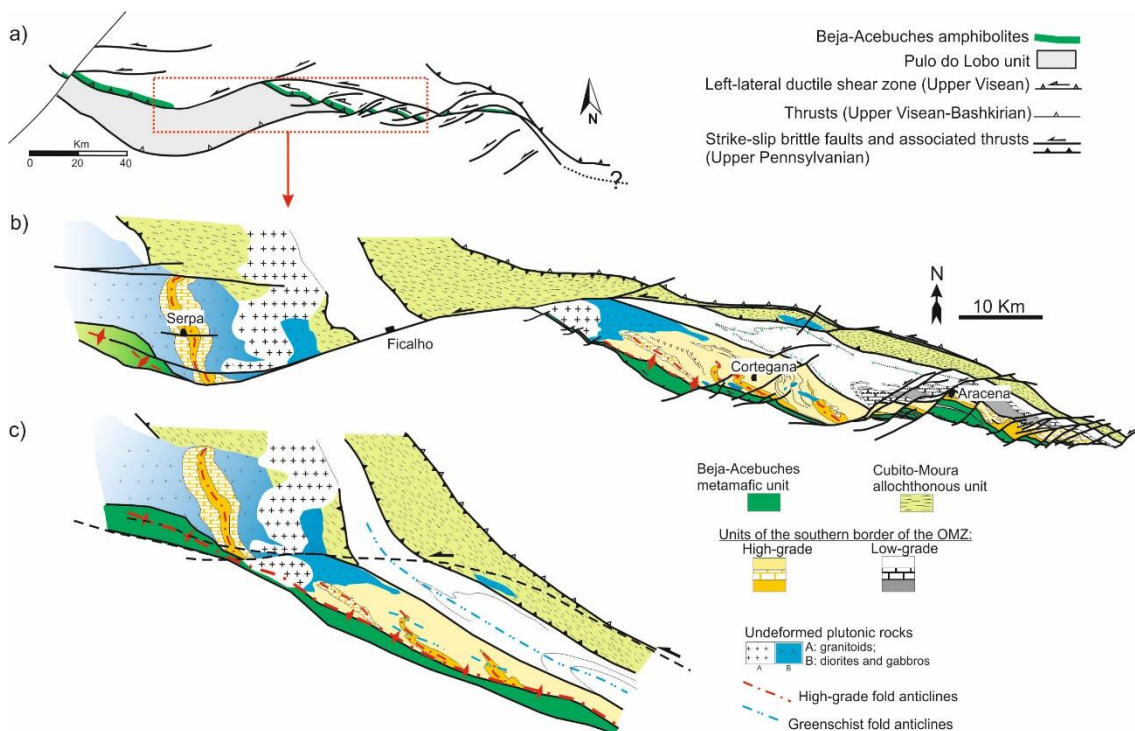
Figure 5.9. a) Schematic map of the main late Variscan faults affecting the OMZ–SPZ boundary. Compare with Fig. 1c for location. b) Map of the central part of the OMZ–SPZ boundary, showing the main Ficalho fault and the set of shorter faults affecting the Aracena–Cortegana sector. c) Reconstruction of this central part before the brittle faulting.

12. Discussion and conclusions

From Middle–Late Devonian to Pennsylvanian period, the collisional evolution of SW Iberia is characterized by oblique left-lateral convergence between three continental terranes: the CIZ (representing the northern margin of Gondwana), the OMZ (a fragment of the Gondwana margin) and the SPZ (the southern margin of Avalonia). Oblique convergence resulted in strain partitioning with the boundaries between the terranes accumulating preferentially the left-lateral component, and the interior of them exhibiting both orthogonal and lateral components of deformation.

12.1. The big numbers of SW Iberia Variscan transpression

This paper is the first attempt to evaluate regional left-lateral displacement in SW Iberia due to the oblique collision of continental terranes during the Variscan orogeny. We are aware of the approximate nature of our calculations, but we contend that the big numbers thus obtained have strong regional significance. As a synthesis, the quantification of the Variscan deformations in SW Iberia described above yields the following results, from north to south (Fig. 5.10):

(i) CIZ–OMZ boundary

- The ductile shearing that occurred in the BCSZ during the Upper Devonian-Mississippian period has been quantified to ≈ 150 km of left-lateral displacement, roughly parallel to the CIZ–OMZ boundary.

- The late Variscan strike-slip fault system that developed at the CIZ–OMZ boundary produced ≈ 85 km of left-lateral displacement parallel to this boundary.

(ii) Inner OMZ

- The Devonian SW-vergent folds and thrusts of the OMZ terrane might have accumulated ≈ 290 km of NE–SW-directed shortening with a left-lateral component parallel to the CIZ–OMZ boundary of ≈ 185 km.

- The Carboniferous upright folds of the OMZ terrane accumulated ≈ 80 km of NE-SW shortening with a left-lateral component parallel to the CIZ–OMZ boundary of ≈ 55 km.

- The rotation of the OMZ Carboniferous folds to a Z shape has been modeled as being due to left-lateral shearing plus with limited perpendicular shortening, thus resulting in ≈ 225 km of displacement subparallel to the OMZ boundaries.

The sum of left-lateral displacements due to Devonian and Carboniferous deformation inside the OMZ amounts to ≈ 465 km, according to the above data. However, plausible calculations yield lower values of ≈ 425 km and ≈ 355 km. Thus, we suggest an alternative value of ≈ 400 km.

(iii) OMZ–SPZ boundary

- The Devonian subduction/exhumation on the southern margin of the OMZ, as represented by the allochthonous Cubito-Moura unit, took place in a left-lateral setting that amounts to ≈ 140 km of displacement parallel to the OMZ–SPZ boundary.

- The displacement figures of the transtensional Early–Middle Mississippian stage that gave way to the BA oceanic-like realm cannot be evaluated, though this event most probably

occurred in a continued left-lateral tectonic setting. An alike scenario can be envisaged for the subsequent obduction of the BA unit, though with renewed transpression.

- The Southern Iberian shear zone that deformed the BA unit reveals ≈ 10 km of left-lateral displacement parallel to the OMZ–SPZ boundary.

- The late Variscan strike-slip fault system that developed at the OMZ–SPZ boundary produced ≈ 80 km of left-lateral displacement parallel to the boundary.

(iv) Inner SPZ

- The transpressional fold-and-thrust belt of the SPZ terrane produced ≈ 90 km of left-lateral displacement parallel to the OMZ–SPZ boundary with ≈ 60 km of orthogonal shortening.

The above numbers are estimations that must be considered as valuable but approximate to the real ones, given the variety of uncertainties in the kinematic analysis performed.
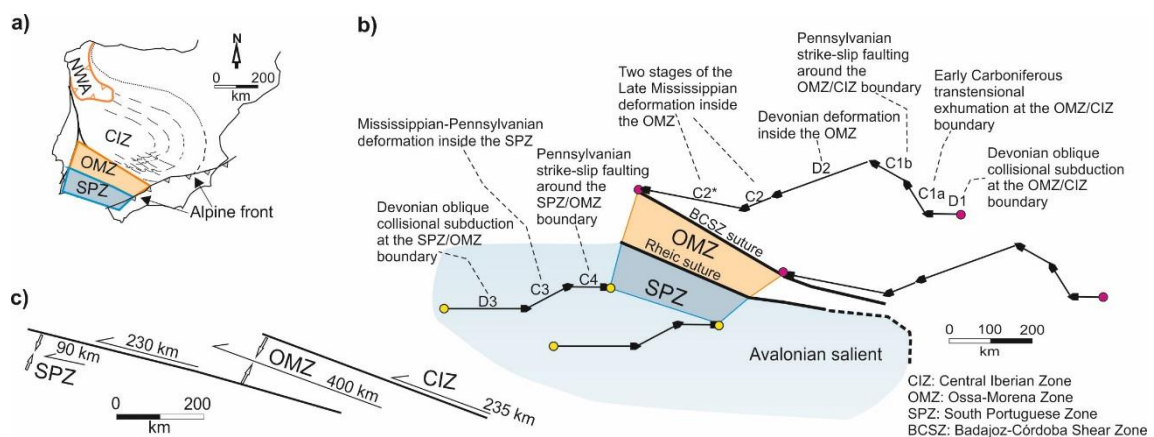
Figure 10. a) Sketch of the Iberian Massif with location of the CIZ, OMZ, SPZ and the NW Iberia allochthon (NWA). b) Vectors showing the relative displacements between the southern Iberia terranes, according to our calculations. c) Sketch emphasizing the left-lateral displacements parallel to terrane boundaries.

12.2. Relative displacements of SW Iberian terranes

Considered altogether, the total collisional convergence recorded in SW Iberia is E–W-oriented and surpasses 1000 km. The left-lateral component parallel to terrane boundaries is estimated to be ≈ 1000 km, half of which accumulated as strike-slip shearing at the two suture boundaries (Fig. 5.10c). This main conclusion brings up an image of the paleoposition of SW Iberian continental terranes just before the Devonian–Carboniferous Variscan collision. The remarkable left-lateral oblique kinematics during the Variscan plate convergence in SW Iberia, as opposed to the dominant right-lateral kinematics of the Variscan/Alleghanian orogen (Fig. 5.1a), is also inferred from our kinematic analysis. We interpret that the reason for the singular kinematics of SW Iberia is the existence of an Avalonian salient, currently represented by the SPZ (Fig. 5.1a and 5.10b).

Finally, it is important to emphasize that in-between these regions with opposite kinematics (left-lateral oblique convergence in SW Iberia and right-lateral oblique convergence in

central Europe), an intermediate one with rather orthogonal convergence must have existed (Fig. 5.1a), which would had to accommodate the > 1000 km of collisional convergence evaluated above. In NW Iberia, a major unrooted allochthonous pile with continental and oceanic-like units has been described for the para-autochthonous CIZ (Martínez Catalán et al., 1997). Thus, NW Iberia may represent this intermediate region with orthogonal collision.

Acknowledgements

References

Abalos, B., Gil Ibarguchi, J.I. and Eguiluz, L.: Cadomian subduction/collision and Variscan transpression in the Badajoz-Córdoba shear belt, southwest Spain. Tectonophysics, 199, 51-72, 1991.

Araújo, A., Fonseca, P., Munhá, J., Moita, P., Pedro, J. and Ribeiro, A.: The Moura Phyllonitic Complex: An accretionary complex related with obduction in the southern Iberia Variscan suture. Geodinamica Acta, 18, 375-388, 2005.

Azor, A., González Lodeiro, F. and Simancas, J.F.: Tectonic evolution of the boundary between the Central Iberian and Ossa-Morena zones (Variscan Belt, southwest Spain). Tectonics, 13, 45-61, 1994.

Azor, A., Rubatto, D., Simancas, J.F., González Lodeiro, F., Martínez Poyatos, D., Martín Parra, L.M. and Matas, J.: Rheic Ocean ophiolitic remnants in Southern Iberia questioned by SHRIMP U-Pb zircon ages on the Beja-Acebuches amphibolites. Tectonics, 27, TC5014, doi: 10.1029/2009TC002527, 2008.

Bandrés, A., Eguiluz, L., Pin, C., Paquette, J.L., Ordóñez, B., Le Fèvre, B., Ortega, L.A. and Gil Ibarguchi, J.I.: The northern Ossa-Morena Cadomian batholith (Iberian Massif): magmatic arc origin and early evolution. International Journal of Earth Sciences, 93, 860-885, 2004.

Bard, J.P.: Signification tectonique des métatholeites d'affinité abyssale de la ceinture de basse pression d'Aracena (Huelva, Espagne). Bulletin de la Société géologique de France, 19, 385-393, 1977.

Booth-Rea, G., Simancas, J.F., Azor, A., Azañón, J.M., Gonzalez Lodeiro, F. and Fonseca, P.: HP-LT Variscan metamorphism in the Cubito-Moura schists (Ossa-Morena Zone, southern Iberia). Comptes Rendus Geoscience, 338, 1260-1267, 2006.

Braid, J.A., Murphy, J.B. and Quesada, C.: Structural analysis of an accretionary prism in a continental collisional setting, the Late Paleozoic Pulo do Lobo Zone, Southern Iberia. Gondwana Research, 17, 422-439, 2010.

Burg, J.P., Iglesias, M., Laurent, P., Matte, P. and Ribeiro, A.: Variscan intracontinental deformation: the Coimbra-Córdoba Shear zone (SW Iberian Peninsula). Tectonophysics, 78, 161-177, 1981.

Castro, A., Fernández, C., De la Rosa J.D., Moreno Ventas, I. and Rogers, G.: Significance of MORB-derived amphibolites from the Aracena metamorphic belt, southwest Spain. Journal of Petrology, 37, 235-260, 1996.

Castro, A., Fernández, C., El-Hmidi, H., El-Biad, M., Díaz-Azpiroz, M., De la Rosa, J. and Stuart, F.: Age constraints to the relationships between magmatism, metamorphism and tectonism in the Aracena metamorphic belt, southern Spain. International Journal of Earth Sciences, 88, 26-37, 1999.

Crespo-Blanc, A.: Evolución geotectónica del contacto entre la zona de Ossa-Morena y la zona Surportuguesa en las sierras de Aracena y Aroche (Macizo Ibérico Meridional): Un contacto mayor en la cadena Hercínica Europea. Ph. D. Thesis, Univ. de Granada, 327 pp, 1991.

Crespo-Blanc, A.: Structure and kinematics of a sinistral transpressive suture between the Ossa-Morena and the South Portuguese Zones, South Iberian Massif. Journal of the Geological Society, London, 149, 401-411, 1992.

Crespo-Blanc, A. and Orozco, M.: The southern Iberian shear zone: a major boundary in the Hercynian folded belt. Tectonophysics, 148, 221-227, 1988.

Czeck, D.M. and Hudleston, P.J.: Testing models for obliquely plunging lineations in transpression: a natural example and theoretical discussion. Journal of Structural Geology, 25, 959-982, 2003.

Czeck, D.M. and Hudleston, P.J.: Physical experiment of vertical transpression with localized non vertical extrusion. Journal of Structural Geology, 26, 573-581, 2004.

Dahn, D.R.L., Braid, J.A., Murphy, J.B., Quesada, C., Dupuis, N. and McFarlane, C.R.M.: Geochemistry of the Peramora Melange and Pulo do Lobo schist: geochemical investigation and tectonic interpretation of mafic melange in the Pangean suture zone, Southern Iberia. International Journal Earth Sciences, 103, 1415-1431, 2014.

Dallmeyer, R.D., Fonseca, P.E., Quesada, C. and Ribeiro, A.: $^{40}Ar/^{39}Ar$ Mineral age constraints for the Tectonothermal Evolution of a Variscan Suture in Southwest Iberia. Tectonophysics, 222, 177-194, 1993.

Dewey, J., Holdsworth, R.E. and Strachan, R.A.: Discussion on transpression and transtension zones. Journal of Geological Society of London, 156, 1048-1050, 1999.

Dias, R. and Ribeiro, A.: Constriction in a transpressive regime: an example in the Iberian branch of the Ibero-Armorican Arc. Journal of Structural Geology, 16, 1545-1554, 1994.

Díaz-Azpiroz, M. and Fernández, C.: Kinematic analysis of the southern Iberian shear zone and tectonic evolution of the Acebuches metabasites (SW Variscan Iberian Massif). Tectonics, 24, TC3010, doi: 10.1029/2004TC001682, 2005.

Dutton, B.J.: Finite strains in transpression zones with no boundary slip. Journal of Structural Geology, 19, 1189-1200, 1997.

Eden, C.P.: Tectonostratigraphic analysis of the northern extent of the oceanic exotic terrane, Northwestern Huelva Province, Spain. Ph. D. Thesis, Univ. of Southampton, 214 pp, 1991.

Eden, C. and Andrews, J.: Middle to upper Devonian melanges in SW Spain and their relationship to the Meneage formation in south Cornwall. Proceedings of the Ussher Society, 7, 217-222, 1990.

Ellis, M.A. and Watkinson, A.J: Reply on "Orogen-parallel extension and oblique tectonics: The relation between stretching lineations and relative plate motions. Geology, 16, 857-861, 1988.

Expósito, I.: Evolución estructural de la mitad septentrional de la Zona de Ossa-Morena y su relación con el límite Zona de Ossa Morena/Zona Centroibérica. Ph. D. Thesis, Univ. de Granada, 296 pp, 2000.

Expósito, I., Simancas, J.F., González Lodeiro, F., Azor, A. and Martínez Poyatos, D.: Estructura de la mitad septentrional de la zona de Ossa-Morena: Deformación en el bloque inferior de un cabalgamiento cortical de evolución compleja. Revista de la Sociedad Geológica de España, 15, 3-14, 2002.

Fernández, C. and Díaz-Azpiroz, M.: Triclinic transpression zones with inclined extrusion. Journal of Structural Geology, 31, 1225-1269, doi: 10.1016/j.jsg.2009.07.001, 2009.

Fernández, C., Czeck, D.M. and Díaz-Azpiroz, M.: Testing the model of oblique transpression with oblique extrusion in two natural cases: Steps and consequences. Journal of Structural Geology, 54, 85-102, doi: 10.1016/j.jsg.2013.07.001, 2013.

Fonseca, P. and Ribeiro, A.: Tectonics of the Beja-Acebuches Ophiolite - a Major Suture in the Iberian Variscan Foldbelt. Geologische Rundschau, 82, 440-447, 1993.

Fonseca, P., Munhá, J., Pedro, J., Rosas, F., Moita, P., Araújo A. and Leal, N.: Variscan ophiolites and high-pressure metamorphism in southern Iberia. Ofioliti, 24, 259-268, 1999.

Fossen, H. and Tikoff, B.: The deformation matrix for simultaneous simple shearing, pure shearing and volume change, and its application to transpression-transtension tectonics. Journal of Structural Geology, 15, 413-422, 1993.

Franke, W.: The mid-European segment of the Variscides: Tectonostratigraphic units, terrane boundaries and plate tectonic evolution. In: Orogenic Processes: Quantification and Modelling in the Variscan Belt, edited by W. Franke, V. Haak, O. Oncken and D. Tanner. Geological Society of London Special Publications, 179, 35-61, 2000.

Gómez-Pugnaire, M.T., Azor, A., Fernández-Soler, J.M. and López Sánchez-Vizcaíno, V.: The amphibolites from the Ossa-Morena/Central Iberian Variscan suture (southwestern Iberian Massif): Geochemistry and tectonic interpretation. Lithos, 68, 23-42, 2003.

Harland, W.B.: Tectonic transpression in caledonian Spitsbergen. Geological Magazine, 108, 27-41. 1971.

Holdsworth, R.E. and Strachan, R.A.: Interlinked system of ductile strike slip and thrusting formed by Caledonian sinistral transpression in northeastern Greenland. Geology, 19, 510-513, 1991.

Jackson, P. and Sanderson, D.J.: Scaling of fault displacements from the Badajoz-Cordoba shear zone, SW Spain. Tectonophysics, 210, 179-190, 1992.

Jiang, D.: Sustainable transpression: An examination of strain and kinematics in deforming zones with migrating boundaries. Journal of Structural Geology, 29, 1984-2005, doi: 10.1016/j.jsg.2007.09.007, 2007.

Jiang, D. and Williams, P.F.: High-strain zones: a unified model. Journal of Structural Geology, 20, 1105-1120, 1998.

Jones, R.R., Holdsworth, R.E. and Bailey, W.: Lateral extrusion in transpression zones; the importance of boundary conditions. Journal of Structural Geology, 19, 1201-1217, 1997.

Jones, R.R., Holdsworth, R.E., Clegg, P., McCaffrey, K. and Tavarnelli, E.: Inclined transpression. Journal of Structural Geology, 26, 1531-1548, 2004.

Lin, S., Jiang, D. and Williams, P.F.: Transpression (or transtension) zones of triclinic symmetry: natural example and theoretical modelling. In: Continental Transpression and Transtension

Tectonics, edited by R.E. Holdsworth, R.A. Strachan, and J.F. Dewey. Geological Society of London Special Publications, 135, 41-57, 1998.

Lin, S., Jiang, D. and Williams, P.F.: Discussion on transpression and transtension zones. Journal of Geological Society of London, 156, 1045-1048, 1999.

Linnemann, U., Gehmlich, M., Tichomirowa, M., Buschmann, B., Nasdala, L., Jonas,P., Lützner, H. and Bombach, K.: The Cadomian Orogen: Neoproterozoic to Early Cambrian crustal growth and orogenic zoning along the periphery of the West African Craton - Constraints from U-Pb zircon ages and Hf isotopes (Schwarzburg Antiform, Germany). Precambrian Research, 244, 263-278: 2014.

López Sánchez-Vizcaíno, V., Gómez Pugnaire, M.T., Azor, A. and Fernández Soler, J.M.: Phase diagram sections applied to amphibolites: a case study from the Ossa-Morena/Central Iberian Variscan suture (Southwestern Iberian Massif). Lithos, 68, 1-21, 2003.

Martínez Catalán, J.R., Arenas, R., Díaz García, F. and Abati, J.: Variscan accretionary complex of northwest Iberia: terrane correlation and succession of tectonothermal events. Geology, 25, 1103-1106, 1997.

Martínez Poyatos, D.: Estructura del borde meridional de la Zona Centroibérica y su relación con el contacto entre las Zonas Centroibérica y de Ossa-Morena. Ph. D. Thesis, Univ. de Granada, 295 pp, 1997.

Matte, P.: Accretionary history and crustal evolution of the Variscan belt in Western Europe. Tectonophysics, 196, 309-337, 1991.

Matte, P.: The Variscan collage and orogeny (480-290 Ma) and the tectonic definition of the Armorica microplate: a review. Terra Nova, 13, 122-128, 2001.

Munhá, J., Oliveira, J.T., Ribeiro, A., Oliveira, V., Quesada, C. and Kerrich, R.: Beja-Acebuches ophiolite, characterization and geodynamic significance. Boletim da sociedade Geologica de Portugal, Maleo, 2, 31, 1986.

Murphy, J.B. and Nance, R.D.: A supercontinent model for the contrasting character of Late Proterozoic orogenic belts. Geology, 9, 469-472, 1991.

Oliveira, J.T.: Part VI: South Portuguese Zone, stratigraphy and synsedimentary tectonism. In: Pre-Mesozoic Geology of Iberia, edited by R.D. Dallmeyer and E. Martínez García. Springer, 334-347, 1990.

Ordóñez-Casado, B.: Geochronological Studies of the Pre-Mesozoic Basement of the Iberian Massif: The Ossa-Morena Zone and the Allochthonous Complexes within the Central Iberian Zone. Ph. D. Thesis, ETH, Zürich, 235 pp, 1998.

Pereira, M.F., Apraiz, A., Chichorro, M., Silva, J.B. and Armstrong, R.A.: Exhumation of high pressure rocks in northern Gondwana during the Early Carboniferous (Coimbra-Cordoba shear zone, SW Iberian Massif): tectonothermal analysis and U-Th-Pb SHRIMP in-situ zircon geochronology. Gondwana Research, 17, 440-460, 2010.

Pérez-Cáceres, I., Martínez Poyatos, D., Simancas, J.F. and Azor, A.: The elusive nature of the Rheic Ocean suture in SW Iberia. Tectonics 34, 2429-2450, doi: 10.1002/2015TC003947, 2015.

Pin, C., Liñán, E., Pascual, E., Donaire, T. and Valenzuela, A.: Late Neoproterozoic crustal growth in the European Variscides: Nd isotope and geochemical evidence from the Sierra de Córdoba Andesites (Ossa-Morena Zone, Southern Spain). Tectonophysics, 352, 133-151, 2002.

Ponce, C., Simancas, J.F., Azor, A., Martínez Poyatos, D., Booth-Rea, G. and Expósito, I.: Metamorphism and kinematics of the early deformation in the Variscan suture of SW Iberia. Journal of Metamorphic Geology, 30, 625-638, 2012.

Quesada, C. and Dallmeyer, R.D.: Tectonothermal evolutionof the Badajoz-Córdoba shear zone (SW Iberia): characteristics and $^{40}Ar/^{39}Ar$ mineral age constraints. Tectonophysics, 231, 195-213, 1994.

Quesada, C., Fonseca, P.E., Munhá, J., Oliveira J.T. and Ribeiro, A.: The Beja-Acebuches Ophiolite (Southern Iberia Variscan fold belt): geological characterization and significance. Boletín Geológico y Minero, 105, 3-49, 1994.

Ramsay, J.G. and Huber, M.I.: The Techniques of Modern Structural Geology, vol. 2, Folds and Fractures. Springer, 393 pp, 1987.

Ribeiro, A. and Silva, J.B.: Structure of the South Portuguese Zone. In: The Carboniferous of Portugal, edited by M.J.L. Sousa, J.T. Oliveira. Memória dos Serviços Geológicos de Portugal, 29, 83-89, 1983.

Ribeiro, A., Pereira, E. and Severo, L.: Análise da deformaçao da zona de cisalhament Porto-Tomar na transversal de Oliveira de Azeméis. Comunicações dos Serviços Geológicos de Portugal, 66, 3-9, 1980.

Robardet, M.: Alternative approach to the Variscan Belt in southwestern Europe: pre-orogenic paleobiogeographical constraints. In: Variscan-Appalachian Dynamics: The Building of the Late Paleozoic Basement, edited by J.R. Martínez Catalán, R. Hatcher, R. Arenas, F. Díaz García. Geological Society of America Special Paper, 364, 1-15, 2002.

Robin, P.Y.F. and Cruden, A.R.: Strain and vorticity patterns in ideally ductile transpressional zones. Journal of Structural Geology, 16, 447-466, 1994.

Rodríguez-Alonso, M.D., Peinado, M., López-Plaza, M., Franco, P., Carnicero, A. and Gonzalo, J.C.: Neoproterozoic-Cambrian synsedimentary magmatism in the Central Iberian Zone (Spain): geology, petrology and geodynamic significance. International Journal of Earth Sciences, 93, 897-920, 2004.

Rubio Pascual, F.J., Matas, J. and Martín Parra, L.M.: High-pressure metamorphism in the Early Variscan subduction complex of the SW Iberian Massif. Tectonophysics, 592, 187-199, 2013.

Sánchez Carretero, R., Eguiluz, L., Pascual, E. and Carracedo, M.: Ossa-Morena Zone: Igneous rocks. In: Pre-Mesozoic Geology of Iberia, edited by R.D. Dallmeyer, E. Martínez García. Springer, 292-313, 1990.

Sanderson, D.J. and Marchini, W.R.D.: Transpression. Journal of Structural Geology, 6, 449-458, 1984.

Shelley, D. and Bossière, G.: A new model for the Hercynian Orogen of Gondwanan France and Iberia. Journal of Structural Geology 22(6), 757-776, 2000.

Silva, J.B., Oliveira, J.T. and Ribeiro, A.: South Portuguese Zone, estructural outline. In: Pre-Mesozoic Geology of Iberia, edited by R.D. Dallmeyer, E. Martínez García. Springer, 348-362, 1990.

Silva, J.B. and Pereira, M.F.: Transcurrent continental tectonics model for the Ossa-Morena Zone Neoproterozoic-Paleozoic evolution, SW Iberian Massif, Portugal. International Journal of Earth Sciences, 93, 886-896, 2004.

Simancas, J.F.: Geología de la Extremidad Oriental de la Zona Sudportuguesa. Ph. D. Thesis, Univ. de Granada, 439 pp, 1983.

Simancas, J.F.: La deformación en el sector oriental de la zona Surportuguesa. Boletín Geológico y Minero, 82, 239-268, 1986.

Simancas, J.F., Martínez Poyatos, D., Expósito, I., Azor, A. and González Lodeiro, F.: The structure of a major suture zone in the SW Iberian Massif: the Ossa-Morena/Central Iberian contact. Tectonophysics, 332, 295-308, 2001.

Simancas, J.F., Carbonell, R., González Lodeiro, F., Pérez-Estaún, A., Juhlin, C., Ayarza, P., Kashubin, A., Azor, A., Martínez Poyatos, D., Almodóvar, G.R., Pascual, E., Sáez, R. and Expósito, I.: Crustal structure of the transpressional Variscan orogen of SW Iberia: SW Iberia deep seismic reflection profile (IBERSEIS). Tectonics 22, 1062, doi: 10.1029/2002TC001479, 2003.

Simancas, J.F., Expósito, I., Azor, A., Martínez Poyatos, D. and González Lodeiro, F.: From the Cadomian orogenesis to the Early Palaeozoic Variscan rifting in Southwest Iberia. Journal of Iberian Geology 30, 53-71, 2004.

Simancas, J.F., Tahiri, A., Azor, A., González Lodeiro, F., Martínez Poyatos, D. and El Hadi, H.: The tectonic frame of the Variscan-Alleghanian orogen in southern Europe and northern Africa. Tectonophysics, 398, 181-198, 2005.

Stampfli, G.M. and Borel G.D.: A plate tectonic model for the Paleozoic and Mesozoic constrained by dynamic plate boundaries and restored synthetic oceanic isochrones. Earth and Planetary Science Letters, 196, 17-33, 2002.

Teyssier, C. and Tikoff, B.: Fabric stability in oblique convergence and divergence. Journal of Structural Geology, 21, 969-974, 1999.

Teyssier, C., Tikoff, B. and Markley, M.: Oblique plate motion and continental tectonics. Geology, 23, 447-450, 1995.

Tikoff, B. and Fossen, H.: Three-dimensional deformations and strain facies. Journal of Structural Geology, 21, 1497-1512, 1999.

Tikoff, B. and Teyssier, C.: Strain modeling of displacement-field partitioning in transpressional orogens. Journal of Structural Geology, 16, 1575-1588. 1994.

Chapter VI

Conclusions

This last chapter summarizes the main findings already exposed in detail in the previous ones, with the purpose of underlining the main contributions of this Thesis. The Variscan tectonometamorphic evolution of SW Iberia has been studied by applying different approaches to particular units of the region, in combination with all of the available data. Special attention has been paid to the boundary between the Ossa-Morena Zone and the South Portuguese Zone, and this has resulted in challenging previous interpretations.

Regarding the Neoproterozoic to Paleozoic tectonics of SW Iberia:

(1) A compilation of all the available pre-Cryogenian inherited zircons in SW Iberian and related terranes has enabled the proposal of a large-scale tectonic/paleogeographic evolution of northern Gondwana from Neoproterozoic to Paleozoic times. This model is based on the examination of sectors containing only Paleoproterozoic zircon populations (derived from West Africa) or both Paleo- and Mesoproterozoic ones (Fig. 2.9). The juxtaposition of West Africa derived terranes (e.g. OMZ, and southernmost CIZ) with East Africa derived terranes (e.g. the rest of CIZ, WALZ, and CZ) was due to a dominant dextral shear zone subparallel to the Cadomian subduction along northern Gondwana. This dextral shear zone would result from deformation partitioning of the oblique Cadomian subduction (Fig. 2.10).

Regarding the characterization and evolution of the tectonic units around the OMZ/SPZ boundary:

(2) A good deal of inherited detrital zircons from metasediments of the northern SPZ were dated (SHRIMP U/Pb) to constrain maximum depositional ages and explore provenance sources (pre-Variscan paleogeographic affinity). The supposed Avalonian affinity of the SPZ cannot unambiguously be tested based on this method because the rocks that would attest the drifting from Gondwana (Ordovician-Silurian) do not crop out in the SPZ. Nevertheless, the obtained inherited zircon populations still provide with some arguments in favor of that hypothesis. Particularly, the latest Devonian Horta da Torre formation (northernmost Pulo do Lobo unit) shows abundant Mesoproterozoic and Caledonian zircon populations, implying a nearby Avalonian-type (Amazonian-Baltican) foreland; thus, this formation can be considered as the only "exotic" formation in the SPZ. On the other hand, the similar zircon content of the Ribeira de Limas formation (Pulo do Lobo unit) and the Ronquillo formation (Iberian Pyrite unit), together with their similar age, lithology and polyphasic deformation, make them correlatable and extends the Pulo do Lobo unit further east. Moreover, a close similarity in detrital zircon content has been also found between the Santa Iría formation (Pulo do Lobo unit) and the PQ formation (Iberian Pyrite unit), both featuring a Variscan volcanic arc missing at outcrop but denoted by a 365-375 Ma zircon population.

(3) The new Mississippian protolith ages ($\approx$340-335 Ma; SHRIMP U/Pb on zircons) obtained from low-grade MORB-featured metamafic rocks of the Pulo do Lobo force a reinterpretation of the Peramora Mélange (previously considered as a Rheic subduction-related accretionary prism), since regional data support that the Rheic Ocean had already disappeared in the Upper Devonian and collision had already started. Together with the Beja-Acebuches Amphibolite (BAA) unit, with similar protolith ages ($\approx$340-335 Ma; SHRIMP U/Pb on zircons), this mafic magmatism is now interpreted in the context of an

Early Carboniferous intraorogenic transtensional event that temporally interrupted the Variscan collision (Fig. 3.4).

(4) The structure of the BAA unit has been characterized as a kilometer-scale south-vergent synmetamorphic fold mapped in Portugal (Fig. 3.9), whose inverted limb is mainly represented by the outcropping segment of this unit in Spain. Prior to folding, the BAA unit obducted northwards onto the southern OMZ, in connection with north-vergent folding in the Pulo do Lobo unit. These north-vergent structures represent the first Carboniferous deformation after the intraorogenic transtensional event. The folding of the BAA unit was coeval to high- to low-temperature left-lateral shearing that dismembered the amphibolites into variable-sized lozenges separated by low-grade shear zones and faults (Fig. 3.8). New protolith ages obtained from deformed metavolcanic rocks (SHRIMP U/Pb on zircons) constrain at 337 ± 3 Ma the maximum age for the low-temperature metamorphism. The BAA folding was the starting point of the southwards migration of the middle/late Carboniferous deformation in the SPZ (Fig. 3.14).

(5) Structural analysis in the Pulo do Lobo unit shows a complex Variscan evolution. The Devonian lower formations are affected by three penetrative deformation phases; these formations are unconformably covered by the latest Devonian to Mississippian upper formations, where only the last two deformation phases are recognized. The third deformation in the Pulo do Lobo unit produced upright to south-vergent folds that propagated southwards through the SPZ; the second deformation produced north-vergent folds, while the first foliation appears only at small-scale microcrenulated at high angles with respect to the second foliation (Fig. 3.11). The lower formations of the Pulo do Lobo unit show striking similarities when compared with those of similar age in the Iberian Pyrite unit located to the south in the inner SPZ, thus undermining the previous interpretation of the Pulo do Lobo unit as exotic with respect to the SPZ.

(6) A multidisciplinary study (X-Ray diffraction, EPMA compositional maps and chlorite thermometry, and Raman spectrometry of carbonaceous matter) has been performed on the very low- to low-grade metasediments of the Pulo do Lobo unit. Two metamorphic events have been recognized in relation to the two older regional foliations. The first event (Devonian) occurred at epizone conditions, while the second (middle/late Carboniferous) did not exceed anchizone/epizone boundary conditions. The white-mica b parameter and celadonite content indicate low-pressure gradients that conflict with the classical interpretation of the Pulo do Lobo unit as a subduction-related accretionary prism.

Regarding the kinematics of the collisional deformation in SW Iberia:

(7) The dominant left-lateral oblique kinematics inferred for the whole Variscan evolution of SW Iberia, opposite to the right-lateral kinematics dominant elsewhere in the orogen, has been roughly quantified. The Variscan transpressional displacements in the SW Iberian terranes and suture units have been estimated by applying simple calculations and transpressional models. The Devonian to Carboniferous oblique convergence between the SW Iberia terranes may have surpassed 1000 km along an approximate E-W direction (present-day coordinates). The zone boundaries (CIZ/OMZ and OMZ/SPZ) accumulated preferentially the left-lateral component, while the major part of the frontal shortening occurred at the interior of the zones (Fig. 5.10).

Regarding the evolution and significance of the OMZ/SPZ boundary:

(8) The new structural, metamorphic and geochronological data reported in this Thesis, together with other robust information from previous works, partially confirm the previous interpretations proposed by some authors on the Variscan evolution of the OMZ/SPZ boundary, though some issues have been reinterpreted. Accordingly, the main landmarks of this evolution are as follows (Fig. 5.2): (i) After closing the Rheic Ocean, the Variscan collisional evolution at the OMZ/SPZ boundary is characterized by two stages of left-lateral transpression separated by a Mississippian transtensional and magmatic stage. (ii) No clear evidence supports the interpretation of the Pulo do Lobo unit as an exotic Rheic subduction-related accretionary prism; instead, the Pulo do Lobo unit most probably represents a detritic platform at the northern part of the SPZ, which started to deform in Late Devonian time. (iii) As a consequence of the imprints due to the Mississippian transtensional and magmatic event and the subsequent complex Carboniferous transpression, the Rheic suture in SW Iberia has a very obscure, nearly cryptic appearance.

Conclusiones

Este capítulo recopila los principales resultados expuestos detalladamente en los capítulos precedentes, con el propósito de destacar las contribuciones principales de esta Tesis. Se ha estudiado la evolución tectonometamórfica del SO de Iberia aplicando metodologías variadas a unidades particulares de esta región. Se ha prestado especial atención al límite entre las zonas de Ossa-Morena (ZOM) y Sudportuguesa (ZSP).

Respecto a la evolución tectónica Neoproterozoica a Paleozoica del SO de Iberia:

(1) La compilación de todas las edades de circones heredados pre-Criogénicos del SO de Iberia y regiones colindantes ha permitido proponer una evolución tectono-paleogeográfica a gran escala del norte de Gondwana durante el Neoproterozoico y Paleozoico. Este modelo se basa en el estudio de sectores que contienen solo poblaciones de circones paleoproterozoicas (procedentes del Cratón de África Occidental) frente a los que contienen paleo- y mesoproterozoicas (Fig. 2.9). La yuxtaposición de terrenos derivados de África occidental (e.g. la ZOM y la parte meridional de la Zona Centro Ibérica; ZCI) con terrenos derivados de África oriental (e.g. el resto de la ZCI, la Zona Astur-occidental Leonesa y la Zona Cantábrica) se considera debida a un cizallamiento dextro subparalelo a la zona de subducción cadomiense existente a lo largo del borde norte de Gondwana. Este cizallamiento dextro resultaría de la partición de la deformación debido a la componente de la subducción oblicua cadomiense (Fig. 2.10).

Respecto a la caracterización y evolución de las unidades tectónicas del límite ZOM/ZSP:

(2) Se ha datado (SHRIMP U/Pb) una gran cantidad de circones detríticos de los metasedimentos devónicos y carboníferos de la parte norte de la ZSP para obtener edades máximas de sedimentación y examinar las fuentes de procedencia (afinidad paleogeográfica pre-Varisca). La supuesta afinidad avaloniana de la ZSP no puede verificarse de forma fehaciente mediante este método, dado que las rocas que atestiguarían la separación entre Avalonia y Gondwana (Ordovícico-Silúrico) no afloran en la ZSP. No obstante, los datos obtenidos muestran algunos argumentos a favor de esta hipótesis. En especial, la formación Horta da Torre del Devónico Superior (que aflora en la parte septentrional de la unidad Pulo do Lobo) muestra abundantes circones mesoproterozoicos y caledonianos, lo que implica una fuente cercana de tipo avaloniano (Amazonia-Báltica). Por lo tanto, esta formación puede considerarse como la única realmente "exótica" con respecto a la ZSP. Por otro lado, los resultados similares en edades de circones en la formación Ribeira de Limas (unidad Pulo do Lobo) y en la formación Ronquillo (Faja Pirítica Ibérica), a la vez que sus similitudes en edad de sedimentación, litología y deformación polifásica, hace que estas dos formaciones sean correlacionables y que la unidad Pulo do Lobo se extienda más hacia el este. Además, también existe similitud en el contenido de circones detríticos de las formaciones Santa Iría (unidad Pulo do Lobo) y PQ (Faja Pirítica Ibérica), y ambas avalan la existencia de un arco volcánico Varisco (con circones de 365-375 Ma) que no afloría.

(3) Se han obtenido nuevas edades de protolitos (≈340-335 Ma; SHRIMP U/Pb en circones) en rocas metamáficas de afinidad MORB de la unidad Pulo do Lobo. Estos datos hacen necesaria una reinterpretación de la Mélange de Peramora (previamente considerada como un prisma de acreción relacionado con la subducción del Océano Rheico), ya que en

el Devónico Superior el Océano Rheico ya había al haber comenzado ya la colisión Varisca. De igual modo que ocurrió con las Anfibolitas de Beja-Acebuches (ABA), con protolitos de edades similares (≈340-335 Ma; SHRIMP U/Pb en circones), este magmatismo máfico se reinterpreta ahora en el contexto de un evento intraorogénico transtensivo que interrumpió temporalmente la colisión Varisca (Fig. 3.4).

(4) La estructura interna de la unidad ABA consiste en un pliegue sinmetamórfico vergente al sur de escala kilométrica, cartografiado en Portugal (Fig. 3.9). Su flanco inverso está representado en el segmento que aflora en España. Previamente a este plegamiento, la unidad ABA obdujo hacia el norte sobre la parte meridional de la ZOM, coetáneamente al desarrollo de pliegues vergentes al norte en la unidad Pulo do Lobo. Estas estructuras vergentes al norte representan la primera deformación carbonífera después del evento transtensivo intraorogénico. El plegamiento de la unidad ABA se produjo simultáneamente al cizallamiento izquierdo de alta a baja temperatura que desmembró las anfibolitas en boudines de tamaño variable separados por zonas de cizalla de grado bajo y fallas (Fig. 3.8). También se han obtenido edades de protolitos de rocas metavolcánicas deformadas (SHRIMP U/Pb en circones), que constriñen la edad máxima para el metamorfismo de baja temperatura en 337 ± 3 Ma. El plegamiento de la unidad ABA fue el punto de partida de la propagación de la deformación hacia el sur durante el Carbonífero medio-superior a través de la ZSP (Fig. 3.14).

(5) El análisis estructural realizado en la unidad Pulo do Lobo muestra una evolución Varisca compleja. Tres fases de deformación penetrativa afectan a las formaciones inferiores (Devónico), mientras que las formaciones superiores (Devónico más alto a Misisipiense) están discordantes y sólo muestran las dos últimas fases de deformación. La tercera fase de deformación en la unidad Pulo do Lobo produjo pliegues entre verticales y vergentes al sur, que se propagaron hacia el sur a través de la ZSP. La segunda fase de deformación produjo pliegues vergentes al norte, mientras que la primera foliación aparece sólo microcrenulada formando ángulos altos con respecto a la segunda foliación (Fig. 3.11). Las formaciones inferiores de la unidad Pulo do Lobo muestran un gran parecido con las formaciones de la misma edad de la Faja Pirítica Ibérica, que se localiza en el interior de la ZSP. Por tanto, la interpretación previa de la unidad Pulo do Lobo como exótica respecto a la ZSP queda desacreditada.

(6) Se ha realizado un estudio multidisciplinar (difracción de Rayos-X, mapas composicionales obtenidos con microsonda electrónica y espectrometría Raman en materia carbonácea) en los metasedimentos de grado bajo a muy bajo de la unidad Pulo do Lobo. Se reconocen dos eventos metamórficos en relación con las dos primeras foliaciones. El primer evento (Devónico) se produjo en condiciones de epizona, mientras que el segundo (Carbonífero medio-superior) no sobrepasó las condiciones del límite anquizona/epizona. El parámetro b de la mica blanca y su contenido en celadonita indican gradientes de baja presión, que ponen en duda la interpretación clásica de la unidad Pulo do Lobo como un prisma de acreción subductivo.

Respecto a la cinemática de la deformación colisional en el SO de Iberia:

(7) La cinemática colisional Varisca dominantemente senestra en todo el SO de Iberia (contrariamente a la cinemática dextra dominante en el resto del Orógeno Varisco) se ha estimado semicuantivamente. Los desplazamientos Variscos transpresivos del SO de Iberia

han sido evaluados aplicando cálculos simples y diversos modelos transpresivos. La convergencia oblicua devono-carbonífera entre los terrenos del SO de Iberia superó los 1000 km en dirección aproximada E-O (coordenadas actuales). Los límites ZCI/ZOM y ZOM/ZSP acumularon preferentemente la componente lateral izquierda, mientras que el acortamiento frontal se produjo preferentemente en el interior de las zonas (Fig. 5.10).

Respecto a la evolución y el significado del límite ZOM/ZSP:

(8) En esta tesis se aportan nuevos datos estructurales, metamórficos y geocronológicos, que junto con la revisión de la información de trabajos anteriores, confirman parcialmente las interpretaciones previas propuestas sobre la evolución Varisca de este límite, aunque algunas otras merecen reinterpretación. De modo resumido, los principales episodios evolutivos son los siguientes (Fig. 5.2): (i) después del cierre del Océano Rheico, la evolución colisional Varisca en el límite ZOM/ZSP se caracterizó por dos estadios de transpresión izquierda separados por un estadio magmático y transtensivo misisipiense. (ii) no hay evidencias claras de la interpretación de la unidad Pulo do Lobo como una unidad exótica ni como un prisma de acreción subductivo; más probablemente, la unidad Pulo do Lobo representa una plataforma detrítica de la parte septentrional de la ZSP, que empezó a deformarse en el Devónico Superior. (iii) Los efectos producidos por el evento magmático y transtensivo misisipiense, más la compleja transpresión carbonífera posterior, dieron lugar a que la sutura del Océano Rheico en el SO de Iberia tenga una apariencia difusa, casi críptica.

Appendix

Appendix 1. UTM coordinates of detrital zircon samples (Chapter II)

	UTM coordinates		Band: 29 S	
SAMPLE	FORMATION	UNIT	X (E)	Y (N)
PLB-63	Ribeira de Limas	South Portuguese Zone: Pulo do Lobo belt	618285	4194680
PLB-78			658262	4194726
PLB-83			657768	4189514
PLB-90			669869	4188826
PLB-28	Horta da Torre		706352	4192584
PLB-68			699255	4192328
PLB-69			694421	4193766
PLB-94			689520	4194928
PLB-53			691935	4194647
PLB-50	Santa Iría		688125	4194335
PLB-67			650293	4199914
PLB-72			656925	4201977
PLB-75			657820	4200151
RNQ-01	El Ronquillo	South Portugese Zone: Iberian Pyrite belt	748396	4173911
RNQ-02			750683	4178836
RNQ-04			748779	4180265
RNQ-07			757880	4161615
RNQ-08	PQ Group		750852	4171762
RNQ-09			750726	4171618
SH-01	Sehoul Cambrian metasandstones	Sehoul Block (North Morocco)	707964	3757730
SH-02			707956	3757806
SH-03			707951	3757858
SH-04			732226	3751232
SH-05			732226	3751232
SH-06			732110	3751222

Appendix 2. Cathodoluminiscence images of representative zircon grains and thin section microphotographs (Chapter II)

RIBEIRA DE LIMAS
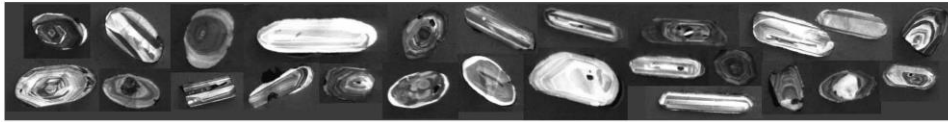
100 μm

500 μm

100 μm

HORTA DA TORRE

100 μm

500 μm

500 μm

SANTA IRÍA

100 μm

500 μm

500 μm

RONQUILLO
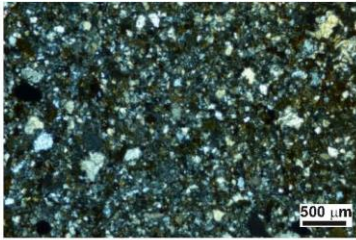

100 μm

500 μm

100 μm

PQ

100 μm

500 μm

100 μm

SEHOUL

100 μm

500 μm
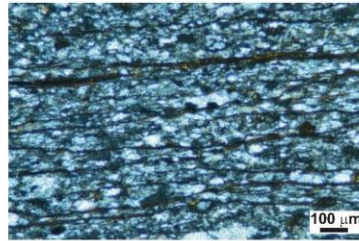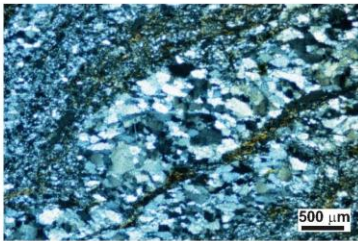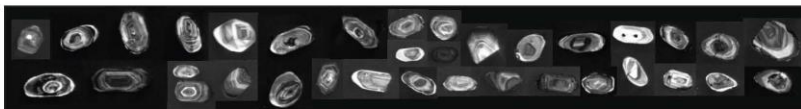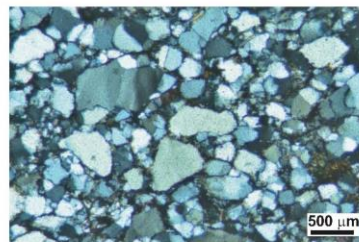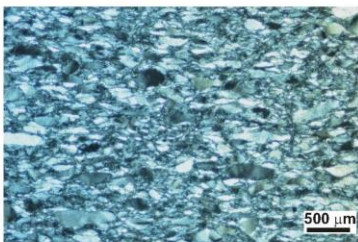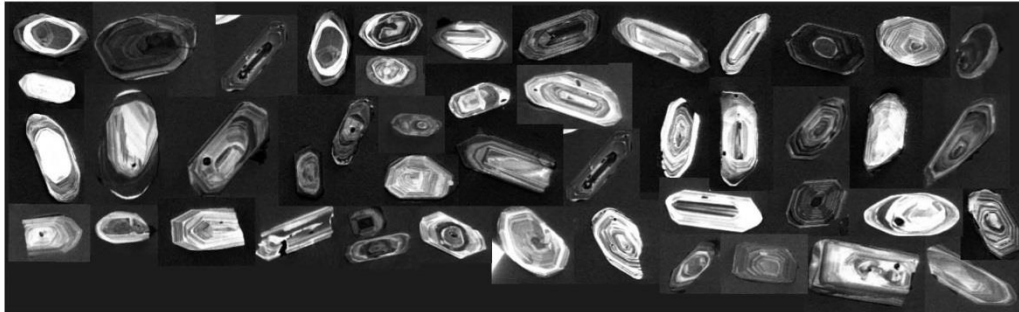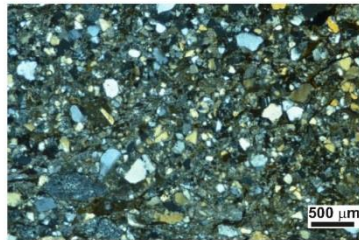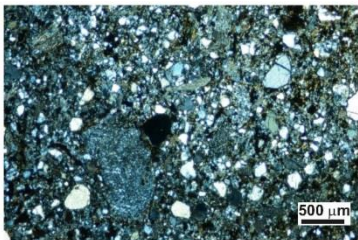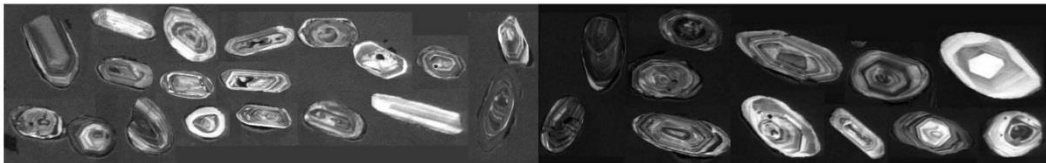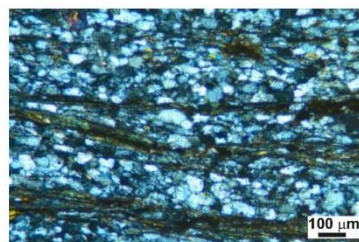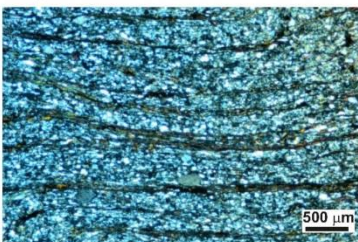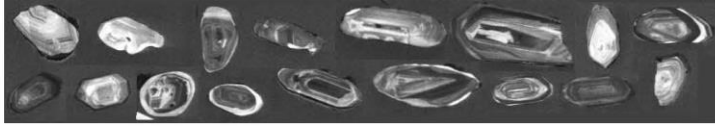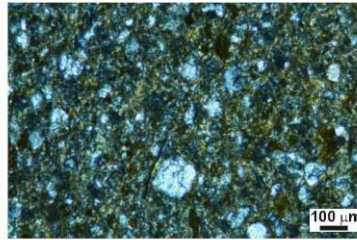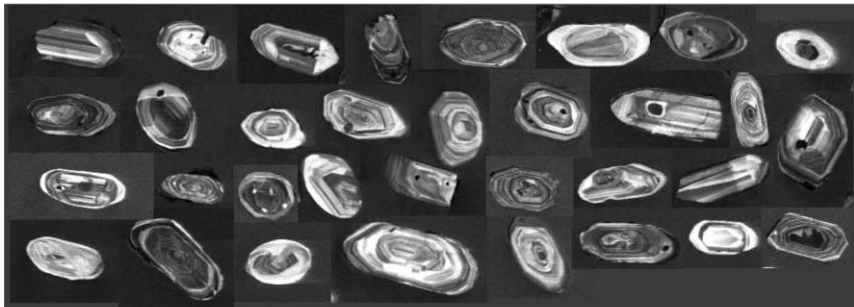
100 μm
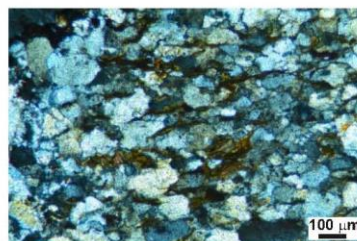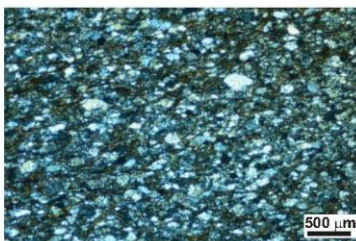
Appendix 3. SHRIMP analytical procedure (Chapter II and III)

U-Th-Pb Geochron analytical procedure used in the SHRIMP IIe/mc instrument of the IBERSIMS lab (UGR)

Zircon grains were separated using panning and magnetic techniques. Hand-picked zircons from the studied samples, several grains of the TEMORA-1 standard (for isotope ratios; Black et al., 2003), one grain of the SL13 zircon standard (for U concentration, Claoué-Long et al., 1995), plus a few grains of the REG zircon (plenty of common lead, for calibrating the masses) were cast on a 3.5 cm diameter epoxy mount (megamount), polished and documented using optical (reflected and transmitted light) and scanning electron microscopy (secondary electrons and cathodoluminescence). After extensive cleaning, mounts were coated with ultra-pure gold (8-10 nanometers-thick) and inserted into the SHRIMP for analysis.

The analytical method followed that described by Williams and Claesson (1987). Each selected spot was rastered with the primary beam for 120 s prior to the analysis, and then analyzed 6 scans, following the isotope peak sequence $^{196}Zr_2O$, ^{204}Pb, $^{204.1}$background, ^{206}Pb, ^{207}Pb, ^{208}Pb, ^{238}U, ^{248}ThO, ^{254}UO. Every peak of every scan was measured sequentially 10 times with the following total counting times per scan: 2 s for mass 196; 5 s for masses 238, 248, and 254; 10 s for masses 204, 206, and 208; and 15 s for mass 207. The primary beam, composed of $^{16}O^{16}O^+$, was set to an intensity of about 5 nA, with a 120 microns Kohler aperture, which generated 17 x 20 micron elliptical spots on the target. The secondary beam exit slit was fixed at 80 microns, achieving a resolution of about 5000 at 1% peak height.

All calibration procedures were performed on the standards included on the same mount. Mass calibration was done on the REG zircon (ca. 2.5 Ga, very high U, Th and common lead content). Every analytical session started by measuring the SL13 zircon, that was used as a concentration standard (238 ppm U). The TEMORA-1 zircon (416.8 ± 1.1 Ma), used as isotope ratios standard, was then measured every 4 unknowns.

Data reduction was done with the SHRIMPTOOLS software (available from www.ugr.es/~fbea), specifically developed for IBERSIMS by F. Bea. This software is a new implementation of the original PRAWN software developed for the SHRIMP, and has been extensively checked against PRAWN and Ludwig's SQUID. SHRIMPTOOLS is platform-independent and runs on any Windows, Mac or Unix computer, regardless of language, time, and date system settings. It has been written in the programming language of the STATA commercial package, which implements powerful algorithms for robust regression, outlier detection and time-series analysis. The software calculates the intensity of each measured isotope in two steps. First, it uses the STATA letter-value display algorithm to find outliers in the ten replicates measured in each peak during each scan, discarding them and averaging the rest once normalized to the SBM measurements. Then, it calculates the 204/206, 207/206, 208/206, 254/238 ratios using Dodson's (1978) double linear interpolation method. The 206/238, 206/195, 238/195, and 248/254 ratios are calculated by dividing the value at the mid-time of the analysis of each isotope calculated

from the robust regression lines of the peak average of each scan vs the time at which it was measured. Errors for Dodson interpolated ratios are calculated as the standard error of the (scans-1) interpolations for each ratio. Errors for isotope ratios calculated by regression result from propagating accordingly standard error of the linear prediction at the mid-point of the analysis. $^{206}Pb/^{238}U$ is calculated from the measured $^{206}Pb+/^{238}U+$ and $UO+/U+$ following the method described by Williams (1998). The error reported for $^{206}Pb/^{238}U$ includes: (1) the error in $UO+/U+$, (2) the error in the regression line $\ln(UO+/U+)$ vs $\ln(^{206}Pb/^{238}U)$, and (3) the standard error in the replicate measurements of the TEMORA zircon. For high-U zircons (U > 2500 ppm), $^{206}Pb/^{238}U$ is further corrected by using the algorithm of Williams and Hergt (2000). Negative ^{204}Pb values may arise from subtracting the blank to the 204 peak measurement when the latter is very low, zero, one or two counts per 10 seconds. Zero counts on 204 peak and 1 count on 204.06 (the blank) result in negative 204/206 ratios. Despite negative isotope ratios have no physical meaning, there is a general agreement amount the SHRIMP users community that negative ^{204}Pb values should be kept to (1) balance averages between different measurements and (2) counter-effect anomalously high blank measurements. Given that the blank is subtracted to masses 206 and 207, negative ^{204}Pb helps approximating the correct 207/206 ratio. Though seldom necessary, the software also permits correction for instrumental drift with time using the sequence of replicate measurements of the TEMORA zircon.

References

Black, L. P., Kamo, S. L., Allen, C. M., Aleinikoff, J. A., Davis, D. W., Korsch, J. R., Foudolis, C., 2003. TEMORA 1: a new zircon standard for Phanerozoic U-Pb geochronology. Chemical Geology 200, 155-170.

Claoue-Long, J. C., Compston, W., Roberts, J., Fanning, C. M. (1995). Two Carboniferous ages: a comparison of SHRIMP zircon dating with conventional zircon ages and $^{40}Ar/^{39}Ar$ analysis. In: Berggren, W. A., Kent, D. V., Aubry, M. P., Hardenbol, J. (Eds.), Geochronology Time Scales and Global Stratigraphic Correlation. SEPM (Society for Sedimentary Geology) Special Publication No. 4. (pp. 3-21).

Dodson, M. H. (1978) A linear method for second-degree interpolation in cyclical data collection. Journal of Physics E: Scientific Instruments 11, 296.

Williams, I. S., & Claesson, S. (1987). Isotopic evidence for the Precambrian provenance and Caledonian metamorphism of high grade paragneisses from the Seve Nappes, Scandinavian Caledonides. II: Ion microprobe zircon U-Th-Pb. Contribution to Mineralogy and Petrology, 97, 205-217.

Williams, I. S., Hergt, J. M. (2000). U-Pb dating of Tasmanian dolerites: a cautionary tale of SHRIMP analysis of high-U zircon. In: Woodhead, J. D., Hergt, J. M., Noble, W. P. (Eds.), Beyond 2000: New Frontiers in Isotope Geoscience, Lorne, 2000; Abstracts and Proceedings (pp. 185-188).

Williams, I. S. (1998). U-Th-Pb Geochronology by Ion Microprobe. In: McKibben, M. A., Shanks III, W. C., Ridley, W. I. (Eds.), Applications of microanalytical techniques to understanding mineralizing processes. Reviews in Economic Geology v.7. (pp. 1-35).
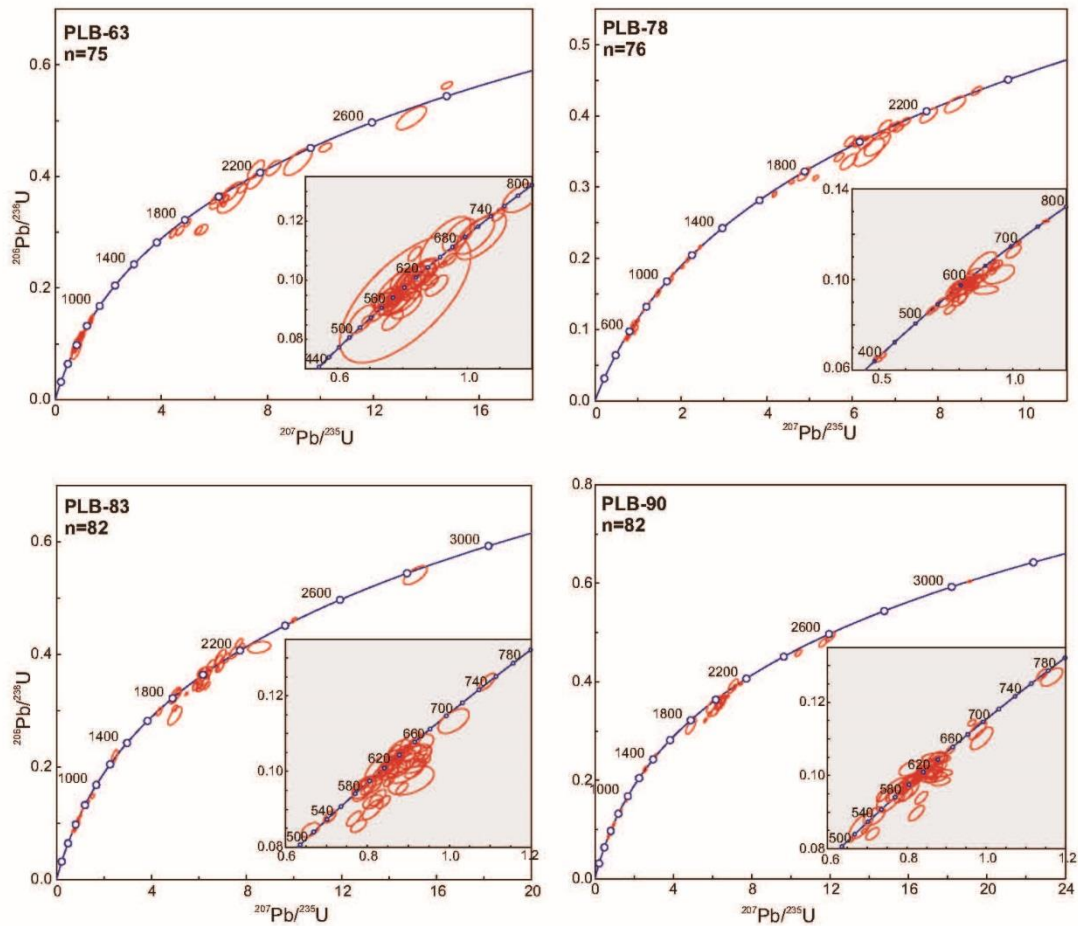
Appendix 4. SHRIMP U-Th-Pb analytical data of zircons (Chapter II).

The gross tables can be found as excel file in the digital version of this Ph. D. Thesis (CD).

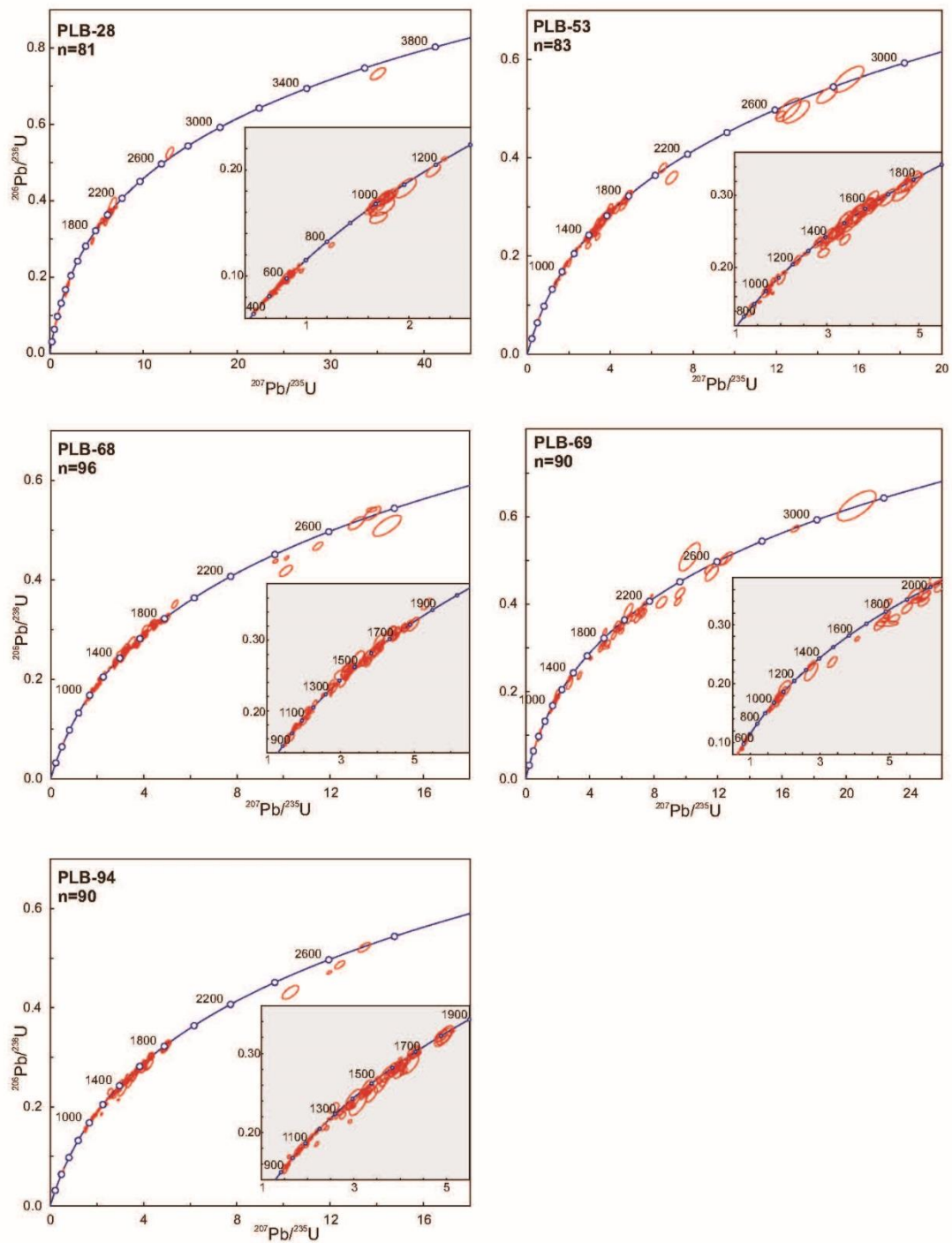**Appendix 5. Wetherill plots of detrital zircon samples (Chapter II)**
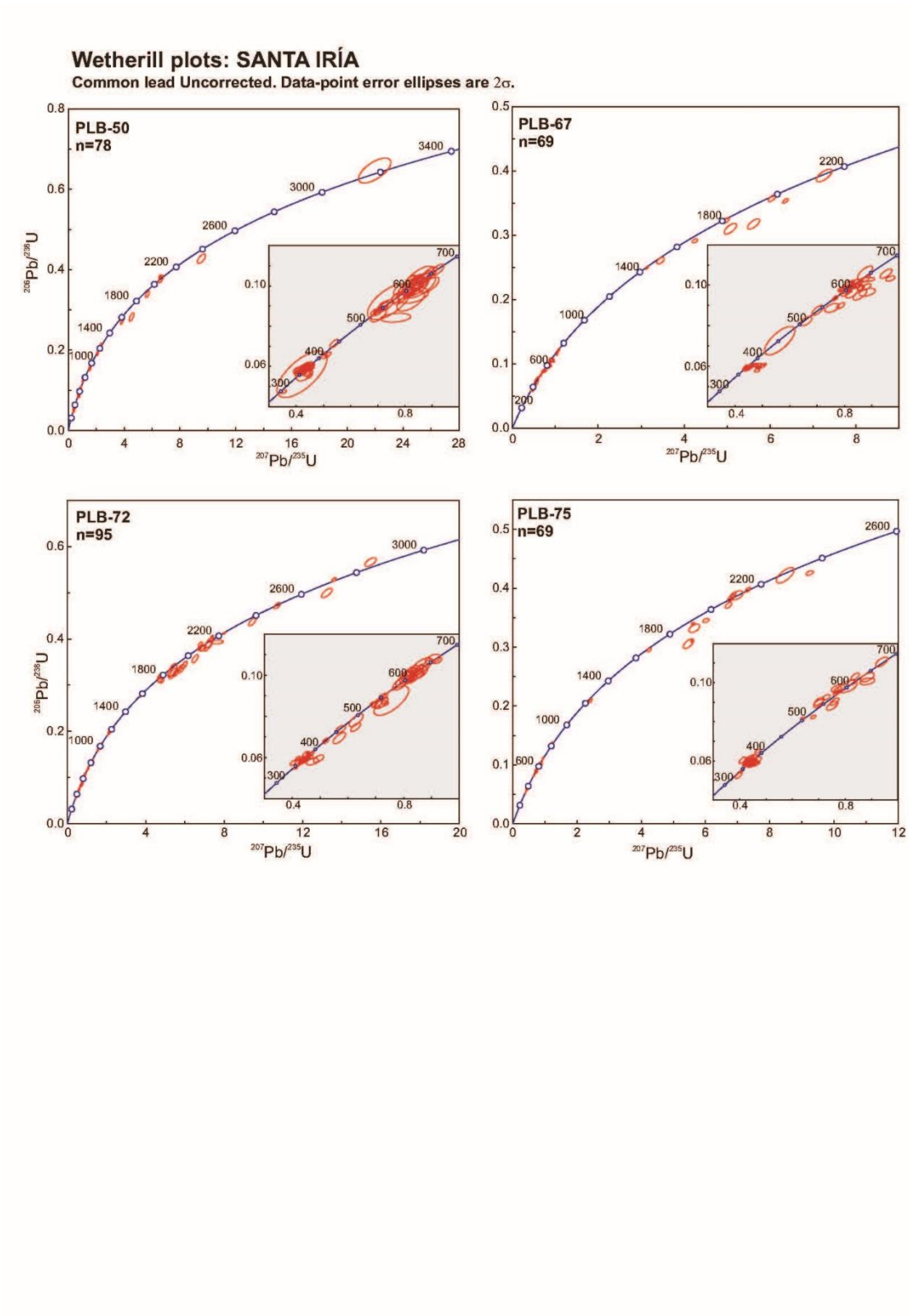
Wetherill plots: HORTA DA TORRE
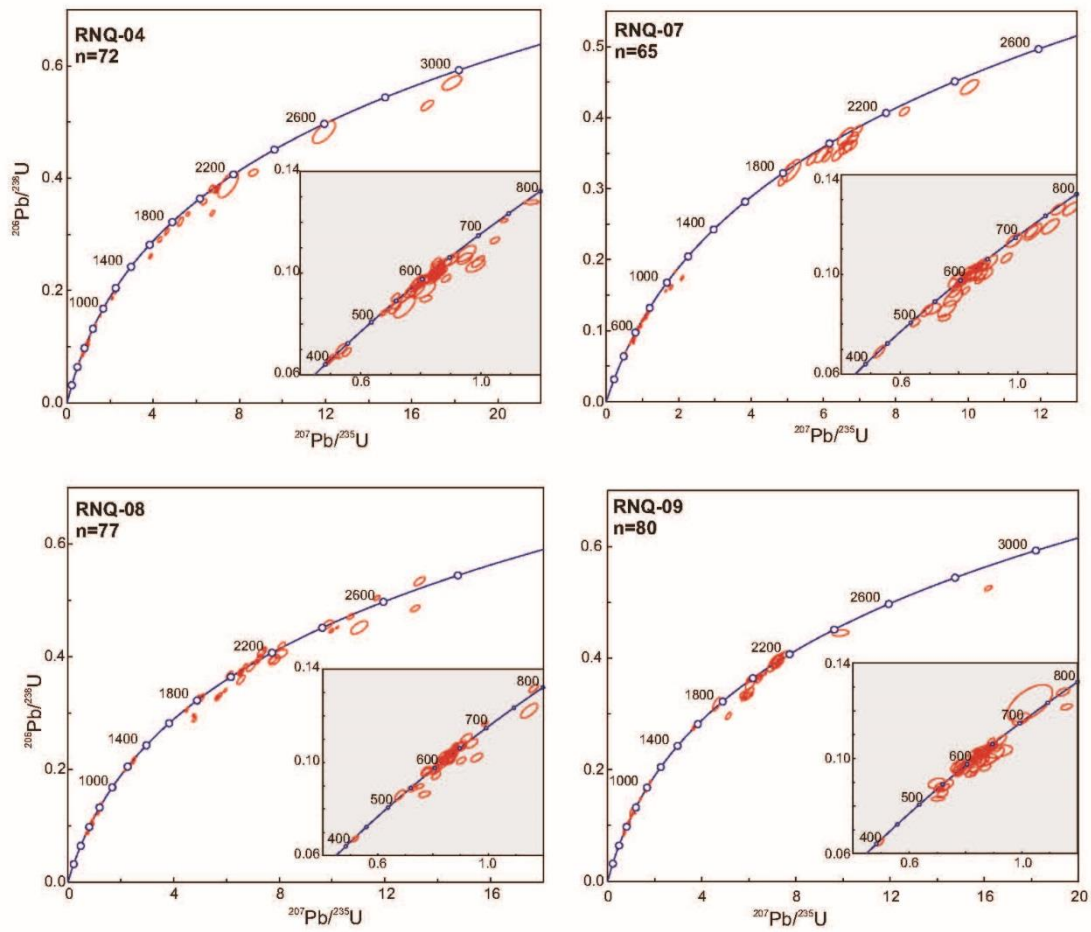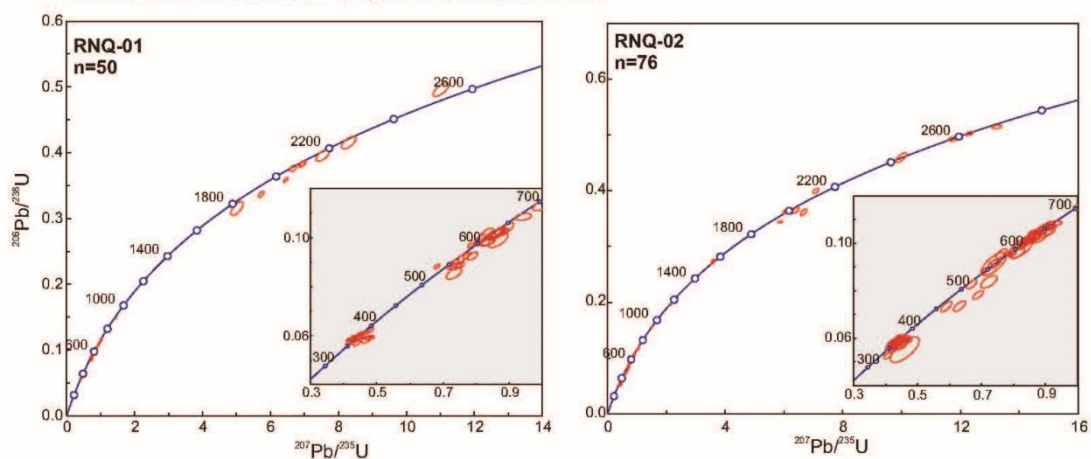Common lead Uncorrected. Data-point error ellipses are 2σ.

Wetherill plots: SANTA IRÍA
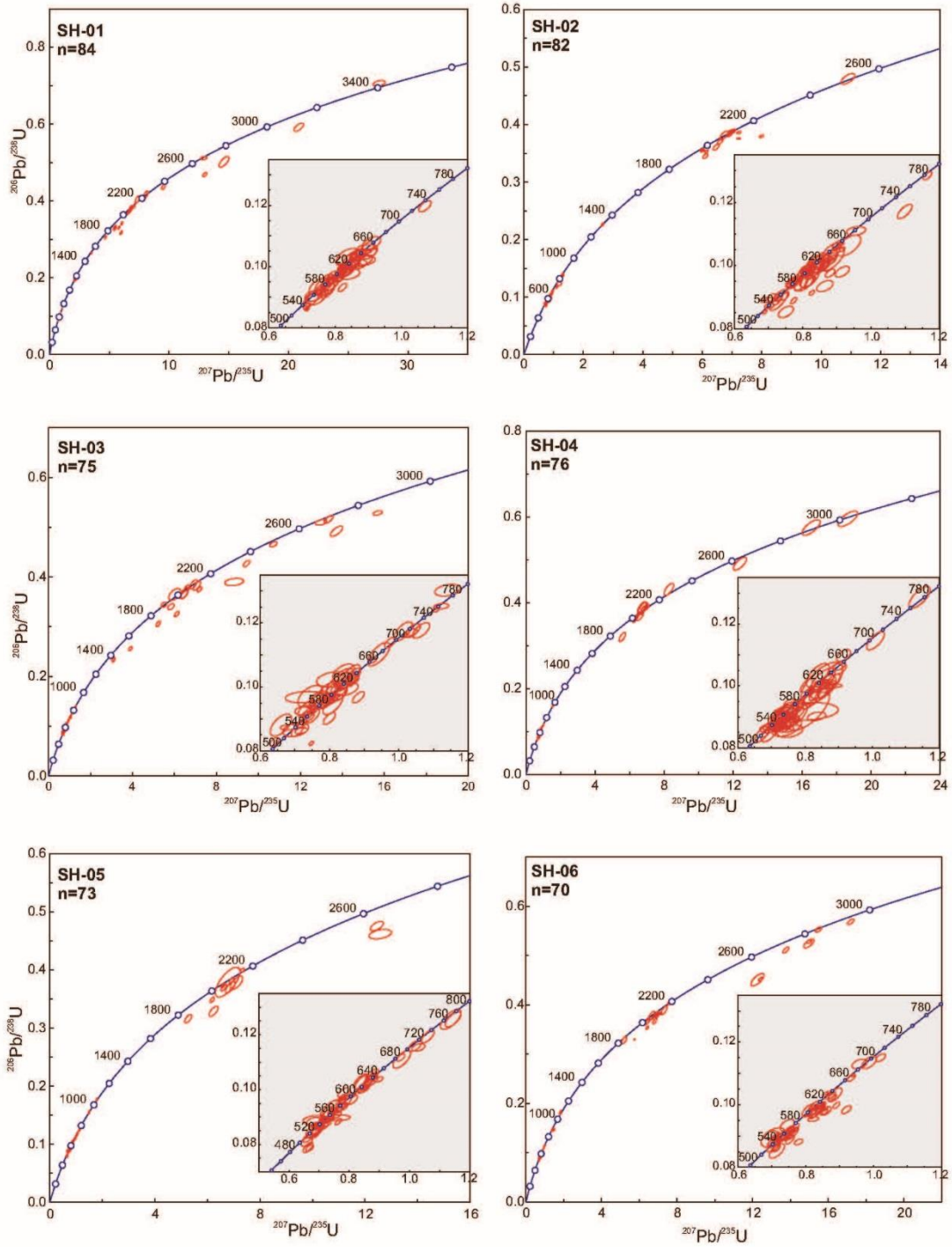Common lead Uncorrected. Data-point error ellipses are 2σ.

Wetherill plots: RONQUILLO
Common lead Uncorrected. Data-point error ellipses are 2σ.

Wetherill plots: PQ
Common lead Uncorrected. Data-point error ellipses are 2σ.

Wetherill plots: SEHOUL
Common lead Uncorrected. Data-point error ellipses are 2σ.

Appendix 6. Sample description (Chapter III)

POR-17: Sample collected in Guadiana River (UTM: 29S, 618542 m E, 4193515 m N). It is a meta-igneous intermediate rock with porphyrytic texture located between the metasediments of the Pulo do Lobo Fm. It is not foliated and the principal mineral is plagioclase. The grain-size is medium and it has some plagioclase porphyroblasts of more than 1 millimeter.

POR-26: Sample collected in the metabasalts from the Peramora olistostrome, (UTM: 29S, 675231 m E, 4196977 m N). It is a fine-grained metabasic rock mainly constituted by plagioclase, Ca-amphibole and epidote, and chlorite, titanite and magnetite as accessory minerals. It has porphyritic texture and it is defined by a foliation and affected by the shearing.

Next three samples were collected in the south of Alájar, where there are some porphyritic-texture rocks between the metasediments of Horta da Torre Fm. (Pulo do Lobo unit), very affected by the shearing:

PLB-19: (UTM: 29S, 705825 m E, 4193270 m N). Foliated ultramilonite meta-igneous intermediate rock where the deformation was intense. It has small grain-size constituted by plagioclase, quartz, feldspar, garnet and some phyllosilicates in the matrix.
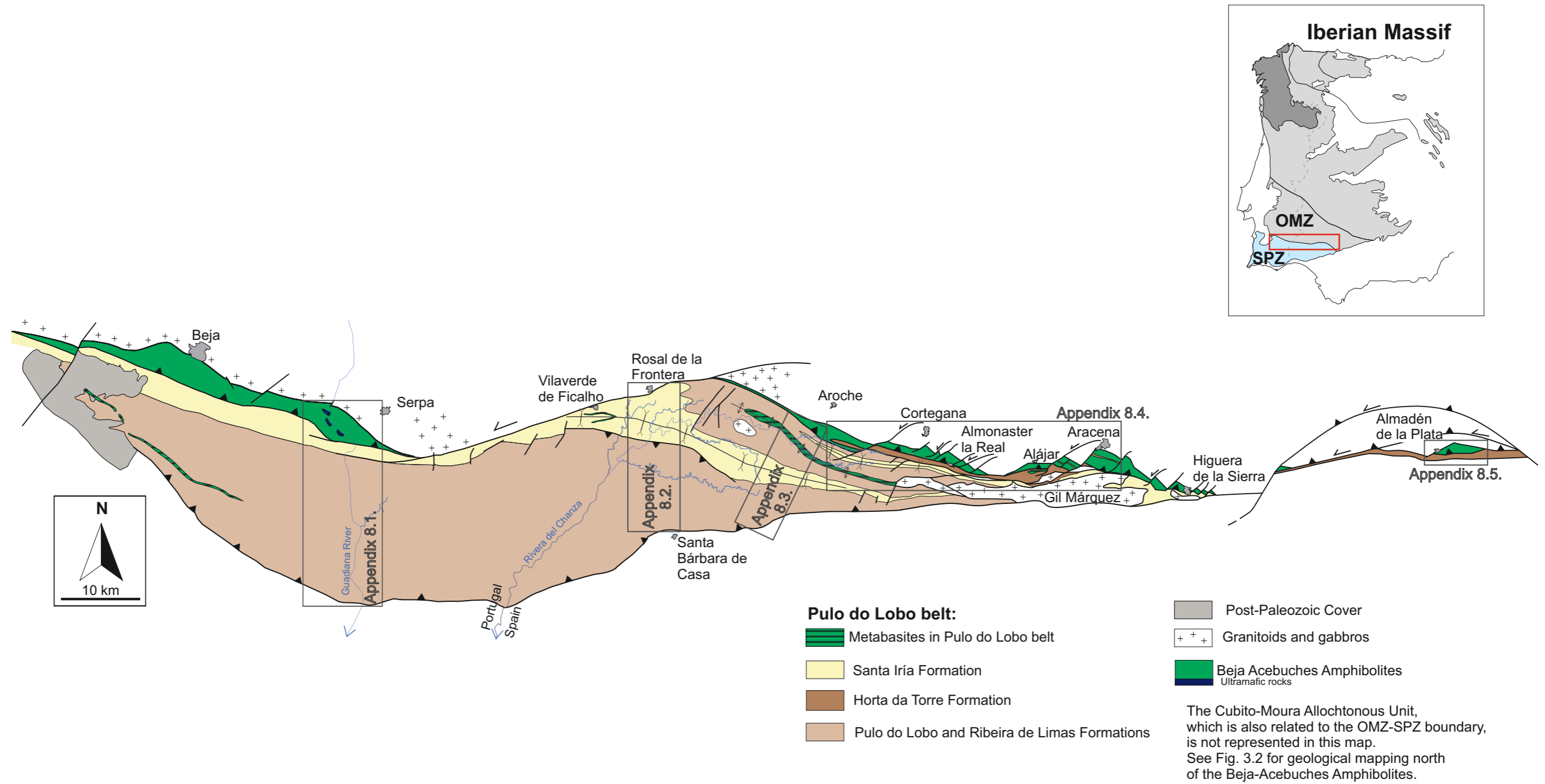
PLB-20: (UTM: 29S, 705885 m E, 4193198 m N). Very similar to PLB-19 is a strongly foliated ultramilonite rock with quartz, plagioclase, garnet and phyllosilicates.

PLB-27: (UTM: 29S, 706352 m E, 4192584 m N). Slightly deformed meta-igneous porphyritic-acid rock, located in a "lozenge" between the foliated metasediments strongly affected by the shearing. The main minerals are millimetric plagioclase porphyroblasts and smaller volcanic quartzs.
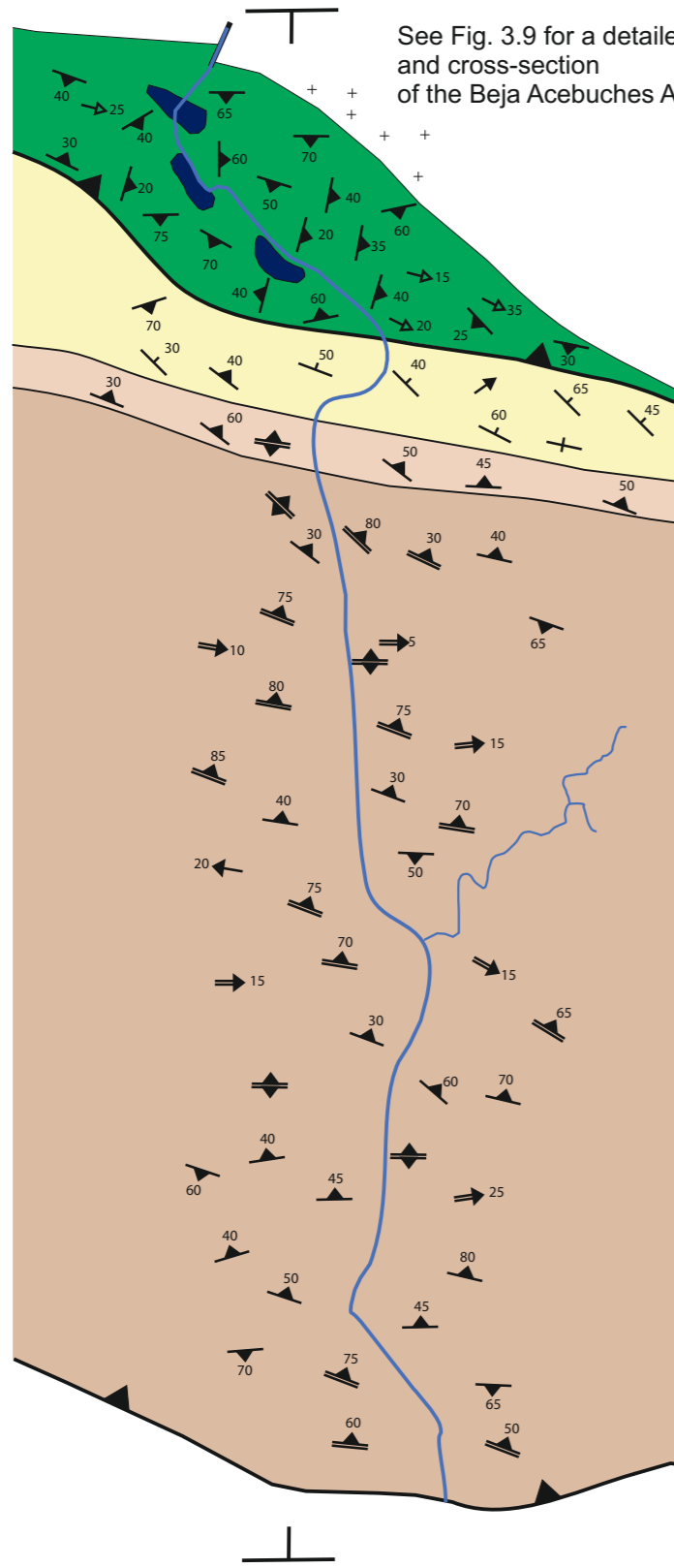
Appendix 7. SHRIMP U-Th-Pb analytical data of zircons (Chapter III).

The gross tables can be found as excel file in the digital version of this Ph. D. Thesis (CD).

**Appendix 8. Geological map of the Ossa-Morena/South Portuguese boundary**

Iberian Massif

OMZ

SPZ

N

10 km

Beja

Serpa

Rosal de la Frontera

Vilaverde de Ficalho

Aroche

Cortegana

Almonaster la Real

Appendix 8.4.

Aracena

Alájar

Almadén de la Plata

Appendix 8.5.

Higuera de la Sierra

Gil Márquez

Appendix 8.1.

Appendix 8.2.

Appendix 8.3.

Santa Bárbara de Casa

Guadiana River

Rivera del Chanza

Portugal

Spain

Pulo do Lobo belt:

Metabasites in Pulo do Lobo belt

Santa Iría Formation

Horta da Torre Formation

Pulo do Lobo and Ribeira de Limas Formations

Post-Paleozoic Cover

Granitoids and gabbros

Beja Acebuches Amphibolites
Ultramafic rocks

The Cubito-Moura Allochtonous Unit,
which is also related to the OMZ-SPZ boundary,
is not represented in this map.
See Fig. 3.2 for geological mapping north
of the Beja-Acebuches Amphibolites.

Appendix 8.1

See Fig. 3.9 for a detailed map
and cross-section
of the Beja Acebuches Amphibolites

Cross-section of the Pulo do Lobo belt in Fig. 3.11-b.
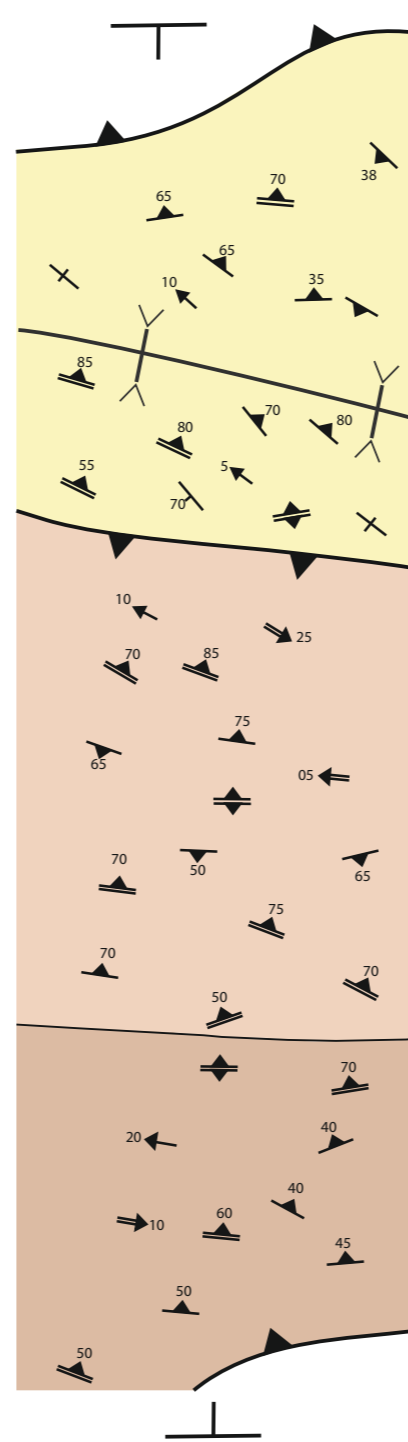
Appendix 8.2

Cross-section in Fig. 4.1-c.1.

N

5 km

Appendix 8.3
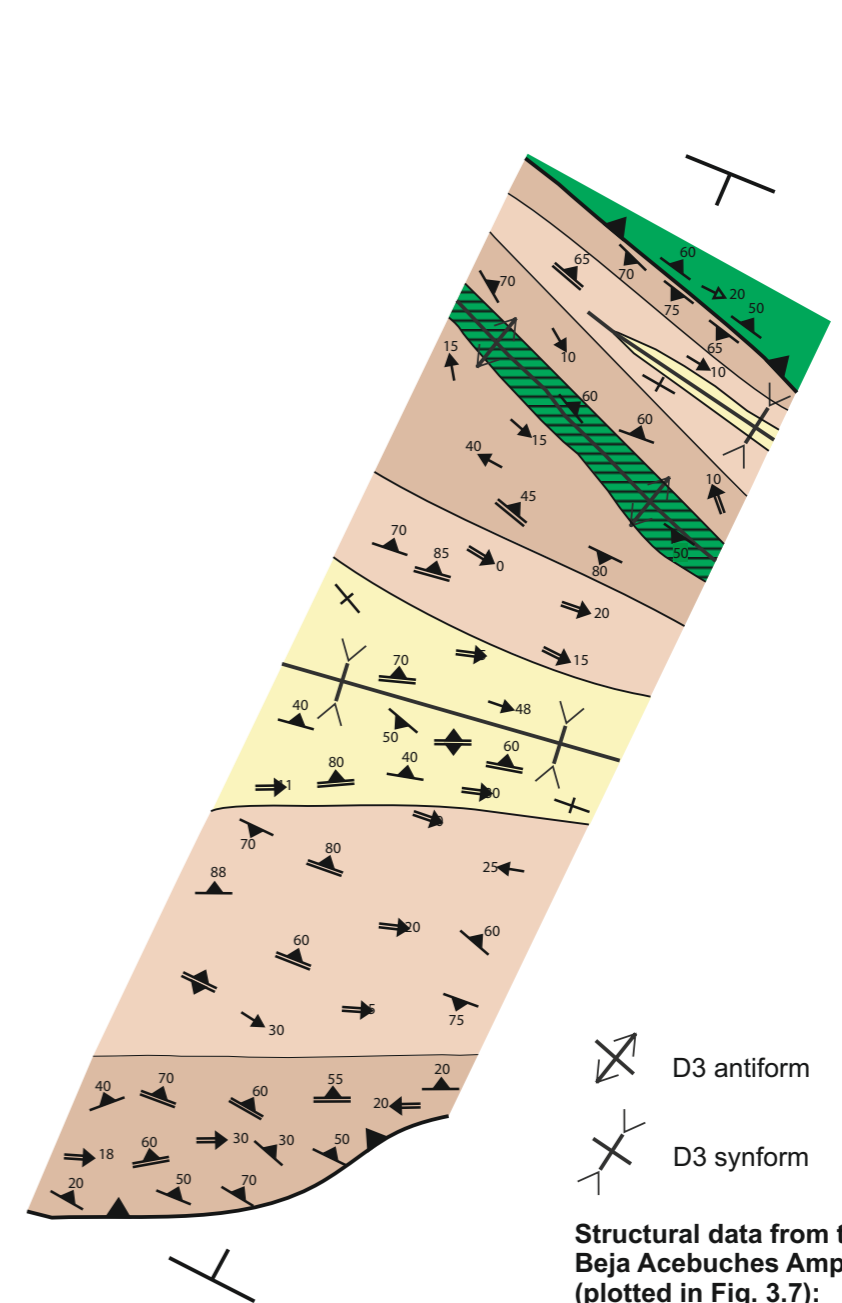
Cross-section in Fig. 3.11-a.

⬠ D3 antiform

✕ D3 synform

**Structural data from the
Beja Acebuches Amphibolites
(plotted in Fig. 3.7):**
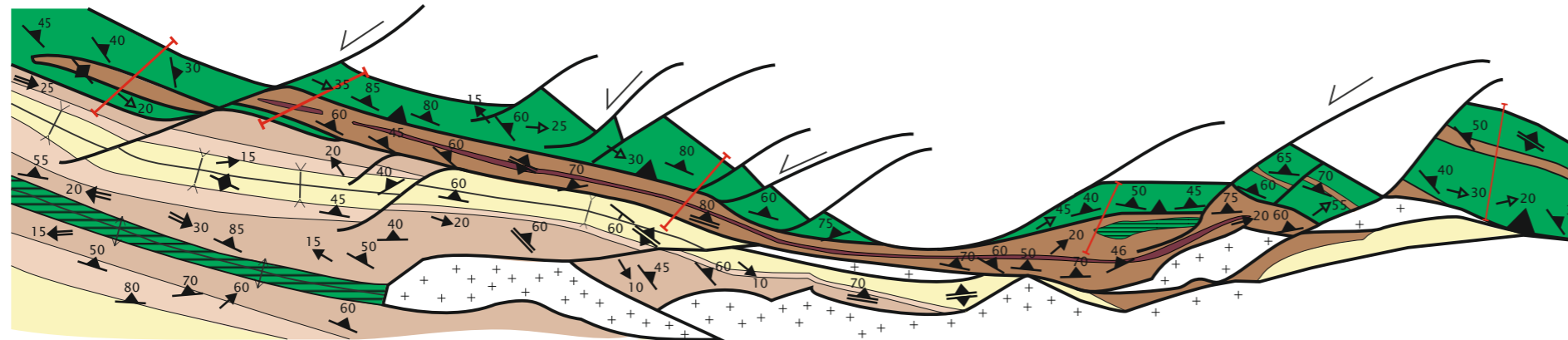
→ Stretching lineation

◢ Mylonitic foliation

**Structural data from the
Pulo do Lobo belt
(plotted in Fig. 3.11):**

→ L1* and L2

⇒ L2* and L3

✕ S0 in Santa Iría Formation

◢ S1* and S2

◢ S2* and S3

⊞ Granitoids

■ Beja Acebuches Amphibolites
Ultramafic rocks

Pulo do Lobo belt:

▤ Metabasites in the Pulo do Lobo belt

□ Santa Iría Formation

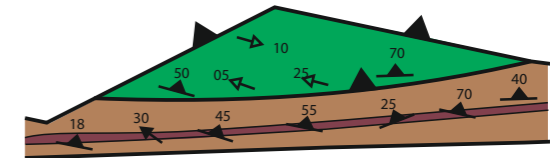□ Ribeira de Limas Formation

□ Pulo do Lobo Formation

Appendix 8.4

Appendix 8.5

Cross-sections in Fig. 3.8 (red lines).

N

5 km

Granitoids

Beja Acebuches Amphibolites

Pulo do Lobo belt:

Metabasites in Pulo do Lobo belt

Santa Iría Formation

Horta da Torre Formation
Quartzite band

Ribeira de Limas Formation

Pulo do Lobo Formation

D3 antiform

D3 synform

**Structural data from the
Beja Acebuches Amphibolites
(plotted in Fig. 3.7):**

Stretching lineation

Mylonitic foliation

**Structural data from the
Pulo do Lobo belt
(plotted in Fig. 3.11):**

L1* and L2

L2* and L3

S0 in Santa Iría Formation

S1* and S2

S2* and S3